



**HAL**  
open science

# GEOCHEMICAL AND ENVIRONMENTAL STUDY OF A COASTAL ECOSYSTEM: MASSACIUCCOLI LAKE (NORTHERN TUSCANY, ITALY)

Ilaria Baneschi

► **To cite this version:**

Ilaria Baneschi. GEOCHEMICAL AND ENVIRONMENTAL STUDY OF A COASTAL ECOSYSTEM: MASSACIUCCOLI LAKE (NORTHERN TUSCANY, ITALY). Geochemistry. UNIVERSITÀ CA' FOSCARI VENEZIA; Università degli studi Ca' Foscari di Venezia, 2007. English. NNT : . tel-00400140

**HAL Id: tel-00400140**

**<https://theses.hal.science/tel-00400140>**

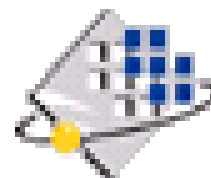
Submitted on 30 Jun 2009

**HAL** is a multi-disciplinary open access archive for the deposit and dissemination of scientific research documents, whether they are published or not. The documents may come from teaching and research institutions in France or abroad, or from public or private research centers.

L'archive ouverte pluridisciplinaire **HAL**, est destinée au dépôt et à la diffusion de documents scientifiques de niveau recherche, publiés ou non, émanant des établissements d'enseignement et de recherche français ou étrangers, des laboratoires publics ou privés.



CO-TUTORED DOCTORAL DISSERTATION  
BETWEEN:



UNIVERSITÀ CA' FOSCARI VENEZIA  
DIPARTIMENTO DI SCIENZE AMBIENTALI  
DOTTORATO DI RICERCA IN SCIENZE AMBIENTALI, 19° CICLO  
(A.A. 2003/2004 – A.A. 2005/2006)

UNIVERSITE PARIS-SUD XI  
FACULTE DES SCIENCES D'ORSAY  
ECOLE DOCTORALE "DYNAMIQUE ET PHYSICO-CHIMIE DE LA TERRE  
ET DES PLANETES"

## **GEOCHEMICAL AND ENVIRONMENTAL STUDY OF A COASTAL ECOSYSTEM: MASSACIUCCOLI LAKE (NORTHERN TUSCANY, ITALY)**

A dissertation submitted the 16<sup>th</sup> March 2007 by  
Doctoral Candidate: Ilaria BANESCHI  
European Doctorate label

### Supervisors:

Prof. Giovanni Maria ZUPPI	Università Cà Foscari, Venezia, Italy
Dr. Jean Luc MICHELOT	UMR-IDES, Université Paris IX, France
Dr. Massimo GUIDI	IGG-CNR, Pisa, Italy
Prof. Roberto GONFIANTINI	IGG-CNR, Pisa, Italy

### Examiners:

Prof. Roberto GONFIANTINI	IGG-CNR, Pisa, Italy	President
Prof. Kazimierz ROZANSKI	AGH, Krakow, Poland	Rapporteur
Prof. Yves TRAVI	Université d'Avignon, France	Rapporteur
Prof. Luigi MARINI	Università di Genova, Italy	Examineur

*To my grandfather Giuseppe,  
To Brunella,  
for all they represent to my life.*

## ACKNOWLEDGMENTS

---

This research was fuelled by several small grants and contributions and by the graciousness of many people. I wish to thank everybody who contributed to this work.

At first, I gratefully acknowledge Dott. Massimo Guidi, without whose patient, guidance, constant support and valuable suggestions, this research would not be accomplished, and my tutor Prof. Gian Maria Zuppi, who gave me the opportunity to carry out this work and following me. I would like to thank Dr. Jean Luc Michelot and Prof. Roberto Gonfiantini for his precious advices.

I would like to thank all the members of the IGG group and in particular Dott. Roberto Cioni, who gave me helpful suggestions, Dott.ssa Maddalena Pennisi for her experiences in boron analyses and her helpfulness and Dott. Gianni Cortecchi.

I am very grateful to Prof. Gabriello Leone for his advices and encouragements.

I also would like to thank Prof. Luigi Marini who helped me to review the English version.

I would like to thank Aldo Pescia for his irreplaceable technical expertise in the laboratory and for his kindness.

This research required chemical and isotopic analyses from several laboratories. In particular, I thank Prof. Emanuele Argese, director of the chemical laboratory at Venice University and Lorena Gobbo. I am grateful to the IDES Laboratories of Orsay (France) for the kind hospitality and, in particular, Marc Massault for the time and attention they gave to my research Elena Crespi and Philippe Pradel (Diffraction RX Laboratory). Other laboratories deserving of recognition include: the Institute of Ecosystem Study of Pisa, in particular Lamberto Lubrano and Cristina Macci; the Stable Isotopes Laboratory of IGG-CNR of Pisa (above all, Enrico Calvi). I thank Dott. Matteo Lelli (IGG-CNR) to perform trace metals analysis of my samples by running the ICP-AES and Daniela Andreani for her collaboration for Boron isotopes analyses.

I would express thanks to the Prof. Roberto Spandre and Dott. Laurent Bergonzini.

Access to Massaciuccoli lake would have been nearly impossible without Andrea Fontanelli and all of the employees of the LIPU of Massaciuccoli, and the support of Migliarino- San Rossore Massaciuccoli Park. I would also like to thank Andrea Tozzi for the help during samplings.

Many thanks to Massarosa municipality, to the Ing. Leonardo Gianneccchini of the 'Consorzio di Bonifica Versilia Massaciuccoli'.

Without the help of my colleagues and students the scope of this project could not have been as extensive as it was. Many thanks to: Matia Menichini, Elisa Carletti, Oriana Gava, Chiara Pistocchi, Simona Bosco, Vania Campigli, Stefano, Daniele Picciaia and Ing. Andrea Scozzari.

A special thank to Daniela Melai for the bibliography revision and the irreplaceable support.

I also would like to thank my friend colleagues: Maura Bussolotto, Manuëlla Delalande, Aurélie Noret, Alban Duriez, Marina Gillon, Christelle Chabault, Bernard Adiaffi, Thierry Richard, Vincent Schneider, Anna Laura Palpacelli, Miss Thi-Kim-Ngan Ho, Broust family, Miss Monique Peron and all people who help and enjoyed me during French stage.

Moreover, I am grateful to all of my friends who supported during these years, and above all: Virginia Barros, Samanta Del Soldato, Nicoletta Cavaleri, Eloisa Di Sipio, Francesca Frediani, Marina Cervelli, Michele Amadori, Mariella Tataranni. I want to remember my friends in Parlascio and Cecilia.

## ABSTRACT

---

The Massaciuccoli palustrine marsh is amongst the most important wetlands in Tuscany. It is a coastal lagoon of fresh to brackish water, which drains a total basin area of about 112 km<sup>2</sup> and opens to the sea by way of an artificial channel, known as Burlamacca.

In the palustrine area there are old quarries (30 m max depth and 2.5 km<sup>2</sup> total area) which have been left by the previous sand extraction activity. Sewage, wastewaters of reclamation lands and wastewaters of cattle-breeding and of a food-industry are the main polluting sources. Within the basin, there are two landfills and several agricultural farming activities.

This research, attempts to study 1) the anthropogenic impact on water chemistry; 2) the seawater inflow, the groundwater infiltration and the evaporation rate; 3) the role of the excavation area and 4) the function of the biotic processes, by applying geochemical techniques and chemical (Br, B, Cl and nutrients) and isotopic ( $\delta^{18}\text{O}$ ,  $\delta^{11}\text{B}$ ,  $\delta^2\text{H}$ ,  $\delta^{13}\text{C}$ ,  $\delta^{34}\text{S}_{\text{SO}_4}$  and  $\delta^{18}\text{O}_{\text{SO}_4}$ ) tracers.

This study highlighted some important methodological aspects concerning:

- 1-the role of biotic processes to regulate the contents of several dissolved chemical compounds
- 2-the application of isotopes to trace the chemical-physical processes, taking place at the interface between the different compartments, to establish the origin of the elements and to get dating.

In particular we point out:

- i. the distribution in the system of trace elements depends on the presence and intensity of biotic activity
- ii. the importance of isotope geochemistry to trace the origin of water and active, chemical-physical processes
- iii. the increase in the radiocarbon activity of the sedimentary organic matter, corresponding to the atomic experiments carried out during the 60's, at different depths in the sediments from different sites in the lake.

We can conclude that geochemical research allowed us to underline the influence of agricultural activity on the chemical composition of lake water, the hydrodynamic equilibrium and superficial sediment composition.

The quarries, because of their high water volume, represent a hydraulic barrier for seawater intrusion into the lake. They act also as a sink for nutrients and they have a positive hydraulic function to prevent lake contamination. However, in future, they will become a serious problem if the stratification (chiefly due to chemical stability) disappears or if they are filled up.

## RIASSUNTO

---

L'area palustre del Massaciuccoli è la più importante zona umida della Toscana settentrionale. E' una laguna costiera contenente acque da dolci a salmastre, che drena un bacino di circa 112 km<sup>2</sup> di superficie totale. L'area palustre è connessa con mare mediante un canale artificiale, noto come Burlamacca.

Nell'area palustre sono presenti ex-cave (profondità massima di 30 m e 2.5 km<sup>2</sup> di estensione totale), residuo della passata attività di estrazione della sabbia silicea. Le principali fonti inquinanti sono rappresentate da scarichi urbani e industriali ed acque di drenaggio dalla bonifica agricola. Nel bacino sono presenti due discariche e varie aziende agricole.

Questo progetto di ricerca si pone l'obiettivo di studiare: 1) l'impatto antropico sulla chimica delle acque del bacino del lago di Massaciuccoli; 2) l'apporto di acqua marina, l'infiltrazione di acque sotterranee ed il tasso di evaporazione del lago; 3) il ruolo svolto dalle ex-cave, e 4) la funzione esercitata dai processi biotici. Tali obiettivi sono stati raggiunti applicando tecniche geochimiche e traccianti chimici (Br, B, Cl e nutrienti) ed isotopici ( $\delta^{18}\text{O}$ ,  $\delta^{11}\text{B}$ ,  $\delta^2\text{H}$ ,  $\delta^{13}\text{C}$ ,  $\delta^{34}\text{S}_{\text{SO}_4}$  e  $\delta^{18}\text{O}_{\text{SO}_4}$ ).

Lo studio ha evidenziato alcuni aspetti metodologici importanti, che riguardano:

- 1- il ruolo dei processi biotici nell'influenzare il contenuto dei composti chimici disciolti nelle acque
- 2- l'applicazione delle tecniche isotopiche sia per tracciare i processi chimico-fisici, che hanno luogo all'interfaccia tra i diversi comparti ambientali, sia per stabilire l'origine degli elementi e per effettuare delle datazioni.

In particolare, abbiamo evidenziato che:

- i. la distribuzione nel sistema in esame degli elementi dipende dalla presenza e dall'intensità dell'attività biotica
- ii. l'importanza della geochimica isotopica nel tracciare l'origine delle acque ed i processi chimico-fisici
- iii. datazioni effettuate sulla materia organica dei sedimenti con il <sup>14</sup>C, evidenziano la presenza di un picco dell'attività radioattiva, che corrisponderebbe agli esperimenti atomici effettuati negli anni '60, a profondità diverse del sedimento nei diversi siti del lago campionati.

In conclusione, questo lavoro ha permesso di evidenziare l'influenza dell'attività agricola sulla composizione chimica dell'acqua del lago, sull'equilibrio idrodinamico e sulla composizione del sedimento superficiale. Inoltre, le cave presenti nella zona palustre, per la loro estensione e profondità, costituiscono una barriera idraulica all'ingresso di acqua di mare nel lago. Tali ambienti rappresentano anche un sink di nutrienti e prevengono la contaminazione del lago. L'interesse per le zone di escavazione è giustificata anche dal fatto che, se in futuro le acque, adesso stratificate, si rimescolassero o se tali buche venissero riempite, potrebbero diventare un serio problema per l'equilibrio dell'intero ecosistema palustre.

## RÉSUMÉ

---

Le marais de Massaciucoli est la plus importante zone humide de la Toscane septentrionale. C'est une lagune côtière qui draine un bassin d'environ 112 km<sup>2</sup> de surface totale et qui est caractérisée par des eaux à salinité très variable. Cette zone est reliée à la mer par un canal artificiel, appelé « Burlamacca ».

Dans cette zone palustre, on retrouve de vieilles carrières (profondeur maximum : 30 m., superficie totale : 2,5 km<sup>2</sup>), témoignage d'une ancienne activité d'extraction de sable siliceux. Les principales sources polluantes sont représentées par les déchets urbains et industriels et par les eaux de drainage agricole ; au sein du bassin, il y a en effet 2 décharges et plusieurs entreprises agricoles.

Ce projet de recherche se propose d'étudier : 1) l'impact anthropique sur la chimie des eaux du bassin du lac de Massaciucoli ; 2) l'apport de l'eau de mer, l'infiltration des eaux souterraines et le taux d'évaporation du lac ; 3) le rôle exercé par les anciennes carrières, et 4) le rôle des processus biologiques.

Les résultats ont été obtenus en appliquant des techniques géochimiques et en utilisant des traceurs chimiques (Br, B, Cl et des éléments nutritifs) et isotopiques ( $\delta^{18}\text{O}$ ,  $\delta^{11}\text{B}$ ,  $\delta^2\text{H}$ ,  $\delta^{13}\text{C}$ ,  $\delta^{34}\text{S}_{\text{SO}_4}$  et  $\delta^{18}\text{O}_{\text{SO}_4}$ ).

L'étude a mis en évidence des aspects méthodologiques importants, concernant :

1. l'influence des processus biologiques sur le contenu des composés chimiques dissous dans les eaux
2. l'application des techniques isotopiques qui, non seulement, a permis de suivre les processus chimiques et physiques qui se développent à l'interface entre les différents compartiments, mais qui a permis aussi d'établir l'origine des divers éléments et d'effectuer des datations.

Notamment, on a mis en évidence les points suivants:

- a. la distribution des éléments dans le système étudié est fonction de la présence et de l'intensité de l'activité biologique
- b. la géochimie est importante pour tracer l'origine des eaux et des processus chimiques et physiques.
- c. Les datations effectuées sur la matière organique des sédiments avec le <sup>14</sup>C mettent en évidence la présence d'un pic de l'activité radioactive, qui correspond aux essais atomiques effectués dans les années '60. La profondeur, à laquelle on peut trouver ces évidences, varie selon les différents sites échantillonnés.

En conclusion, ce travail a permis de mettre en évidence l'influence de l'activité agricole sur la composition chimique de l'eau du lac, sur l'équilibre hydrodynamique et sur la composition du sédiment superficiel. En outre, les carrières, en relation à leur extension et profondeur, représentent une barrière hydraulique à l'intrusion de l'eau marine dans le lac ; la disparition de la stratification des eaux des carrières ou un éventuel remplissage de ces dernières pourrait devenir un problème très sérieux pour l'équilibre de l'écosystème palustre.

# INDEX

---

---

<b>Acknowledgments</b> .....	iii
<b>Abstract</b> .....	iv
<b>Riassunto</b> .....	v
<b>Résumé</b> .....	vi
<b>1 PROBLEMATICS AND RESEARCH OUTLINES</b> .....	3
1. INTRODUCTION .....	3
1.1.1 <i>The transition ecosystems: the coastal area</i> .....	4
1.1.2 <i>Anthropogenic impact on the hydrodynamic pattern and on the environmental quality of the basin</i> .....	4
1.2 OBJECT AND RESEARCH STRATEGY .....	6
<b>2 RESEARCH AREA</b> .....	8
2.1 GEOGRAPHICAL SETTING .....	8
2.1.1 <i>Climate</i> .....	11
2.1.2 <i>Tides</i> .....	13
2.1.3 <i>Bathymetry and lake level</i> .....	13
2.2 GEOLOGY AND GEOMORPHOLOGY .....	15
2.3 HYDROLOGY .....	19
2.3.1 <i>Water balance: an overview</i> .....	21
2.3.2 <i>Summary: hydrogeologic data</i> .....	22
<b>3 METHODOLOGY</b> .....	23
3.1 WATER SAMPLING AND INSTRUMENTATION .....	23
3.1.1 <i>Analytical methods</i> .....	25
3.2 SEDIMENT SAMPLING AND INSTRUMENTATION .....	27
3.2.1 <i>Analytical methods</i> .....	28
<b>4 WATER GEOCHEMISTRY</b> .....	30
4.1 WATER CLASSIFICATION .....	30
4.2 GEOCHEMICAL PROCESSES .....	38
4.2.1 <i>Ionic relations</i> .....	38
4.2.2 <i>Processes affecting carbon content</i> .....	46
4.2.3 <i>Boron and boron isotopes</i> .....	53
4.3 SOME CONCLUSIONS .....	58
4.4 EVAPORATION PROCESS .....	60
<b>5 GEOCHEMICAL PROCESSES IN THE DEEP AREA</b> .....	66
5.1 THERMAL AND CHEMICAL STRATIFICATION .....	67
5.1.1 <i>Density Calculations</i> .....	71
5.1.2 <i>Silica: main process</i> .....	73
5.1.2 <i>Redox gradients and Reactions</i> .....	73
5.2 SULPHATE REDUCTION AND SULPHURE ISOTOPES .....	80
5.3 CONCLUSION .....	86
<b>6 SEDIMENTS</b> .....	88
6.1 CARBON DATING .....	90
<b>7 CONCLUSION</b> .....	93
<b>BIBLIOGRAPHY</b> .....	94



<b>ANNEX I</b>	I
TABLE I.1: Chemical-physical analyses carried out in-situ	I
TABLE I.2: Chemical analyses of sampled waters	IV
TABLE I.3: Analyses of nutrients and CO <sub>2</sub> content in waters	VIII
TABLE I.4: Isotopic analyses of the waters	XII
<b>ANNEX II</b>	XV
TABLE II.1: Chemical analyses of OC, TC, TIC, N and LOI in the superficial sediments	XV
TABLE II.2: <sup>13</sup> C and <sup>14</sup> C analyses of the organic carbon of the sediments	XVII

# 1 PROBLEMATICS AND RESEARCH OUTLINES

## 1.1 INTRODUCTION

The Massaciuccoli palustrine marsh is amongst the most important wetlands in Tuscany. It is a coastal lagoon of fresh to brackish water, which drains a total basin area of about 112 km<sup>2</sup>. The basin encloses the town of Viareggio as well as some villages (see Figure 1.1.1), namely: Quiesa, Bozzano, Massaciuccoli, Stiava, Montramito, Torre del Lago, Vecchiano and Migliarino, whose domestic effluents are disposed, mainly without treatments, directly in the lake or in its tributary streams. Sewages, wastewaters of reclamation lands and wastewaters of cattle-breeding and of a food-industry are the main polluting sources.

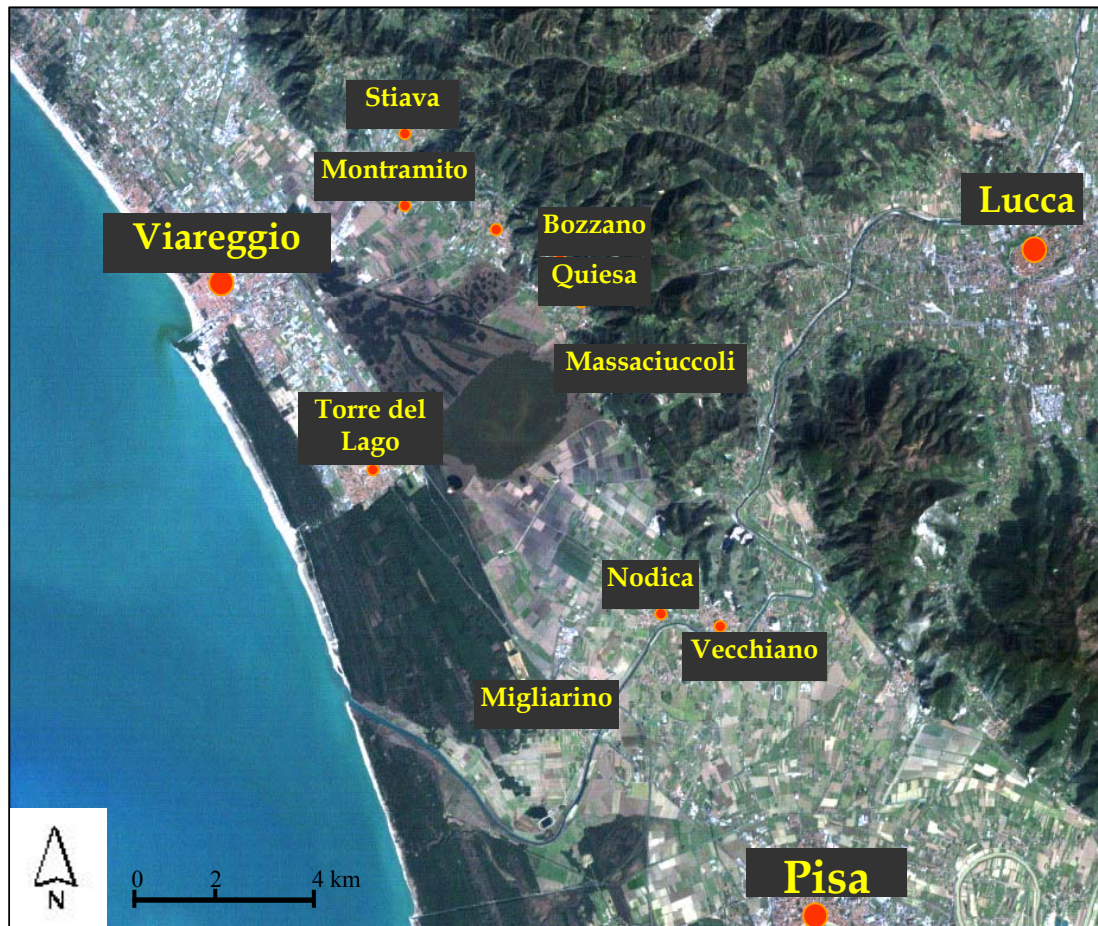


Figure 1.1.1 Localization of the studied area

Within the basin, there are two landfills and several agricultural farming activities.

As the majority of the plain is located under the sea level (from -1 to -3 m a.s.l.), there are some pumping stations constructed in order to force water from reclaimed land into the lake.

In the palustrine area, there are old quarries (30 m max depth and 2.5 km<sup>2</sup> total area) which have been left by the previous sand extraction activity.

The wetland opens to the sea by way of an artificial channel, known as Burlamacca, at the town of Viareggio, on the north. One kilometre before its mouth, there is an old sluice, named "Porte Vinciane", regulating the ingress of marine water. Burlamacca feeds the quarries before reaching the lake.

Eutrophic processes occur at this site as the hydraulic network has carried many nutrients. An artificial channels' network drains both rural and urban zones.

### **1.1.1 THE TRANSITION ECOSYSTEMS: THE COASTAL AREA**

According to the Convention on Wetland (Ramsar, Iran, 1971), wetlands are defined as "areas of marsh, fen, peatland or water, whether natural or artificial, permanent or temporary, with water that is static or flowing, brackish or salt, including areas of marine water the depth of which at low tide does not exceed six metres" (Article 1.1). In addition, the Ramsar Convention (Article 2.1) provides that wetlands "may incorporate riparian and coastal zones adjacent to the wetlands, and islands or bodies of marine water deeper than six metres at low tide lying within the wetlands". As a result, the Ramsar Convention may include not only freshwater resources such as rivers and lakes, but also coastal and shallow marine ecosystems, including artificial water bodies and underground water resources. They are often interconnected with other wetlands, and they frequently constitute rich and diverse transition zones between aquatic ecosystems and terrestrial ecosystems such as forests and grasslands.

As transition zones (or ecotones) between land and water, coastal wetlands are often rich in species diversity and provide critical habitats for migratory and nesting birds, spawning fish, and rare plants. However, various types of development and recreation continue to impact coastal wetlands and limit their capacities to perform important ecosystem functions. The importance of wetlands for performing various ecological services is well documented, and they have long been recognized as one of the most important ecosystems on Earth (Mitsch and Gosselink, 2000). Really, they are amongst the most productive ecosystems in the world, referred to as "biological reserve" because of the rich biodiversity they support. Wetlands are dynamic, complex habitats that depend on water to maintain their ecological functions. Wetlands are not only sites of exceptional biodiversity, they play also an important role in cleaning polluted waters, preventing floods, protecting shorelines and recharging groundwater aquifers. In fact, they commonly diminish the amount of suspended solids, nutrients and heavy metals from water that migrates through them (Gambrell, 1994; Cooke, 1994; Crites *et al.*, 1997). Therefore, they are sinks for various non-point source pollutants. Wetlands are also important as carbon sinks on a global scale.

In addition to their ecological importance, wetlands are indirectly responsible for considerable economic and social benefits, including maintenance of fisheries, provision of water supplies (maintenance of quality and quantity), support to agriculture, wildlife resources and timber production, providing energy resources (peat and plant matter), transport, supporting important recreational and tourism opportunities. Wetlands also contribute to climatic stability through their role in global water and carbon cycles.

### **1.1.2 ANTHROPOGENIC IMPACT ON THE HYDRODYNAMIC PATTERN AND ON THE ENVIRONMENTAL QUALITY OF THE BASIN**

Many of world's lakes and coastal wetlands have deteriorated due to exploitative use and improper management, causing irreparable damage to the existing ecosystems. Actually, wetlands are easily affected by external events, such as pesticides, fertilizers or other chemicals. Therefore, there is a serious national and international concern about the state and fate of these ecosystems, which have begun to be monitored and restored.

In the past 50 years, the rate of wetlands loss has increased dramatically and is still growing. Agriculture has been one of the main reasons for this (Table 1.1.2.1). It seems likely that more than half of the world's wetlands may have been destroyed during this century. In particular, in the Mediterranean areas, their reduction had begun since ancient time, but at slower rate than nowadays. During roman domain in Italy, for example, wetlands extended for 30000 km<sup>2</sup>, while they reduced to 13000 km<sup>2</sup> in the XX<sup>th</sup> century and 3000 km<sup>2</sup> in 1991 (Table 1.1.2.2). In Europe, people have a long tradition of farming the floodplains of many large river basins. Such practices were carried out in a consistent, regulated manner in keeping with seasonal water cycles and respecting natural resources. Each year, fodder and grazing rights would be decided and respected; fallow periods were common and extensive. Changing practices, however, have meant

a reduction (and loss) of such fallow periods, with increased agriculture and altered flood regimes by means of dams and canalisation projects. In the past few centuries, they have been commonly regarded as unproductive and unhealthy lands. Many countries have made considerable efforts to convert them from a "worthless" existence to economically viable systems for agriculture or fisheries production. Many have been filled with domestic and industrial wastes (some of which have been of a toxic nature), while others have been drained to create additional land for development.

**Table 1.1.2.1** Reasons of the wetland losses and degradation in Europe (from Hollis, 1992)

<b>Reasons</b>	<b>Diffusion</b>
Anthropogenic pressure (in particular the hunting)	35 %
Pollution	33 %
Agriculture	20 %
Urbanization	15 %
Water resource management	11 %
Abandon of traditional activity	11 %

Irrigation and waterlogging may also lead to salinization of soils and loss of productivity, as water near the surface evaporates and leaves behind a damaging residue of salt. Some 17% of the world's agricultural land is irrigated: some countries rely almost entirely on irrigation - Pakistan (77%) and Egypt (100%), for example. According to some estimates, waterlogging and salinization may be sterilising some 80 million to 110 million hectares of fertile soil worldwide (Ramsar Convection).

**Table 1.1.2.2** Loss of wetlands in Europe

<b>State</b>	<b>% of lost wetlands</b>	<b>References</b>
Italy	66 % from 1938 to 1984	ISTAT & ISMEA, 1992
Great Britain	50% since 1949	Baldock, 1984
France	67% since c.a. 1900	Min. de l'Environnement, 1993
Germany	57% since 1950 to 1985	OECD, 1989
The Netherlands	55% since 1950 to 1985	OECD, 1989
Spain	60% since 1948 to 1990	Casado <i>et al.</i> , 1992
Greece	63% since 1920 to 1991	Psilovikos, 1992
Danube delta	25%	Munteanu and Toniuc, 1992

## 1.2 OBJECT AND RESEARCH STRATEGY

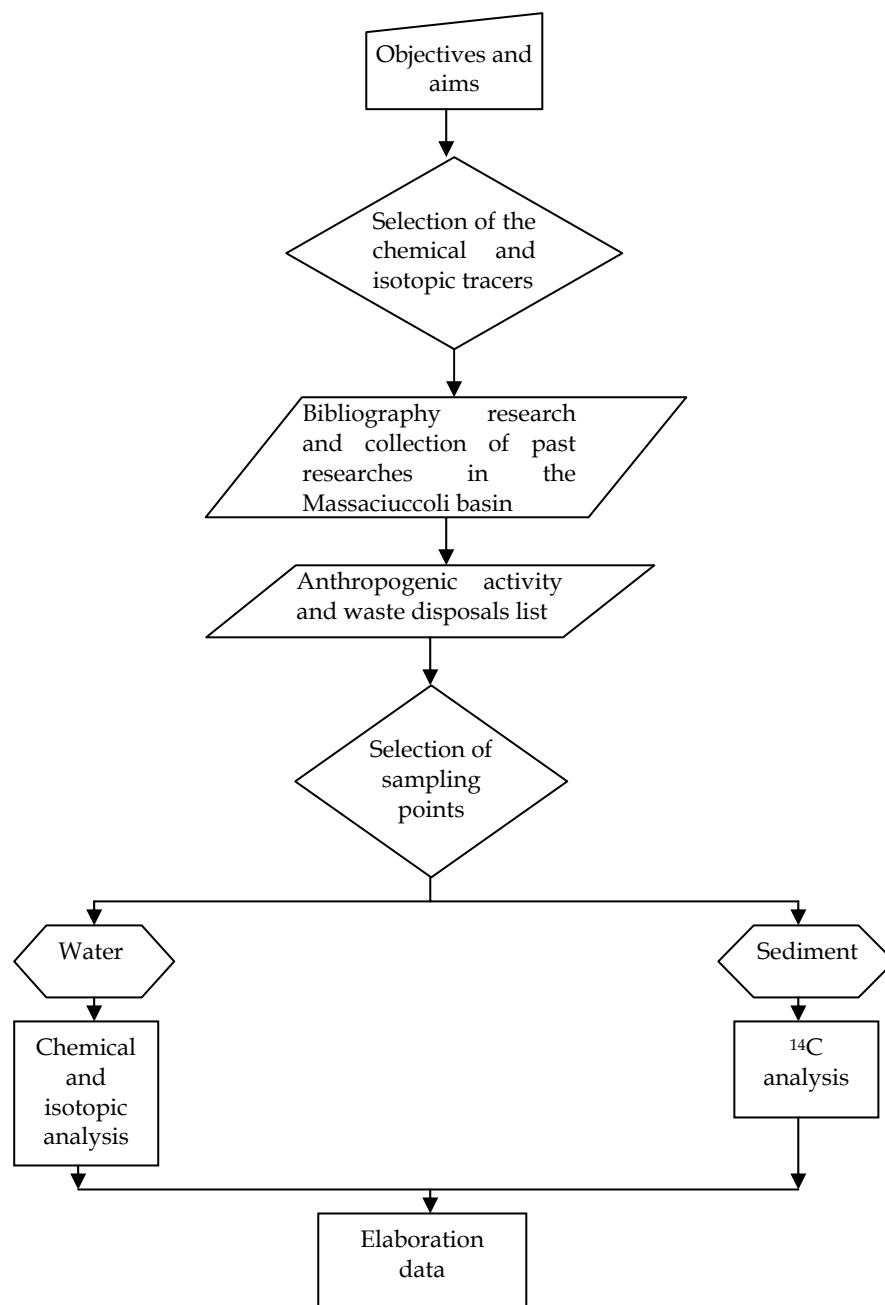
This research focuses on the spatial and temporal variability of the chemical composition of the Massaciuccoli lake. In order to gain a comprehensive overview of the environmental status in the basin, we attempt to study in depth the following items:

- 1) the anthropogenic impact on water chemistry
- 2) the seawater inflow, the groundwater infiltration and the evaporation rate
- 3) the role of the excavation area
- 4) the function of the biotic processes.

An analytical chemistry and geochemical modelling approach was taken to provide answers to these questions. In order, it has been applied:

- 1) geochemical elaborations and isotopic techniques ( $\delta^{11}\text{B}$  and  $\delta^{13}\text{C}$ )
- 2) chemical (Br, B, Cl and nutrients) and isotopic ( $\delta^{18}\text{O}$ ,  $\delta^{11}\text{B}$  and  $\delta^2\text{H}$ ) tracers
- 3) geochemical elaborations and isotopic tracers ( $\delta^{13}\text{C}$ ,  $\delta^{34}\text{S}_{\text{SO}_4}$  and  $\delta^{18}\text{O}_{\text{SO}_4}$ ).

The following flow diagram summarizes the research study.



Lake water samples were collected along depth profiles during the summer 2004 and surface water samples were collected at various locations within the lake. Inflowing stream and sewage effluent discharges were sampled to determine the role of stream and sewage inputs on lake chemistry. The lake and its inflows were sampled three times in 2004-2005 to observe temporal variations due to changing lake and inflow conditions. Quarries water samples were also collected along depth profiles.

## 2 RESEARCH AREA

The location of Massaciuccoli basin is given in Figure 2.1.

A description of the studied area, that aims to unravel the factors that determine the geochemical variability of the waters and sediments, should therefore address both the natural and human history of the territory. Geology is undoubtedly a key natural factor in basin formation and composition. With respect to human activities, the interest is in the local processes that led to the current landscape and water chemistry. Understanding the parent materials and human activities provides insight into the patterns of variation of the Massaciuccoli ecosystem.

This chapter gives an overview of both the geographical aspects and the human activities of the Massaciuccoli wetland.

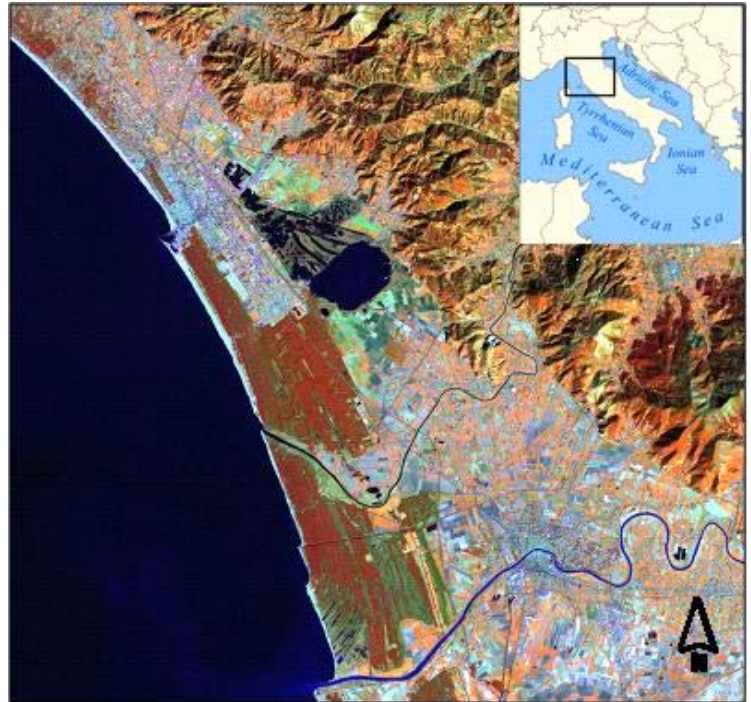


Figure 2.1 Localization map of the studied area

### 2.1 GEOGRAPHICAL SETTING

The studied area embraces the southern part of the Versilian plain and continues to SE with the Pisa plain. It is a coastal plain, delimited Eastward by the Apuane Alps and Massarosa-Pisa Mountains. Alluvial cones, built up in a multi-step process throughout Pleistocene and Holocene (Federici, 1987), connect plain and mountain areas. The marshy area with a thick peat layer comprises the Massaciuccoli lake (7 km<sup>2</sup>) and the palustrine area, referred as “Padule di Massaciuccoli” (13 km<sup>2</sup>) residue of a larger marsh which had been reclaimed and used for intensive cultivation (Pedreschi, 1956). The lake is approximately 10 km far from the town of Pisa, centred on N 43 49' 59.5' and E 10 19' 50.7'. It is approximately 2.5 km by 3.5 km in size and the maximum depth is 2.5 m. The lake is ring-shaped because of filling process and because of land reclaiming and draining, above all in the southern part of the area.

47% of the territory is located in the Massarosa municipality, 37% in the Vecchiano municipality, 13% in the Viareggio municipality and 4% in the Lucca municipality. The total population is 46697 of inhabitants (Allegretti *et al.*, 2002; Pagni *et al.*, 2004).

The lake system is thought to be no more than 20,000 years old, when it became isolated from the sea by the beach ridges' development. It is a typical coastal lake, although it is 4 km far from the sea due to the progressive progradation of the coastal plain favoured by sedimentary supply from the Serchio and Arno Rivers. The progradation of the Versilian plain occurred following consecutive continental and marine sediment deposition, within the evolution of a post-orogenic subsident tecto-sedimentary basin (Versilian basin), mostly submerged at the present (Federici, 1987). Moving from the sea toward the interior, there are the following structural and morphological units (Figure 2.1.1):

- the sand belt, ~~under~~ 3.5 m a.s.l. (D, S)
- the central plain occupied by the wetland (T)
- the piedmont belt ( $g_1$ ,  $g_2$ )

- the mountain chain in the western part, with Mount Ghirlandona (465 m a.s.l.) as the maximum altitude. It occupies one tenth of the territory (A)

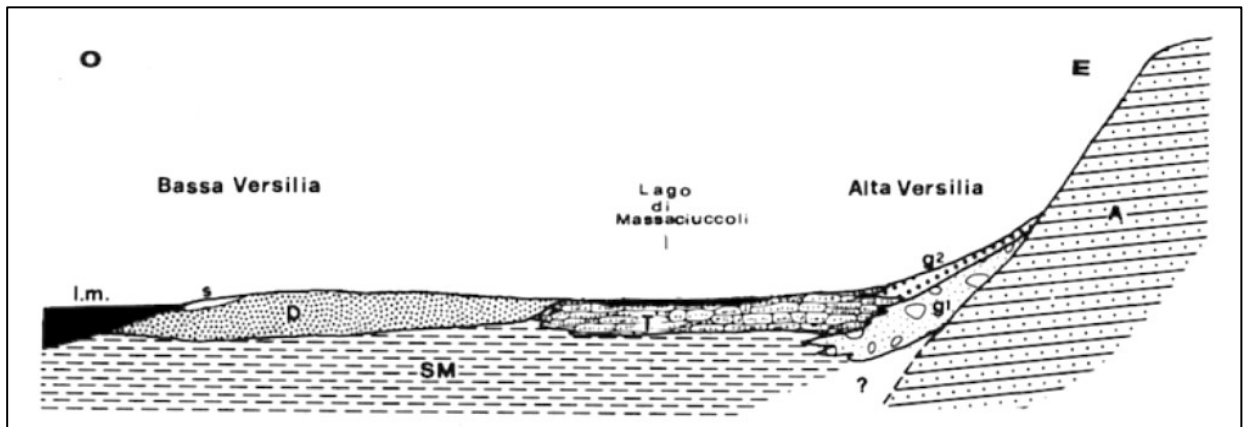


**Figure 2.1.1** Massaciuccoli Lake's territory. A= Apuane Alpes and Pisa-Massarosa mountains; g1=Pleistocene fan; g2= recent fan; T= peat soil; D= eolian sands' bars; S= marine sands; SM= Versilian sands (Federici, 1987 modified)

The Massaciuccoli marsh has been particularly impacted by the wastes from culture lands and the polluted runoff from sub-urban and agricultural areas. Additionally, there are an olive-refinery and two landfills, one of which has become recovered even if a heavy metal (Pb and Cr) contamination occurred (Geoser, 1995). Figure 2.1.2 shows the potentially pollution sources around the lake.

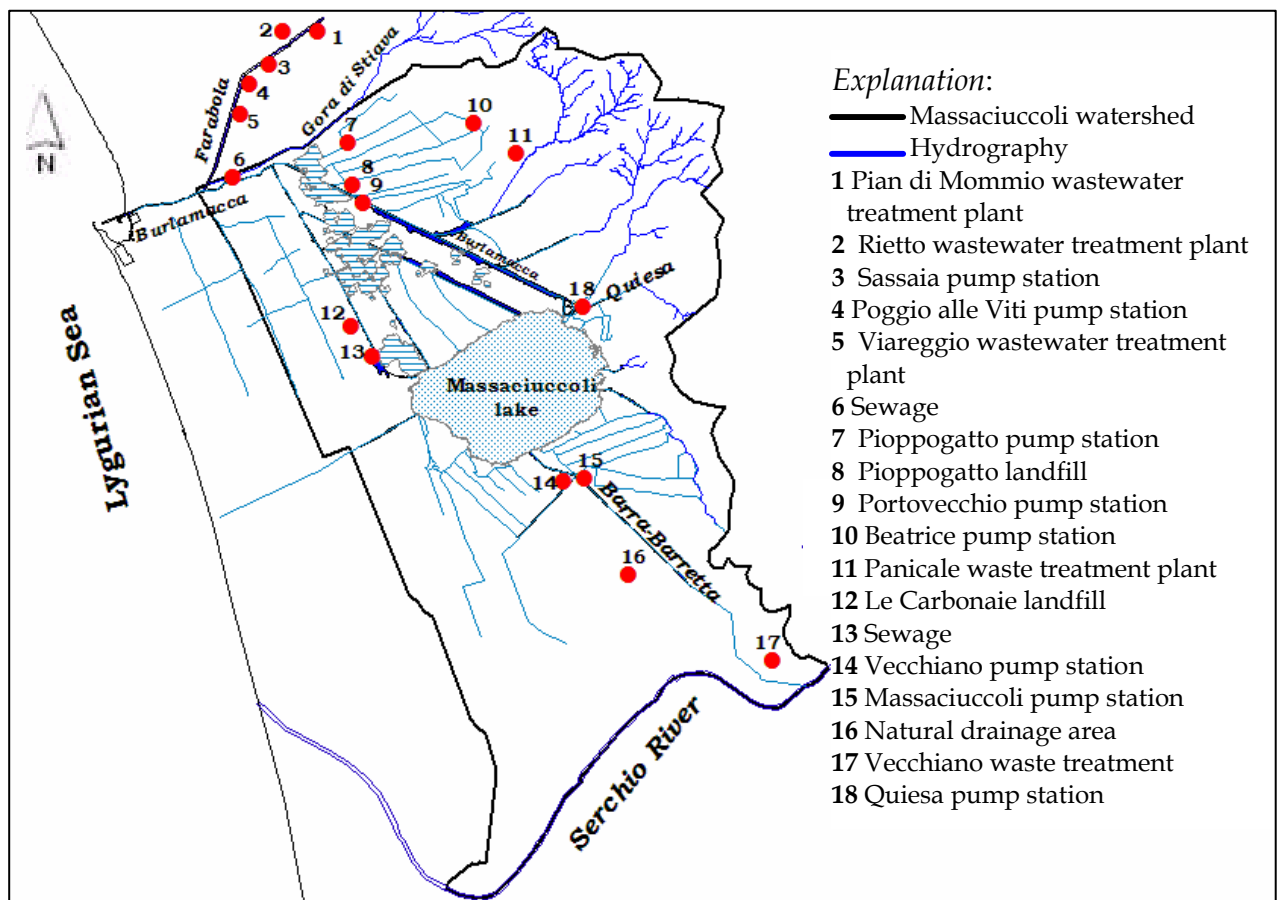


**Figure 2.1.2** Pollution sources in the Massaciuccoli area



Since the XIX century, the Massaciuccoli wetland has been affected by the extraction of peat first and siliceous sand afterwards. The excavation area, about 10 km<sup>2</sup>, is located NNW of the lake and it consists of several artificial lakes corresponding to the zones of siliceous sand withdrawal. In this zone, the peat level above the siliceous sand deposit was thinner (5-6 m thickness). Two air photos (Figure 2.1.3), taken in 1954 and 1993, underline the high impact of the excavation activity on the area. In the '70s, the extraction activity stopped but the quarries (30 m max depth) have never been recovered.

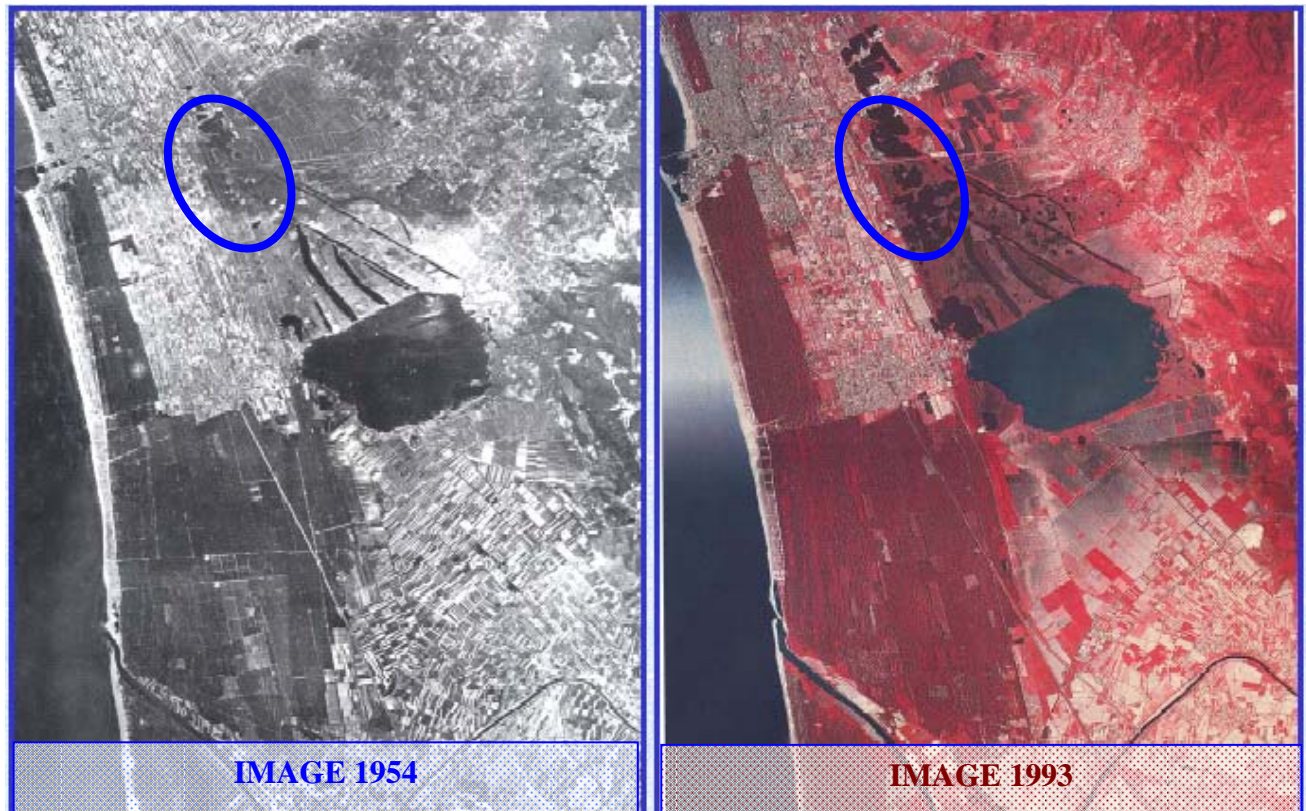


**Figure 2.1.3** Air photos of Massaciuccoli wetland. The circle underlines the excavation area in 1954 and 1993 respectively

The total area of the Massaciuccoli wetland is about 93.58 km<sup>2</sup> and 51% of it is devoted to agriculture (Figure 2.1.4). About 30.89 km<sup>2</sup> of agricultural areas are olive-plantations, vineyards and orchards (Regione Toscana, 2005). The main crops are corn, greens such as spinach and tomatoes, grain leguminous for fodder. Livestock is cattle. The economic role of agriculture is significant for the studied area, as 17% of the employment is in the agricultural sector (Tomei, 1972; Focardi, 1987; ISTAT, 2002; ISTAT, 2005; Forzieri, 2000).

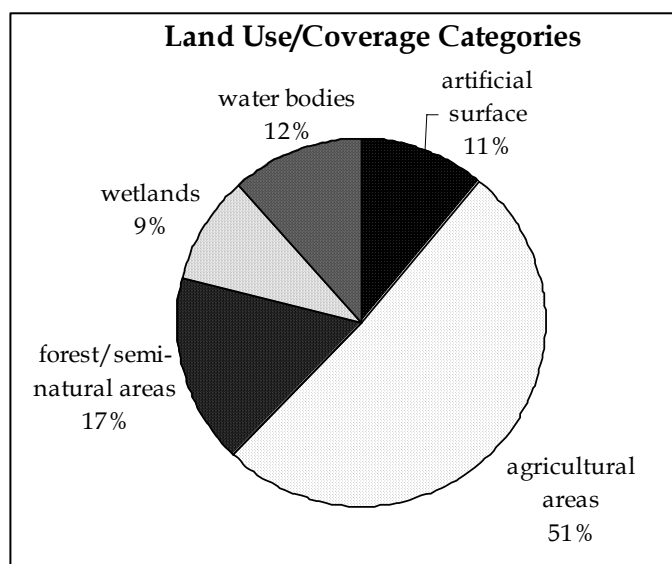


**Figure 2.1.4** The various land cover/use categories as a percentage of the total area

The Massaciuccoli ecosystem is a site of exceptional biodiversity, supporting high levels of endemic species and including significant numbers of at-risk species and plant communities, such as *Orchis palustris* (Del Prete and Tomei, 1980), *Utricularia australis*, *Hydrocotyle ranunculoides* and *Hibiscus palustris* (Tomei, 1983), the association *Sphagno-droseretum rotundifoliae* (Tomei *et al.* 1997; Tomei *et al.*, 1985; Rapetti *et al.*, 1986). There are three different environmental units: the foredune, the pinewood of *Pinus pinaster* and the marsh (Cavalli *et al.*, 1995; Garbari, 2003). The diverse habitat zones shelter slightly different fauna and flora, providing a great variety of microhabitats for plants and animals (Alessio *et al.*, 1992, 1995; Mori *et al.*, 1996; 1998). The Massaciuccoli wetland has been recognized as Special Area for Conservation (EU Habitats Directive) and Special Protection Area (EU Birds Directive) for *Botaurus stellaris* (Cenni, 1999). The growing nutrient concentration promotes algal blooms some of which are toxic, such as *Prymnesium Parvum* and *Microcystis aeruginosa* (Simoni, 1977; Simoni *et al.*, 1985; D'Errico *et al.*, 1994). Indeed, exotic species, such as *Procambarus clarkii* (Girard, 1832) bother macrophyte populations.

### 2.1.1 Climate

According to the climatic classification of Köppen the climate symbol of the studied area is 'Csa', that is Mediterranean climate with dry summers and mild winters (Köppen, 1936; McKnight and Hess, 2000); while according to Thornthwaite it can be classified as Mesothermic climate (Thornthwaite, 1948; Thornthwaite and Mather, 1957; Vittorini, 1972; Rapetti *et al.*, 1986).

The average temperature is around 15.5°C, ranging from 7°C in winter to 22°C in summer. The only thermometric sensor within the studied area is in the Viareggio weather station (UTM: E 602495; N 4858869) until 2002 (Servizio Idrologico Regionale of Pisa). The graphic of Figure 2.1.1.1, referring to the monthly average values between 1980 and 2002, shows that January and December present the lowest annual temperatures, while July has the highest one.

Insolation data are collected only in Pisa by the "Servizio Meteorologico dell'Aeronautica Militare" (Rapetti, 2003). The mean annual solar insolation is 2349 hours, with a minimum value of 94 hours in December and a maximum of 324 hours in July (Rapetti, 2003). The mean annual solar radiation is 283 cal/cm<sup>2</sup>/day, with minimum and maximum of 470 and 96 cal/cm<sup>2</sup>/day, in December and July respectively (Rapetti, 2003).

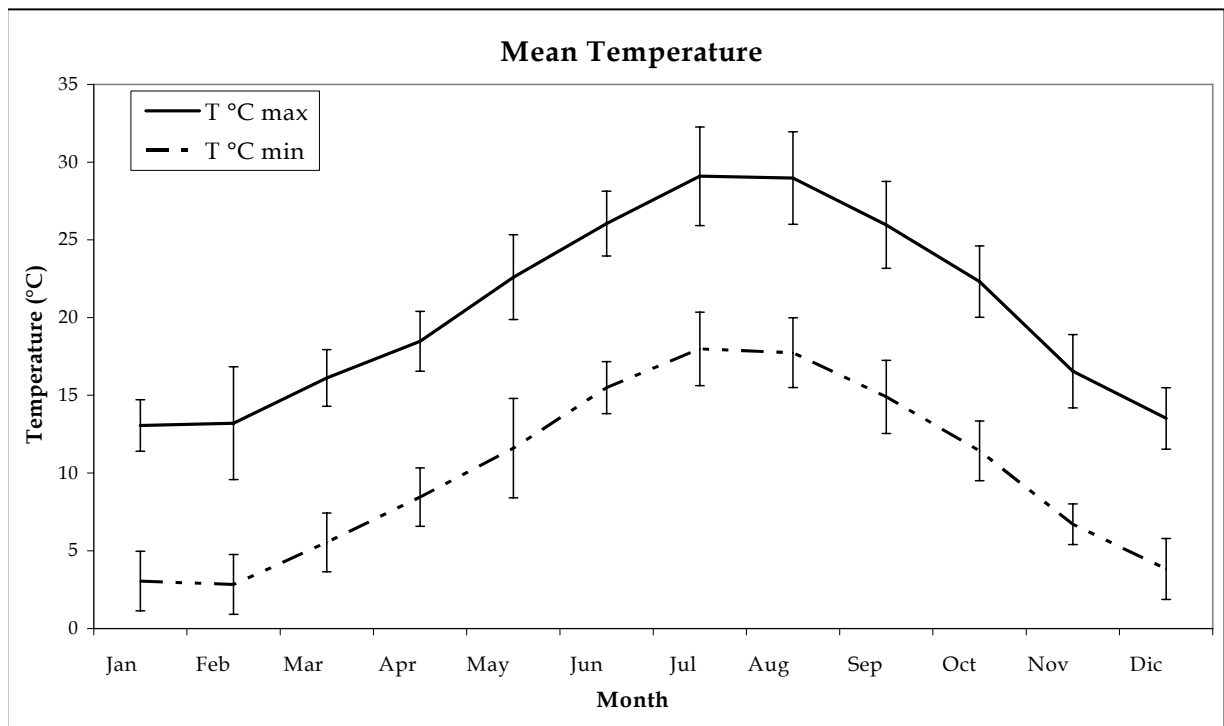


**Figure 2.1.1.1** Temperature record registered at the Viareggio station from 1980 to 2002. Standard deviation for each month is reported

There is no meteorological station for air humidity within the basin. Humidity values in Pisa range from 88% in winter to 61% in summer period.

The wet winter/dry summer seasonality of precipitation is typical of Mediterranean climate. Total annual rainfall is about 900 mm and is intense during fall and winter periods. Orographic precipitation, reaching values of 2000 mm (M. Ghirlandona), occurs on the Oltre Serchio and Massarosa mountain belt, that is aligned NW-to-SE and oriented across a prevailing wind from the sea. The Bagnoulds-Gausson diagram (Figure 2.1.1.2), relating temperature with precipitation, emphasizes an aridity period during the summer months.

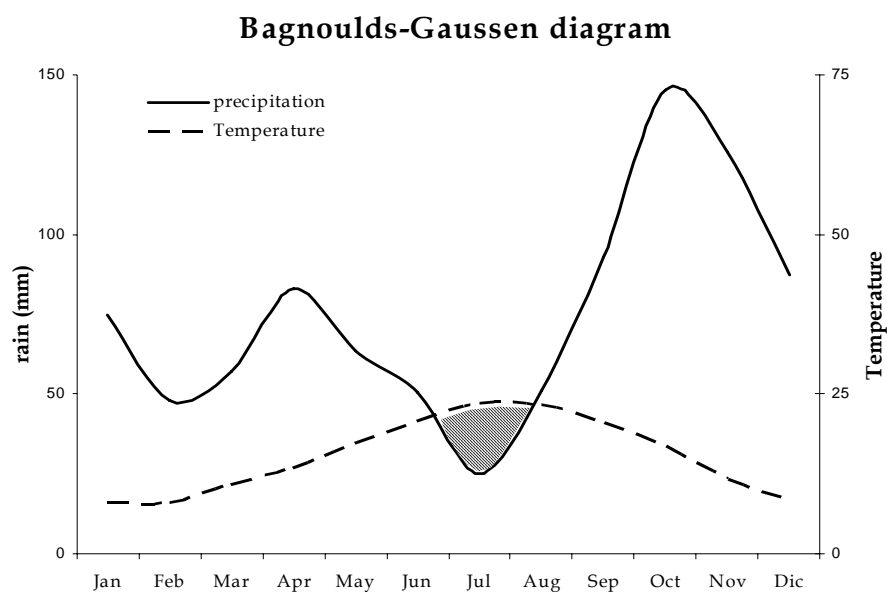


**Figure 2.1.1.2** Bagnoulds-Gausson diagram, relating temperature with precipitation from 1980 to 2002 in Viareggio

The main winds are from NNW, so they can prevent the discharge of water from the lake.

### 2.1.2 Tides

Tides influence the Massaciuccoli lake through the Burlamacca channel, preventing water discharge and affecting salinization of palustrine area. The tides in the Burlamacca channel are mixed with semidiurnal (two high waters and two low waters of each tidal day approximately equal in height, each 12h 30') dominance and diurnal spring tide. The mean tidal amplitudes in Livorno range from 14 cm during neap tides to 50 cm during spring tides (Istituto Idrografico della Marina). A tidal monitoring is located before the Porte Vinciane cataract. The diagram 2.1.2.1 describes the tidal flow measured at Livorno and at the Porte Vinciane. The semidiurnal cycle is evident.

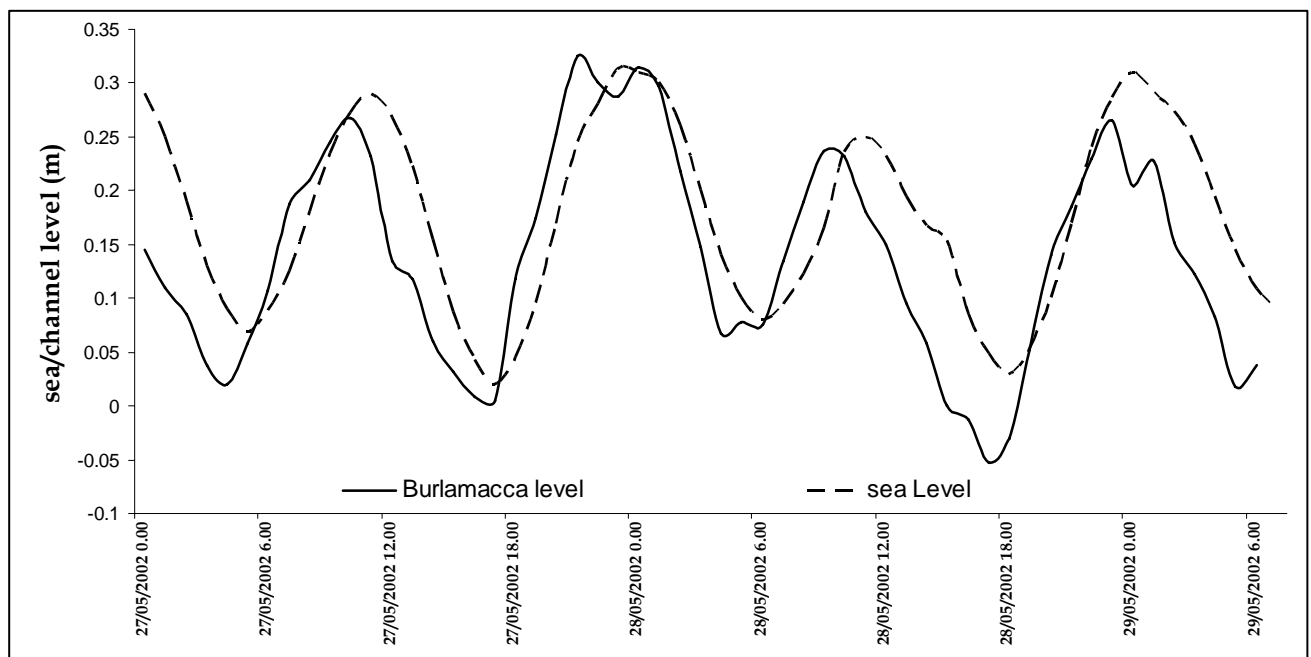


**Figura 2.1.2.1** Tides in Burlamacca channel and in Livorno

### 2.1.3 Bathymetry and lake level

The bathymetric survey, performed in 2003 by IGG-CNR and Southampton University, showed the lake to be extremely flat and shallow (Figure 2.1.3.1). The average depth is 2 m, though isolated depressions are evident on the western side (about -10 m a.s.l.) and along the southern margin of the lake (about -6 m). The lake is shallowest in the east (1 m) and shows a gentle gradient to the west where depths are 2 m on average (Amos *et al.*, 2004; Pedreschi, 1956; AQUATER, 1980; Duchi *et al.*, 1990).

The lake level long-term trend underlines that the lake level remains under sea level from April to September; the minimum value of -0.64 m was reached on August-September 1962 (Regione Toscana, 1973). The mean level lake during the 2001-2006 period is illustrated in Figure 2.1.3.2. The lake level has reached the lowest level of -0.5 m on September 2003, at the end of a very dry and hot summer.

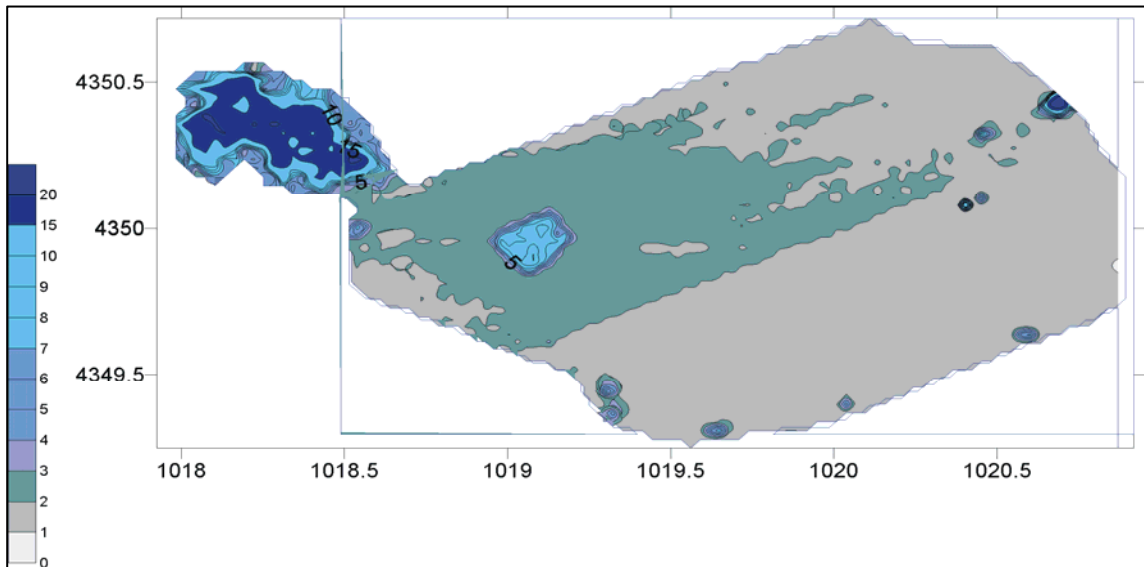


**Figure 2.1.3.1** Bathymetry of Massaciuccoli lake and Sisa quarry

The lake level follows very well the precipitation and the pumping station discharge. Therefore, the meteorological conditions of the area are the most important variables conditioning the water balance of the lake.

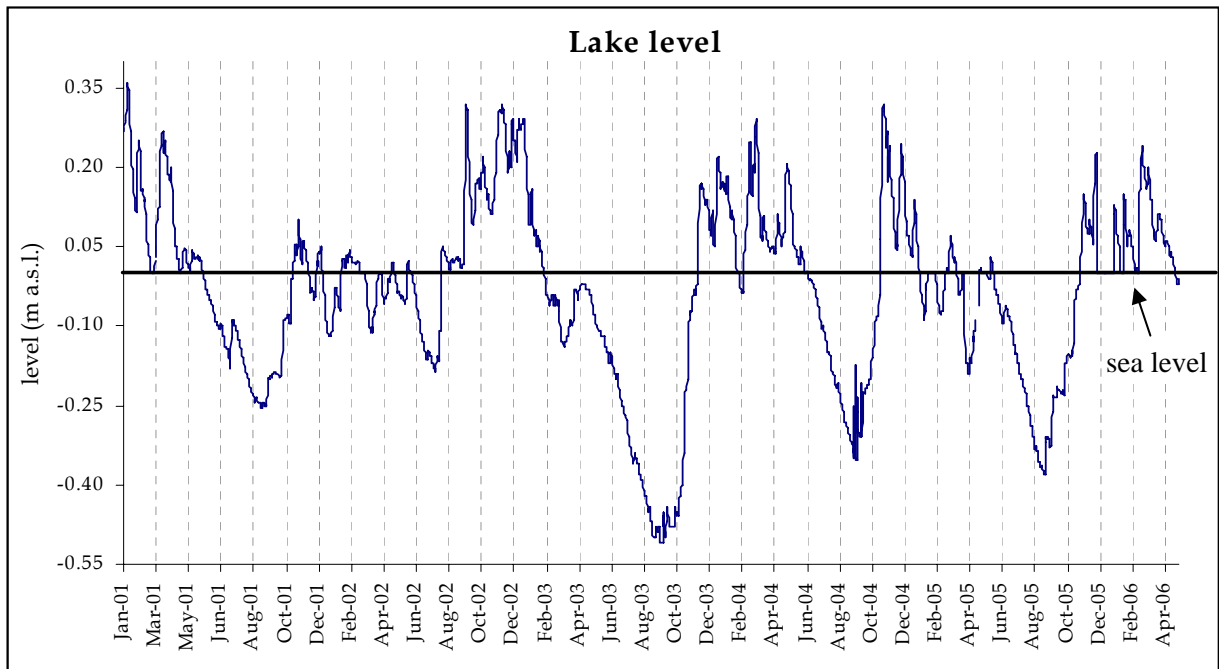


**Figure 2.1.3.2** Lake level variation measured at Torre del Lago

## 2.2 GEOLOGY AND GEOMORPHOLOGY

The Pisa-Versilian coastal plain has been thoroughly studied since many decades. Investigations on regional geology and geomorphology were carried out by Giannini (1950), Blanc *et al.* (1953), Romagnoli (1957), Giannini and Nardi (1965), Ghelardoni *et al.* (1968), Mazzanti and Pasquinucci (1983), Della Rocca *et al.* (1987), Federici (1987), Mazzanti *et al.* (1983), Baldacci *et al.* (1993) and Pascucci (2005).

Contemporary stratigraphy and paleoclimatic reconstruction has been attempted by Pantanelli (1905), Blanc *et al.* (1953), Marchetti (1943), Federici (1983, 1993), Bianciardi (1999), Antonioli *et al.* (2000) and Gulia *et al.* (2004).

### Mountain belt

The Northern Apennine (Figure 2.2.1) is a fold-thrust chain, formed during the Tertiary because of the interaction between various microplates in the Eurasia-Africa collision belt (Carmignani *et al.*, 2001; Vai and Martini, 2001). The Neogene-Quaternary basins of Northern Tuscany are mainly interpreted as graben or half-graben (Ghelardoni *et al.*, 1968), related to a post-collision extensional tectonics which began in late Miocene and still causes a subsidence motion (Patacca *et al.*, 1990; Bossio *et al.*, 1993; Carmignani *et al.*, 1994; Pascucci, 2005). These basins are separated by structural highs made up of allocthonous units of Mesozoic to Paleogene age, belonging to the Ligurian, Subligurian and Tuscan Domains, that were overthrust mostly in Early Miocene times (Baldacci *et al.*, 1967; Carmignani and Kligfield, 1990; Vai and Martini, 2001; Cantini *et al.*, 2001). The basins are segmented by transverse, NE-SW lineaments (Vai and Martini, 2001).

The outcropping substrate of the mountain belt is represented by the following nappe-units from the top (Giovannini, 1993; Nolledi *et al.*, 2003):

- Late Cretaceous-Eocene Ligurid and Subligurid Units made up of argillites and limestones

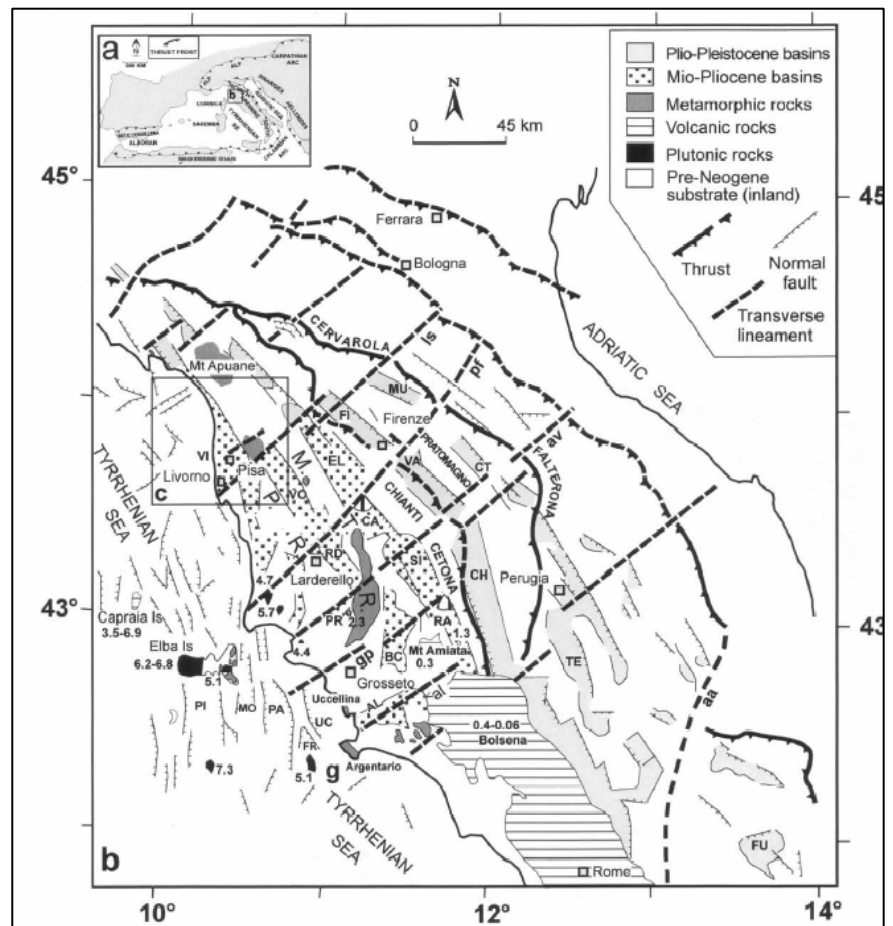


**Figure 2.2.1** Generalized structural maps: **a** Schematic map showing the mountain chains of the Mediterranean region and geologic subdivision of the Apennines; **b** Neogene-Quaternary basins of the Northern Apennines (Basins: AL: Albegna, BC: Baccinello; CA: Casina; CH: Chiana; CT: Casentino; EL: Elsa; FI: Firenze; FR: Formiche; FU: Fucino; MO: Montecristo; MU: Mugello; PA: Punta Ala; PI: Pianosa; RA: Radicofani; RD: Radicondoli; SI: Siena; TE: Tiberino; UC: Uccellina; VA: Valdarno; VI: Viareggio; VO: Volterra; Transverse lineaments: aa: Olevano-Antrodoco, al: Albegna; av: Albia-Marecchia; gp: Grosseto-Pienza; ls: Livorno-Sillaro; pf: Piombino-Faenza; MTR: Middle Tuscany Ridge; PR: Perityrrhenian Ridge; 3.5 radiometric age of igneous rocks in Ma. (from Pascucci, 2005)

- Tuscan Nappe subdivided in Upper Triassic –Lower Cretaceous carbonates (Calcare cavernoso), Late Cretaceous–Eocene argillite (Scaglia Formation), and Upper Oligocene–Lower Miocene turbiditic sandstone (Macigno Formation)
- Metamorphic units consisting of Upper Triassic siliciclastic metasediments (Verrucano Formation), anhydrites and dolomites followed by a metamorphosed sedimentary succession equivalent to the Tuscan Nappe succession.

The Macigno formation is the main unit of the mountains in the Massarosa area (Giannini and Nardi, 1965). The Bastione mountain is characterized by the geologic unit of the “Tuscan Nappe” (Trevisan *et al.*, 1968). The Scaglia formation, Diaspri and Maiolica crop out between Quiesa, Bozzano and Chiatri (Figure 2.2.2).

#### The coastal plain

The Versilian Basin is oriented NW-SE and bordered by the Mts Pisani to the NE, by the Meloria-Maestra shoal to the SW, and by the Mts Livornesi to the SE (Bossio *et al.*, 1993; Della Rocca *et al.*, 1987). Toward the north it closes offshore of Carrara Marina and is limited by the Apuane Alps. The Viareggio Basin has a well-developed offshore portion, actually covered by continental Quaternary deposits mainly related to the evolution of the Arno and Serchio rivers (Federici and Mazzanti, 1988; Aguzzi *et al.*, 2005), and an inshore part. The basin is filled by up to 2500 meters of upper Miocene Serravalian-early Tortonian-Present deposits (Foresi *et al.*, 1997), mainly composed of alternate sands and clays, resting unconformably on the Oligocene-early Miocene Macigno sandstone, the uppermost part of the Tuscan Unit. Since Pleistocene, tectonic phases and eustatic variations of sea level have determined an alternation of continental sediments (gravels, sands and silts) and marine deposits (mainly sands). Post-Versilian sandy beach ridge systems, separated by low-energy water bodies («*lame*» auctorum, Federici, 1993), started to be built up since 3000±4000 years.

In the coastal belt the eolian sands crop out and become silty in the eastern sector. The overlying peat deposit occupies most of the plain with thickness increasing from 1 m in Torre del Lago to 8 m near Massaciucoli (Villa Ginori drilling) and exceeding 10 m towards Massarosa. The peat contains a lot of water and it can be classified as temperate eutrophic peat (Federici, 1987). It originated peat soil classified as histosol (Sartori and Levi-Minzi, 1985).

The coastal Pisa and Viareggio plains also include a sequence of quaternary alluvial and lacustrine deposits. Federici and Mazzanti (1995) and Federici (1987, 1993) give an overview of the lithostratigraphy of the Versilian plain, recognizing the following lithostratigraphic units from the top to the bottom:

- peat layers and current alluvial deposits, sandy-clayey deposits sometime with gravel
- clay and lacustrine peat related to the 3<sup>rd</sup> cold period (Wurm III) and to the successive post-glacial period
- eolian and marine sand with *Purpura haemastoma*, attributed to the Versilian transgression. These deposits pinch-out in the piedmont belts. <sup>14</sup>C dating of shells, found out at -26 m and -15 m, yields an age of 5646±200 and 8940±273 years respectively (Ferrara *et al.*, 1959, 1961). Peat blocks had been found within these deposits (Blanc, 1934; Marchetti and Tongiorgi, 1936)
- lacustrine clay interstratified with peat, belonging to 2<sup>nd</sup> cold period (Wurm II) of the last glaciation
- marine sand, belonging to the 1<sup>st</sup> warm period between the Wurm I and Wurm II
- continental clay with some sand, corresponding to the Wurm I
- continental gravel and pre-wurmian clay, present under 150 - 130 m depth.





Federici (1993) reconstructed the climatic evolution of the Versilian plain since the Pleistocene period, considering the lithological and chronological data available (Ferrara *et al.*, 1957, 1961; Federici, 1987; Alessio *et al.*, 1964; Broeker *et al.*, 1956). In the 1998, ENEA carried out a continuous core to 90 m depth at SE of the lake for a chronological and paleo-environmental interpretation of the marine holocenic transgression, based on several  $^{14}\text{C}$  and U/Th dates (Antonioli *et al.*, 2000). The first 75 cm are topsoil; clay and peat is present from -75 cm to -7 m.  $^{14}\text{C}$  dating on superficial peat gives ages of  $2327\pm 52$  years BP at -1 m of depth, and  $2716\pm 37$  years BP at -2.1 m. These peat levels denote high compaction values, which reflected the soil drop due both to a natural processes and anthropogenic influence (Auterio *et al.*, 1978; Antonioli *et al.*, 2000). Dating of a wood fragment at 3 m depth give an age of  $4490\pm 90$  years BP (Bianciardi, 1999; Grassi *et al.*, 2000).

## 2.3 HYDROLOGY

The 119-km<sup>2</sup>-large drainage basin (including the lake area) represents a complex hydrological landscape, consisting of 35 km<sup>2</sup> of naturally drained mountain area and 84 km<sup>2</sup> of coastal plain (Giovannini, 1993). Since the Gora di Stiava and Farabola streams drain a further area of 22km<sup>2</sup>, the actual Massaciuccoli catchment extends over 97 km<sup>2</sup>, of which 7 km<sup>2</sup> are occupied by sand dunes discharging to the sea through the basement. As in the mountain belt marly and clayey terrains prevail, only 25% of the rains infiltrate (Giovannini, 1993).

The hydrography (Figure 2.3.1) is poorly developed and the lack of great tributaries is due to both the little extent of the lake itself and the basin geomorphology (Pedreschi, 1956; Mazzanti and Trevisan, 1978; Mazzanti, 1983; Della Rocca *et al.*, 1987; Federici and Mazzanti, 1988). Besides, a remarkable network of ditches and channels, parallel to the coast line, complicates the hydrographic system and conveys waters to the lake. Owing to the presence of lands situated under the sea level (-3.5 m a.s.l.), a great reclamation work was carried out (Pedreschi, 1956; Melis, 1969).

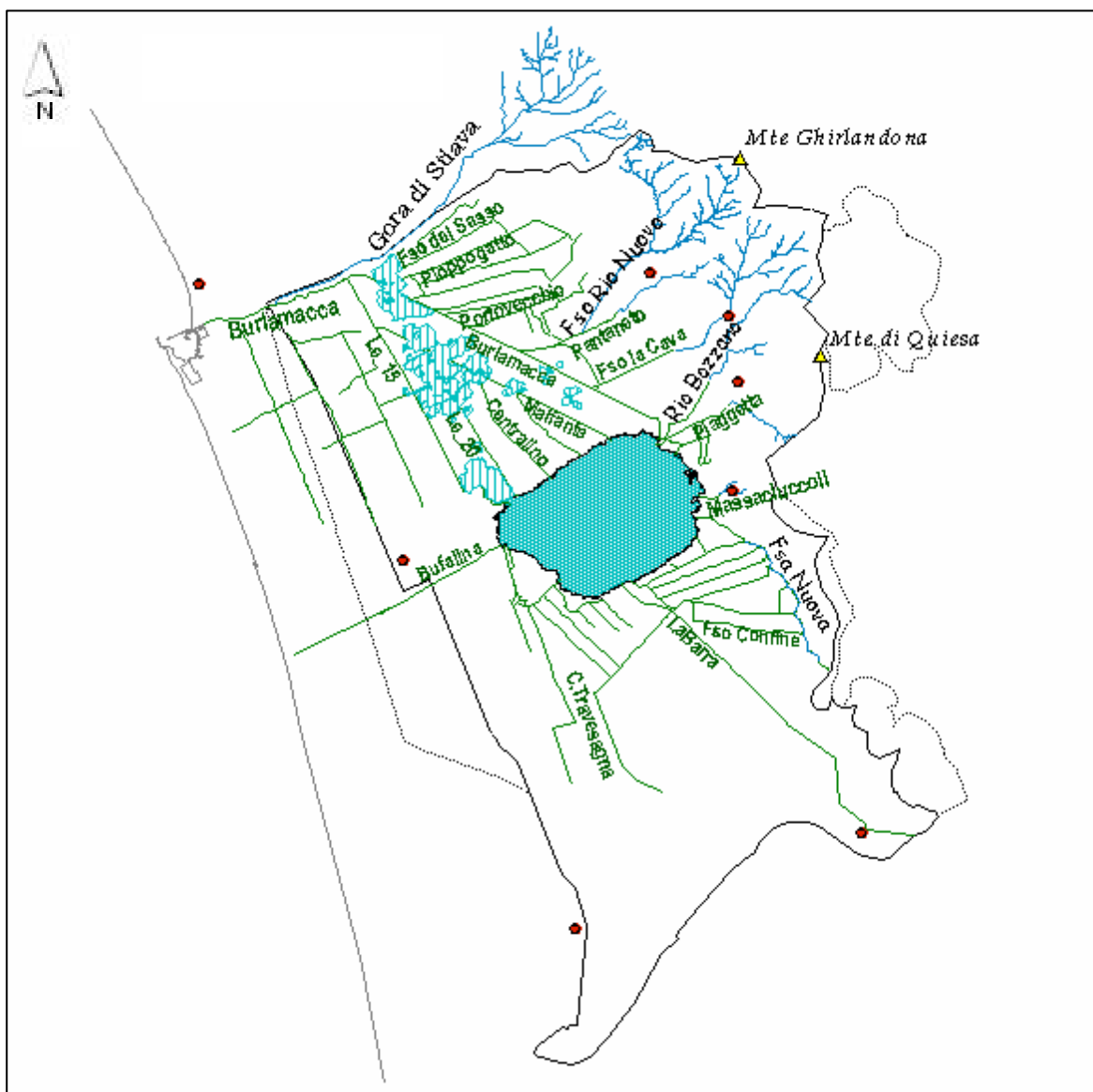


Figure 2.3.1 Hydrographic pattern

At present, the Burlamacca channel represents the main outlet discharging waters from the lake, but occasionally a flux of marine water occurs close to its bottom towards the lake (Spandre, 1975; Meriggi, 1995; Baneschi, 2003; Frediani, 2003).

Natural and artificial tributaries feed directly the lake. They are:

- the Barra channel that receives water from two pumping stations, Vecchiano and Massaciuccoli. It drains all the southern agriculture and industrial basin. It has been believed the main cause of the organic pollution and suspended matter loading lake waters
- Fossa Nuova
- Quiesa channel, which is fed by groundwater and the Villa Spinola spring.

Some other streams, flowing from the mountain belt, do not feed directly the lake, but flow into the Burlamacca channel (Dalle Mura, n.p.; Giovannini, 1993).

The general hydrogeologic pattern hypothesized for the basin (Nolledi *et al.*, 2003) consists of two aquifers confined between three aquicludes, according to the following succession:

- basal aquiclude, corresponding to the impermeable or slightly permeable "Verrucano" formations
- inferior aquifer, formed by the "Calcare Cavernoso" and "Calcare Selcifero" formations
- intermediate aquiclude, represented by the "Diaspri" siliceous-marly level
- superior aquifer, hosted into the "Maiolica" limestone
- top aquiclude, including all the formations above the "Maiolica", from the "Scaglia Rossa" to the "Alberese".

As far as it is the plain concerned, the hydrogeological scheme is simple, since it is linked with the distribution of eolian and marine sands, which represent the phreatic aquifer. The succession is described below, from the top to the bottom:

- little permeable deposits, made up of silts or silty-clays with intercalations of peats and clays
- marine and eolian sands
- silty-clayey impermeable formations.

In the piedmont areas near Massaciuccoli, an artesian aquifer is present (Nolledi *et al.*, 2003).

Over sixty springs are known to be present in the area (Chines and Nolledi, 1982), chiefly in the mountain belt. The four main springs originate by deep circulation and have a large recharge basin along the Apuane boundary. They are:

- **Montramito** springs, whose waters flow into the "Maiolica" limestone (superior aquifer) as suggested by the Ca-HCO<sub>3</sub> composition, while the waters percolating towards the inferior aquifer acquire a Ca-sulphate composition, owing to interaction with the Calcare Cavernoso formation. The main spring discharges on average 65.6 l/sec
- **Stiava** springs, originated by faults connecting the inferior limestone aquifer with the surface. The chemical composition is Ca-sulphate
- **Villa Spinola** spring, classified as an "overflow" spring with an average discharge of 165 l/sec, is located near Quiesa at 60 m a.s.l. It has a Ca-sulphate chemical composition (Masini, 1958) and the same anions and cations percentages of the Stiava springs. Isotopic data (Nolledi, 2003) suggest a complex recharge pattern. Owing to both its localization with respect to the lake and the availability of chemical data, these data were included in the analytical database in order to understand the possible influence of waters of this hydrochemical facies on lake geochemistry
- **Bozzano** spring, named as "**II Fontanone**", collects water from the carbonate aquifer hosted into the "Maiolica" and calcarenite formations.

Along the southern piedmont margin, in correspondence to the boundary between the alluvial plain and the carbonate formations, there are some other springs such as Case Rosse and "Il Paduletto", which are of Ca-HCO<sub>3</sub> type. There is also a thermomineral spring known as "Acque Rugginose".

### 2.3.1 Water balance: an overview

The hydrogeologic watershed is assumed to correspond with the drainage basin, even if underground exchanges are possible particularly along the piedmont belt, where carbonate formations are present.

The lake contains 14 Mm<sup>3</sup> of water in hydrostatic equilibrium with the superior aquifer. Strong raining events make the groundwater to discharge directly in the sea possible, allowing the groundwater to flood into the urbanization areas.

The Massaciuccoli basin can be divided into two sectors (Duchi *et al.*, 1990; Franceschi, 1992), where some sub-basins are individuated, corresponding to the reclamation zones with respective pumping stations.

1. Southern sector, between the lake and the Serchio river, includes:

- 6.5 km<sup>2</sup> of naturally-drained lands
- 14.4 km<sup>2</sup> of palustrine-wooded lands
- 16.7 km<sup>2</sup>, belonging to Vecchiano sub-basin and mechanically drained
- 5.2 km<sup>2</sup> constituting the Massaciuccoli sub-basin.

2. The northern sector, from the Apuane Alps to both the sea (at SW) and the lake (at SE), is divided into six sub-basins, mechanically drained, of which three belong to the Massaciuccoli basin:

- Massarosa
- Portovecchio
- Quiesa.

In addition to meteoric waters, whose summer effect is cancelled out by the evapotranspiration processes (AQUATER, 1980; Spandre, 1975), the Massaciuccoli basin receives run-off and groundwater recharge. As previously mentioned, the mountains around the plain feed the phreatic aquifer. Besides, in the southern sector, limited by the artificial right bank of the Serchio river, underground flows exist on NS direction and vice versa. In general, the Serchio river drains the aquifer with limited, sporadic inversions (Ghezzi, 1994).

The piedmont recharging area includes six districts:

- a) Camaiore valley
- b) "Piano di Conca" and "Conca di Stiava" areas
- c) Montramito
- d) Conca di Massarosa
- e) Bozzano-Quiesa zone
- f) Massaciuccoli - Case Rosse pedemontan belt.

In the middle part of the plain, where the Massaciuccoli lake and its drainage network are found, the superficial waters are in equilibrium with groundwaters, influenced and/or maintained by the draining effect of pumping stations. In fact, the phreatic system converges towards the piezometric lows, located in correspondence with the pumping stations. Isophreatic lines trend underlines the presence of an internal low zone under sea level, aligned in the direction Massaciuccoli lake - Montramito and culminating in a minimum (-2 m a.s.l.) at Pian del Quercione. The piezometric minimum corresponds not only with the pumping station but also with a morphological depression, where stagnant waters and peat deposits had existed for long a time. Successively, the hydraulic reclamation stressed the morphological low by the compactation caused by peat, with an average value of 3 m during the last 65 years (Auterio *et al.*, 1978). The highest phreatic values (2 m a.s.l.) are near Nodica along the mountain belt (Simoni *et al.*, 1999). In the west, the aquifer flow to the sea, but near the coast the coastal dune hinders the water discharge. In fact, at "Migliarino Macchia" the aquifer becomes a dunal 20 m-thick aquifer (AQUATER, 1980; Nollodi *et al.*, 2003), directly fed by precipitations. This high piezometric value works as a barrier for the marine ingression. The SEV (vertical electrical soundings and/or resistivity profiles) survey on the coast (Marchisio and d'Onofrio, 1997) underlines that the salt-water wedge stops at 1 km from the shoreline due to the presence of a clay level at -15/-20 m a.s.l.. Nevertheless, some piezometers and

wells along the “Le Quindici” channel have high conductivity values. Some authors (Geotecneco, 1975; Aquater, 1980) hypothesized the presence of fossil waters with high salinity in the palustrine area. However, recent studies (Meriggi, 1995; Baneschi, 2003; Frediani, 2003; Autorità di bacino del Serchio, 2005) recognized the presence of marine waters infiltrating near the bottom of the Burlamacca channel and stratified in the quarries, particularly in S. Rocchino quarry. Spandre (1975) supports the diffusion of marine waters through the sand aquifer toward the area around the lake. The channels in the northern palustrine zone are considered to be in hydraulic equilibrium with the lake (Giovannini, 1993), but water exchange is influenced by the periodic inflow of marine waters from the Burlamacca channel, in particular during the summer period. Unfortunately, it is not possible to compute the water balance for Massaciuccoli basin owing to lack of information concerning groundwater inflow and outflow, as well inflow from the sea. Some authors had attempted to calculate this water balance obtaining differing results:

- ⇒ 56 Mm<sup>3</sup>/year (Regione Toscana, 1973)
- ⇒ 41.6 Mm<sup>3</sup>/year (Spandre, 1975)
- ⇒ 43-45 Mm<sup>3</sup>/year (AIC Progetti, 1982)
- ⇒ 47.8 Mm<sup>3</sup>/year (Duchi *et al.*, 1990)

The Burlamacca flow is estimated to have an average value of 1.22 according to Spandre (1975) and Regione Toscana (1973), and 1.38 m<sup>3</sup>/s according to AIC Progetti (1982).

### 2.3.2 Summary: hydrogeology data

This section described the geological and hydrological setting of the studied area and it introduced the environmental problems. It has come out that Massaciuccoli ecosystem is extremely complex due to the presence of water inflows with an unknown flow and many pollution sources (point and non-point) for the different land-uses and the urbanization processes, other than exploitation of the wetland resources.

The information about the discharge of springs and groundwater in the lake are inaccurate and the lack of measures about inflows makes mass balance estimation impossible.

However, in the following sections chemical and isotopic techniques are applied in order to identify and to characterize the different water types and pollutant inflows in the lake. Considering these aims, the hydrological characteristic of the area and the inflow taken into account on this study are summarized in the table 2.3.2.1.

**Table 2.3.2.1** Hydrogeologic data

Parameter	Extention	Inflow/outflow
Hydrologic basin	114 km <sup>2</sup> *	
Hydrogeologic basin	170 km <sup>2</sup> *	
Lake area	6.9 km <sup>2</sup>	
Lake area and surface waters	13 km <sup>2</sup> *	
Lake volume	15 Mm <sup>3</sup>	
Sandpit area	2.5 km <sup>2</sup>	
Sandpit volume	37.5 Mm <sup>3</sup>	
Mean annual precipitation into the basin and into the lake		871 mm/year* 927 mm/year
Mean annual inflow by precipitation within hydrological basin (excluding the lake)		86.2 Mm <sup>3</sup> / year
Mean annual evapotraspiration by land coverage (101 km <sup>2</sup> )		54 Mm <sup>3</sup> / year*
Mean annual outflow to closest basins		2.5 Mm <sup>3</sup> / year*
Outflow by irrigation		2.7 Mm <sup>3</sup> / year*
Total net Inflow in the lake		31 Mm <sup>3</sup> / year 983 l/sec

\*by: Autorità di bacino del fiume Serchio, 2007 (modified)

### 3 METHODOLOGY

#### 3.1 WATER SAMPLING AND INSTRUMENTATION

The aim of water sampling is to investigate both spatial and temporal changes in chemistry in the Massaciuccoli lake and excavation area (old quarries). Accordingly, four samples categories were collected:

- 1) superficial samples (-0.5 m in depth) of the major inflows into the Massaciuccoli lake (Barra, Fossa Nuova, Quiesa, Burlamacca, Gora di Stiava and Farabola)
- 2) samples along vertical profiles (been careful to take a sample about 10 cm from the sediment-water interface) and along 8 different sites of the lake and 7 sites of lake tributaries
- 3) samples along vertical profiles in three quarries within the excavation area
- 4) samples along a salinity profile in the Burlamacca channel, from the sea to the San Rocchino quarry, comprising both superficial and bottom waters.

The samples were collected during three times: July-August 2004 (summer), February-March 2005 (winter) and May 2006 (springtime).

The data set comprises 73 samples of waters from the lake and surrounding channels, collected during the three different seasons; 26 water samples from the excavation area (old quarries); 16 samples from the Burlamacca channel. In addition, one seawater sample from the Viareggio coast, one sample from a deep well (Case Rosse) and one sample from Serchio river (Pisa plain), sampled during summer 2005, were also collected and analyzed (Figure 3.1.1). 54 waters sampled in July-August 2002 (summer), consisting of samples along vertical profiles in the quarries, superficial waters from lake, Burlamacca channel and agricultural drainage, are also included in the database for comparison.

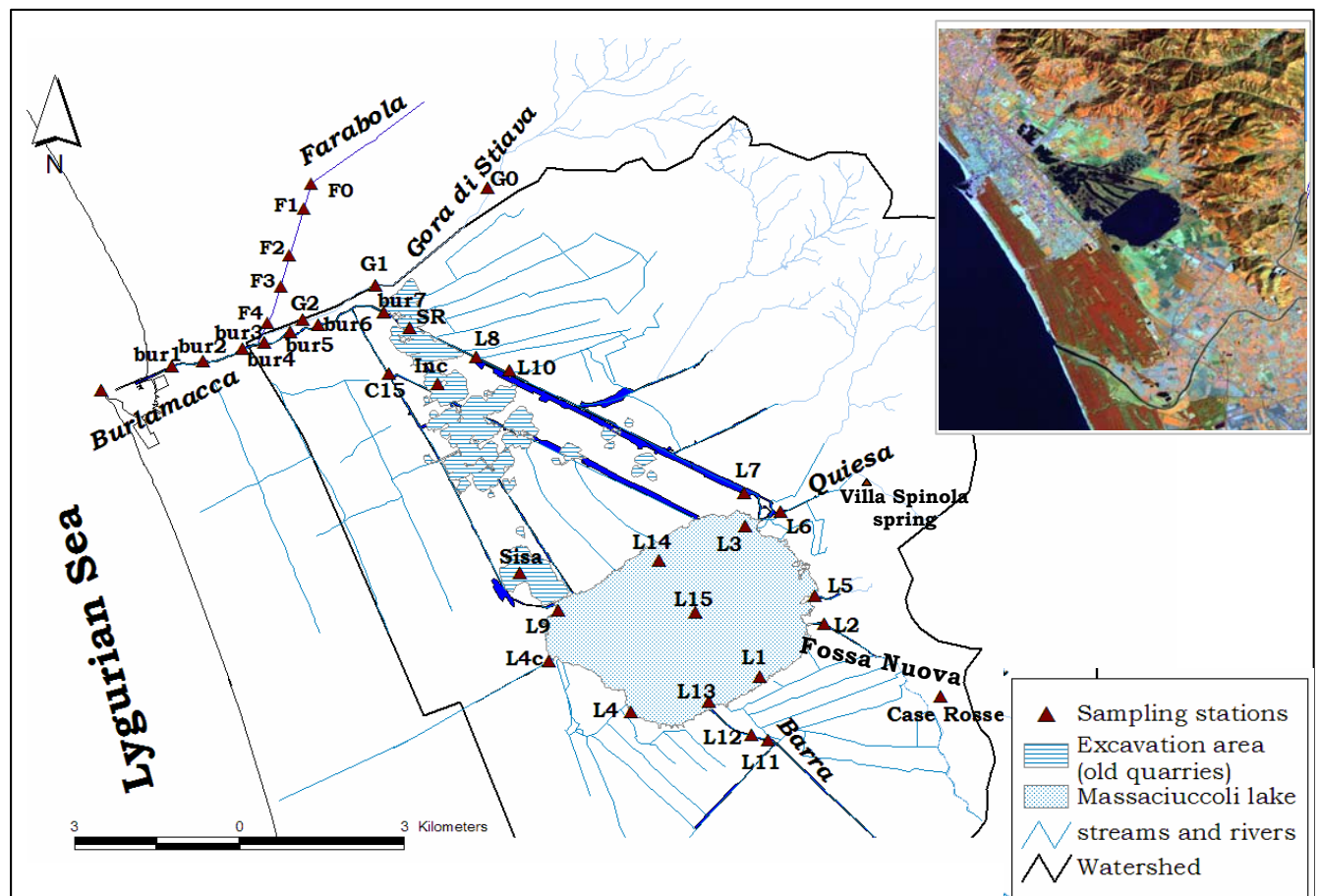
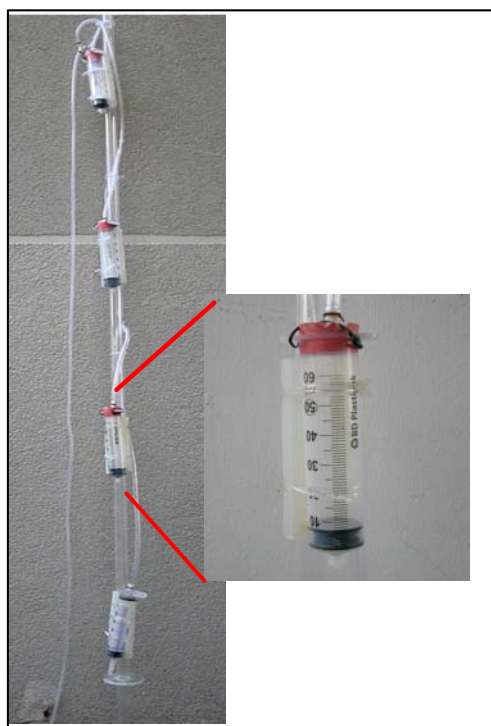


Figure 3.1.1 Sampling points

For each water sample, temperature, dissolved O<sub>2</sub>, pH and electric conductivity (EC) were measured by means of the multiparametric probe OCEAN SEVEN 401-Idronaut. EC, depth, oxygen and pH sensors were calibrated on each sampling trip. The results are reported in appendix I table 1.

Lake and channel waters (with the exception of Farabola and Gora di Stiava) were collected from a boat by submerging a closed bottle to a depth of 50 cm, where it is opened manually. Depth profiles were carried out in summer 2004 collecting waters at discrete depths using a sampler constructed in the IGG laboratory (Figure 3.1.2). It consists of a bar with 4 syringes at 45 cm spacing. The piston of each of them is connected to a polyethylene pipe. The sampler is submerged in the water to the bottom, allowed to stabilize and, with a vacuum pump, the piston of each syringe is lifted to collect the water. Afterwards, a pressure is created in every pipe in order to expel the water, which is collected in different backers. The first 50 ml were discharged.

The samples from quarries were taken at discrete depths, depending on temperature and conductivity gradients, as follows. A polyethylene pipe was lowered at the chosen depth, holding its submerged end close to the Idronaut sensors (Figure 3.1.3). A sampling bottle, equipped with a two-way valve, was connected to the surface end of the pipe and to a manual vacuum pump. First, the pipe was flushed with lake waters, and then the water was allowed to accumulating in the bottle. In all cases, a single large composite sample was obtained. It was further subdivided, at the end of a predefined sampling, as suitable for the analyses to be performed.



**Figure 3.1.2** Device used to collect instrumentation used to collect samples at different depths in shallow waters



**Figure 3.1.3** Multiparametric probe and sampling instrumentation used to collect water from

At each site, alkalinity (typically obtained averaging 3 determinations) was measured immediately in order to prevent precipitation or degassing processes.

Samples for major cations, orthophosphate and nitrate analyses were filtered through 0.45 µm cellulose acetate filters into clean polyethylene (PTE) bottles, previously rinsed with the sampled water. Samples for trace metal analysis were filtered through 0.45 µm cellulose-acetate membranes into glass bottles that had been soaked in 20% ultrapure HNO<sub>3</sub> for 1 day and rinsed with deionized

water. Before collection of the sample, 5 ml of sampled water were passed through the filter as an additional cleaning step. Special care was taken at all stages to minimize contamination and blanks were used as monitors (see below). Samples for metals were preserved immediately in acid-washed bottles by addition of Suprapur HNO<sub>3</sub> (2% v/v); samples for Ca and Mg determinations were acidified to pH < 2 by adding HCl (2% v/v). Samples for sulphide analysis were stored into 100 ml glass bottles containing 0.5 ml of a NaOH 8N solution and a zinc acetate saturated solution was immediately added upon collection. <sup>13</sup>C<sub>DIC</sub> samples were collected in 250 ml PTE bottles, HgCl<sub>2</sub> was added to preserve the sample, and the samples were stored in the dark at 4°C. One litre of water was collected for <sup>34</sup>S<sub>SO<sub>4</sub></sub> and <sup>18</sup>O<sub>SO<sub>4</sub></sub> isotopes measurements. This was preserved in the field by adding a spatula tip of calomel in order to prevent bacterial SO<sub>4</sub> reduction and acidifying with HCl to remove sulphide. In the laboratory BaSO<sub>4</sub> was quantitatively precipitated by adding BaCl<sub>2</sub> (10% solution). BaSO<sub>4</sub> was collected on a 0.45 µm Millipore® filter and washed until no chloride was detected in the effluent (Cl presence was tested by using an AgNO<sub>3</sub> solution). The precipitate was dried at 80°C.

In all cases, the bottles were flushed with sample water and capped without introducing air bubbles. After collection, all samples were placed into an ice-filled cooler and transported to the Institute of Geosciences and Earth Resources, National Research Council (IGG-CNR) laboratory of Pisa. Samples were then kept refrigerated at 4°C until all analyses were completed.

### 3.1.1 Analytical methods

The analyses were performed according to the *Standard Methods for the Examination of Water and Wastewater* (AWWA, 1998).

Total alkalinity was measured in the field by HCl titration according to the Gran's method (Gran, 1952) using methyl-orange as indicator. Nitrite and ammonia analyses were performed in the laboratory immediately after sampling or at most the day after by spectrophotometry (Griess reagent) and potentiometry (gas selective membrane ThermoOrion mod.95-12), respectively. Silica was determined by means of the spectrophotometric method (β-silico-molybdenum blue). Boron concentrations were measured by colorimetry, following the azomethine-H method (Trujillo *et al.*, 1982), and ICP-AES. Total Organic Carbon (TOC) content was quantified spectrophotometrically by measuring the CO<sub>2</sub> produced after acid digestion. Anion analyses (SO<sub>4</sub>, NO<sub>3</sub>, Br) were performed with a Dionex series 100 ion chromatograph, calibrated daily to standard solutions per ion, using an AS14 column. Suppressed conductivity was the method of detection. For the determination of Cl content, titration techniques (Methrom Ag 9100 Herisau) were applied by using AgNO<sub>3</sub> 0.1N. Cation analyses were performed by Atomic Absorption Spectrophotometry (Perkin Elmer) and heavy metals (Fe, Mn, Cd, Cr, Cu, Pb, V, Zn) were analyzed by ICP-AES (Perkin Elmer OPTIMA 3000) by the EPA 6020Rev 0/94 method. Fe and Mn were also analyzed by spectrophotometry using the 3-(2-pyridyl)-5,6-bis(4-phenylsulfonic acid)-1,2,4-triazina method and the formaldehyde oxime method, respectively. A blank was processed in the field by adding nitric acid to distilled water in a similar manner to that used for the samples. The field blanks resulted to have concentrations of heavy metals below the instrumental detection limits.

All major analyses were conducted at the IGG-CNR of Pisa. The results are reported in Appendix I, table 2 and 3.

Data quality was further assessed using the charge balance errors, CBE. Charge balance error is based on the concept that the sum of the positive charges should equal the sum of the negative charges in a solution (Freeze and Cherry 1979). The charge balance equation more commonly used in literature (Fritz, 1994) is:

$$CBE = \frac{(\Sigma^+ - \Sigma^-)}{(\Sigma^+ + \Sigma^-)} \times 100$$

where  $\Sigma^+$  is the sum of the measured, positively-charged equivalents, and  $\Sigma^-$  is the sum of the measured, negatively-charged equivalents. According to Fritz (1994), a %CBE less than 5% is considered good for most applications. With more dilute samples as with these experiments, less



than 10% charge balance error is acceptable. Careful quality controls were undertaken to obtain a reliable analytical dataset with a CBE less than 3%.

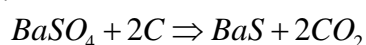
Saturation coefficients were calculated using the USGS hydrogeochemical modeling software PHREEQC 2.8 (Parkhurst and Appelo, 1999), utilizing the MINTEQA thermodynamic database (Allison *et al.*, 1990). The saturation degree for pure phases was quantified by the parameter  $SI = \log(Q/K)$ , where  $K$  is the equilibrium constant and  $Q$  is the activity product of the solute species involved in the reaction. The  $SI$  value is a convenient measure of the amount of departure from thermodynamic saturation; values for the quotient of greater than 0 represent supersaturation, and values less than 0 represent undersaturation.

The oxygen isotopic composition was determined by the water-CO<sub>2</sub> equilibration method at 25°C (Epstein and Mayeda, 1953). The hydrogen isotopic composition was measured following the procedure of Coleman *et al.* (1982), reducing water to H<sub>2</sub> at 460°C using metallic zinc. The two procedures were calibrated according to the recommendations of the International Atomic Energy Agency of Vienna (IAEA). CO<sub>2</sub> and H<sub>2</sub> were analyzed for <sup>18</sup>O/<sup>16</sup>O and <sup>2</sup>H/<sup>1</sup>H ratios by means of a GEO 20-20 and a ThermoFinnigan DELTA XP mass spectrometer, respectively. Results are reported as part per thousand (‰) with respect to the Vienna Standard Mean Ocean Water (V-SMOW), using the  $\delta$  notation (Gonfiantini, 1978). The overall precision of stable isotope determination was 1‰ and 0.2‰ for <sup>2</sup>H and <sup>18</sup>O, respectively.

The  $\delta^{13}\text{C}$  value of the dissolved inorganic carbon (DIC) was measured by converting DIC to CO<sub>2</sub> with 100% phosphoric acid (H<sub>3</sub>PO<sub>4</sub>) followed by cryogenic separation and analysis by mass spectrometry on a GEO 20-20 mass spectrometer (Kroopnick, 1974). The  $\delta^{13}\text{C}$  of DIC was reported in the  $\delta$  notation relative to V-PDB (Vienna PeeDee Belemnite) Standard for carbon. Reproducibility is typically better than  $\pm 0.2\text{‰}$ .

The boron isotopic composition was determined at the IGG-CNR laboratory by PTIMS (Positive Thermal Ionization Mass Spectrometry; Spivack and Edmond, 1986), using a VG Isomass 54E mass spectrometer. Owing to the high water contents of organic matter and colloids, boron was analyzed after alkali fusion of the evaporated samples and extracted via three ion exchange columns according to Tonarini *et al.* (1997, 2003), in order to avoid any interference. The SRM-951 boric acid standard (U.S. National Institute of Standards and Technology) was repeatedly processed to monitor possible isotopic fractionation. Values are reported on the  $\delta$  scale relative to NBS951 boric acid standard. Based on replicate analyses, both precision and accuracy are typically about 0.5 per thousand (‰) or better.

The sulphur isotopic composition was analyzed at the Hydrology and Isotopic Geochemistry Laboratory of the Paris XI University. The  $\delta^{18}\text{O}_{\text{SO}_4}$  was following the technique of Shakur (1982). This is based on the complete conversion of BaSO<sub>4</sub> and C (graphite) into CO<sub>2</sub> and BaS (Figure 3.1.1.1) as described by the reaction:



The oxygen isotope composition of CO<sub>2</sub> was then measured as usual (see above).



**Figure 3.1.1.1** Line for oxygen extraction from the sulphate for  $\delta^{18}\text{O}_{\text{SO}_4}$  analyses

Barium sulphide was first converted to  $\text{Ag}_2\text{S}$  by treatment with a  $\text{AgNO}_3$  solution. Silver sulphide was finally oxidized quantitatively to  $\text{SO}_2$  and its  $\delta^{34}\text{S}$  value measured (Figure 3.1.1.2). Oxygen and sulphur isotopic ratios were determined by conventional dual inlet isotope ratio mass spectrometry using a VG Sira 10. Isotope compositions are reported on the usual  $\delta$  scale, in parts per thousand with respect to the internationally accepted standards, namely CDT (Troilite from the Canyon Diablo meteorite) for sulphur, and V-SMOW for oxygen. Precision was  $\pm 1\text{‰}$  and  $\pm 1.5\text{‰}$  for sulphur and oxygen, respectively. In Appendix I, table 4, are reported the isotopic results.

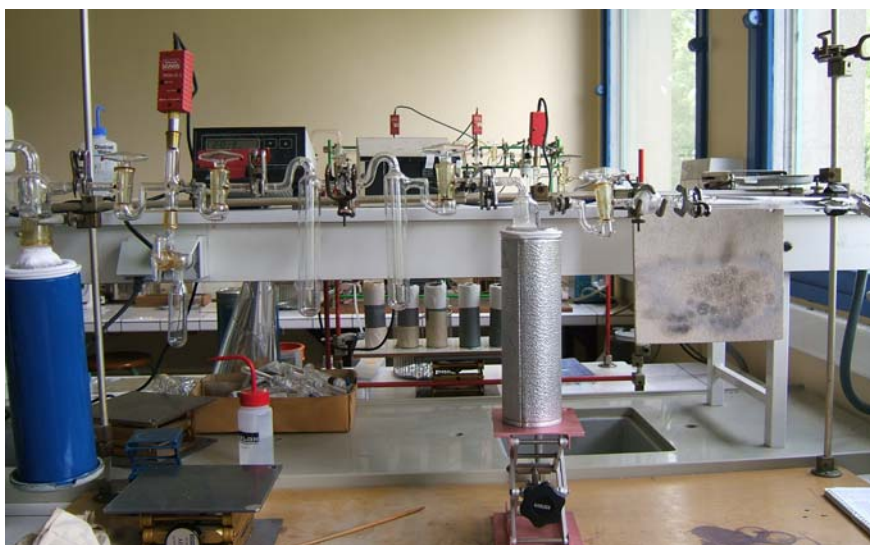


**Figure 3.1.1.2** Line for Sulphur Dioxide for  $\delta^{34}\text{S}$  analyses

### 3.2 SEDIMENT SAMPLING AND INSTRUMENTATION

Sediment samples were taken at the same sampling points as the water-column samples during the summer 2004. Superficial sediments were collected by means of the piston coring method, using a 4-cm-diameter PVC liner in order to prevent any contaminations. The core barrel with the piston is manually placed at the sediment water interface (Figure 3.2.1). This method of coring has the advantages of both keeping the core strata intact, unlike dredge sampling, and minimizing core compression. The piston is held in place while the core barrel is pushed into the sediment. The piston keeps the core under suction so that it can be easily removed from the sediment. As the core is raised, a core cap is placed at the bottom, immediately after removal, to prevent any leakage of the sample.

Cores were typically 50 cm in length. Once brought back to boat, the sedimentological characteristics, grain size, color and occurrence of organic material were described and subsamplings were carried out. This was performed by slicing, generally, the first 5 cm from the top of the core into clean containers like “ziplock” sacs. Then, if layers could not be distinguished, subsamples were taken by slicing 5-10 cm increments of the core. All subsamples were preserved at  $4^\circ\text{C}$  before arrival to the laboratory. In the laboratory, each sediment’s subsample was carefully inspected removing all fragments  $>2\text{mm}$ . Afterward, they were homogenized and a representative aliquot was dried in an oven at  $105^\circ\text{C}$  for 24h until a constant dry weight was observed, in order to estimate the water content, by the difference in weight before and after drying. The water content results are given in table 1 in the Appendix II. The remaining part was dried in a box under air flux. The dried samples were ground to a fine, homogeneous powder using an agate mortar with pestle before further processing.

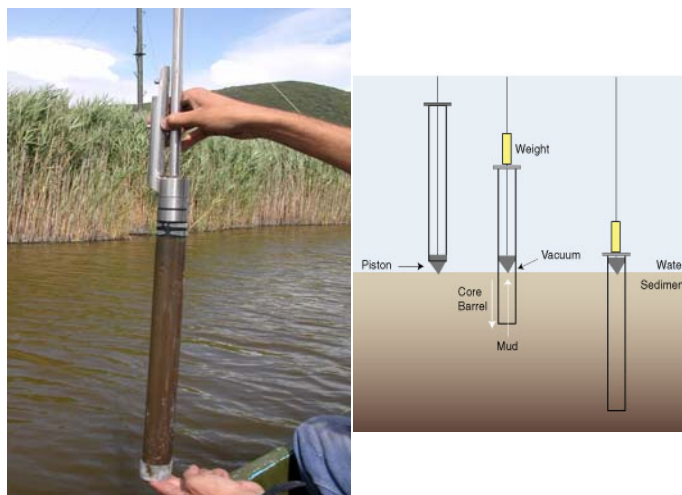


**Figure 3.2.1** Manual piston corer (AFSISTEMI)

### 3.2.1 Analytical methods

Total carbon (TC) and its organic fraction (TOC) were determined by combustion in an oxygen stream at 1200 and 600°C, respectively (Koch and Malissa, 1957). Inorganic carbon (TIC) was calculated as the difference between concentrations of TC and TOC. Total Nitrogen (TN) was analyzed by combustion in a LECO CNS 2000 combustion analyzer set at 1100°C. The results are given in table 1 in the Appendix II.

Sequential loss on ignition followed the method proposed by Heiri *et al.* (2001), with the modification by Bengtsson and Enell (1986) which takes into account the loss of mass at 105°C and the residues after ignition for the calculation of the LOI. The process was:

- (1) Dry the sample 12–24 h at 105°C. Calculate the loss on ignition at 105°C ( $LOI_{105}$ ) as  $LOI_{105} = 100(WS - DW_{105})/WS$ , where  $WS$  is the weight of the air-dried sample and  $DW_{105}$  is the dry weight of the sample heated at 105°C.
- (2) Burn the sample at 550°C for 4 h. Calculate  $LOI_{550} = 100(DW_{105} - DW_{550})/WS$ , where  $LOI_{550}$  is the percentage of loss on ignition at 550°C and  $DW_{550}$  is the weight of the sample after heating at 550°C.
- (3) Heat the sample at 950°C for 2 h; calculate  $LOI_{950} = 100(DW_{550} - DW_{950})/WS$ , where  $LOI_{950}$  is the percentage of loss on ignition at 950°C and  $DW_{950}$  is the weight of the sample after heating at 950°C. The remaining sample, after heating at 950°C, is the residuum ( $LOI_{res}$ ).

The results are presented in table 1 in the Appendix II.

All of the samples (about 10 g) were subjected to the standard protocol for Accelerator Mass Spectrometry (AMS) analyses of  $^{14}C$  organic carbon. The chemical treatment consisted of a strong acid-alkali-acid (AAA) treatment, including hot 10% HCl treatment (30 min at 80°C) to eliminate carbonate contamination, and NaOH treatment (30 min at 80°C) to remove secondary humic acids. A final 10% HCl treatment completed the cleaning procedure. After each acid treatment, the samples were neutralized with repeated washing with distilled water and dried in an oven at 80°C. Subsequently, 10–15 mg of organic carbon were combusted to  $CO_2$  in a quartz ampoule with CuO and silver wool at 850°C for 30 min, under vacuum (Figure 3.2.1.1). The  $CO_2$  gas obtained was purified from pollutant gases (e.g.  $H_2S$ ) to prevent inactivation of iron catalyst during graphitization reaction. The  $CO_2$  purified was reduced to graphite by  $H_2$  on powdered iron catalyst at 650°C for 2 hours.

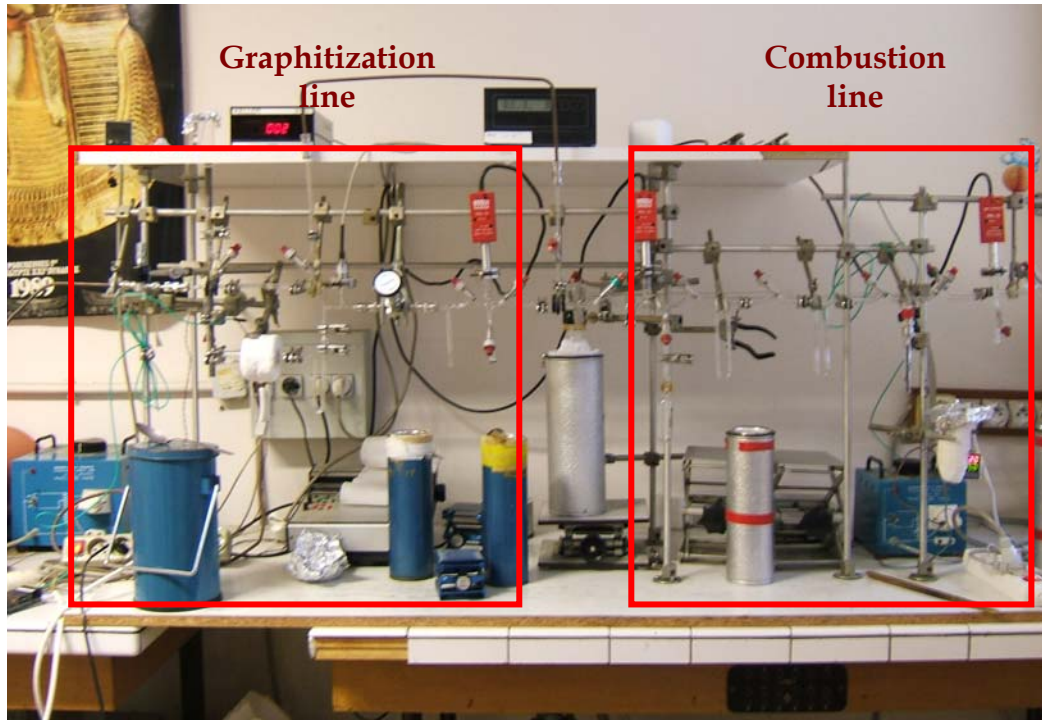


**Figure 3.2.1.3** Line for graphitization of organic carbon

The graphite was pressed into a target holder and analyzed using an accelerator mass spectrometry (Nadeau *et al.*, 1998). Residual CO<sub>2</sub> gas was used for associated <sup>13</sup>C measurement and/or for duplicate if necessary. The graphite sources were prepared in Orsay (Laboratory of Hydrology and Isotope Geochemistry, Orsay, France), and carbon atoms were counted with the accelerator mass spectrometer 3 MeV tandem Pelletron (CEA Saclay). Analytical errors, including laboratory errors, are between 0.5 and 0.8 pMC (percentage of Modern Carbon). The results are reported in Appendix II table 2.

## 4 WATER GEOCHEMISTRY

### 4.1 WATER CLASSIFICATION

Table 4.1.1 summarizes the basic statistics of chemical-physical parameters for each samples' group. As already recalled, the dataset includes not only data obtained during this study, but also data collected during the summer 2002 for comparative purposes. In order to understand better the variability of chemical results, data from the sea, Serchio river and Villa Spinola spring are considered.

**Table 4.1.1** Basic statistics of 11 parameters, relative to the different groups of samples. Mean values are calculated considering data of all samplings (N represents the number of samples considered in the calculations)

	T	pH	Conductivity	TDS	Alk	Cl	SO4	Na	K	Ca	Mg
	°C		µS (20°C)	mg/l	meq/l	mg/l	mg/l	mg/l	mg/l	mg/l	mg/l
<b>Lake</b>											
N	46	46	42	42	46	46	46	46	46	46	46
Mean	23.3	8.62	2009	2009.37	3.04	790.22	366.22	462.03	18.35	120.94	73.1
Median	25.9	8.75	1965	1965.19	2.63	749.08	369.01	442.24	18.52	115.78	71.51
Min.	4.1	7.4	1847	1847.22	2.2	688.25	201.56	408.26	8.79	101.57	63.47
Max.	29.7	9.05	2413	2413.46	7.3	1139.03	435.05	595.36	25.54	174.39	96.66
SD	7.1	0.4	164	164.00	1.05	99.21	43.53	49.42	3.5	15.89	7.33
<b>Agricultural Network</b>											
N	50	50	34	50	50	50	50	50	50	50	50
Mean	22.4	8.159	3513	2249.65	4.11	884.45	365.94	506.79	19.68	140.28	78.94
Median	25.6	8.180	3606	2216.92	3.57	830.66	369.43	469.51	20.20	137.94	76.61
Min.	4.4	6.990	1280	1092.24	2.80	285.35	233.69	158.58	4.00	110.08	31.12
Max.	29.8	8.890	7901	3941.16	8.80	1838.61	526.82	1006.74	40.09	215.70	133.53
SD	7.6	0.457	1539	555.00	1.34	311.61	58.29	171.30	7.38	21.32	19.35
<b>Farabola and Gora di Stiava streams</b>											
N	7	7	7	7	7	7	7	7	7	7	7
Mean	25.0	7.917	7870	4325.87	5.21	1977.14	511.44	1194.22	50.40	134.11	136.40
Median	25.7	7.660	8489	4627.16	5.23	2106.42	594.22	1303.69	54.18	135.25	144.84
Min.	21.8	7.470	1008	718.12	4.03	134.69	142.16	62.74	3.41	103.05	20.90
Max.	26.6	8.90	12432	6540.71	5.70	3201.14	672.22	1905.14	75.85	160.46	214.11
SD	1.7	0.586	3653	1893.76	0.59	984.70	197.65	593.52	23.95	17.14	62.41
<b>Burlamacca Channel</b>											
N	18.0	18.000	11	17	15	23	23	15	15	15	15
Mean	25.7	8.181	43417	13304.30	3.71	9543.25	1474.28	3820.59	142.52	235.07	473.14
Median	25.7	8.185	40291	12940.11	3.70	10548.05	1514.91	1942.92	74.90	191.13	254.00
Min.	22.1	7.450	8825	3804.04	2.93	1759.20	478.39	985.26	38.20	162.18	134.76
Max.	28.4	8.860	69883	23573.70	4.75	20656.97	3027.49	10841.42	393.60	410.55	1221.66
SD	1.6	0.519	24627	7442.74	0.42	6566.20	855.47	3196.50	115.03	79.76	371.56
<b>Quarries</b>											
N	50	50	27	49	50	50	50	49	49	49	49
Mean	17.212	7.680	7469	6206.48	6.43	3093.31	564.28	1670.64	64.00	180.62	211.21
Median	16.595	7.505	4074	4170.68	3.78	1910.47	436.50	1091.80	40.05	158.25	144.96
Min.	6.247	6.870	1635	2005.52	3.00	729.52	12.18	441.98	18.51	121.53	70.00
Max.	28.16	8.78	20868	16941.74	26.59	9068.53	1347.04	5065.84	240.98	414.46	591.04
SD	6.104	0.636	6198	4503.25	4.91	2566.04	308.38	1359.19	53.24	56.17	153.62
<b>Sea</b>											
Mean	26.75	8.11	65076	39076.89	2.68	21485.95	2853.32	12073.52	528.36	452.02	1369.64
<b>Serchio</b>											
Mean	29.4	8.03	868	552.62	3.25	56.3655	146.49	38.62	2.81	95.20	14.88
<b>Villa Spinola spring</b>											
Mean				752.82	3.07	19.65	381.25	8.53	0.93	144.49	10.78
<b>Case Rosse well</b>											
Mean				80.07		35.5	17.01	21.72	0.89		4.96

The degree of salinization due to seawater mixing is generally indicated by an increase in both Total Dissolved Solids (TDS) and nearly all major cations and anions as well. Very wide ranges and high standard deviations are easily recognized for most parameters. In particular, for superficial waters the TDS value has a wide range between 718 (Gora di Stiava stream) and 23573 mg/l (Burlamacca channel). The ranges of Na and Cl ions are also wide: 62.7 (Gora di Stiava stream)-12224.8 mg/l (Burlamacca channel) and 134 (Gora di Stiava stream)-21720 mg/l (Burlamacca channel), respectively. Such wide ranges of solute concentrations suggest that multiple sources and/or complex hydrochemical processes act to generate this spread in chemical composition.

Solute concentrations are shown as box plots in Figure 4.1.1, which underline variability between the different waters' types. The dominance of Na and Cl ions in many water samples suggests the significant influence of seawater through direct mixing, although further hydrogeochemical and isotopic data are needed to validate this hypothesis. Therefore, the chloride and salinity increasing does not indicate necessary a mixing process with seawater.

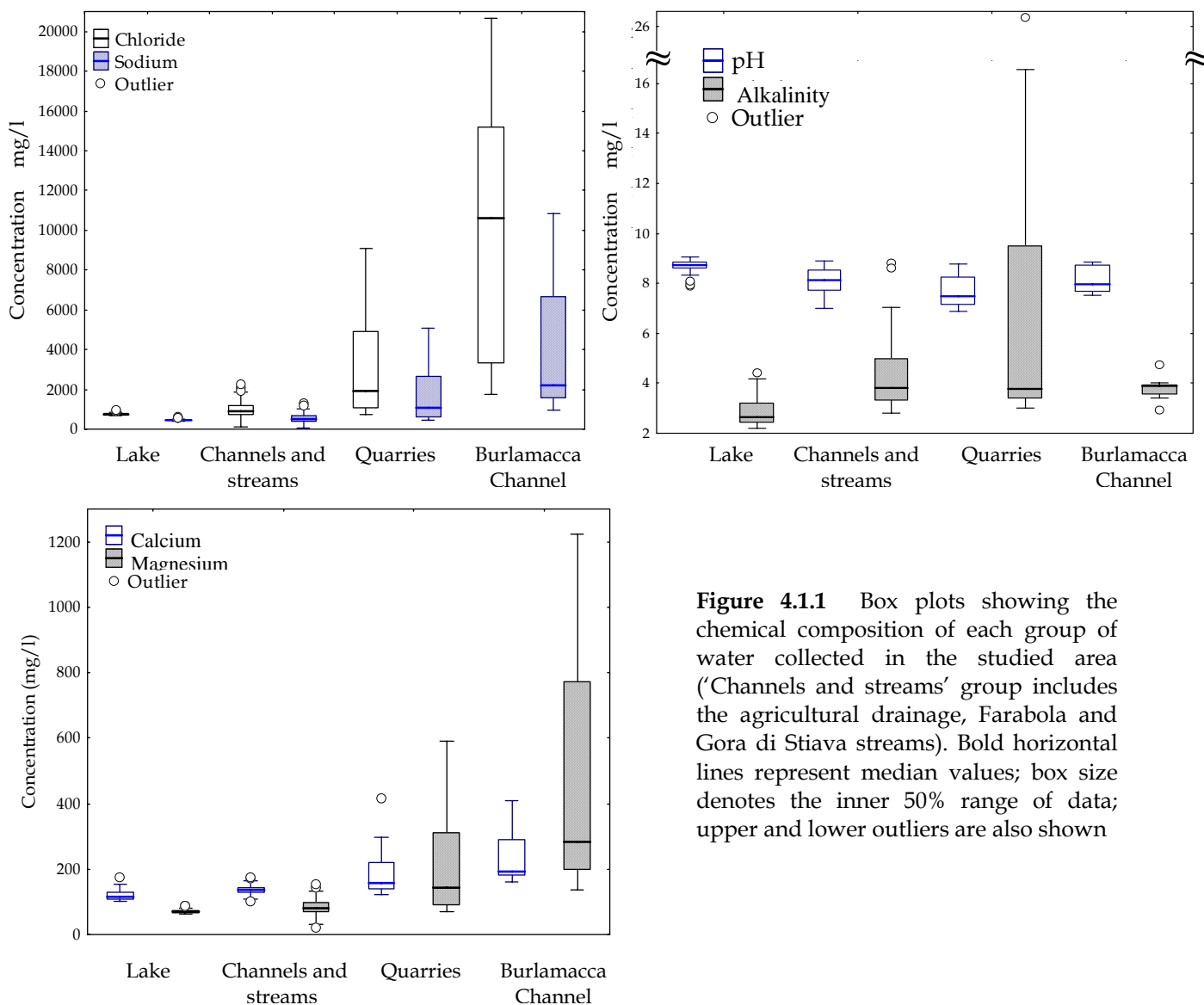


**Figure 4.1.1** Box plots showing the chemical composition of each group of water collected in the studied area ('Channels and streams' group includes the agricultural drainage, Farabola and Gora di Stiava streams). Bold horizontal lines represent median values; box size denotes the inner 50% range of data; upper and lower outliers are also shown

A general view of the chemical characteristics of the studied waters is given by application of the Langelier-Ludwig (or LL) diagram (Langelier and Ludwig, 1944). This diagram is a square plot, where the position of a sample is obtained by first calculating the sum of main anions,  $\Sigma an$ , and of main cations,  $\Sigma cat$ , by means of the following equations:

$$\Sigma an = eCl + eSO_4 + eHCO_3$$

$$\Sigma cat = eCa + eMg + eNa + eK$$

where  $e$  refer to the concentration of each component in eq/l or meq/l. Then the percentage of each component are easily obtained, suitably grouped, and plotted. In general, the sum of selected cations (e.g.  $Na\%+K\%$ ) is plotted on the y-axis, against the percentage of each selected anion (Piper, 1944). Each axis ranges from 0 to 50 meq% (R value). According to Tonani (unpublished reports) the square LL plot represents the base of a compositional pyramid whose edges are the chemical concentrations, in eq/l or meq/l, and whose axis expresses the Total Ionic Salinity (TIS, in the same unit). In Figure 4.1.2 the LL square diagram with  $\%HCO_3$  as x-axis (LL- $HCO_3$ ) is reported; samples can chemically be classified as Na,K-Cl waters, even if few observations (Serchio river, Villa Spinola and Gora di Stiava G0) have a mixed composition. Na and K are the principal cations, except for two samples, G0 and Serchio river, where Ca and Mg dominate.

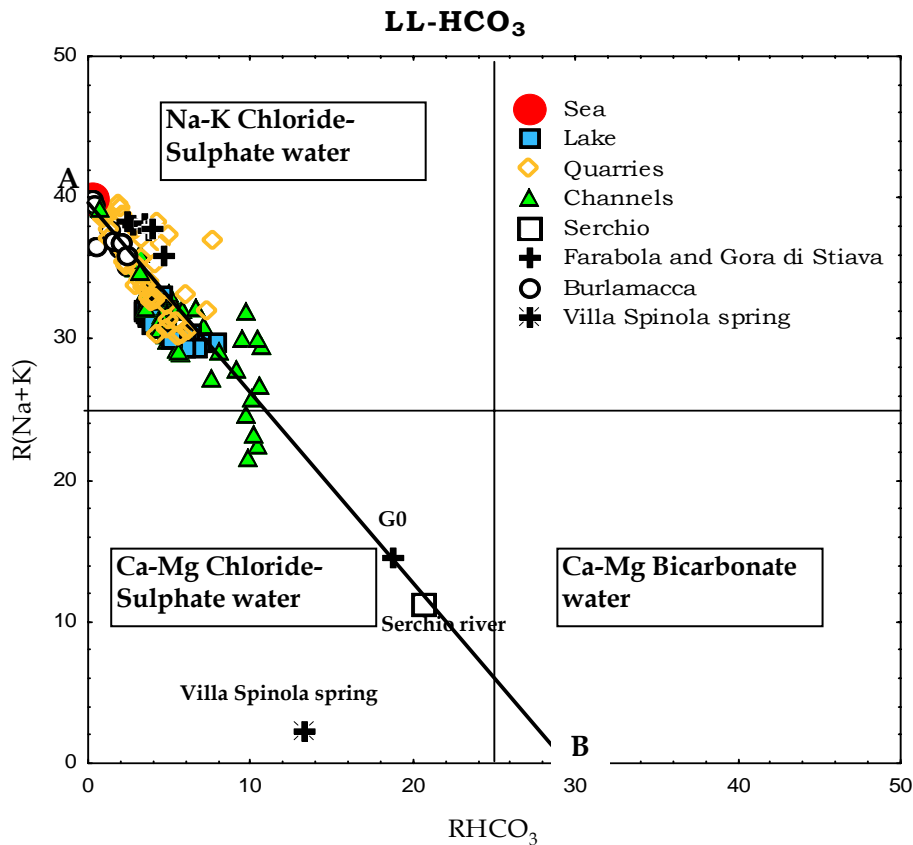


**Figure 4.1.2** LL- $HCO_3$  diagram for all the samples. The line  $\overline{AB}$  represents the trace of the section reported in Figure 4.1.9

The LL-Cl diagram (Figure 4.1.3) underlines the dominance of Cl, while the LL- $SO_4$  plot shows (Figure 4.1.4) the presence of samples situated to the left of the main trend due to a relatively smaller percentage of  $SO_4$ . These latter samples came from different areas, namely:

1. the bottom of the quarries
2. some drainage water (i.e. L6, L12 collected on winter and springtime and L11 on winter), and a lake sample collected during the summer 2002 (L15-02).

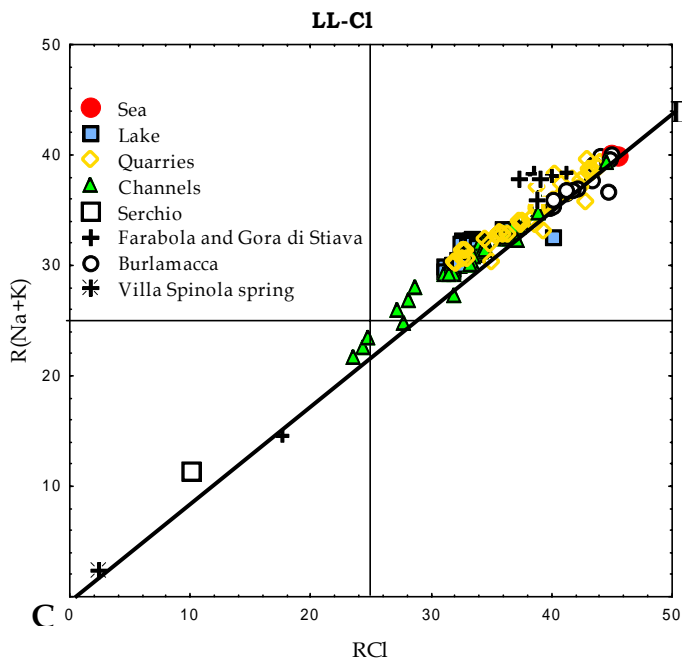


**Figure 4.1.3** LL-Cl diagram for all the samples. The line  $\overline{CD}$  represents the trace of the section shows in Figure 4.1.7.

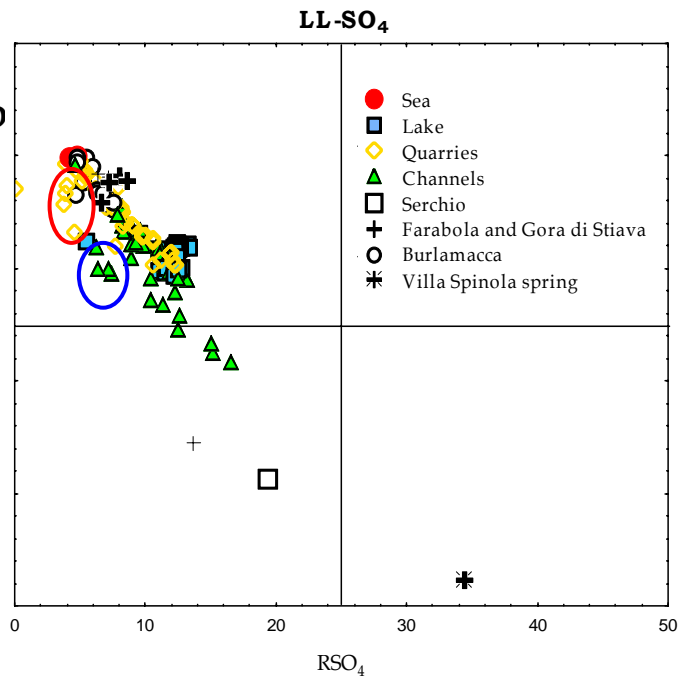


**Figure 4.1.4** LL-SO<sub>4</sub> diagram for all the samples. The red and blue circles encompass the samples from the bottom of the quarries and the samples L6, L11, L12 and L15, respectively

The position of a data point in the Cl-SO<sub>4</sub>-HCO<sub>3</sub> triangular plot is obtained, by first, calculating the sum  $\Sigma an$  of the concentrations  $e$  (meq/l) of all three species involved:

$$\Sigma an = eCl + eSO_4 + eHCO_3$$

Then the percentages of chloride, %Cl, sulphate, %SO<sub>4</sub>, and bicarbonate, %HCO<sub>3</sub>, are evaluated. The triangular diagram (Figure 4.1.5) underlines the dominance of chloride ions and the significant depletion in SO<sub>4</sub> of the samples from the bottom of the quarries (enclosed by the red circle in Figure 4.1.5) in relation the superficial ones. This depletion can be ascribed to the SO<sub>4</sub> bacterial reduction, which is accompanied by the addition of organic HCO<sub>3</sub>, produced through oxidation of organic matter, to the solution.

The K vs Na plot (Figure 4.1.6) points up that the samples classified as chloride-alkaline, based on Figure 4.1.2, 4.1.3 and 4.1.4, belong to the Na-Cl type as Na prevails on K.



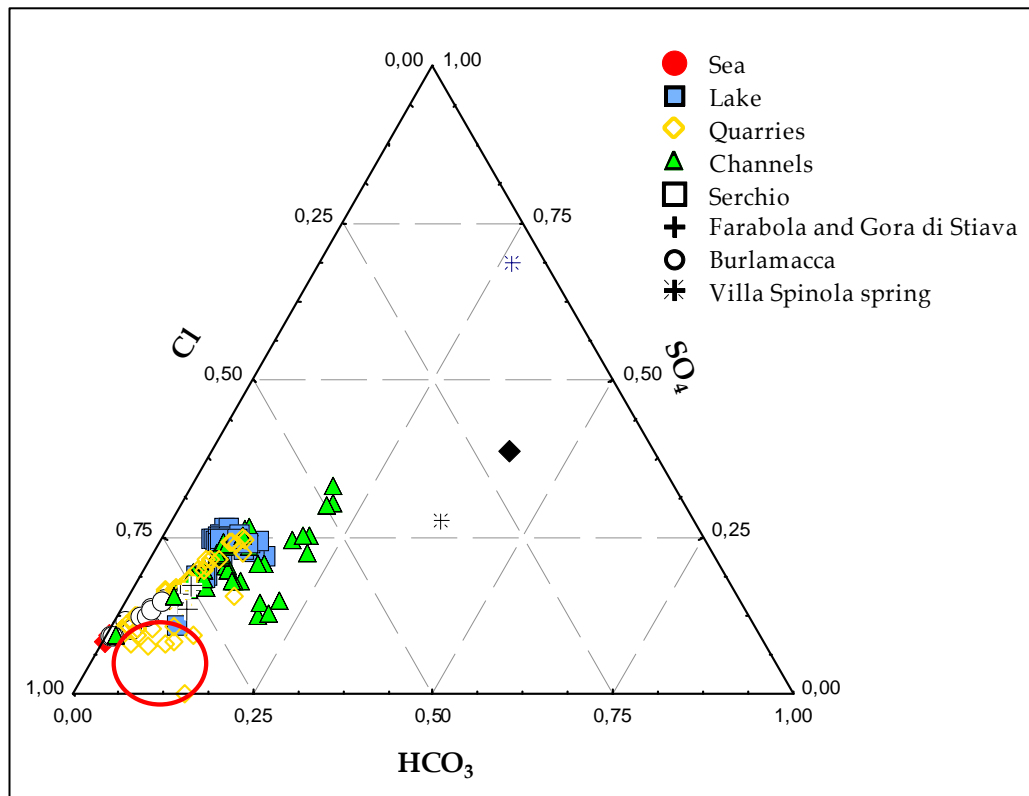


**Figure 4.1.5** Triangular diagram for major anions (meq/l). The red circle encloses the samples from the bottom of the quarries

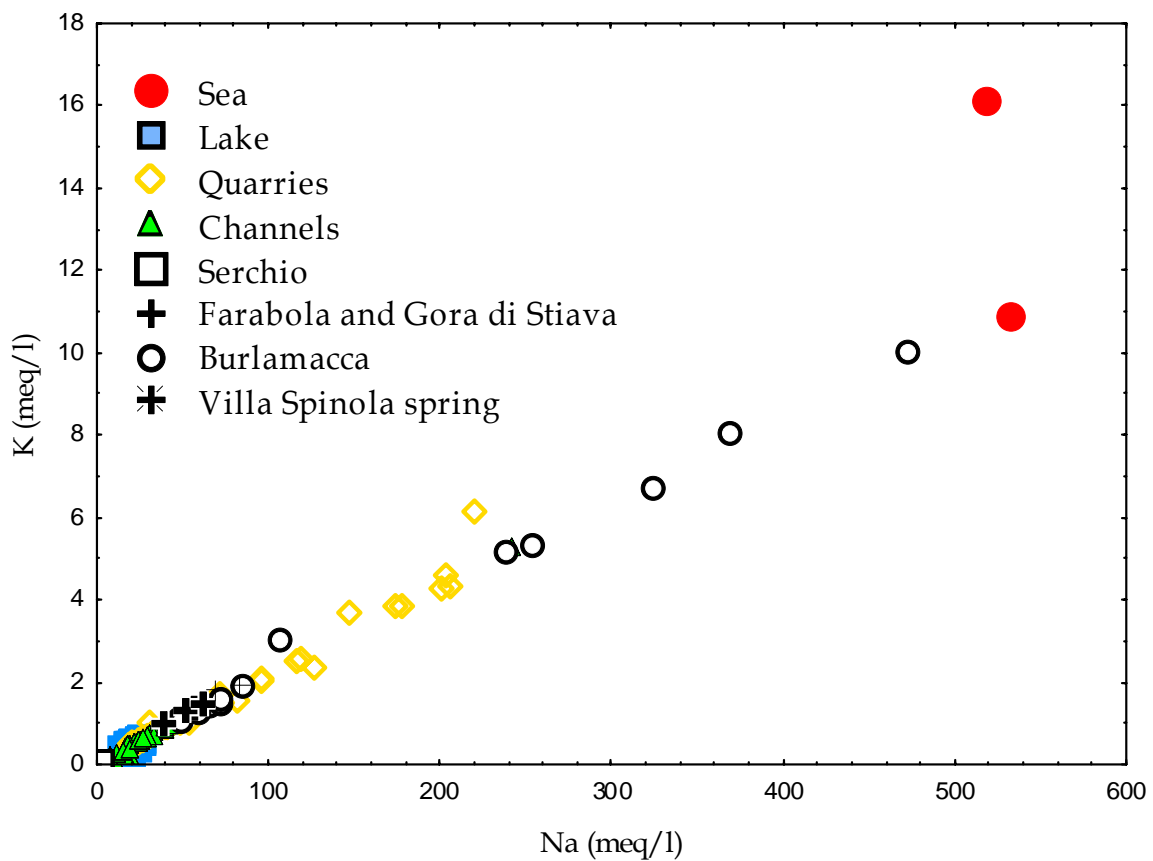


**Figure 4.1.6** Bivariate diagram for samples of the studied system

The LL-HCO<sub>3</sub> and LL-Cl diagrams (Figure 4.1.2 and 4.1.3, respectively) show an evident alignment of samples. Figure 4.1.7 represents the section  $\overline{CD}$  of the LL-Cl diagram, passing through this alignment. The Serchio river and Gora di Stiava (G0) are characterized by the lowest salinity, 16.5 and 20 meq/l, respectively. Samples from the agricultural network and from the lake have intermediate salinity; samples from Burlamacca, quarries and sea have the highest values. Therefore, the alignment recognised on the LL diagram is also evident when salinity is considered. Figure 4.1.8 is an expansion of the section  $\overline{CD}$  of the LL-Cl diagram for lake samples. It shows the occurrence of seasonal differences and, in particular, that the winter and spring samples have the same salinity of the samples collected in summer 2004 but relatively higher contents of Ca and Mg. Samples collected in summer 2002 are characterized by a larger salinity and higher contents of Na and K.

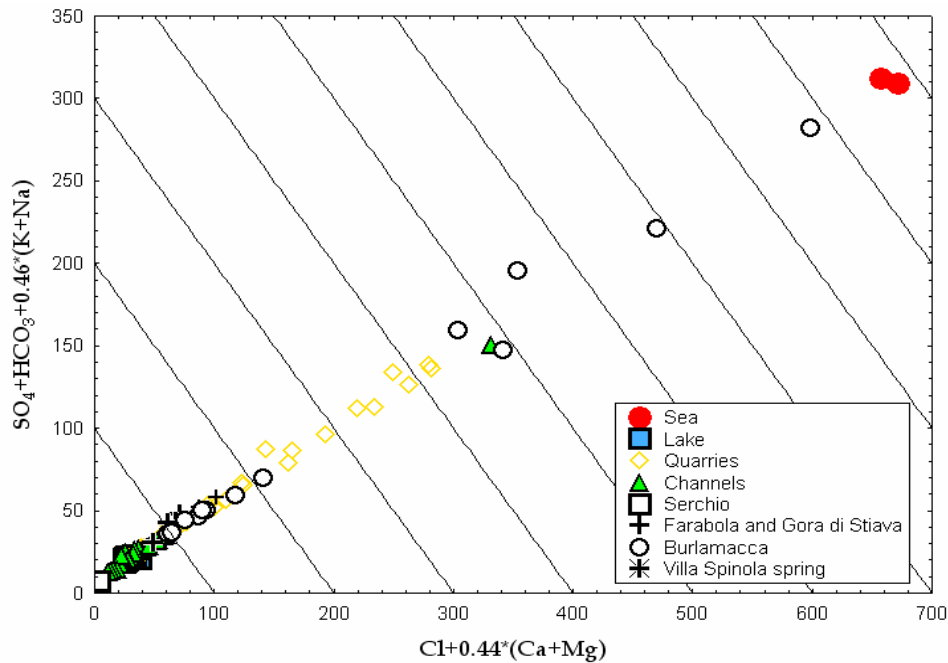


**Figure 4.1.7** Section of the LL-Cl plot through the alignment of water samples

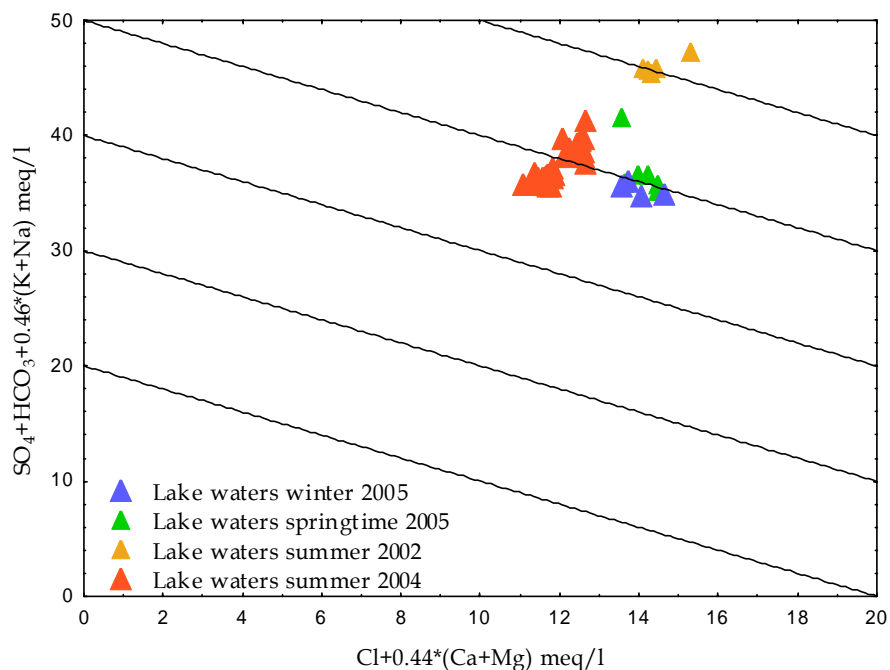


**Figure 4.1.8** Enlargement of the Figure 4.1.7 for lake samples. Seasonal variations are underlined

In details, the LL-HCO<sub>3</sub> section  $\overline{AB}$  (Figure 4.1.9) for the samples collected from the lake and the channels shows that lake waters collected in summer 2004 differ from those collected in winter and springtime and from the drainage network, owing to the relatively lower content of Ca-Mg bicarbonate. Lake waters collected in summer 2002 present a relatively higher content of Na, K chloride and sulphates, as samples collected from the Barra channel in summer 2004. This denotes that there are both a spatial variability and a temporal one in the studied area.

Generally, all the diagrams underscore that the samples from the lake lie along a mixing line, which can not result by mixing between seawater and freshwaters like those of Serchio river.

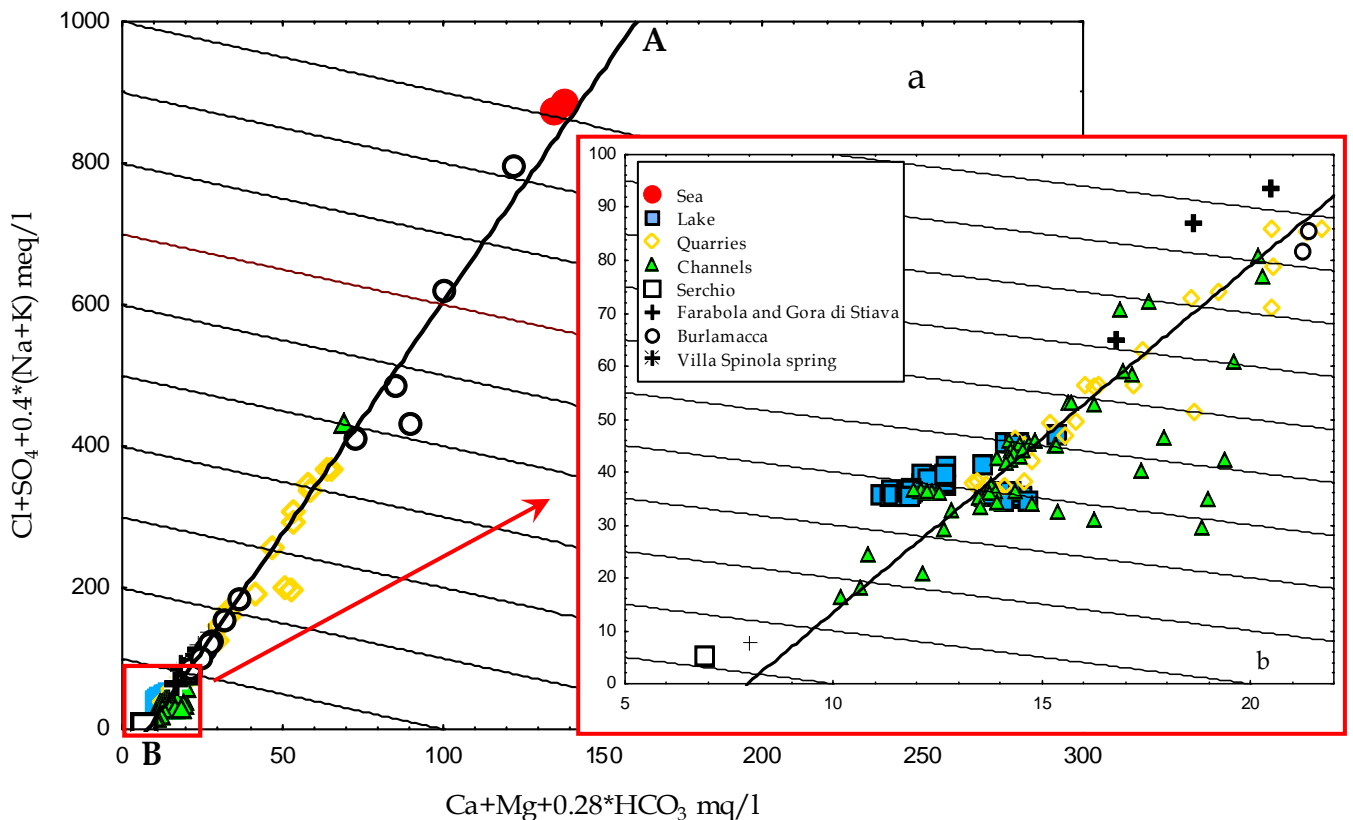


**Figure 4.1.9** (a) Section of LL-HCO<sub>3</sub> plot through the alignment of water samples and (b) enlargement for low-salinity samples

The alignment, connecting the low-salinity waters of the Serchio and Gora di Stiava and high-salinity seawater samples, is clearly evident in Cl/Na plot (Figure 4.1.10).

Summarizing, the majority of the studied waters are of Na-Cl composition, except the Villa Spinola spring which belongs to the Ca-sulphate type, and the Serchio River, Gora di Stiava stream (G0) and two samples of the agricultural network (Quiesa, L6 and Barra, L12, channels) which have a mixed composition.

The following anions sequence can be defined based on the SO<sub>4</sub>/Cl plot (Figure 4.1.11):

- i. Cl > SO<sub>4</sub> > HCO<sub>3</sub>: for most samples
- ii. Cl > HCO<sub>3</sub> > SO<sub>4</sub>: for the Gora di Stiava stream (G0), and the agricultural network
- iii. Cl > SO<sub>4</sub> = HCO<sub>3</sub>: for the Serchio river.

Sodium represents the principal cation in most waters, except the Serchio river, Gora di Stiava stream (G0) and Villa Spinola spring where Ca dominates.

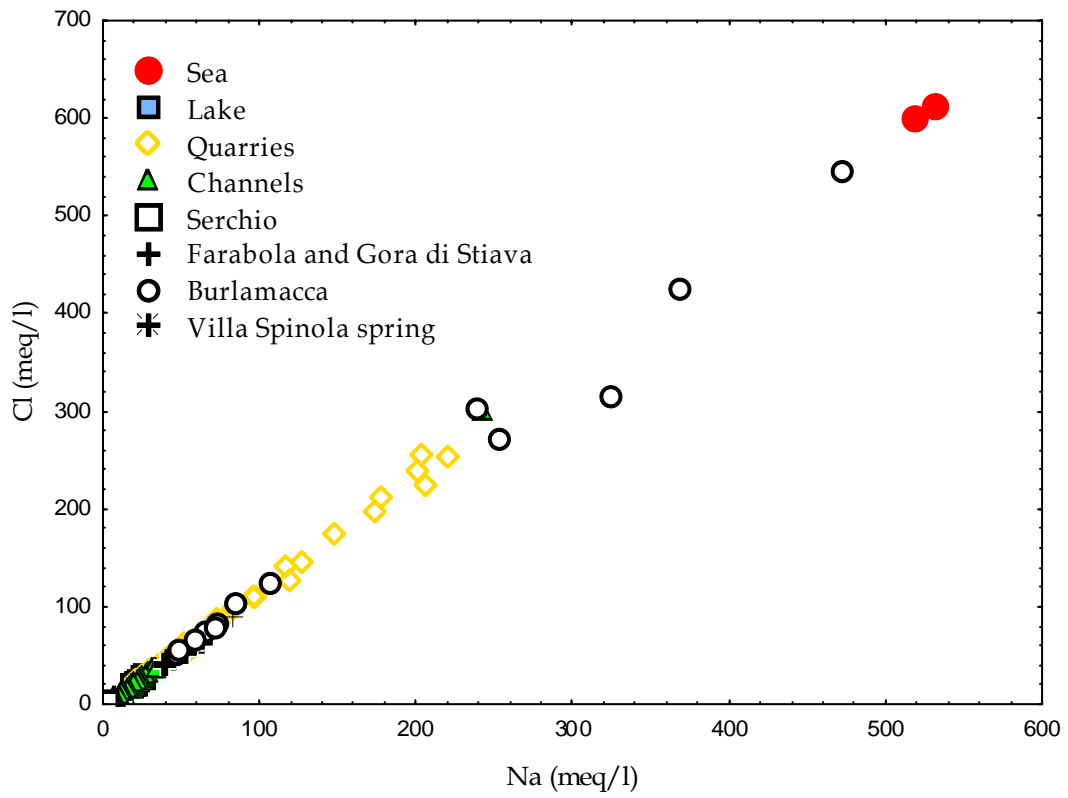


Figure 4.1.10 Cl/Na diagram for samples of the studied area

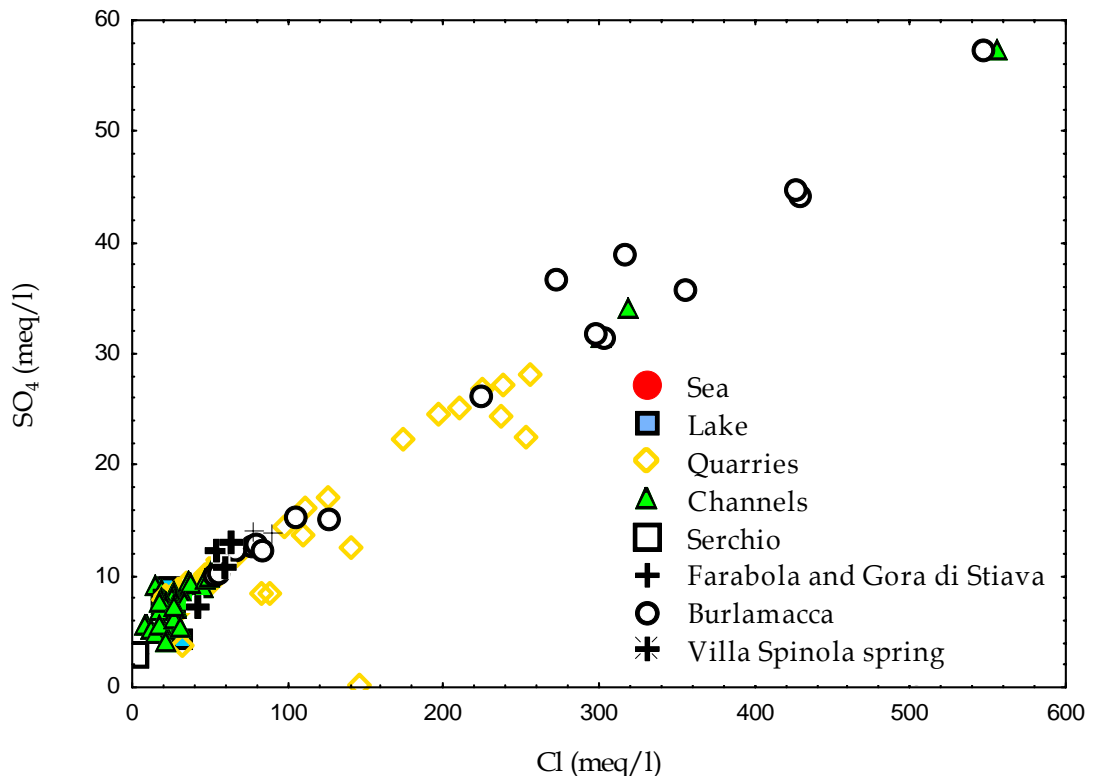


Figure 4.1.11 Bivariate  $SO_4$ -Cl diagram for samples of the entire system

## 4.2 GEOCHEMICAL PROCESSES

### 4.2.1 Ionic relations

In the previous section, we examined the spatial distribution of major elements across the Massaciuccoli basin in order to identify active geochemical processes. To better understand the processes controlling salinity evolution and solute content variations the molar ratios of several elements are taken into account. Na/Cl, B/Cl and Br/Cl ratios are used to identify seawater mixing (Neal *et al.*, 1998; Park *et al.*, 2005; Cartwright *et al.*, 2006) and anthropogenic contamination or vegetation/soil adsorption processes (Faber *et al.*, 2004; Kass *et al.*, 2005). Mg/Ca, Ca/Na, and Ca+Mg/SO<sub>4</sub> ratios are used to determine mineral weathering, dissolution/precipitation of minerals and evaporation of surface and lake water (Yan *et al.*, 2002; Green *et al.*, 2005). However, tracing the origin of salinity is not easy, particularly if multiple nonpoint, saline sources are present within the basin (Vengosh, 2003).

We can hypothesize that the following processes account for changes in the chemical composition of lake waters: (1) net evaporations, prevailing during the summer period, and transpiration, prevailing during spring period, when vegetation has the maximum expansion which increases the content of conservative solutes in the lake. If these were the only processes, the ionic ratios between conservative constituents in lake waters should be identical to those of its tributaries and the Burlamacca channel. (2) Inflows from agriculture network (point sources) that modify lake water composition in accordance to the relative contributions of the inflows. (3) Groundwater discharge (i.e., a non-point source), which gradually modifies lake water composition along the flow due to an increasing fraction of the groundwater component.

In this paragraph, ionic relations and seasonal variations of the chemical composition of lake waters are accurately analysed.

The Ca/Mg diagram (Figure 4.2.1.1) displays two trends:

1. the first includes the samples from the lake and the agricultural network, with a Ca/Mg ratio higher than 1
2. the other includes samples from the sea, the Burlamacca channel and the quarries, with a Ca/Mg ratio of 0.14.

The plot allows one to identify three end members: i) the sea, ii) the groundwater from carbonate rocks and iii) the waters from the reclaimed area with a composition like the Barra water, the principal channel receiving drainage waters. Indeed, the lake waters can be subdivided into three groups:

1. low-Ca samples, collected in the summer 2004 and one sample in the summer 2002 (L4) (group A in the Figure 4.2.1.1b), with a Ca/Mg ratio ranging from 1 to 0.924
2. intermediate-Ca samples, collected in the summer 2002 and one sample in the summer 2004 (L9-m04) (group B) with a Ca/Mg ratio ranging from 0.804 to 0.852. These samples belong to the alignment comprising the Burlamacca channel and the seawater, possibly due to a marine inflow during that period or a lower amount of precipitation
3. high-Ca samples (group C), collected in winter and springtime 2005, except one sample (L9) with a Ca/Mg ratio higher than 1.

The dashed line in Figure 4.2.1.1 represents the regression line ( $r^2=0.77$ ) for the Serchio river and agricultural drainage during winter and spring periods. The Ca excess can be chiefly ascribed to the dissolution of Ca-minerals, such as calcite, gypsum and anhydrite. We can suppose that the agricultural network is the principal responsible of the chemistry of the lake. In fact, the lake in winter and spring periods, when the runoff inflow is the highest, derives from agriculture drainage through CaCO<sub>3</sub> precipitation (which is the principal mineral in lake sediment) and not because of direct seawater mixing. In summer period, two processes are possible: 1) precipitation of calcite-magnesite solid solutions, called Mg-Calcites (Reed, 1983) due to evaporation process (note that dolomite is absent in superficial sediments as expected based on its relatively low precipitation rate) or 2) Mg enrichment due to marine influence. This geochemical pattern is outlined in Figure 4.2.1.2.

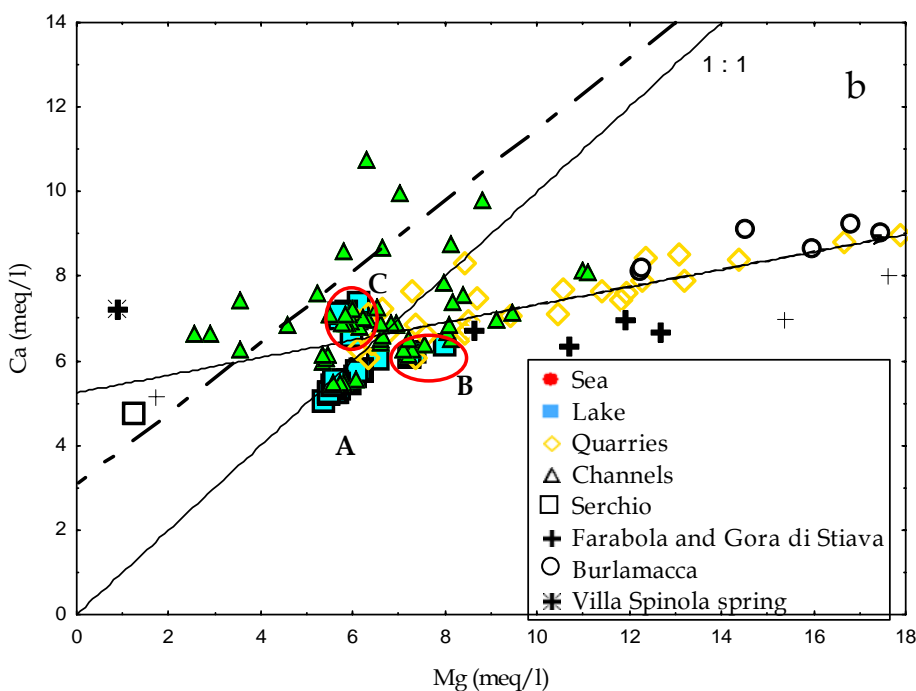
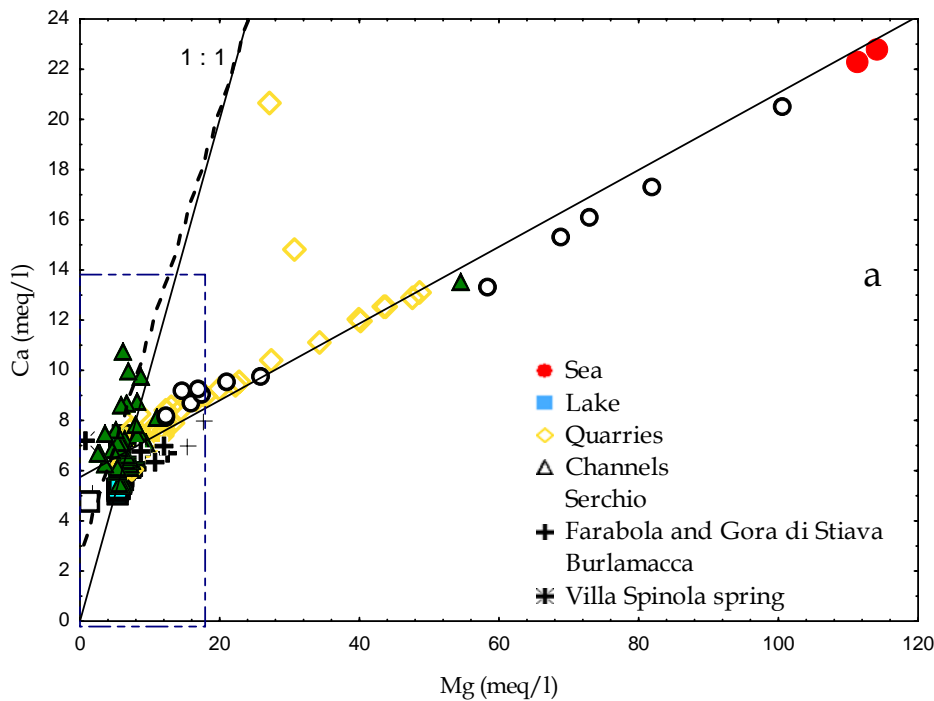


**Figure 4.2.1.1** (a) Bivariate diagram Ca/Mg and (b) enlargement of the dotted square. The letters indicate lake waters and agricultural drainage samples in different seasons: A=summer 2004; B=summer 2002; C=winter 2005. Regression line (dashed line) for the Serchio river and agricultural drainage during winter and spring periods is reported.

The Ca vs  $\text{SO}_4$  diagram (Figure 4.2.1.3) confirms the presence of the two trends and three samples groups, recognised in the Ca/Mg plot (Figure 4.2.1.1-4.2.1.2). Again, one trend is defined by seawater, the Burlamacca channel and the quarries' surface waters; the other consists of the samples from the lake and agricultural network, with a Ca/ $\text{SO}_4$  ratio close to 1. Furthermore, lake waters during summer 2004 (group A in Figure 4.2.1.1b) denote a deficiency of calcium due to  $\text{CaCO}_3$  precipitation. This causes the scatter of samples in relation to the fresh water/sea water mixing line (dashed line), although the possible influence of BSR cannot be ruled out. It is, therefore, confirmed that the present chemical composition of lake waters results from weathering and evapotranspiration processes.

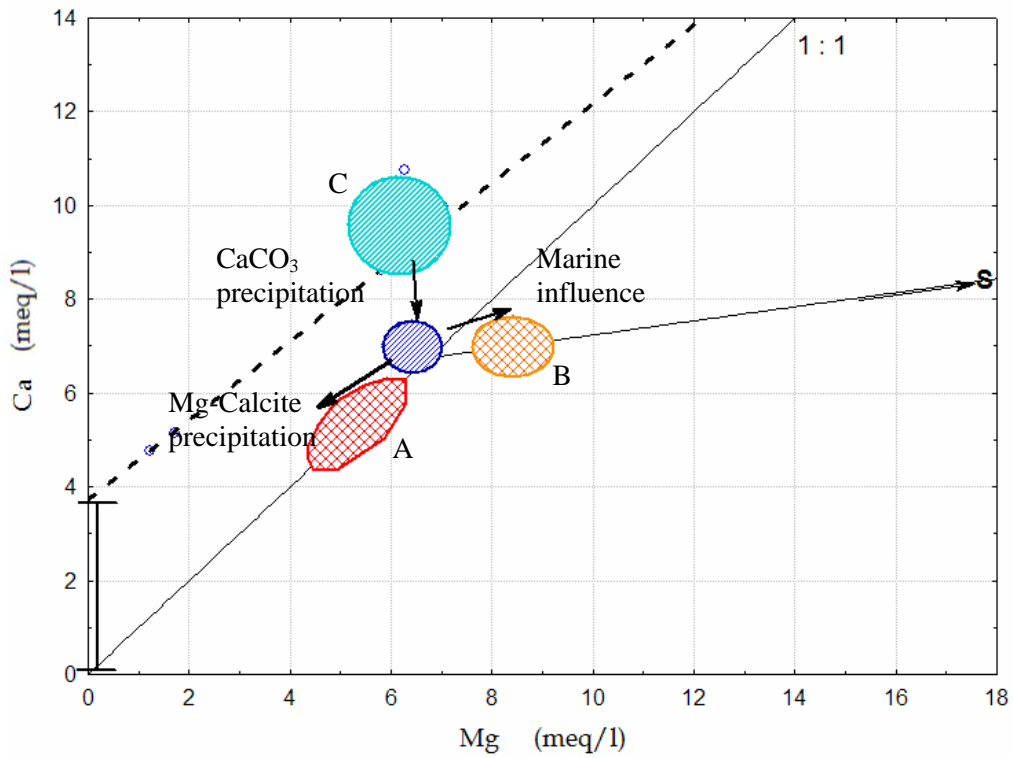


**Figure 4.2.1.2** Schematic model clarifying Ca and Mg variations drainage and lake waters in different seasons

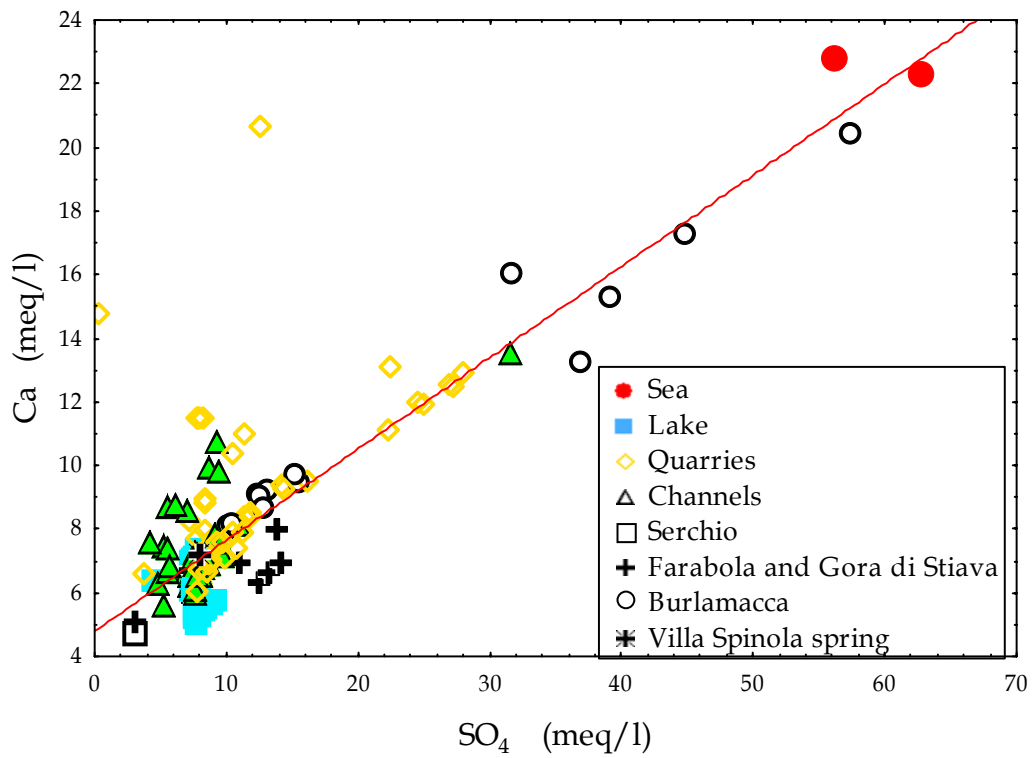


**Figure 4.2.1.3** Ca/SO<sub>4</sub> plot for the overall system.

The  $(Ca+Mg)$  vs  $(SO_4+HCO_3)$  diagram (Figure 4.2.1.4) shows a calcium and magnesium excess, from sources other than carbonates and gypsum, mainly in samples from the Burlamacca channel and the quarries. Samples from the lake, the agricultural network, the Serchio river and the Gora di Stiava stream have a  $\frac{Ca+Mg}{SO_4+HCO_3}$  ratio close to 1, except the samples collected in the lake during the summer 2002, which seem to have a small cation excess, probably due to marine inflow. Dissolution of calcite, dolomite or gypsum releases Ca, Mg,  $SO_4$  and  $HCO_3$  according to a  $(Ca + Mg)/(SO_4 + HCO_3)$  ratio equal to 1 on this diagram. We can suppose that  $CaCO_3$  precipitation (Figure 4.2.1.5) from waters like Barra and Fossa Nuova channels shifts their chemical composition towards that of lake samples, as indicated by full line in Figure 4.2.1.5.

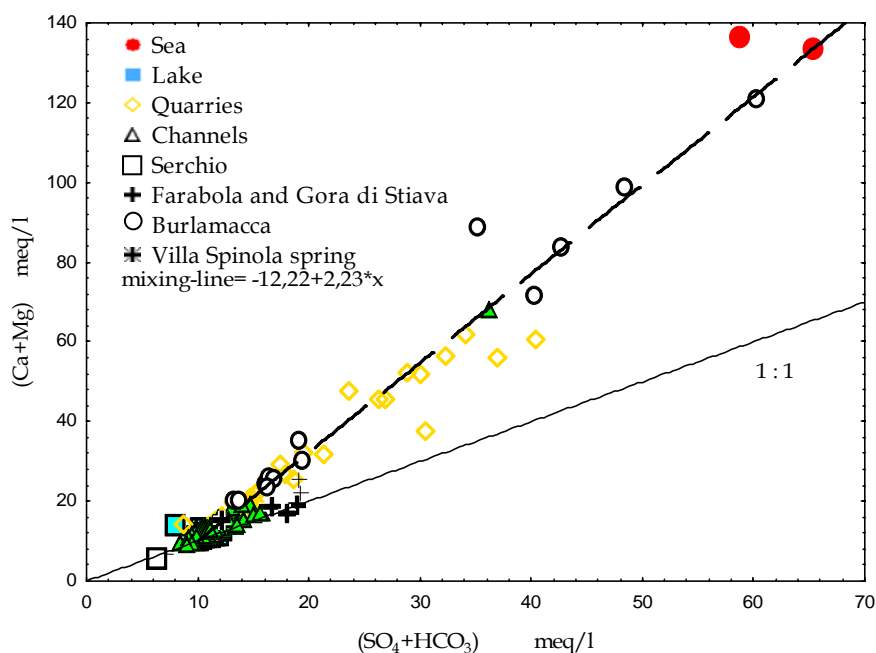


**Figure 4.2.1.4**  $(Ca+Mg)$  vs  $(SO_4+HCO_3)$  plot for the overall system. The 1:1 line (continuous line) and the regression line for the samples from the Burlamacca channel, quarries and sea (dotted line) are reported

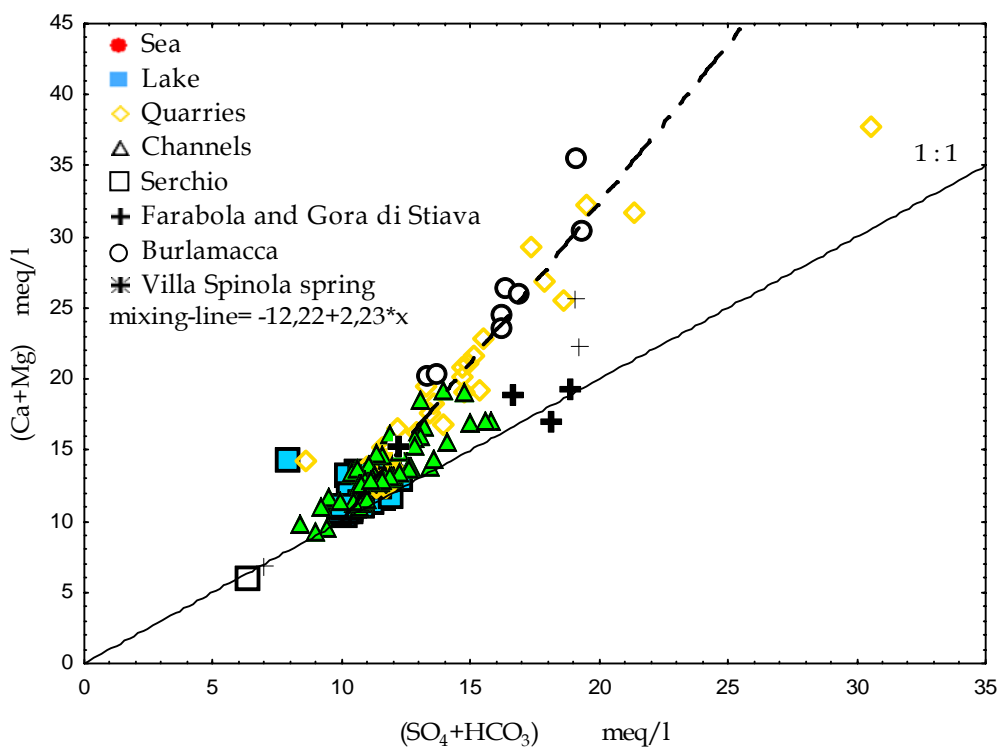


**Figure 4.2.1.5** Enlargement of the Figure 4.2.1.4



We observed that sodium and chloride concentrations generally increase along the flow paths towards the sea water and that such an increase is abrupt along the Burlamacca channel and the excavation area. In the Langelier-Ludwig square diagram with  $\text{HCO}_3\%$  as x-axis (Figure 4.2.1.6), a calculated mixing line between seawater and waters like the Fossa Nuova and the Barra channels is reported. These channels are selected as end-members of the agricultural network because they drain, naturally or mechanically, the agriculture area and represent the major inflows in the lake. The majority of the samples fall between the two mixing lines, even if some samples plot away from these two trends.

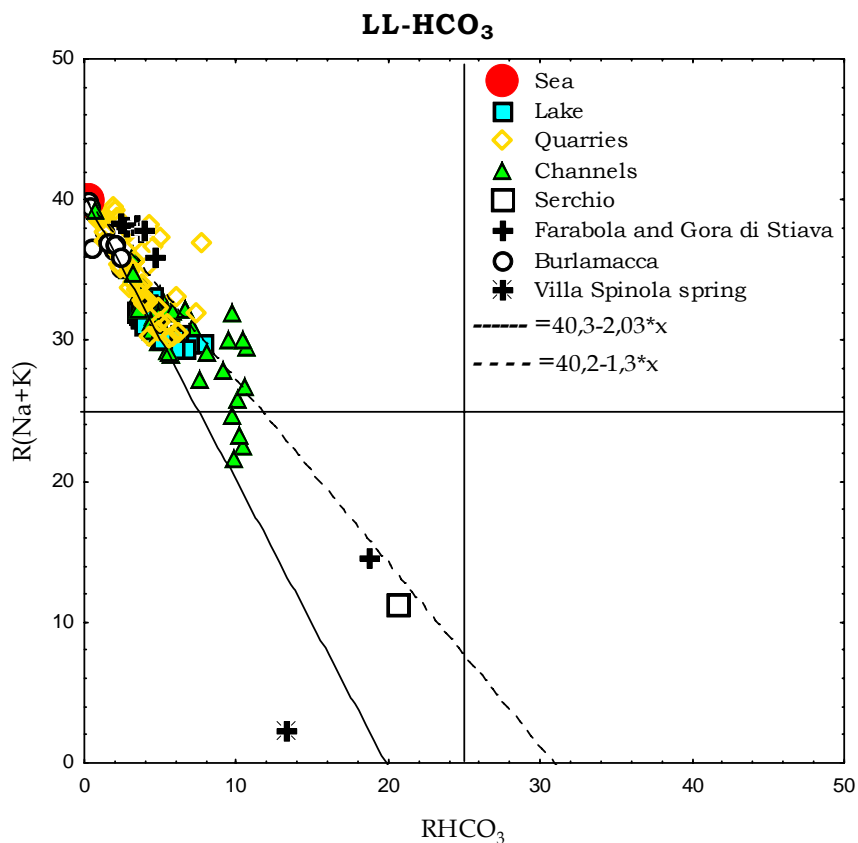


**Figure 4.2.1.6** In this LL-HCO<sub>3</sub> diagram are reported the theoretical mixing lines between sea water and (1) the agricultural water drainage of the Barra channel (dotted line) and (2) the runoff from the southern pedemontana area of Fossa Nuova (continuous line)

The good correlation ( $r^2=0.98$ ) between Cl and Br (Figure 4.2.1.7) for the samples from the quarries, the Burlamacca channel and sea water outlines and confirms the occurrence of seawater intrusion along the Burlamacca channel up to the excavation area. The diagram of Cl/Br vs Cl (Figure 4.2.1.8) allows one to distinguish the following two groups of samples: a) samples with a molar Cl/Br ratio near the seawater value (i.e., 660) and high chloride content and b) samples with a ratio greater than seawater value and low chloride content. Some samples from Burlamacca channel have a Cl/Br ratio  $> 660$ , due to either a chloride excess or a bromide defect with respect to seawater composition. As samples were collected in the urban area of Viareggio where there are industrial and urban wastes, chloride pollution is to be the most likely explanation.

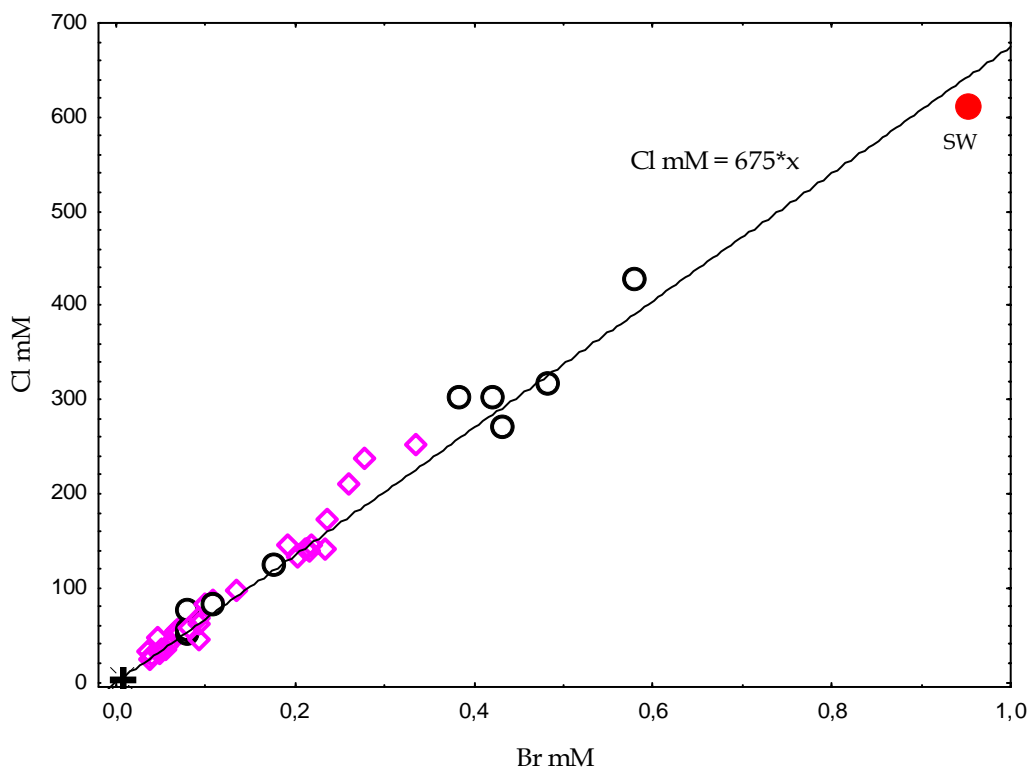


**Figure 4.2.1.7** Cl vs Br plot for samples from the Burlamacca channel (○), seawater (SW, ●), the excavation area (◇) and the Gora di Stiava stream (+)

For samples of the Massaciuccoli lake and the agricultural network, geochemical processes are complex because of interaction with vegetation, phytoplankton, agricultural basin characterized by peat soil, animal manure and urban wastes. For these samples the Cl/Br variations cannot be explicated by chloride variation alone, since the Cl/Br ratio correlates with the bromide content (Figure 4.2.1.9).

First it must be underscored that the diagram does not show clear trends, but each sample results by interaction of various processes occurring in that site. This is a typical example of the complexity of bromide geochemistry which prevents to formulate accurate explications. However, we try to advance some hypotheses about the processes prevailing at each site, underlining the necessity of further detailed studies. We can hypothesize: 1) a decrease in bromide concentration owing to organic uptake and plant assimilation or 2) an increase in bromide content caused by animal waste or release by peat soil.

Despite most samples collected during summer 2002 have a ratio near 660, suggesting sea water intrusion, the mid lake sample (L15-02) has a higher Cl/Br ratio. Therefore, there are other processes influencing bromide distributions in the lake. In particular, the sample collected during the spring 2005 and summer 2002 has a Cl/Br ratio quite constant (1124 and 1178, respectively). Considerable assimilation of bromide by green plants is now well documented (Whitmer *et al.*, 2000) and the high phytoplankton mass that is present in the lake during the summer and spring periods (Simoni *et al.*, 1999; 2002) may be a possible bromide sink. Putschew *et al.* (2003) point out that phototrophic organisms are responsible for the formation of adsorbable, organically-bound bromine (AOBr) in lake waters. This process causes decreasing bromide concentration and consequently increasing Cl/Br ratio.

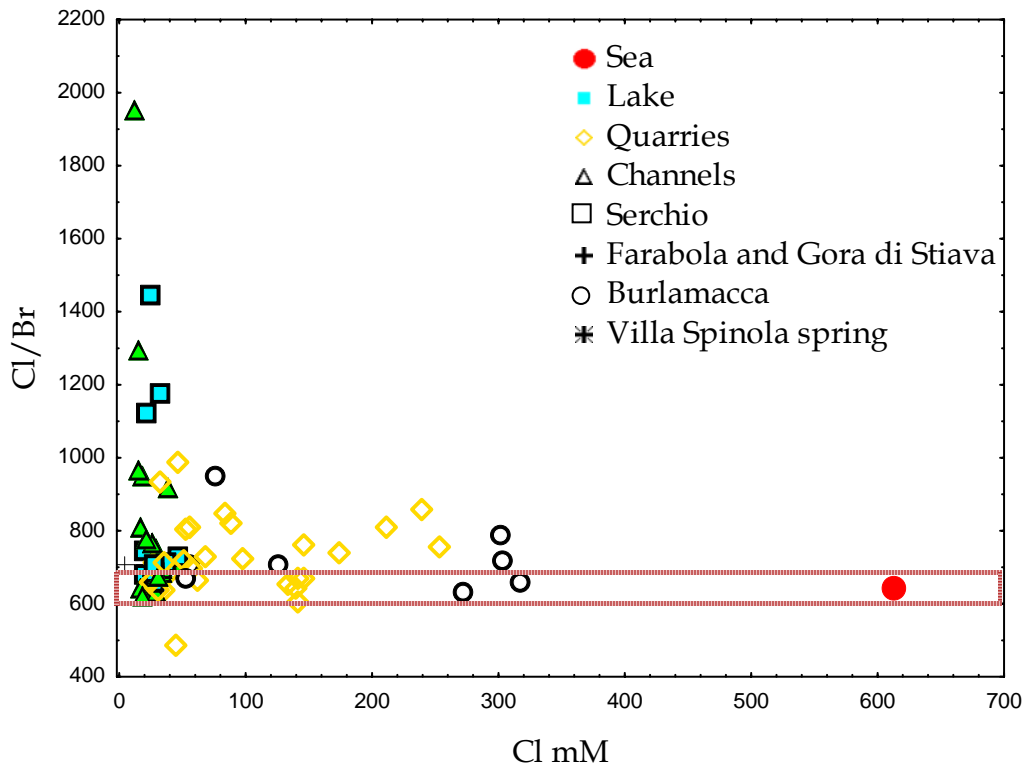


**Figure 4.2.1.8** The diagram describes the Cl/Br molar ratio variation with respect to the chloride content of the samples of the studied area. The band underlines the range of variation of the Cl/Br ratio for seawater

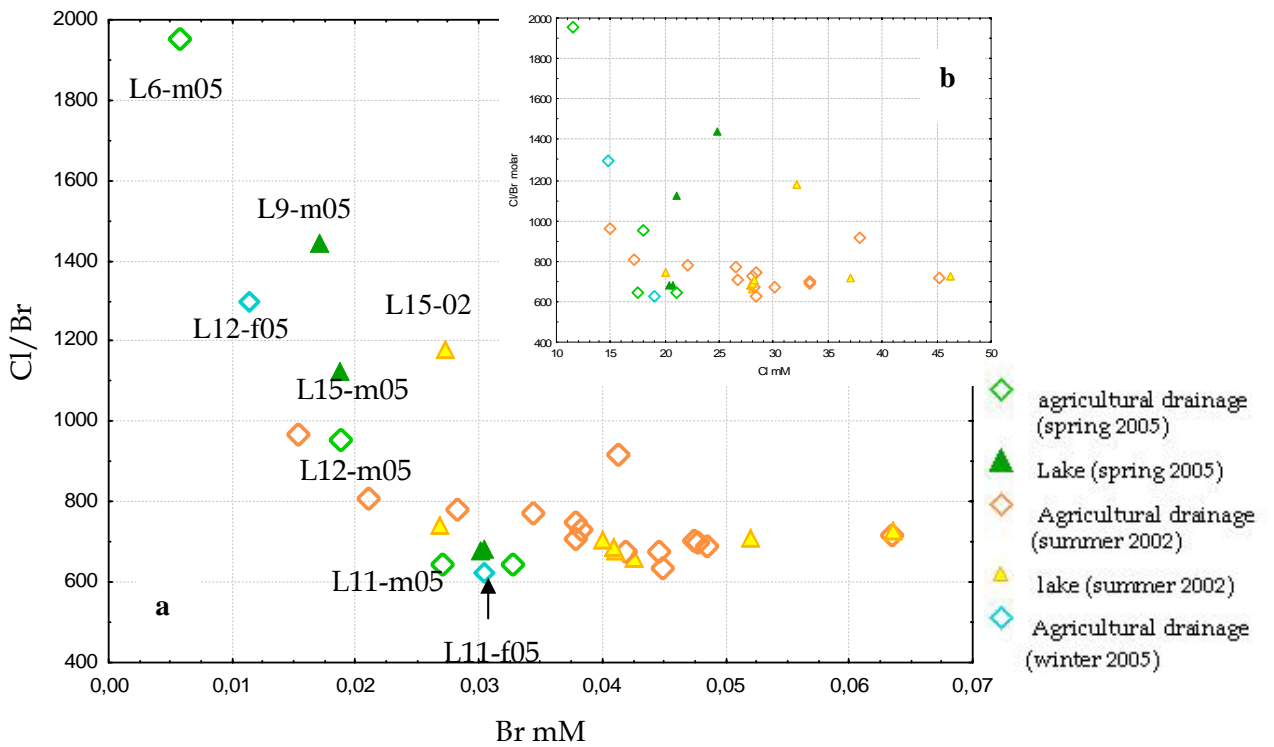


**Figure 4.2.1.9** Distribution of Cl/Br ratio against (a) the bromide content for the lake and agricultural drainage samples and (b) chloride. Seasonal differences are highlighted

Samples collected within the agricultural network have different Cl/Br ratios. In particular, the sample collected from the Barra drainage, upstream of the pump stations, has constantly lower Cl/Br molar ratios and higher bromide contents with respect to the sample collected downstream of these stations (L12-m05), suggesting a source of bromide both by waste and peat release. Besides, sample L12-m05 has a greater DOC content than L11-m05 but a lower Br content, suggesting the probable effect of dissolved organic matter which forms AOBr (Figure 4.2.1.10).

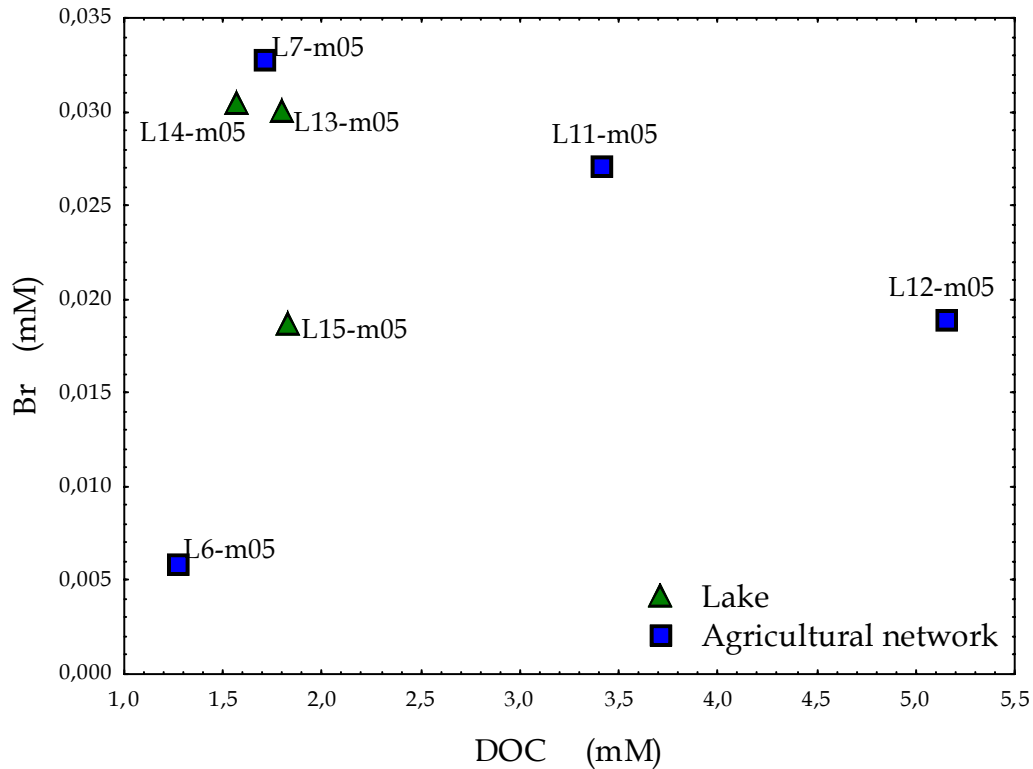


**Figure 4.2.1.10** Br content and dissolved organic carbon (DOC) for some samples of lake and agricultural network during spring period

Hudak and Paul (2003) reported Cl/Br ratios from 79 to 377 for animal leachate ranging. Therefore contamination by animal waste can lower the Cl/Br ratio. The Barra channel receives upstream of the pump stations natural drainage from agricultural areas rich in peat soil. Massaciucoli peat contains 93  $\mu\text{gBr/g}_{\text{dry weight}}$  (Summa and Tateo, 1999) which can be released during the wet season. Laboratory analysis of a leachate from a peat (processing the soil with deionised water, in 1: 50 proportion, for 12h) underlines a release of chloride and bromide with a low molar ratio, 56. Gerritse and George (1988) observed that degradation of soil organic matter lowers the Cl /Br molar ratio in soil water down to 23.

#### 4.2.2 Processes affecting carbon content

Chemistry of carbonate and calcium in most lakes involves essentially two reactions: calcite precipitation and photosynthesis-respiration processes (Sigg *et al.*, 1994; Gaillard, 1995). Saturation indices (SI) for calcite and dolomite for the Massaciucoli lake and agricultural network are generally significantly higher than 1, indicating considerable supersaturation. These elevated saturation indices show a seasonal variation for lake waters (Figure 4.2.2.1), with the highest values during the summer period and the lowest ones during the winter period. Highest SI values, associated with lowest pCO<sub>2</sub> concentrations and highest pH values are observed in summer lake samples, pinpointing the occurrence of the most intense primary production (Wachniew and Rozanski, 1997). The highest supersaturations are typical of mesotrophic lakes (Kuchler-Krischun and Kleiner, 1990); for instance, Wachniew and Rozanski (1997) observed a 7.5-fold supersaturation with respect to calcite in lake Gosciuz, a mid-latitude mesotrophic lake.

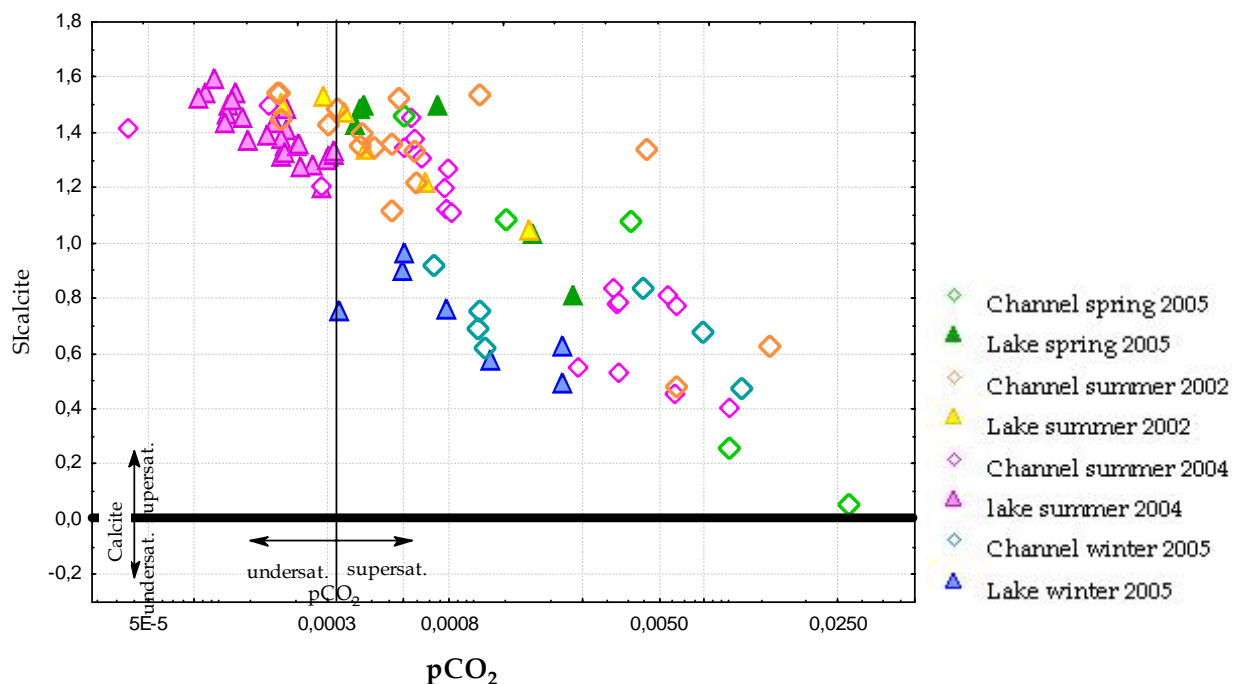


**Figure 4.2.2.1** Saturation index (SI) for calcite is plotted against pCO<sub>2</sub> reported in logarithm scale. Undersaturation and supersaturation for CO<sub>2</sub> refers to equilibrium with the atmosphere

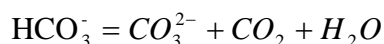
Concentration of CO<sub>2</sub>(aq) were calculated from alkalinity and pH data, considering the temperature dependencies for the equilibrium constants K<sub>CO2</sub>, K<sub>1</sub>, and K<sub>2</sub> regulating the equilibrium between dissolved inorganic carbon species (Plummer and Busenberg, 1982). Values of apparent CO<sub>2</sub> pressure (pCO<sub>2</sub>) were calculated by means of the simple equation:

$$pCO_2 = K_{CO_2} / H_2CO_3$$

considering the temperature dependence of K<sub>CO2</sub> given by Langmuir (1997). The accuracy of these calculations is mainly controlled by the errors on pH and alkalinity.

Dissolved inorganic carbon in lakes (DIC = H<sub>2</sub>CO<sub>3</sub>\* + HCO<sub>3</sub><sup>-</sup> + CO<sub>3</sub><sup>2-</sup>) is derived from various sources (Figure 4.2.2.2), including the atmospheric CO<sub>2</sub>, the oxidized derivatives of carbon compounds produced through microbial mineralization of autochthonous and allochthonous organic matter, and geologically-derived carbon from the watershed delivered by runoff and groundwater inflow (Striegl *et al.*, 2001). Lakes often become greatly undersaturated in CO<sub>2</sub> during photosynthesis because of CO<sub>2</sub> assimilation is faster than resupply by gas exchange from the

atmosphere (Stumm and Morgan, 1996). In general, addition or removal of CO<sub>2</sub> has no direct effect on alkalinity, as long as the equilibrium reaction:



is effective, but these processes affected pH and are responsible for the significant diurnal changes in pH that can be observed in ponds and small lakes. Plant growth also requires the uptake of nitrogen and phosphorus, which affects both pH and alkalinity. These processes, which involve the assimilation of cations and anions such as NH<sub>4</sub><sup>+</sup> and NO<sub>3</sub><sup>-</sup>, affect the alkalinity as a result of the uptake or release of H<sup>+</sup> (or OH<sup>-</sup>) that is required to maintain the charge balance (Stumm and Morgan, 1996). Goldman and Brewer (1980) have examined the alkalinity produced in cultures of marine algae because of nitrate consumption during photosynthesis. Transfer of soil water and agricultural drainage into adjacent water bodies can have significant effects on these aquatic ecosystems. The major reactions and their effects on pH and alkalinity are summarized in Table 4.2.2.1.

**Table 4.2.2.1** Effects on alkalinity of reactions occurring during photosynthesis, respiration and weathering and other redox reactions of geochemical interest (after Hutchhinson, 1957; Stumm and Morgan, 1996; Van Cappellen and Wang, 1996)

PROCESSES	Δ [Alk]
<u>Photosynthesis and respiration:</u>	
106CO <sub>2</sub> + 16NO <sub>3</sub> <sup>-</sup> + HPO <sub>4</sub> <sup>2-</sup> + 122H <sub>2</sub> O+ 18H <sup>+</sup> $\xrightarrow{\text{fotos}}$ [ C <sub>106</sub> H <sub>263</sub> O <sub>110</sub> N <sub>16</sub> P ]+ 138O <sub>2</sub> <small>seaweeds</small>	Increase
[ C <sub>106</sub> H <sub>263</sub> O <sub>110</sub> N <sub>16</sub> P ]+ 107O <sub>2</sub> + 14H <sup>+</sup> $\xrightarrow{\text{resp}}$ 106CO <sub>2</sub> + 16NH <sub>4</sub> <sup>+</sup> + HPO <sub>4</sub> <sup>2-</sup> + 108H <sub>2</sub> O	Increase
[ C <sub>106</sub> H <sub>263</sub> O <sub>110</sub> N <sub>16</sub> P ]+ 424Fe(OH) <sub>3</sub> + 862H <sup>+</sup> → 424Fe <sup>2+</sup> + 16NH <sub>4</sub> <sup>+</sup> + 106CO <sub>2</sub> + HPO <sub>4</sub> <sup>2-</sup> +1166H <sub>2</sub> O	Increase
[ C <sub>106</sub> H <sub>263</sub> O <sub>110</sub> N <sub>16</sub> P ]+212MnO <sub>2</sub> +398H <sup>+</sup> →212Mn <sup>2+</sup> +16NH <sub>4</sub> <sup>+</sup> +106CO <sub>2</sub> +HPO <sub>4</sub> <sup>2-</sup> +298H <sub>2</sub> O	Increase
<u>Redox processes</u>	
-NO <sub>3</sub> <sup>-</sup> + H <sub>2</sub> O+ 2H <sup>+</sup> → NH <sub>4</sub> <sup>+</sup> + 2O <sub>2</sub>	+2 eq
-5CH <sub>2</sub> O+ 4NO <sub>3</sub> <sup>-</sup> + 4H <sup>+</sup> → 5CO <sub>2</sub> + 2N <sub>2</sub> + 7H <sub>2</sub> O	+4 eq
-H <sub>2</sub> S+ 2O <sub>2</sub> → SO <sub>4</sub> <sup>2-</sup> + 2H <sup>+</sup>	+2 eq
- SO <sub>4</sub> <sup>2-</sup> + 2CH <sub>2</sub> O+ 2H <sup>+</sup> →2 CO <sub>2</sub> + H <sub>2</sub> S+ H <sub>2</sub> O	+2 eq
-Fe(OH) <sub>3</sub> + 2 SO <sub>4</sub> <sup>2-</sup> + 4H <sup>+</sup> → FeS <sub>2(s)</sub> + 15/4 O <sub>2</sub> + 7/2 H <sub>2</sub> O	+4 eq
<u>Weathering:</u>	
-CaCO <sub>3(s)</sub> + 2H <sup>+</sup> →Ca <sup>2+</sup> + CO <sub>2</sub> +H <sub>2</sub> O	+2 eq
- CaAl <sub>2</sub> Si <sub>2</sub> O <sub>8(s)</sub> + 2H <sup>+</sup> →Ca <sup>2+</sup> +H <sub>2</sub> O+ Al <sub>2</sub> Si <sub>2</sub> O <sub>5</sub> (OH) <sub>4(s)</sub>	+2 eq
- KAlSi <sub>3</sub> O <sub>8(s)</sub> + H <sup>+</sup> + 9/2 H <sub>2</sub> O → K <sup>+</sup> + H <sub>2</sub> O+ 2H <sub>4</sub> SiO <sub>4</sub> + 1/2 Al <sub>2</sub> Si <sub>2</sub> O <sub>5</sub> (OH) <sub>4(s)</sub>	+1 eq

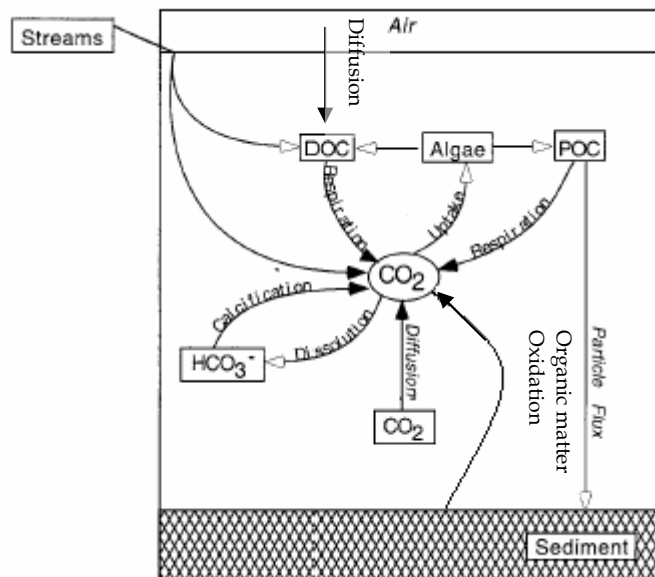


**Figure 4.2.2.2** Conceptual model of processes involved in the carbon cycle. Solid arrows denote  $\text{CO}_2$  sources. The unbalanced 'calcification' and 'dissolution' stand for the reaction  $\text{Ca}^{2+} + 2 \text{HCO}_3^- \leftrightarrow \text{CaCO}_3 + \text{CO}_2 + \text{H}_2\text{O}$ . (Neumann *et al.*, 2001 modified)

The pH/p $\text{CO}_2$  diagram (Figure 4.2.2.3) points out the seasonality of the carbon biogeochemical cycle in the lake system, with summer samples characterized by the highest pH values and the lowest p $\text{CO}_2$  values. Under such high pH circumstances, the input rate of  $\text{CO}_2$  into the lake is more likely to be enhanced by reactions of  $\text{CO}_2$  to form  $\text{HCO}_3^-$  (Stumm and Morgan, 1996). This is correlated to the

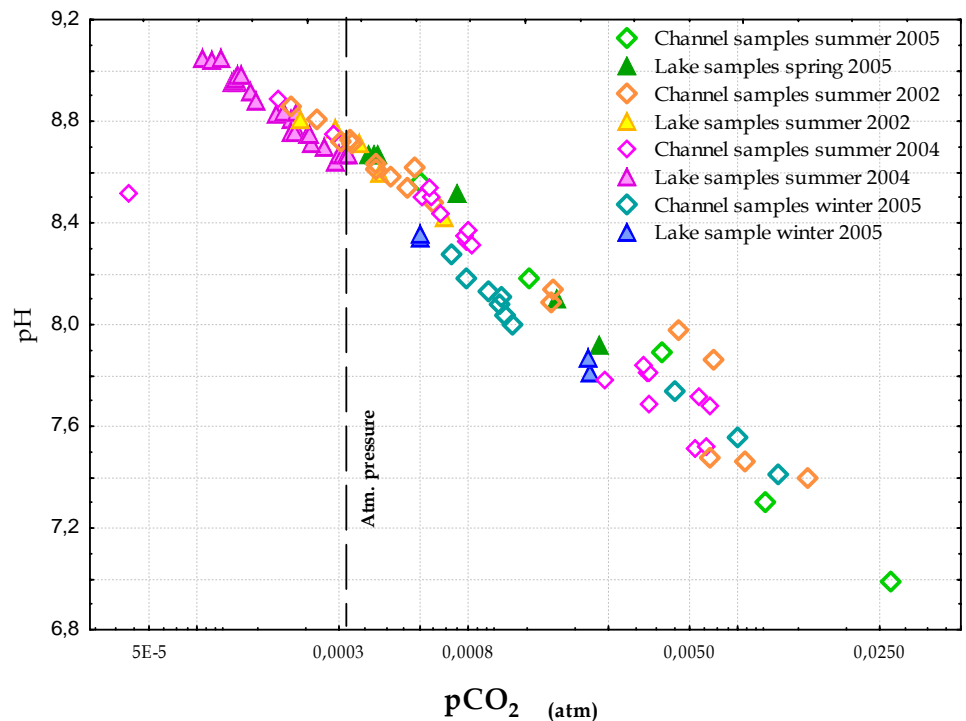


**Figure 4.2.2.3** pH/p $\text{CO}_2$  diagram for lake and agricultural drainage samples. The atmospheric pressure of  $\text{CO}_2$  ( $10^{-3.5}$  atm) is marked with a vertical dotted line

photosynthesis process which uptake  $\text{CO}_2$  from the water. The agricultural network experiences the highest p $\text{CO}_2$  values, although data are highly scattered, suggesting the occurrence of other reactions such as respiration processes. The decomposition of organic matter in presence of

dissolved oxygen (e.g., by oxygen-driven reduction) increases the carbon dioxide content of water and lowers its pH (Telmer and Veizer, 1999). Moreover, summer lake samples denote the lowest  $p\text{CO}_2$  and  $\text{HCO}_3^-$  contents, while channels have the highest  $p\text{CO}_2$  and bicarbonate contents (Figure 4.2.2.4).

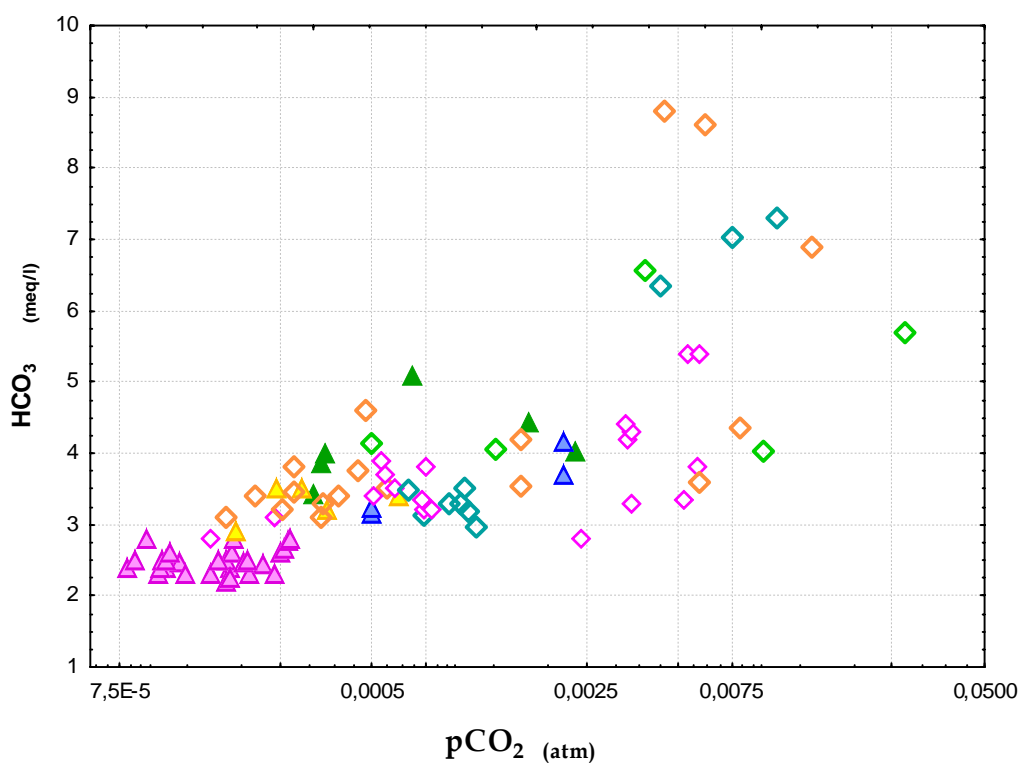


**Figure 4.2.2.4**  $\text{HCO}_3^-/\text{pCO}_2$  diagram for lake and agricultural drainage samples. For legend see Figure 4.2.2.3

An effective way of representing the interaction of respiration and photosynthesis with the aqueous system of interest is to consider the atmospheric  $p\text{CO}_2$  content ( $10^{-3.5}$  atm) as a reference value.  $p\text{CO}_2$  values near  $10^{-3.5}$  atm indicate equilibration with the atmosphere, while values above this threshold are indicative of  $\text{CO}_2$  overpressures, which trigger its transfer to the atmosphere. By the same token, values below this threshold imply undersaturation that causes absorption of atmospheric  $\text{CO}_2$ . By means of an analogous procedure, the partial pressure of atmospheric oxygen, calculated from temperature, quote and chlorinity, was converted to mg of  $\text{O}_2$  by using the Henry's law and then was subtracted from the measured oxygen concentrations. These oxygen differences indicate equilibrium at zero, oversaturation at positive and undersaturation at negative values. This procedure is used by Barth *et al.* (1999) to interpret the carbon cycle in aquatic ecosystems of Ontario. Assuming that oxygen oversaturation together with  $\text{CO}_2$  undersaturation is caused by photosynthesis and the inverse relationship by respiration, the quadrants in Figure 4.2.2.5 can be interpreted as follows: **A**: dominance of photosynthesis; and **B**: prevalence of respiration.

The points around the zero intersect in Figure 4.2.2.5 indicate that these water samples are close to the equilibrium with the atmosphere. In the agricultural drainage decomposition of organic matter prevails during the summer, while in the lake samples collected during the summer 2004, photosynthesis prevails and results in oversaturation of  $\text{O}_2$  and undersaturation of  $\text{CO}_2$ . The pattern of greater  $\text{O}_2$  consumption and  $\text{CO}_2$  production observed in lake in winter and in spring, when rainfalls are higher, could be the result of the decrease in photosynthesis activity and a higher availability of organic material decomposing.



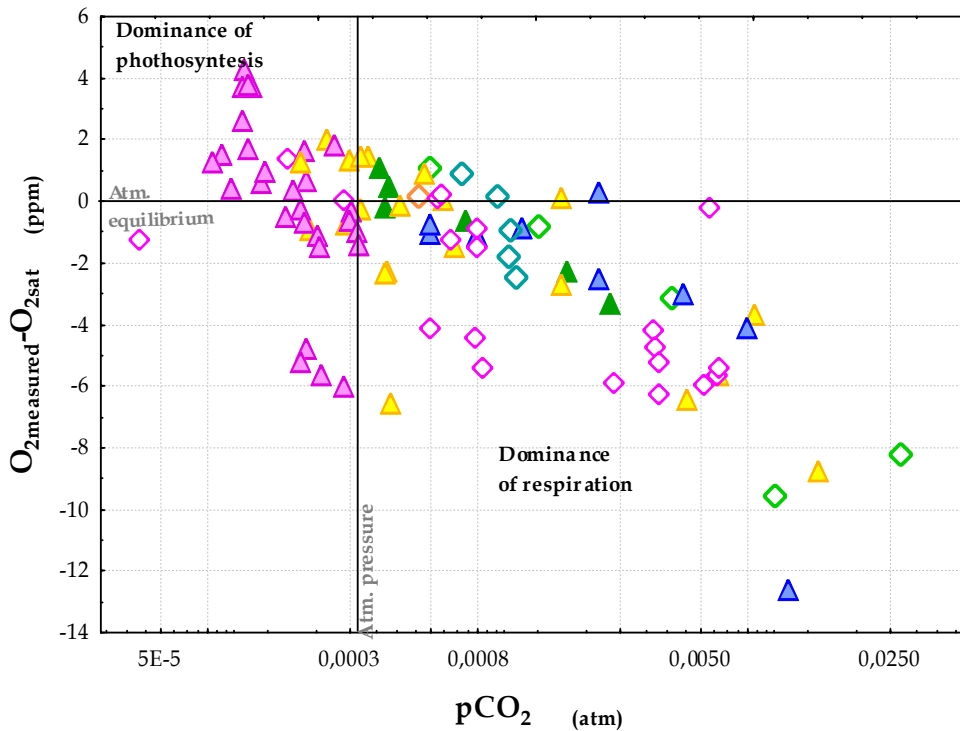
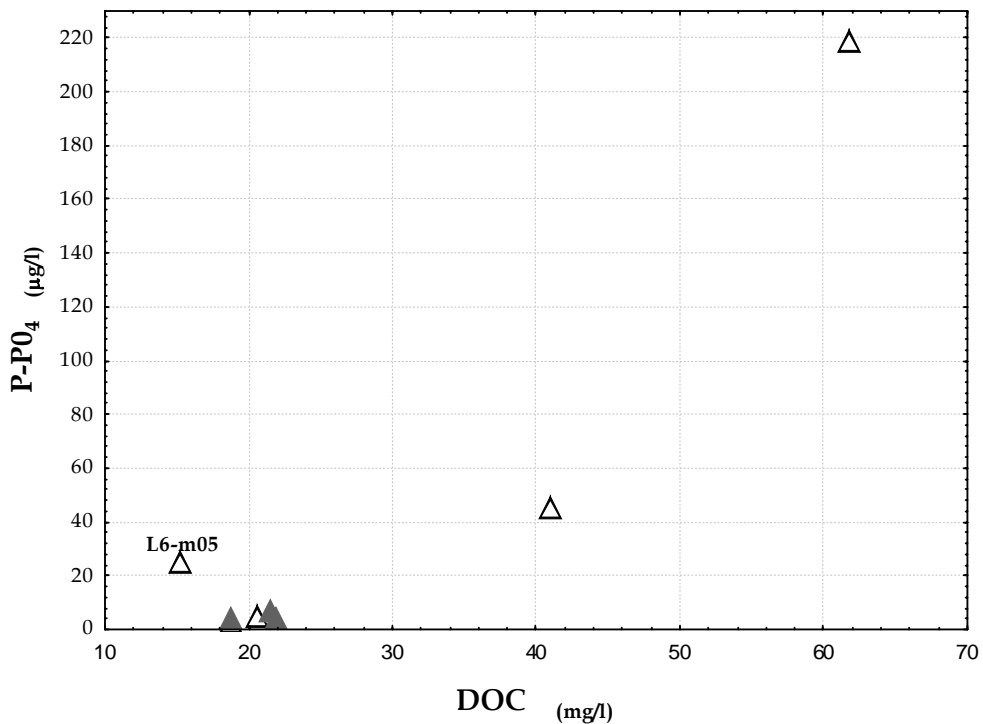


**Figure 4.2.2.5** Differences between the measured oxygen partial pressure and oxygen atmospheric value is reported against pCO<sub>2</sub> values. For legend see Figure. 4.2.2.2

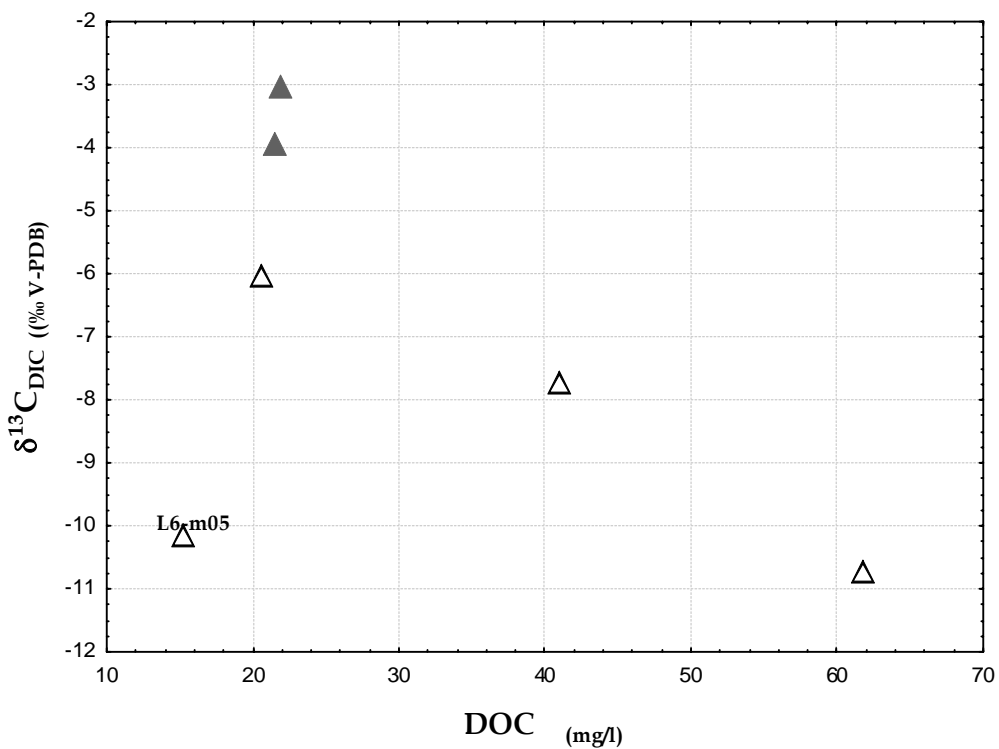
The Figure 4.2.2.6 underlines that lake samples are characterized by low levels of orthophosphate and dissolved organic carbon (DOC). This confirms the dominance of photosynthesis and related orthophosphate uptakes. When the respiration process becomes dominant, orthophosphate and dissolved organic matter increase, suggesting nutrient availability. The sample collected from a drainage channel (L6-m05) is characterized by a low level of DOC related to the PO<sub>4</sub> content. As the pCO<sub>2</sub> is quite elevated, the decomposition process seems to have already consumed all the organic matter.

Carbon cycling, through all the linkages sketched in Figure 4.2.2.2, involves equilibrium and kinetic fractionation of carbon isotopes (Romanek *et al.*, 1992; Zhang *et al.*, 1995; see Bade *et al.*, 2004 for a thorough review). It has long been recognized that lake metabolism plays an important role in influencing the isotope signature of DIC (Oana and Deevey, 1960). Preferential photosynthetic uptake of <sup>12</sup>C increases epilimnetic isotopic values of DIC ( $\delta^{13}\text{C}_{\text{DIC}}$ ) and decomposition of sinking organic matter decreases hypolimnetic  $\delta^{13}\text{C}_{\text{DIC}}$  values; these processes are recognized as major controls on water-column  $\delta^{13}\text{C}_{\text{DIC}}$  value. Bade *et al.* (2004) studied 72 lakes in Northern Wisconsin and the Upper Peninsula of Michigan and concluded that productivity and respiration control the  $\delta^{13}\text{C}_{\text{DIC}}$  values in surface waters of lakes. Increasing productivity should increase  $\delta^{13}\text{C}_{\text{DIC}}$ , whereas increasing respiration should decrease  $\delta^{13}\text{C}_{\text{DIC}}$ . Similarly,  $\delta^{13}\text{C}_{\text{DIC}}$  should be related to those factors controlling productivity and respiration in lakes, such as Total Phosphorus (TP) and dissolved organic carbon (DOC) (Carignan *et al.*, 2000; Prairie *et al.*, 2002; Hanson *et al.*, 2003). This data and models indicate that metabolism creates substantial variations in  $\delta^{13}\text{C}_{\text{DIC}}$  round the potential  $\delta^{13}\text{C}_{\text{DIC}}$  that is set by geochemical factors of the watershed. The diagram of  $\delta^{13}\text{C}_{\text{DIC}}$  vs DOC (Figure 4.2.2.7) for the studied area shows a negative correlation with lighter  $\delta^{13}\text{C}_{\text{DIC}}$  corresponding with higher DOC contents, underlining the dominance of respiration/decomposition of organic matter.

A drainage sample (L6-m05) is characterized by low  $\delta^{13}\text{C}_{\text{DIC}}$  and DOC content, confirming the presence of a degraded environment.

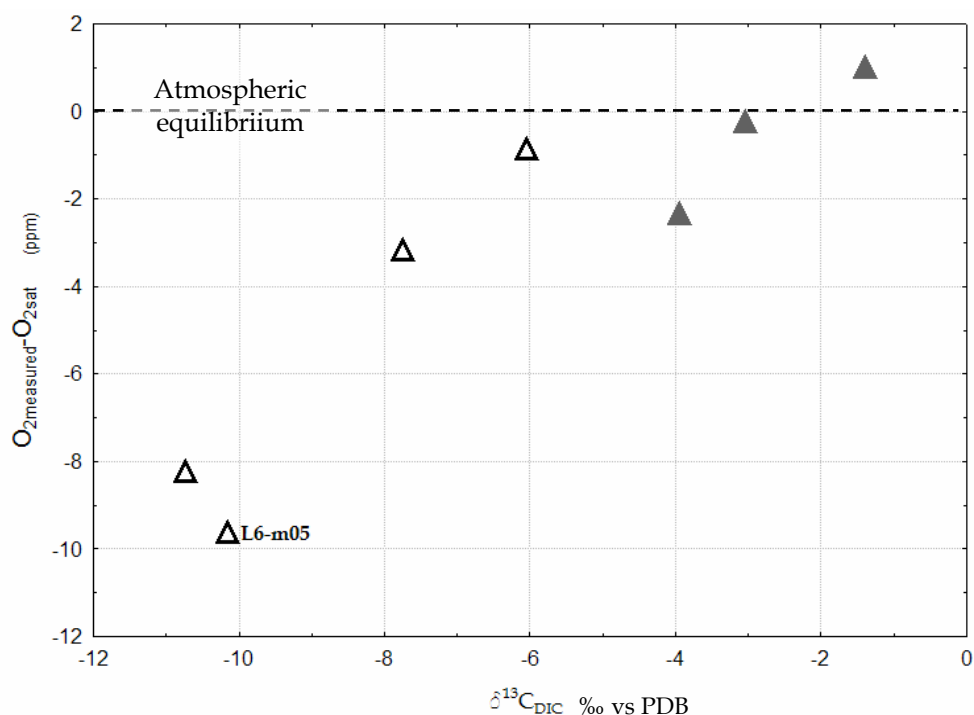


**Figure 4.2.2.6** Orthophosphate content against DOC for lake samples (closed triangle) and agricultural drainage (open triangle)



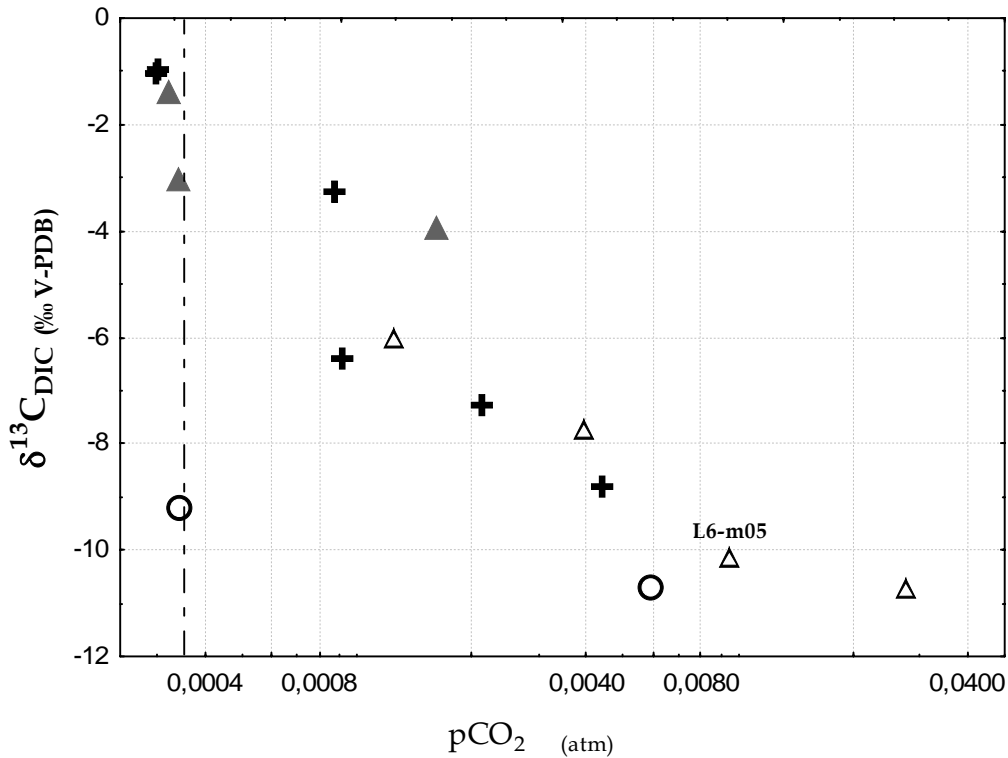
**Figure 4.2.2.7**  $\delta^{13}\text{C}_{\text{DIC}}$  against DOC for lake samples (closed triangle) and agricultural drainage (open triangle)

Figure 4.2.2.8 underlines that  $\delta^{13}\text{C}_{\text{DIC}}$  values correlate positively with oxygen contents and negatively with  $\text{CO}_2$  partial pressure (Figure 4.2.2.9). Samples from the lake where photosynthesis prevails have the highest  $\delta^{13}\text{C}_{\text{DIC}}$  values. In effect, direct oxidation of organic matter produces depleted biogenic  $\text{CO}_2$  with a  $\delta^{13}\text{C}_{\text{DIC}}$  close to that of labile organic matter, whereas photosynthesis enriches the  $\delta^{13}\text{C}_{\text{DIC}}$  (Mook and Tan, 1991) because algae preferentially remove light carbon from the DIC pool (Fry and Sherr, 1984). Atmosphere–water  $\text{CO}_2$  exchange is expected to modify the  $\delta^{13}\text{C}_{\text{DIC}}$  isotopic composition towards the equilibrium value with the atmosphere. The atmospheric  $\delta^{13}\text{C}_{\text{CO}_2}$  composition ranges from -6 to -8‰ PDB (Cerling *et al.*, 1991) and has an average of -7.5‰ PDB (Wachniew and Rozanski, 1997), but undergoes  $^{13}\text{C}$  enrichment after  $\text{CO}_2$  diffusion into water bodies (Zhang *et al.*, 1995). The equilibrium  $\delta^{13}\text{C}_{\text{DIC}}$  depends on both temperature and distribution of DIC species. Theoretical  $\delta^{13}\text{C}_{\text{DIC}}$  values for complete equilibration with atmospheric  $\text{CO}_2$  range from +1 to -2.65‰ PDB (Barth and Veizer, 1999; Telmer and Veizer, 1999).



**Figure 4.2.2.8** Differences between the measured oxygen content and oxygen atmospheric value is reported against  $\delta^{13}\text{C}_{\text{DIC}}$  for lake samples (closed triangle) and agricultural drainage (open triangle)

The carbon isotopic composition of the various plants ranges from ranges between -23 to -33‰ with average of -26‰ in the Calvin cycle (C3), while the carbon isotopic composition of Hatch-Slack (C4) plants ranges from -9 to -16‰ and average of -13‰ (Leman, 1972; Throughton, 1972; Allaway *et al.*, 1974). Depending on the organic source material for  $\text{CO}_2$  production and dissolution of calcite in soils, groundwaters result in  $\delta^{13}\text{C}_{\text{DIC}}$  values of -16‰, if the DIC originates from decay of C3 plants, and -13‰, if it results from decomposition of C4 plants like corn (Salomons and Mook, 1986). The vegetation on the Massaciuccoli watershed follows the C3 photosynthetic pathway, except in areas of intensive cultivation of maize, which follows the C4 photosynthetic pathway. In fact, in the agricultural channel  $\delta^{13}\text{C}_{\text{DIC}}$  values are closed to -11‰ and confirming the importance of the agricultural area in controlling the chemical and isotopic composition of lake waters.



**Figure 4.2.2.9**  $\delta^{13}\text{C}_{\text{DIC}}$  against  $\text{pCO}_2$  for lake sample (closed triangle), agricultural drainage (open triangle), Burlamacca channel (circle) and quarry (cross)

#### 4.2.3 Boron and Boron isotopes

Boron can be used as a tracer in aquatic systems because of its high solubility in aqueous solutions, measurable abundance in natural waters, and the lack of isotopic effects induced by evaporation, volatilization, and oxidation-reduction reactions (Bassett *et al.*, 1995).

Boron exhibits a wide range of concentration in geological environments, from a few ppb in rain (Fogg and Duce, 1985) to several hundreds mg/l in hydrothermal fluids. Except for comparatively rare magmatic environments, boron is always bonded to oxygen, forming both trigonal and tetrahedral complexes. In aqueous solution, boron primarily exists as 3-coordinate  $\text{B}(\text{OH})_3^0$  (boric acid) at acidic and weakly alkaline pHs and 4-coordinated  $\text{B}(\text{OH})_4^{-1}$  (borate) in strongly alkaline solutions (Culberson *et al.*, 1967).

Boron can be considered a conservative element in the oceans, where it occurs in constant proportion to Cl. Since mean concentration in open seawater (4.5 ppm; Uppstroem, 1974) is greater than in rivers and streams (0.01 to 0.2 ppm; Drever, 1981; Lemarchand *et al.*, 2000), relatively high concentrations of boron (B) can be considered as indicators of marine intrusion. Therefore, B and Cl are commonly used to constrain the salinity source and mixing processes between fresh groundwater and seawater. It should be stressed, however, that concentrations of B much higher than in seawater can be found in waters contaminated by pollution from industrial, domestic effluents (1 mg/l, Vengosh *et al.*, 1994), fly ash leachate (14 mg/l, Davidson and Basset, 1993), landfill leachate (7 mg/l, Eisenhut *et al.*, 1996; Eisenhut and Heumann, 1997) or animal manure (i.e., liquid hog manure 0.4 to 8.2 mg/l, Vincini *et al.*, 1994; Komor, 1997). Source apart, B concentration in some waters is related to leaching of rock, boric minerals and clay minerals.

For the Massaciucoli system, the B vs. Cl diagram (Figure 4.2.3.1) reveals a light alignment comprising the samples from the sea, the Burlamacca channel and the quarries. The regression line

is characterized by a good correlation coefficient ( $r^2=0.994$ ) and a slope of 0.0007, relatively close to the molar ratio 1: 8000 of seawater (Rosler and Langer, 1972).

Assuming a mixing model between seawater and freshwater, as previous discussed, for which composition is based on the local freshwaters feeding Burlamacca channel and the northern quarries (i.e. Gora di Stiava stream), calculated seawater percentage for different samples along Burlamacca channel is illustrated in the Figure 4.2.3.1. These values are derived considering Chloride concentrations, which are consistent with percentages calculated with other tracers, as illustrated in Table 4.2.3.1.

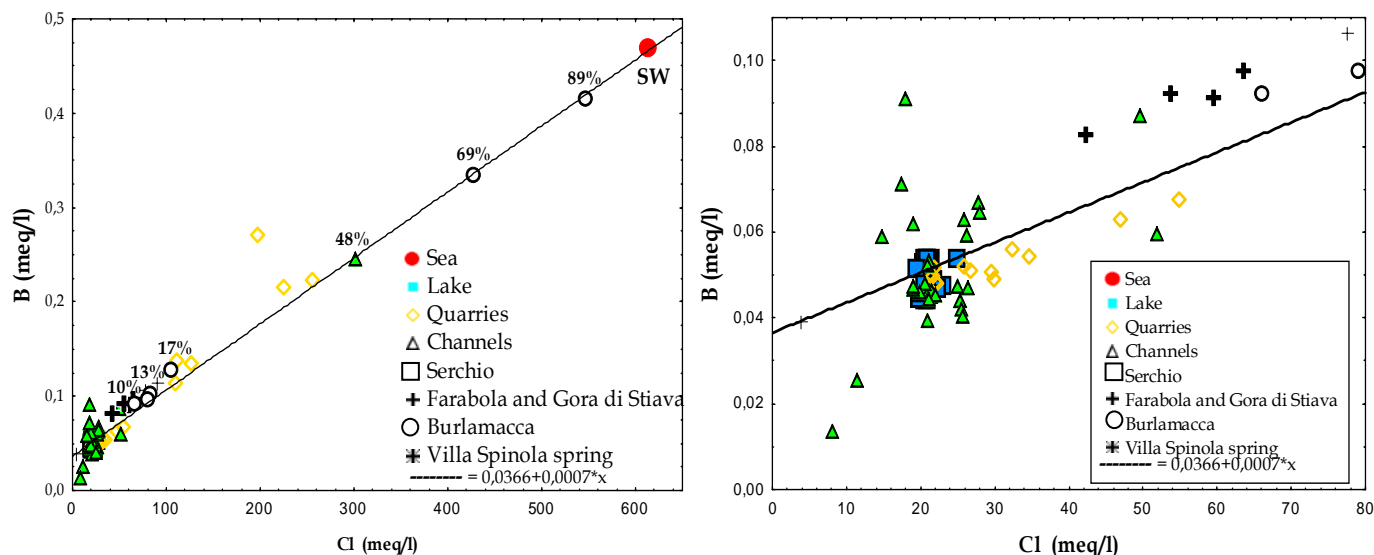


**Figure 4.2.3.1** B/Cl plot for all the samples of the studied system. The regression line for seawater, Burlamacca channel and quarries is reported.

**Table 4.2.3.1** Estimation of seawater percentage using different tracers

Sample	Distance from sea (k m)	Depth sampling (m)	%seawater			
			Cl	Na	Br	B
Bur1-05	0.56	-0.5	89±4	89±4		89±8
Bur2-05	0.95	-0.5	69±4	69±4		69±7
Bur4-05	1.6	-1.65	70±4		61±6	
Bur4-05	1.6	-0.5	13±3	13±3	11±5	15±6
Bur-02bis	1.6	-2	52±3	61±4	50±6	
Bur3-02	1.5	-0.4	49±3	44±3	45±5	
Bur6-05	2.6	-0.5	17±3	15±3		22±6
Bur5-05	2.2	-0.5	12±3	13±3		13±6
Bur7-02	3.6	-1.2	44±3	47±3	45±6	
Bur7-02	3.6	-0.6	12±3	12±3	8±5	
Bur7-05	3.6	-0.5	10±3	11±3		13±5
SR14-sp05	4.05	-14	41±3	38±3	32±5	44±6
SR10-sp05	4.05	-10	36±3	39±3		42±6
SR7-sp05	4.05	-7	32±3	32±3	34±5	55±6
SR3-sp05	4.05	-3	18±3	18±3		24±6
SR2.7-sp05	4.05	-2.7	8±3	9±3		7±6
SR1.5-sp05	4.05	-1.5	4±3	5±3		3±5

Conversely, lake and drainage waters have B/Cl ratios significantly different from the seawater value. This underlines that the influence of seawater is neither the only process nor the main one accounting for the water chemistry of the lake. We could hypothesize that in its lake and in the drainage other processes are essential, such as: concentration variations for mixing or contamination processes, leaching of soil, reaction with clay minerals and complexing with organic matter.

Anthropogenic inputs can be considered to explain the deviation in B/Cl ratio and B concentration in drainage samples. Boric acid and borate minerals are widely utilized in a number of industrial applications such as glass and porcelain manufacture, production of leather, carpets, cosmetics, and photographic chemicals, flame-proofing compounds, corrosion inhibitors and antiseptics, wire drawing, welding and brazing of metals. Boron is also used in cleaning products, agrochemicals and insecticides. The increase in B/Cl ratio in lake and channel waters can be expressed as follows:

$$[B/Cl]_{\text{sea}} = 0.0007$$

$$[B/Cl]^* = 0.0007 + A$$

where A is the chemical deviation factor with respect to the seawater ratio, the asterisk indicates the B/Cl ratio of Massaciucoli water, and  $[B/Cl]_{\text{sea}}$  is the ratio in sea water with a mean dissolved chloride and boron of 612 and 0.47 meq/l, respectively. Assuming that the B/Cl ratio is constant both in sea water and in meteoric waters we can write:

$$A = (B/Cl)^* - 0.0007$$

where  $(B/Cl)^*$  is the ratio measured in the samples.

The A factor was calculated and plotted in a diagram of A vs (B/Cl) (Figure 4.2.3.2). The points lay obviously along a straight line, but it is interesting to underline that the samples from the agricultural network are characterised by the highest deviation values, while the samples from the sea and the Burlamacca channel exhibit the lowest ones. This suggests an extra source of boron, related to the agricultural practices, as it is a micronutrient, apart from seawater. In particular, samples collected during spring and winter show the highest boron excess, reflecting the seasonality of agricultural practices and runoff intensity. The Gora di Stiava sample is characterized by an anomalously high deviation factor, which is probably due to sewage contamination, in line with its location in an urban area. Lake samples are between the agricultural pool and the marine pool, even if nearest to the first one.

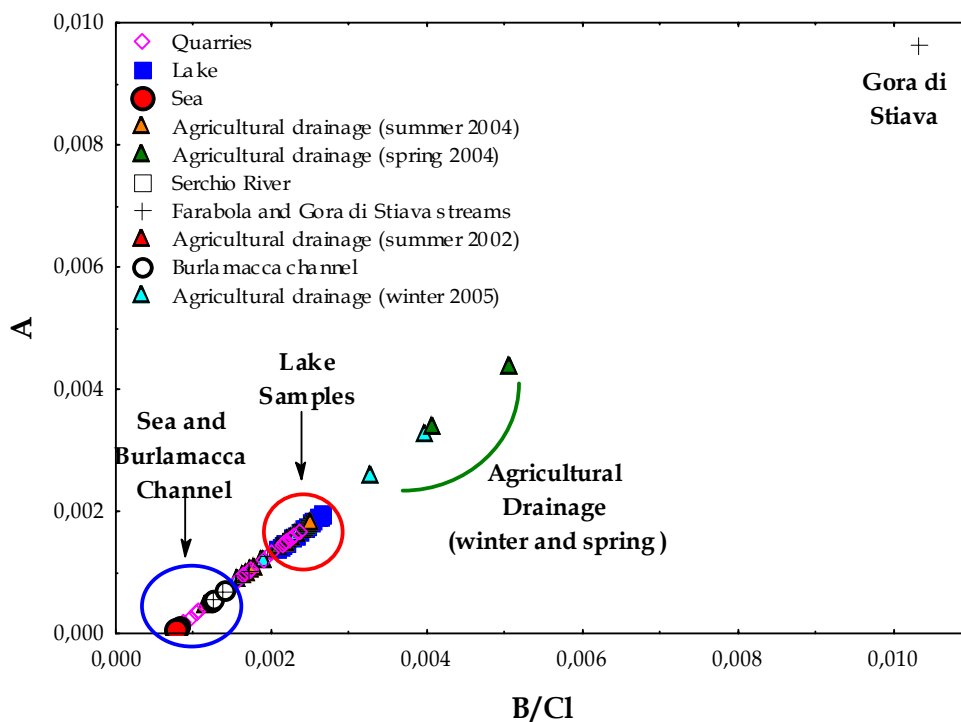


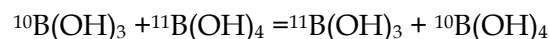
Figure 4.2.3.2 Deviation factor A against B/Cl ratio. The different types of samples are indicated

In order to identify and discriminate between the different boron sources, boron isotopes were investigated.

The large relative mass difference between the two stable isotopes of B,  $^{10}\text{B}$  and  $^{11}\text{B}$ , leads to a wide range of B isotope variations in nature, with  $\delta^{11}\text{B}$  ranging from  $-16$  to  $90\%$  (Barth, 1993). This implies significant contrasts between different B sources and, therefore, the possibility to distinguish them.

Boron isotopes of fluids are mainly controlled by the composition of the boron sources, mixing of fluids from different reservoirs, and fractionation of boron isotopes related to differential uptake of the two dominant aqueous boron species, undissociated boric acid  $\text{B}(\text{OH})_3$  (trigonal) and the borate anion  $\text{B}(\text{OH})_4$  (tetrahedral), whose relative abundances are a sensitive function of pH, as well as salinity and cation concentrations (Spivack and Edmond, 1987; Harshey *et al.*, 1986).  $^{11}\text{B}$  separates preferentially into dissolved boron in a solution (mainly composed of undissociated boric acid  $\text{B}(\text{OH})_3$ ), whereas  $^{10}\text{B}$  is preferentially incorporated in the form of the tetrahedral species in the solid phase. The isotope fractionation factor between boric acid and borate anion in aqueous solution at  $25^\circ\text{C}$  ( $\alpha_{\text{V-III}} = [^{11}\text{B}/^{10}\text{B}]_{\text{IV}}/[^{11}\text{B}/^{10}\text{B}]_{\text{III}}$ ) is equal to 0.981 (Kakahana *et al.*, 1977).

During interaction of fluids with sediments boron can be taken up by clay minerals. The uptake is proportional to the concentration of boron in the solution, pH, salinity, clay content and mineralogy, clay particle size, organic carbon, cation exchange capacity, and nature of exchangeable cation. Isotopic fractionation of boron isotopes occurs via an equilibrium exchange process between the two dominant aqueous boron species because of their differential uptake during adsorption of boron onto active surfaces, mainly by displacement of  $\text{H}_2\text{O}$  and  $\text{OH}$  from surface sites of  $\text{Al}_2\text{O}_3$  phases. Since the affinity of the clay edges for the  $\text{B}(\text{OH})_4$  ion is much stronger than for  $\text{B}(\text{OH})_3$ , adsorption increases with increasing pH values, up to pH of maximum adsorption (Spivack and Edmond, 1987). The isotopic fractionation of boron is controlled by the exchange reaction of its species, given by:



Since the  $\text{B}(\text{OH})_3$  species is enriched in  $^{11}\text{B}$  relative to the  $\text{B}(\text{OH})_4$  species due to larger isotopic reduced partition function ratios, preferential removal of the  $^{10}\text{B}(\text{OH})_4$  ion onto the clay edges results in isotopic fractionation in which dissolved boron (predominantly composed of  $\text{B}(\text{OH})_3$  species) is enriched in  $^{11}\text{B}$  (Palmer *et al.*, 1987). Hence, during an adsorption process,  $^{10}\text{B}$  would preferentially enter the adsorbed boron complex, whereas dissolved boron would become enriched in  $^{11}\text{B}$  relative to  $^{10}\text{B}$ , accompanied by removal of elemental boron from solution. Adsorption-related fractionation of boron isotopes is exemplified by the pronounced  $^{11}\text{B}$  enrichment of seawater (worldwide constant  $\delta^{11}\text{B}$  value of about  $+40\%$ ) by about  $40$ – $50\%$  relative to average continental crust. Adsorption of boron on to organic matter (Gu and Lowe, 1990; Yermiyahu *et al.*, 1995) also would be expected to preferentially remove  $^{10}\text{B}(\text{OH})_4$  from solution. High concentrations of organic matter are available in soils and rivers, boron sorption on these materials, especially in soils of high pH, is likely to yield significant  $^{11}\text{B}$  enrichments in soil solutions and rivers. In the same manner as its adsorption (and coprecipitation) on clays or Fe oxyhydroxides, boron surface complexation on organic ligands may explain, to a significant extent, the isotopic shift which can be observed in river waters (Lemarchand *et al.*, 2002) or in soil minerals (Rose *et al.*, 2000) compared to the continental crust.

B isotopes have been also applied as tracers of human impact on water resources focusing on the identification of waste waters and sewages dominated by synthetic B products (Bassett, 1990; Vengosh *et al.*, 1994; Bassett *et al.*, 1995; Barth, 1998; Vengosh and Pankratov, 1998) as well as on the impact of fly ash leachate (Davidson and Bassett, 1993). Isotope signatures of inputs related to agriculture (e.g. hog manure, cattle feedlot runoff and synthetic fertilizers) has also been reported (Komor, 1997; Kloppmann, 2003; Widory *et al.*, 2004; 2005). Vengosh *et al.* (2005) utilizes the isotopic composition of boron for tracing sewage effluent and natural saline sources in the coastal plain aquifer of Israel.

In the Massaciuccoli area, boron isotopic composition ranges from +37‰ to +17‰. The highest values, from +30 to +37‰, were measured in the samples along the coast and are consistent with the  $\delta^{11}\text{B}$  mean value for seawater, +39.5‰ (Spivack and Edmund, 1987).

Decreasing values are found in samples progressively far from the sea and nearest the agricultural area. Figure 4.2.3.3 shows that the B/Cl ratio increases for decreasing  $\delta^{11}\text{B}$  values. Hence, the samples with higher B/Cl values are the lightest ones, except a sample from an agricultural drainage (L12) with high B/Cl ratio and intermediate  $\delta^{11}\text{B}$  value.

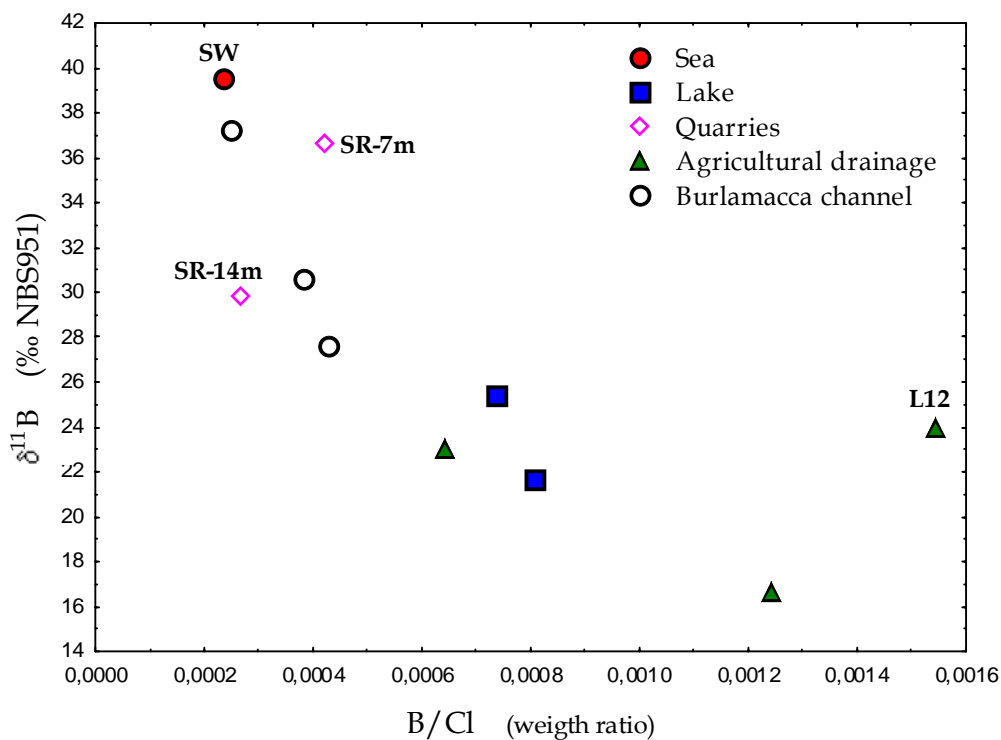


Figure 4.2.3.3  $\delta^{11}\text{B}$  vs B/Cl plot

The sample collected from the bottom water of the San Rocchino quarry (SR14) is characterized by a molar ratio similar to the seawater one, but its  $\delta^{11}\text{B}$  is lower than the seawater value. As the San Rocchino quarry receives water directly from the sea and it is stratified near the bottom, we expected a higher isotopic composition. This surprisingly light value can be explained as follows: it must be recalled that  $^{10}\text{B}$  preferentially forms tetrahedrally coordinated chelates with organic functional groups (Oxspring *et al.*, 1995; Taylor *et al.*, 1996; Schmitt-Kopplin *et al.*, 1998), and it is adsorbed as tetragonal complexes on the surface of humic acid (Lemarchand *et al.*, 2005); because in the bottom waters in contact with peat-rich sediments sulphate reduction oxidize organic matter, as discussed above, release of light boron isotopes can occur. Nevertheless, this hypothesis has to be confirmed by a more detailed study on the excavation area and on the isotopic composition of superficial sediments.

The isotopic boron signal can differentiate different water types. For the Massaciuccoli basin, analyses of boron composition of sediment, soil, sewage effluent and fertilizers used in agriculture are currently not available. Therefore, literature values are considered and summarized in Figure 4.2.3.4. The isotopic boron signal differentiates the agricultural network and lake samples with  $\delta^{11}\text{B}$  lower than seawater. The  $\delta^{11}\text{B}$  value measured in agricultural drainage was reported for the isotopic composition range of animal manure (Komor *et al.*, 1997; Kloppman, 2003; Widory *et al.*, 2004; 2005; 2006).



We can conclude that boron isotopes represent the most discriminating source indicators. We have at least a binary mixing system with a drainage influenced by manure and fertilizer and seawater as extreme end-members.

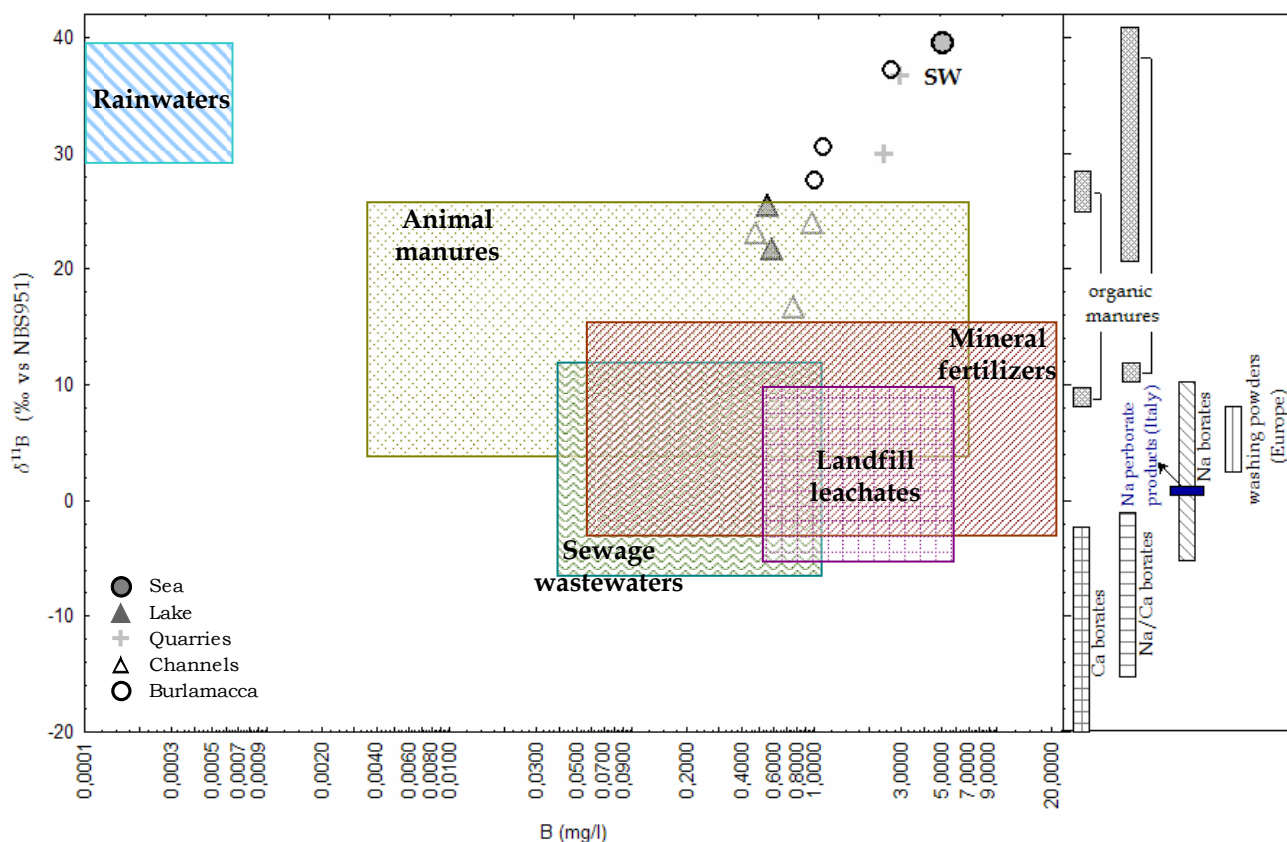


**Figura 4.2.3.3**  $\delta^{11}\text{B}$  vs B content. Typical values for different materials are underlined. Data from: McMullen *et al.*, 1961; Finely *et al.*, 1961; Swihart *et al.*, 1986; Xiao *et al.*, 1988; Oi *et al.*, 1989; Palmer and Helvacı, 1995; Barth 1998, 2000a, 2000b; Basset *et al.*, 1995; Gellenbeck, 1994; Komor, 1997; Eisenhut and Heumann, 1997; Leenhouts *et al.*, 1998; Vengosh *et al.*, 1994, 1999; Mather and Porteous, 2001; Widory *et al.*, 2003, 2005, 2006; Ladouche and Ghyselinck, 2004; Nguyen-Thé and Widory, 2006)

### 4.3 SOME CONCLUSIONS

The classic method for water classification is used to identify the hydrochemical facies of lake water. The chemical characteristics of the waters collected within the basin change both in space and in time. I used it to pinpoint different water type which control the chemistry of lake water, and their interaction.

The lake water and the waters from the northern palustrine area (including sandpit and Burlamacca channel) belong to the Na-Cl type.

The amples from the southern and eastern agricultural network (Quiesa, L6 and Barra, L12, channels) have a mixed composition, such the inflow from Gora di Stiava stream on the N.

The Villa Spinola spring on the E belongs to the Ca-sulphate type.

This treatment, however, does not allow recognizing the geochemical processes such as mixing, evaporation and biotic process occurring in different compartment of the Massaciucoli wetland. Therefore:

- Na vs Cl, B vs Cl and Br vs Cl binary diagrams are used to determine and to distinguish between mixing process with seawater and reaction with dissolved organic matter

- Mg vs Ca, Ca vs Na, Ca+Mg vs SO<sub>4</sub> binary diagrams are used to establish the continental inflow.

These diagrams underline that i) mixing process with seawater affect the northern area of the basin, that is Burlamacca channels and sandpits; ii) anthropogenic activity, especially agriculture, influences the lake and the southern basin.

In order to differentiate the geochemistry of carbon species into the lake and into the agricultural network, I analyse the  $\delta^{13}\text{C}_{\text{DIC}}$ . By the application of this tracer, I realized that i) equilibrium with respect to atmospheric CO<sub>2</sub> and carbonate phases prevails in the middle part of the lake; ii) the dissolved inorganic carbon into the waters of agricultural channels and near lake shore originates from the oxidation of organic matter.

In order to characterize the human impact (agriculture and sewage) on the lake boron isotopes analyses were performed on lake waters and in the channel draining the southern basin. This tracer, indeed, allows distinguishing between the seawater inflow and/or weathering reaction and pollution since binary diagrams cannot differentiate in the Massaciucoli system these different inputs.

#### 4.4 EVAPORATION PROCESSES

As discussed in previous paragraphs, the chemical composition of the Massaciucoli lake cannot be explained by seawater mixing alone but several intermixed processes that include evaporation processes and groundwater inflows control it. However, based on the absolute and relative concentrations of specific solutes such as Cl, Na, Br and B we are not able to discriminate the effect of seawater mixing from evaporative processes. In order to characterize the influence of the evaporation and transpiration processes on the Massaciucoli lake and to understand its hydrogeochemical variations, we have investigated stable isotopes ratios  $\delta^2\text{H}$  and  $\delta^{18}\text{O}$ .

As a preliminary step of this study, we have used the isotope GNIP/ISOHIS database (IAEA, 2004) to calculate the Local Meteoric Water Line (LMWL), obtaining the equation:  $\delta^2\text{H} = 7.6 \cdot \delta^{18}\text{O} + 7.5$ , which is significantly different from the global meteoric water line (Craig, 1961):  $\delta^2\text{H} = 8 \cdot \delta^{18}\text{O} + 10$ . All samples fall below the LMWL, except a sample from a channel that received water from a pumping station.

The Massaciucoli basin can be supposed into hydrodynamic equilibrium between the Ligurian sea and the drainage network. In the  $\delta^2\text{H}$  vs  $\delta^{18}\text{O}$  plot of Figure 4.4.1, however, the lake is not along a mixing line between seawater and local continental waters. In contrast, such a mixing process can be supposed for the samples from the Burlamacca channel and San Rocchino and Incrociata sandpits that plot along the mixing line described by the following equation:  $\delta^2\text{H} = 6.7 \cdot \delta^{18}\text{O} + 0.1$ .

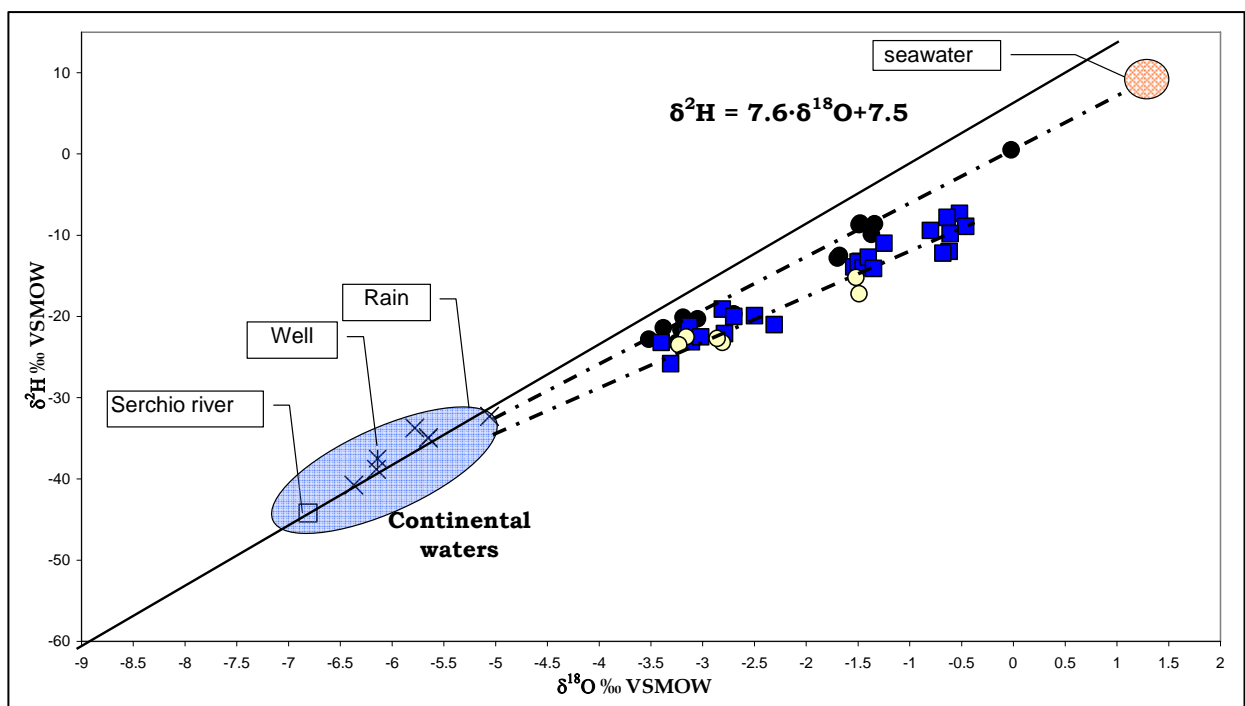


**Figure 4.4.1**  $\delta^2\text{H}$  versus  $\delta^{18}\text{O}$  plot for the Massaciucoli lake (■), channels (▲), Burlamacca channel, San Rocchino and Incrociata sandpits (●), Sisa sandpit (○) and local seawaters (⊗)

In detail, the isotopic composition of lake waters changes significantly, ranging from -3.13‰ to -0.46‰ and -21.2‰ to -8.9‰ for  $\delta^{18}\text{O}$  and  $\delta^2\text{H}$ , respectively. As expected, the highest isotopic ratios are recorded in the summer period and the lowest ones in the winter. In the  $\delta^2\text{H}$  versus  $\delta^{18}\text{O}$  diagram (Figure 4.4.2), the samples from the lake and channels identify an evaporative enrichment in heavy isotopes, which is described by the Evaporation Line:  $\delta^2\text{H} = 5.4 \cdot \delta^{18}\text{O} - 5.9$ . The intersection

between the evaporation line and the LMWL gives the mean initial isotope composition of the water before evaporation:  $\delta^{18}\text{O}=-6.5\text{‰}$  and  $\delta^2\text{H}=-41.6\text{‰}$ .

The samples collecting in Sisa sandpits have an isotopic composition different from that one of San Rocchino or Incrociata sandpits. In particular, the samples taken from different depth are along the LEL, suggesting that the evaporation during summer period is the main process and that the seawater does not affect this system. Stable isotopes point out the different behaviour of Sisa sandpits compared with San Rocchino and Incrociata sandpits.

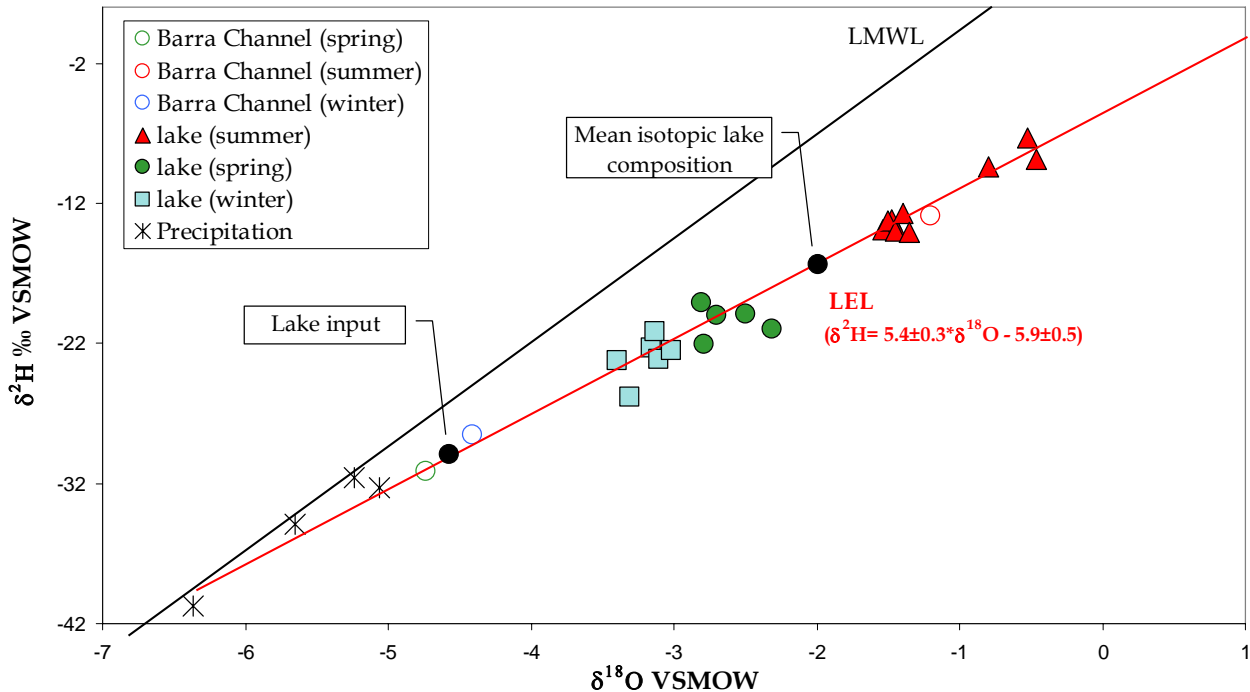


**Figure 4.4.2**  $\delta^2\text{H}$  versus  $\delta^{18}\text{O}$  plot for the Massaciuccoli lake during summer, springtime and winter. Values for local rain and groundwater (\*) are also reported. The Local Evaporation Line (LEL) is shown

The isotopic enrichment is not associated with a concurrent change in chloride concentration (Figure 4.4.3), suggesting that the main active process involves an exchange of water molecules between the atmosphere and the lake, whereas the net change in the mass of water is less important. The latter process causes, in fact, a small change in chloride concentration (see below). This plot underlines also the seasonal effects of evaporation processes on lake waters, since the  $\delta^{18}\text{O}$  signal increases of about 3‰ from winter to summer. Meanwhile, the Cl concentration changes only from 688mg/l to 783mg/l, with a variation of 13%.

The lake's mean volume does not change significantly through the year, although the water level varies considerably, rising to +30 cm a.s.l. in winter and falling to -40 cm a.s.l. in summer (Figure 4.4.4).

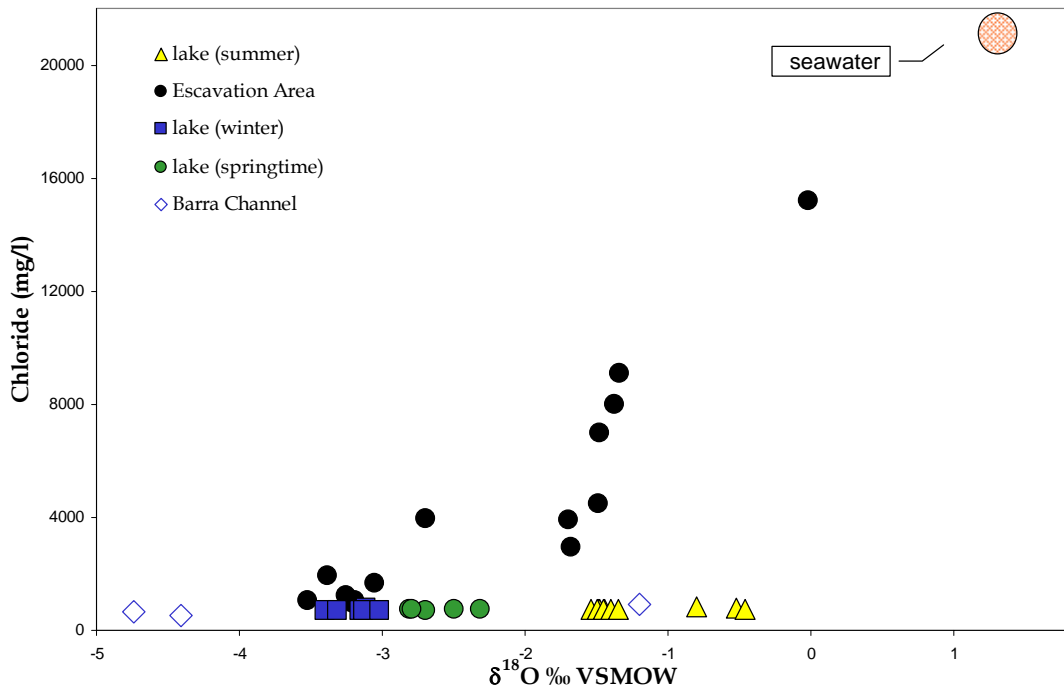


**Figure 4.4.3** Cl versus  $\delta^{18}\text{O}$  diagram for the Massaciucoli lake during summer, springtime and winter, samples from the Burlamacca channel and excavation area and local seawater are also plotted

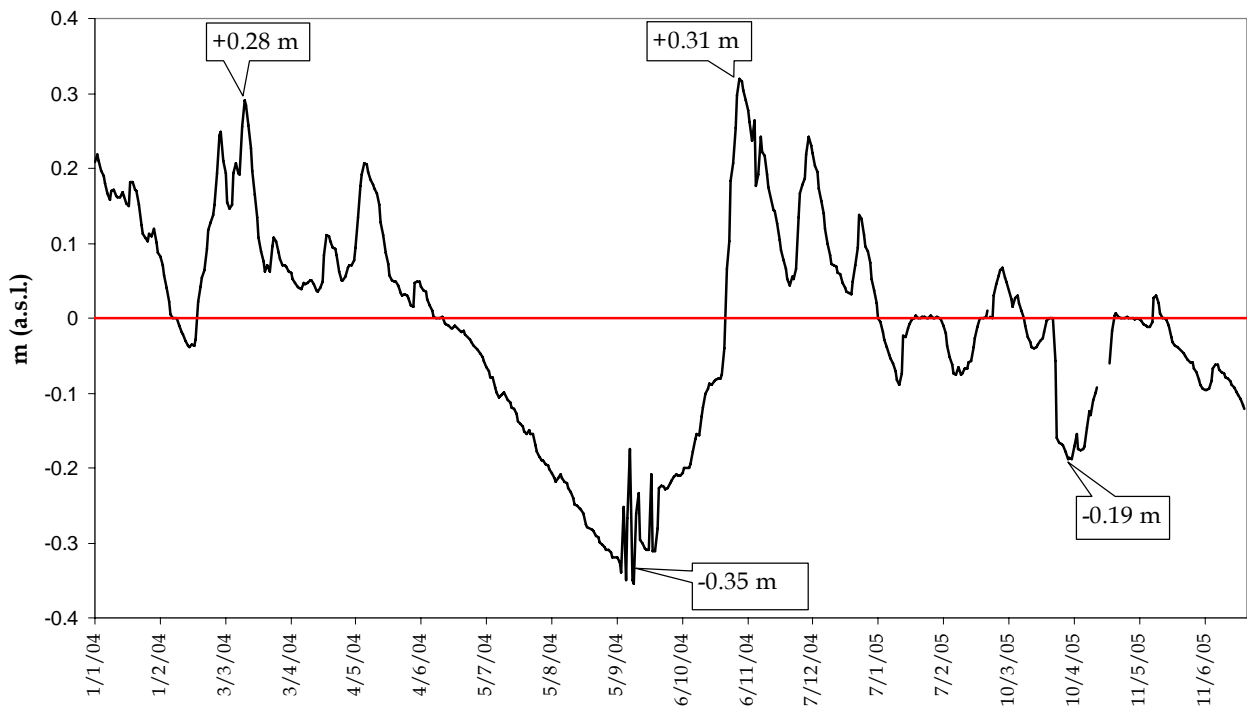


**Figure 4.4.4** Lake level variation from January 2004 to June 2006

As first assessment, it can be assumed that the annual volumetric changes are minor (i.e.  $dV/dt \approx 0$ , when  $dt=1$  year) and hydrologic fluxes remain constant. So, the lake can be considered as close to hydrologic steady-state, with continuous inflow balanced by a combination of outflow via evaporation and liquid outflow (i.e.  $I = Q + E$ ).

In a scenario where lake water has an initial isotopic composition close to that of input water, it will undergo progressive enrichment in the heavy isotopes as evaporation during residence time, given by  $\tau = V/I$  ( $V$  is lake volume and  $I$  is the inflow to the lake).

In this situation, the steady-state isotopic composition of the lake is described by the equation (Gonfiantini, 1986), assuming that other parameters are invariant and have values corresponding to their mean annual values:

$$\delta_L^{S^{18}O} \approx \frac{k \cdot (h\delta_a^{18}O + \Delta\varepsilon + \frac{\varepsilon}{\alpha}) + (1 - h + \Delta\varepsilon) \cdot \delta_i^{18}O}{(1 - k) \cdot (1 - h + \Delta\varepsilon) + \frac{k}{\alpha}}$$

where  $\delta_i^{18}O$  is the initial isotopic composition of lake water;  $k$  is the fraction of water lost by evaporation;  $\delta_a^{18}O$  is the isotopic composition of atmospheric water vapour above the evaporating surface, in the region of turbulent transport;  $h$  is the relative humidity of the atmosphere above the evaporating surface on top of the laminar layer;  $\alpha$  is the isotope equilibrium fractionation factor between water and water vapour at the temperature of the lake surface;  $\varepsilon = 10^3(1 - 1/\alpha) + \Delta\varepsilon$  is the total isotope enrichment, where  $\Delta\varepsilon$  stands for kinetic enrichment. The kinetic enrichment is usually expressed by the following equations (Vogt, 1978):  $\Delta\varepsilon = 14.3 \cdot (1 - h)$  for  $^{18}O$ . The values of the equilibrium fractionation factor, as a function of temperature are usually derived from the empirical formulae of Majoube (Majoube, 1971).

The equation can be used to evaluate the fraction of water lost by evaporation:

$$k = \frac{(\delta_L^{S^{18}O} - \delta_i^{18}O) \cdot (1 - h + \Delta\varepsilon)}{h \cdot (\delta_a^{18}O - \delta_L^{S^{18}O}) + (\delta_L^{S^{18}O} + 1) \cdot (\Delta\varepsilon + \frac{\varepsilon}{\alpha})}$$

The waters feeding the lake come principally from the drainage network and they have been already evaporated. Nevertheless, during summer, when their waters are heavily enriched ( $\delta^{18}O$  around  $-1.2$  ‰ for the main inflow, Barra channel), they do not feed the lake because evaporation is greater than precipitation (Autorità di Bacino del Fiume Serchio, 2007). Moreover, their waters are used for irrigation. Considering the input for precipitation during fall, winter and spring periods in the basin and directly into the lake, not including possible groundwater feeding the lake due to lack of information (see table 2.3.2.1 for the data used in the calculation), I estimated the  $\delta_i^{18}O$ .

$$\delta_i^{18}O = \frac{(I_{PB} - ET) \cdot \delta_{Ch}^{18}O + I_{PL} \cdot \delta_p^{18}O}{I_{PB} - ET + I_{PL}} = \frac{(78 - 40) \cdot -4.55 + 6 \cdot -5.3}{78 - 40 + 6} = -4.65 \text{ ‰}$$

where  $I_{PB}$  is the total precipitation ( $Mm^3$ ) during fall, winter and spring period within the hydrological basin (excluding lake area);  $ET$  is the evapotranspiration ( $Mm^3$ ) in the same periods;  $I_{PL}$  is the total precipitation ( $Mm^3$ ) during fall, winter and spring period into the lake;  $\delta_p^{18}O$  is the weighted mean isotopic value for precipitation in Pisa;  $\delta_{Ch}^{18}O$  is the mean isotopic composition of the water from channels during spring and winter periods. Using lake volume ( $15 Mm^3$ ) and total input ( $44 Mm^3$ ), the mean residence time is approximately 4 months.

Unfortunately, the atmospheric moisture above the lake is unknown. The isotopic composition of marine vapour ranges from -11 to -14‰ (Gat, 2000), vapour moisture in Madrid and Lisbona are -15 and -14‰, respectively (IAEA, 2005), whereas a value of -13‰ was estimated for atmospheric moisture around the Bracciano Lake (Gonfiantini *et al.*, 1962). All in all, a value of  $\delta_a^{18}O$  of -13‰ has been considered for the Massaciuccoli lake. The relative humidity has been estimated at 70% from values measured in Pisa.

In the table 4.4.1 are summarized the all the parameters used to estimate the fraction of water lost by evaporation.

**Table 4.4.1** Data used to estimate k.

Parameters	$\delta^{18}O$	
Rainwater	-5.3	
Mean isotopic composition of inflow from channel	-4.55	
$\delta_i^{18}O$	-4.65	
$\delta_L^{18}O$	-2.1	
$\delta_a^{18}O$	-13	
T		15.5°C
h		70%

In this way, the mean fraction of water lost by evaporation is estimated as about 10%.

The uncertainty in a function  $f(x_1, x_2, \dots, x_n)$  due to the uncertainty from each of the individual variables  $x_1, x_2, \dots, x_n$  characterized by an uncertainty  $\sigma_1, \sigma_2, \dots, \sigma_n$  is given by following relation:

$$\sigma_{f(x_1, x_2, \dots, x_n)} = \sqrt{\left(\frac{\partial f(x_1, x_2, \dots, x_n)}{\partial x_1}\right)^2 \sigma_{x_1}^2 + \left(\frac{\partial f(x_1, x_2, \dots, x_n)}{\partial x_2}\right)^2 \sigma_{x_2}^2 + \dots + \left(\frac{\partial f(x_1, x_2, \dots, x_n)}{\partial x_n}\right)^2 \sigma_{x_n}^2}$$

The basic idea is to determine by how much  $f$  would change if the individual variables were changed by its uncertainty. Such knowledge is important for (a) evaluating the applicability of the model, (b) determining parameters for which it is important to have values that are more accurate. I estimate uncertainty calculating the variations directly by a finite difference such as:

$$\sigma_{f(x_1, x_2, \dots, x_n)} = \sqrt{\left(\frac{f(x_1 + dx, x_2, \dots, x_n) - f(x_1, x_2, \dots, x_n)}{dx}\right)^2 \sigma_{x_1}^2 + \left(\frac{f(x_1, x_2 + dx, \dots, x_n) - f(x_1, x_2, \dots, x_n)}{dx}\right)^2 \sigma_{x_2}^2 + \dots + \left(\frac{f(x_1, x_2, \dots, x_n + dx) - f(x_1, x_2, \dots, x_n)}{dx}\right)^2 \sigma_{x_n}^2}$$

using the individual variables uncertainty reported in table 4.4.2.

Considering the error affecting this evaluation, the  $k$  value can estimated as  $(10 \pm 5) \%$ . The parameter that much affecting the uncertainty of the  $k$  estimation is the isotopic composition of the atmospheric moisture because it is difficult to evaluate this parameter with sufficient accuracy.

**Table 4.4.2** Individual variables uncertainty

Parameters	values
$\sigma(\delta_i^{18}O)$	0.5‰
$\sigma(\delta_L^{S18}O)$	0.5‰
$\sigma(\delta_a^{18}O)$	3‰
$\sigma(T \text{ } ^\circ\text{C})$	2
$\sigma(h \text{ } \%)$	5
$\sigma(\alpha)$	0.18‰
$\sigma(\varepsilon)$	0.18‰
$\sigma(\Delta\varepsilon)$	0.71‰



## 5 GEOCHEMICAL PROCESSES IN THE DEEP AREA OF THE MASSACIUCCOLI BASIN

The excavation area, called 'sandpits' is located north of the Massaciuccoli lake, in the palustrine area between the Burlamacca channel and the highway connecting Torre del Lago and Viareggio (Figure 5.1). The area extends for about 2.5 km<sup>2</sup> and includes numerous artificial lakes with an average depth of 15 m and a maximum depth of 25 m. These were excavated to extract siliceous sand. The estimated water volume of these lakes is about 37.5 Mm<sup>3</sup>, that is 2.5 time the water volume of the Massaciuccoli lake. This points out the relevance of the excavation area in any hydrologic study of the Massaciuccoli system.

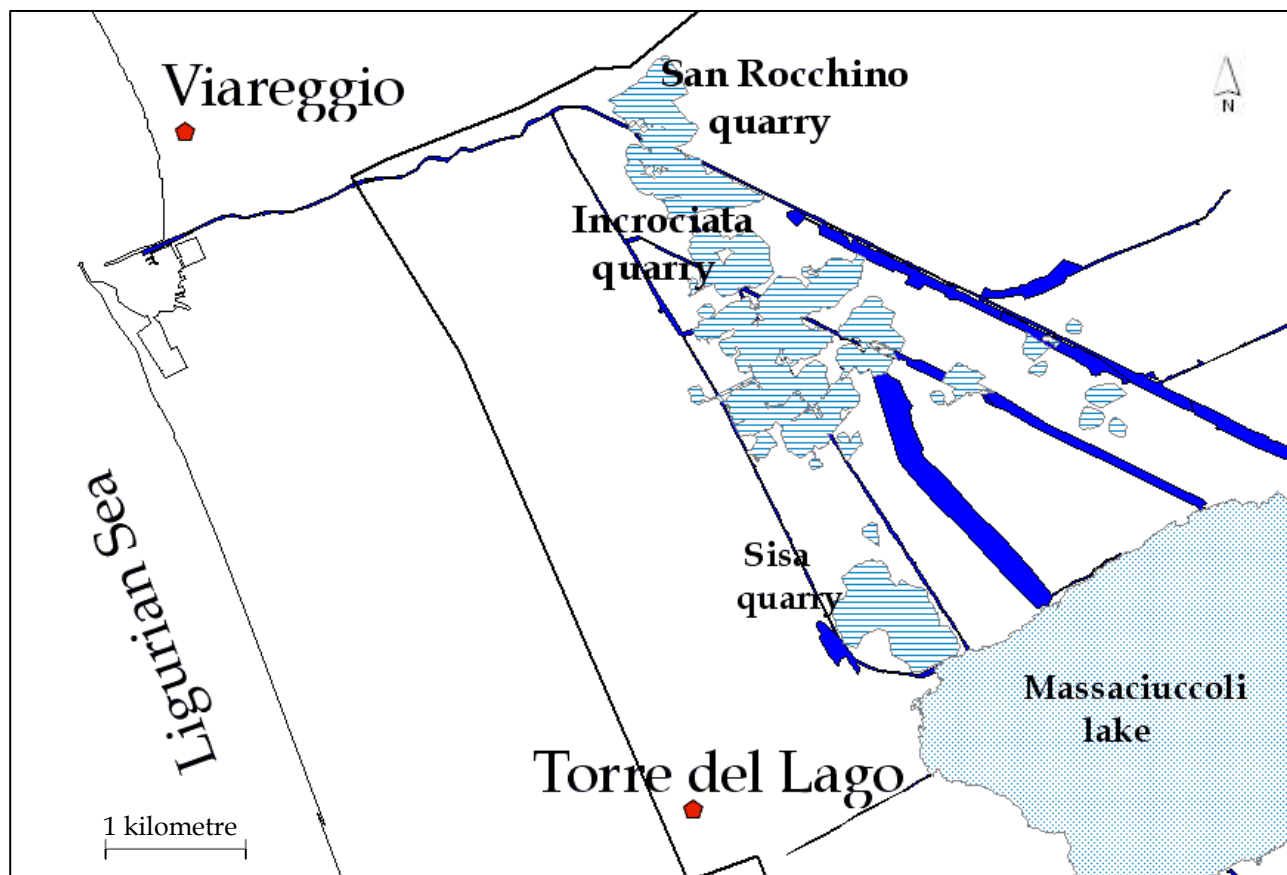
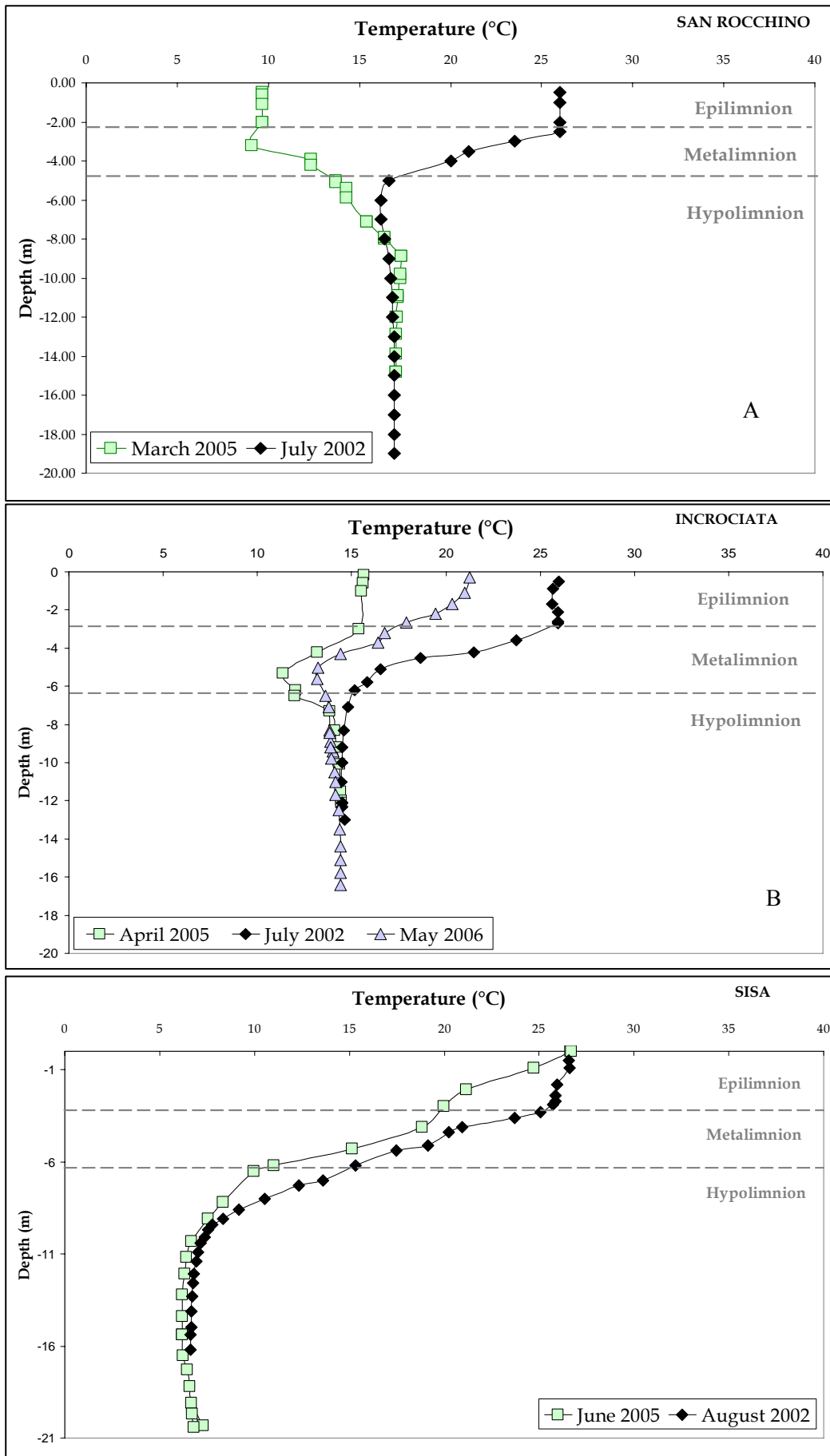


Figure 5.1 Sandpit ponds localization

During spring 2005, physical and chemical profiles were carried out in San Rocchino, Incrociata and Sisa sandpits. Incrociata sandpit was studied also during spring 2006. In this the section the physical and chemical characteristics of each sandpit are discussed.

## 5.1 THERMAL AND CHEMICAL STRATIFICATION

Water temperature is an important factor in the limnology for several reasons, including its influence on the rate of biochemical reactions and thermodynamic equilibrium. Even more important, in combination with the intensity of wind and lake geometry, water temperature affects water density, determining the degree of surface waters mixing with deeper waters and, as a result, influencing important processes within the lake. Unlike the Massaciuccoli lake, which is shallow and characterized by well-mixed waters throughout the year, the depth of the sandpits are great enough to cause the development of layers of differing water temperature on a seasonal basis. As the intensity of solar radiation increases during the spring and early summer months, thermal stratification occurs, with the development of a layer of warm surface water, called the "epilimnion", over the deeper, cooler waters below. The depth of the epilimnion is directly related to the degree of wind-generated turbulence at the surface. During the summer period, the superficial waters of the sandpits reach the maximum temperature whereas the water in the deepest portion of the lake remains relatively cool throughout the summer and is referred to as "hypolimnion". Between these two layers the area of most rapid change in temperature with depth is referred to as "metalimnion" (Figure 5.1.1). The picture is reversed during winter period, when the superficial waters reach the minimum temperature while the deepest portion of the lake preserves a relatively constant temperature value. During autumn, the epilimnion cools and there is a time when the temperature of the entire column from top to bottom is more or less the same. Figure 5.1.1B shows that in springtime, when the epilimnion warms, its temperature is similar to that of bottom waters. At this point, stratification could break down and a lake circulation could take place. However, San Rocchino and Incrociata sandpit are exposed to a salt water supply, as mentioned above, which causes a vertical (chemical) density gradient and some water remains unmixed. Therefore, these sandpits are in a state of chemical stratification, or "meromixis" (Findenegg, 1935) in which the upper, less saline layer of the lake fails to mix with the more saline water below. The perennial stagnant layer of a meromictic system is called monimolimnion, the uppermost layer is called mixolimnion and the intermediate layer chemocline (Wetzel, 1983). The vertical location of physicochemical discontinuities in the water column is evident based on the content of oxygen, temperature and conductivity (Figure 5.1.2, Figure 5.1.3 and Figure 5.1.4). In general, mixolimnetic waters the chemocline are well-oxygenated, whereas monimolimnetic waters below the chemocline are anoxic and may contain reduced substances such as ammonia and sulphide. Water density preserves this separation. However, Sisa sandpit could experience circulation during winter.



**Figure 5.1.1** Temperature profiles in waters of San Rocchino (A), Incrociata (B) and Sisa (C) sandpits

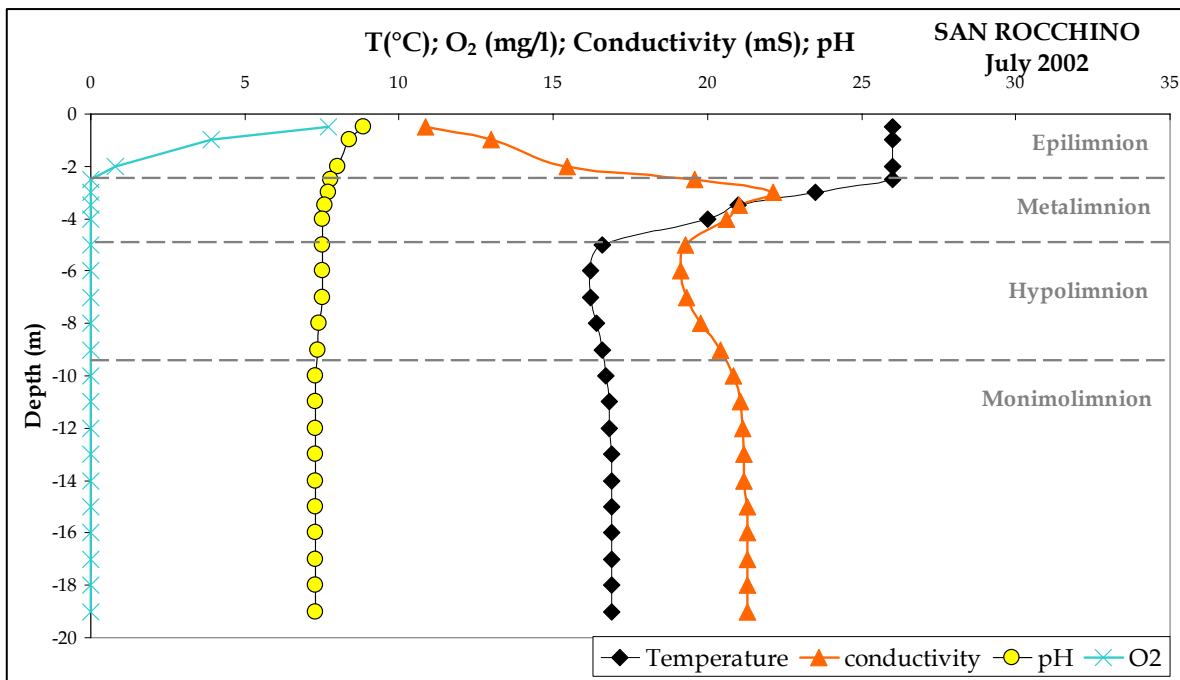
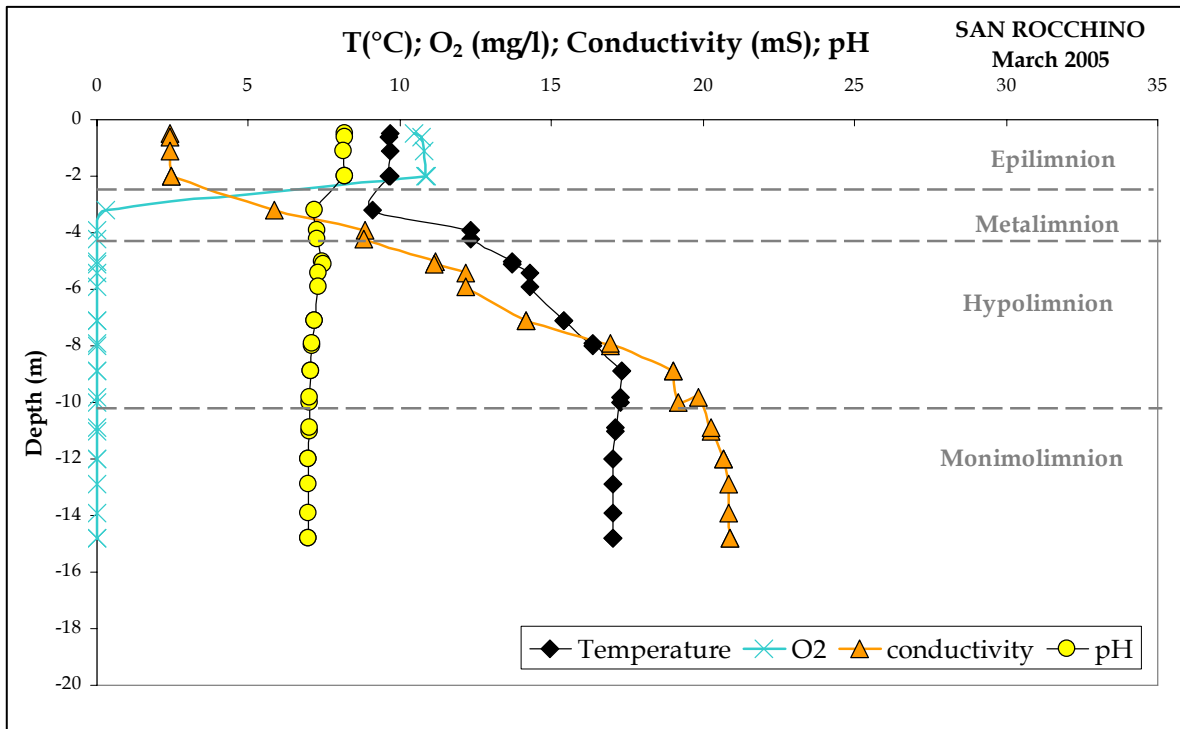


**Figure 5.1.2** Temperature, conductivity, oxygen dissolved and pH profiles in San Rocchino quarry

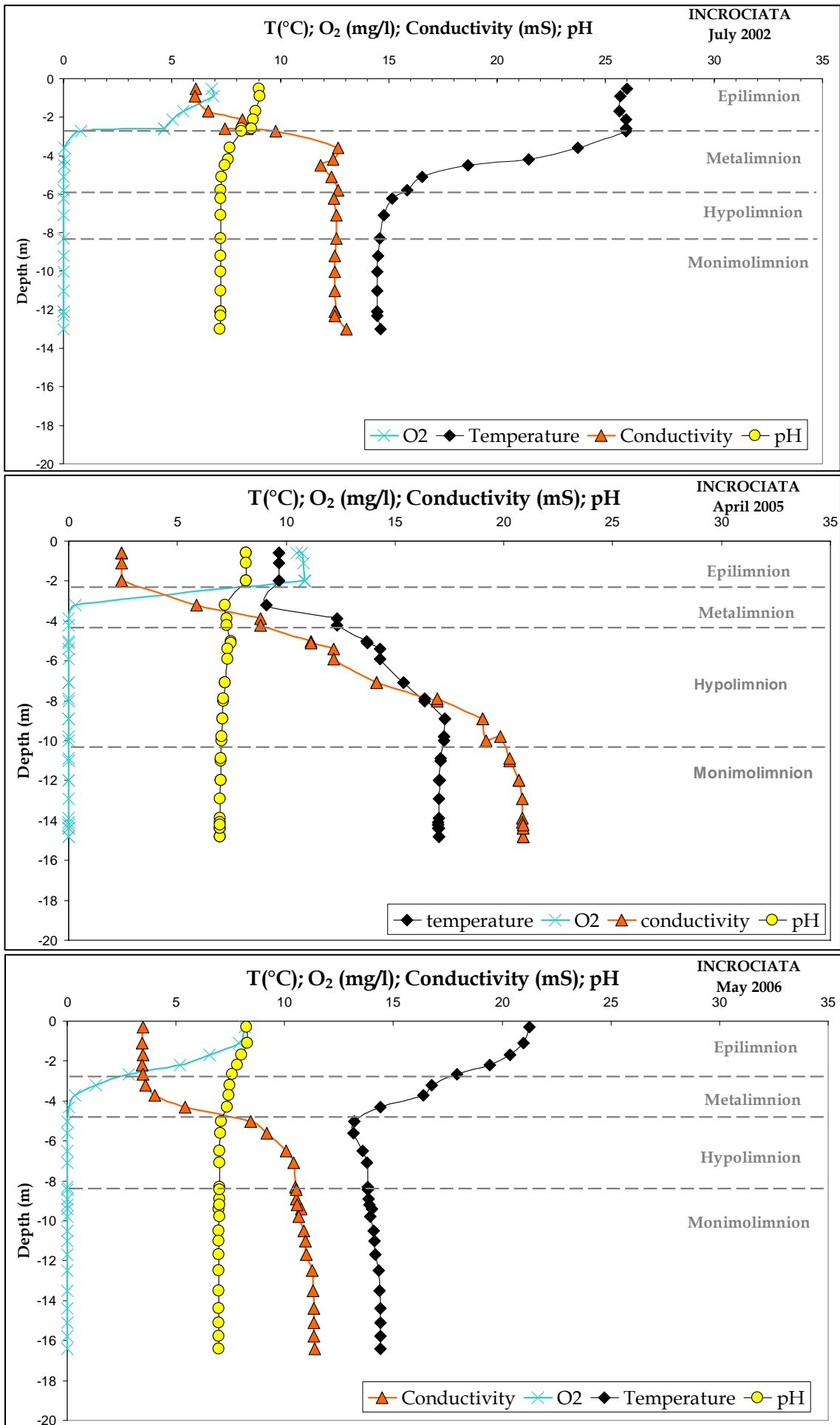


Figure 5.1.3 Temperature, conductivity, oxygen dissolved and pH profiles in Incrociata quarry

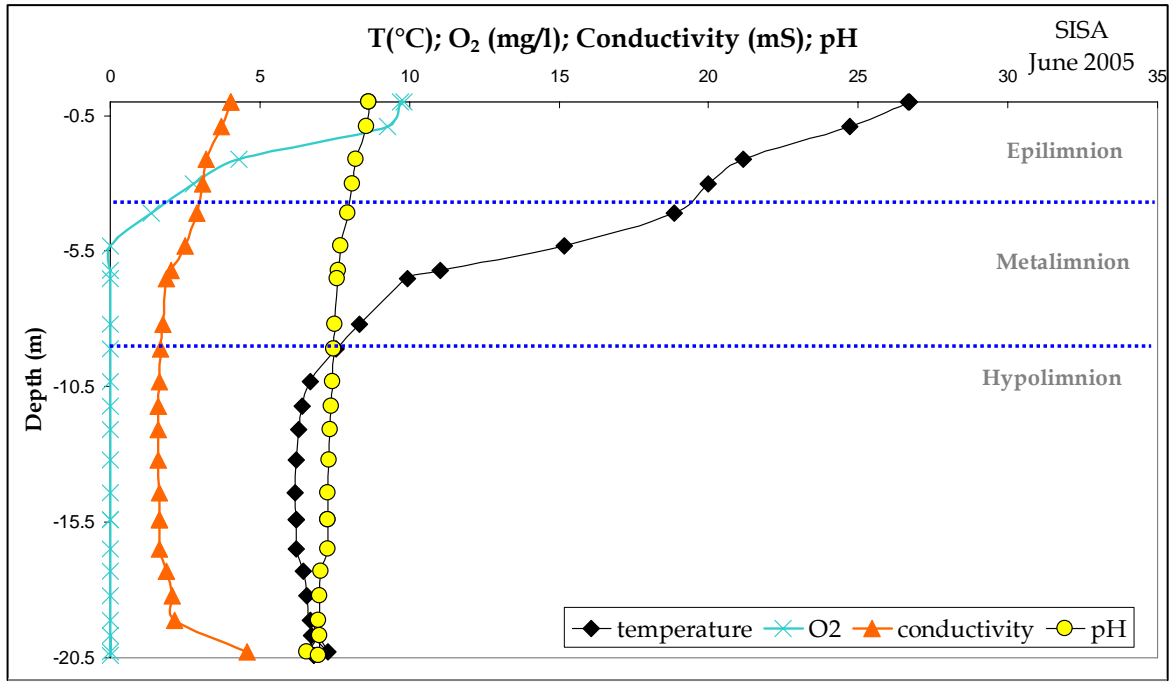


Figure 5.1.4 Temperature, conductivity, oxygen dissolved and pH profiles in Sisa quarry

It is interesting to analyse the temperature profile in the sandpit Sisa, where the temperature at depth is about 7°C while the temperature at depth in the other sandpits is approximately 15°C. This sandpit is adjacent to the lake, of which it can be considered an extension. The lake water temperature in winter drops to about 5-6°C, like the temperature value measured during summer period at depth in Sisa sandpit. During summer, the increase of surface temperature does not affect deep water, which therefore remains cold. This is confirmed by the fact that the isotopic composition of the deep water during summer period keeps the signal of winter lake water, as well chemistry. Thus, Sisa sandpit during cool period is completely mixed and it is fed by lake water, and this is proved by some additional isotopic measurements especially during winter period.

### 5.1.1 Density calculations

The density of fresh water is a complex function of temperature (T), salinity (S) and pressure (p). Empirical relation of  $\rho(T, S, p)$  is given by Chen and Millero (1986):

$$\rho(T, S, p) = \rho^0(T, S) \left( 1 - \frac{p}{K_m} \right)^{-1}$$

$$\rho^0(T, S) = 0.9998395 + 6.7914 \times 10^{-5} T - 9.0894 \times 10^{-6} T^2 + 1.0171 \times 10^{-7} T^3 +$$

$$- 1.2846 \times 10^{-9} T^4 + 1.1592 \times 10^{-11} T^5 - 5.0125 \times 10^{-14} T^6 + \rho^1(T, S)$$

$$\rho^1(T, S) = S(8.181 \times 10^{-4} - 3.85 \times 10^{-6} T + 4.96 \times 10^{-8} T^2)$$

where  $\rho$ ,  $\rho^0$ ,  $\rho^1$  (g cm<sup>-3</sup>) are contributions to density of water, T (°C) is water temperature, S(‰) is salinity, p(bar) is pressure and

$$K_m^{-1} = \gamma = \frac{1}{\rho} \left( \frac{\partial \rho}{\partial T} \right)_{S,p}$$

is compressibility of water (cm<sup>3</sup> g<sup>-1</sup> bar °C<sup>-1</sup>).

Density for waters at different depths and temperatures in each sandpit was calculated in order to assess the water stability evolution during the year. The results are summarized in Figure 5.1.1.1

and 5.1.1.2, where water density values are reported against depth. Density trends were also simulated assuming that the temperature of the first five meters falls down to 4°C.

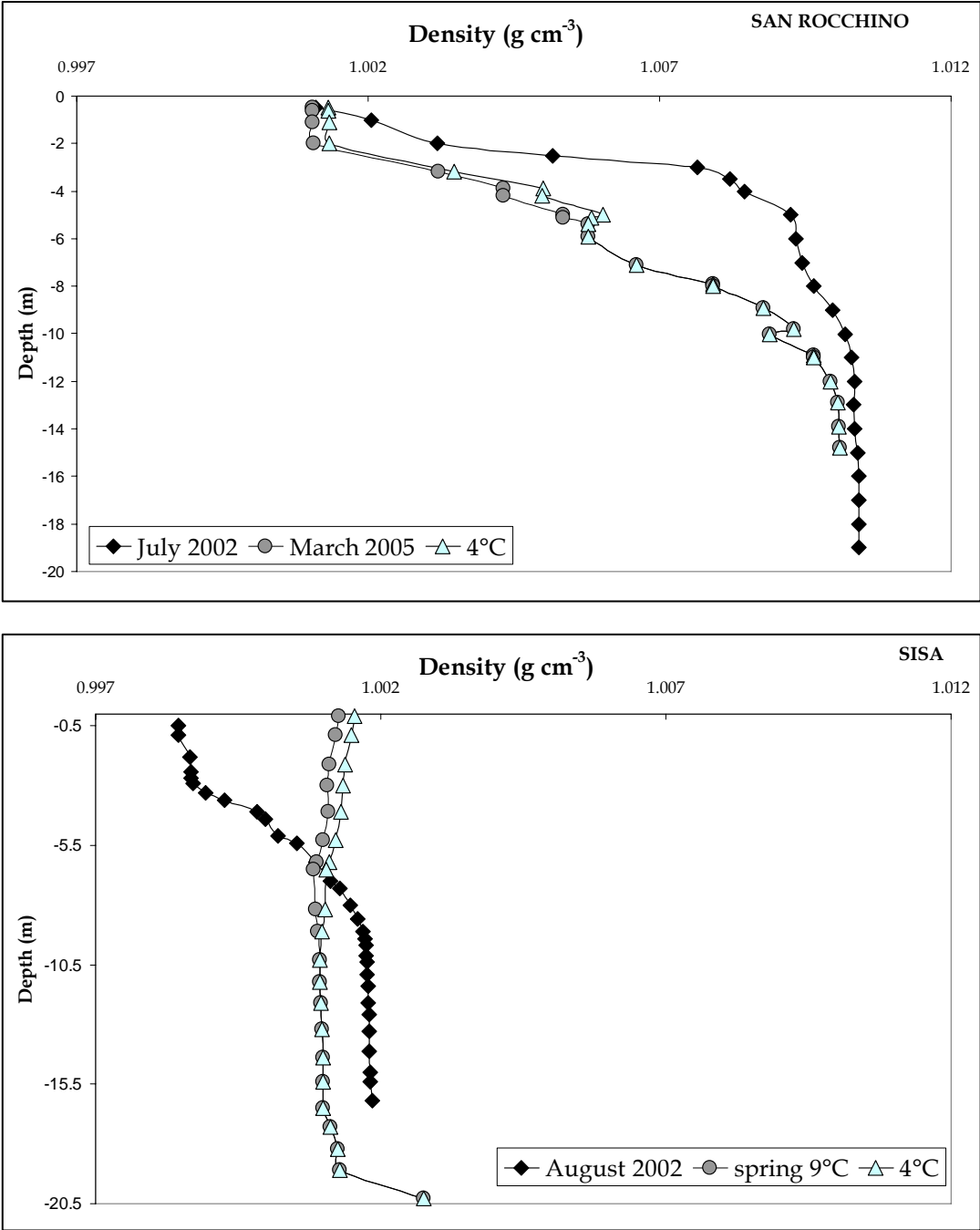


**Figure 5.1.1.1** Density variations along the water column of San Rocchino and Incrociata sandpit

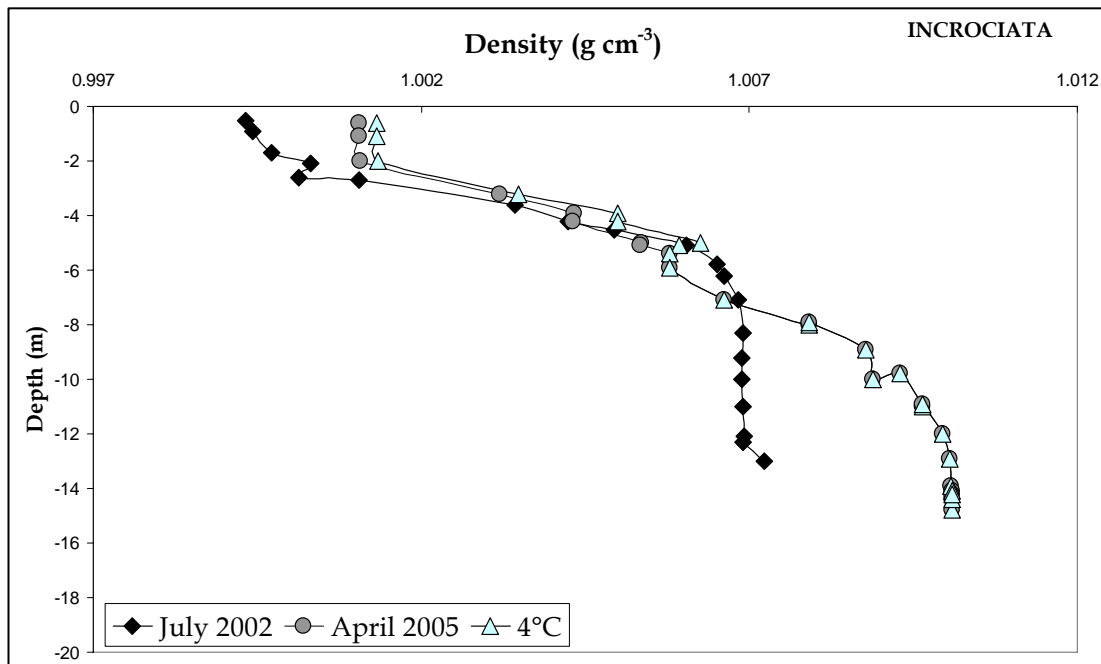
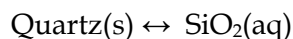


**Figure 5.1.1.2** Density variations along the water column of Sisa sandpit

Based on these calculations, it is likely that San Rocchino and Incrociata sandpits preserve stratification also during the winter and spring periods and waters in the deepest portions never mix. For what concerns San Rocchino during spring, fall and winter, the superficial water up to 2 m depth can mix and oxygen exchange with the atmosphere can take place. At -6 m, corresponding to the limit between thermocline and hypolimnion, water can also mix. For Incrociata, the pattern is very similar to that of San Rocchino, but during the summer period the first 3 m are mixed. The Sisa sandpit shows a holomictic behaviour, with circulation when temperature fall down to 15°C in the first 5 m.

### 5.1.2 Silica: main process

The SiO<sub>2</sub>-Si concentrations displayed a marked pattern in relation to the water depth (Figure 5.1.2.1) and it is supposed to be controlled by mineral equilibrium with quartz and not by phytoplankton community dynamics. The Figure 5.1.2.2 illustrates that some samples from the bottom of the sandpits have silica content as expected by the equilibrium with quartz:



Moreover, they are subsaturated in relation to the amorphous silica. We can hypothesize that the siliceous sands, which constitute the sediments, dissolved and dissolved silica increase in the water.



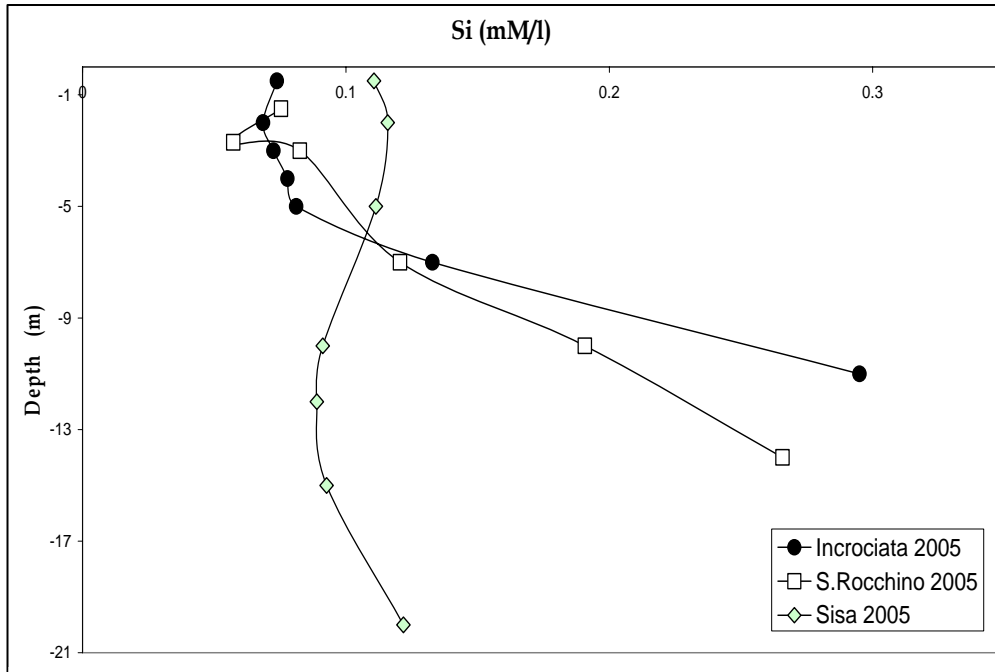


**Figure 5.1.2.1** The variation of monomeric silica along the water column of the sandpits

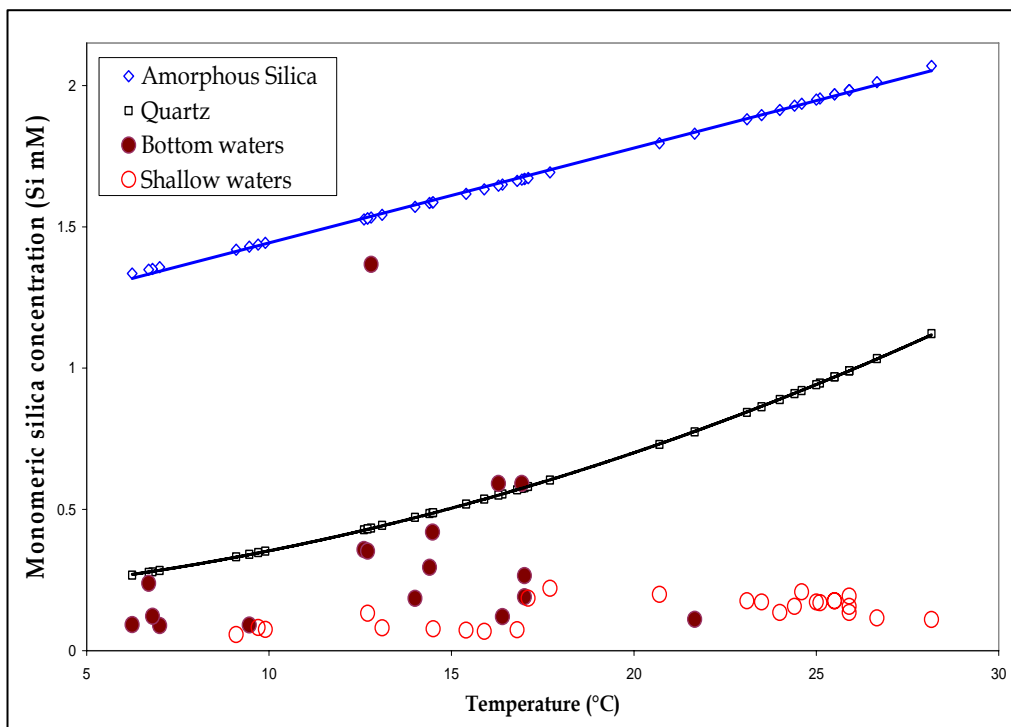


**Figure 5.1.2.2** The effect of temperature on equilibrium of amorphous silica and quartz. Samples are also reported

### 5.1.3 Redox gradients and reactions

Vertical profiles of all sandpits indicate the presence of strong redox gradients. Figures 5.1.2, 5.1.3 and 5.1.4 highlight that oxygen decreases rapidly within the first 4-5 m to virtually nil values. Stratification acts as a barrier that prevents mixing between superficial waters rich in oxygen and the anoxic waters.

Trend in  $p\text{CO}_2$  and alkalinity with depth can be observed in the three sandpits, besides  $\text{O}_2$ , chloride and sulphate variations. We have to recall that the sandpits directly receive marine waters, which fall near the bottom, and experience thermal and chemical stratification. Figures 5.1.3.1 and 5.1.3.2 illustrate the variation of  $p\text{CO}_2$ , alkalinity,  $\text{O}_2$  and  $\text{N-NH}_4$  in each sandpit. Three sectors can be identified: a) the shallow oxic part, b) the transitional zone, where oxygen decreases and 3) the anoxic bottom zone depleted in oxygen. The upper portion of the sandpits is oxic and devoid of  $\text{H}_2\text{S}$ , while the lower portion is characterised by presence of dissolved sulphide and  $\text{NH}_3$ . In the Incrociata and San Rocchino sandpits  $p\text{CO}_2$  and alkalinity increase abruptly in the anoxic zone (below 4-5 m depth for Incrociata and below 2-3 m depth for San Rocchino), while in Sisa the  $p\text{CO}_2$  variation is gradual and alkalinity increases less markedly, from 3.8 to 6.8 meq/l.

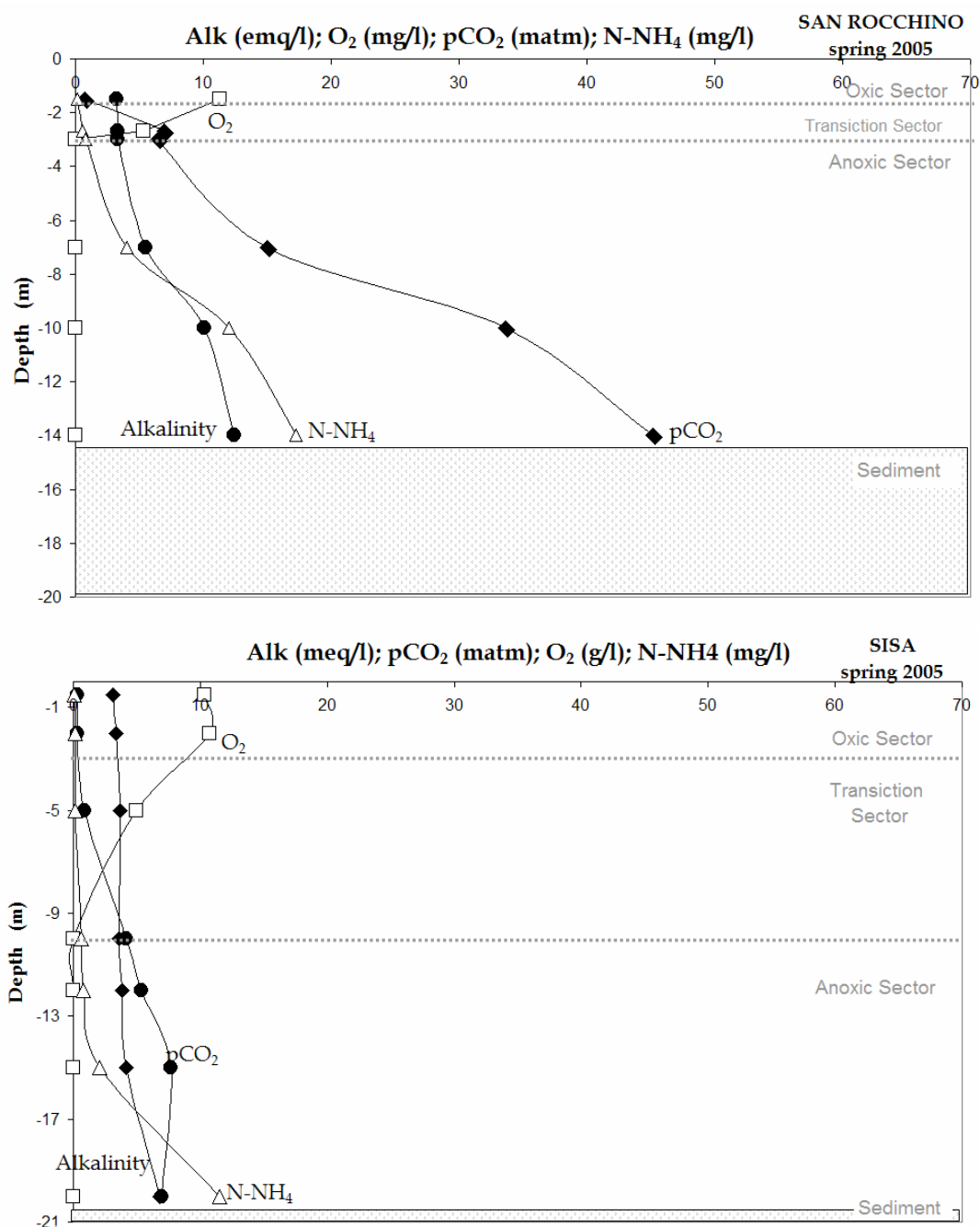


**Figure 5.1.3.1** Alkalinity, oxygen dissolved,  $p\text{CO}_2$  and ammonia profiles in San Rocchino and Sisa sandpit

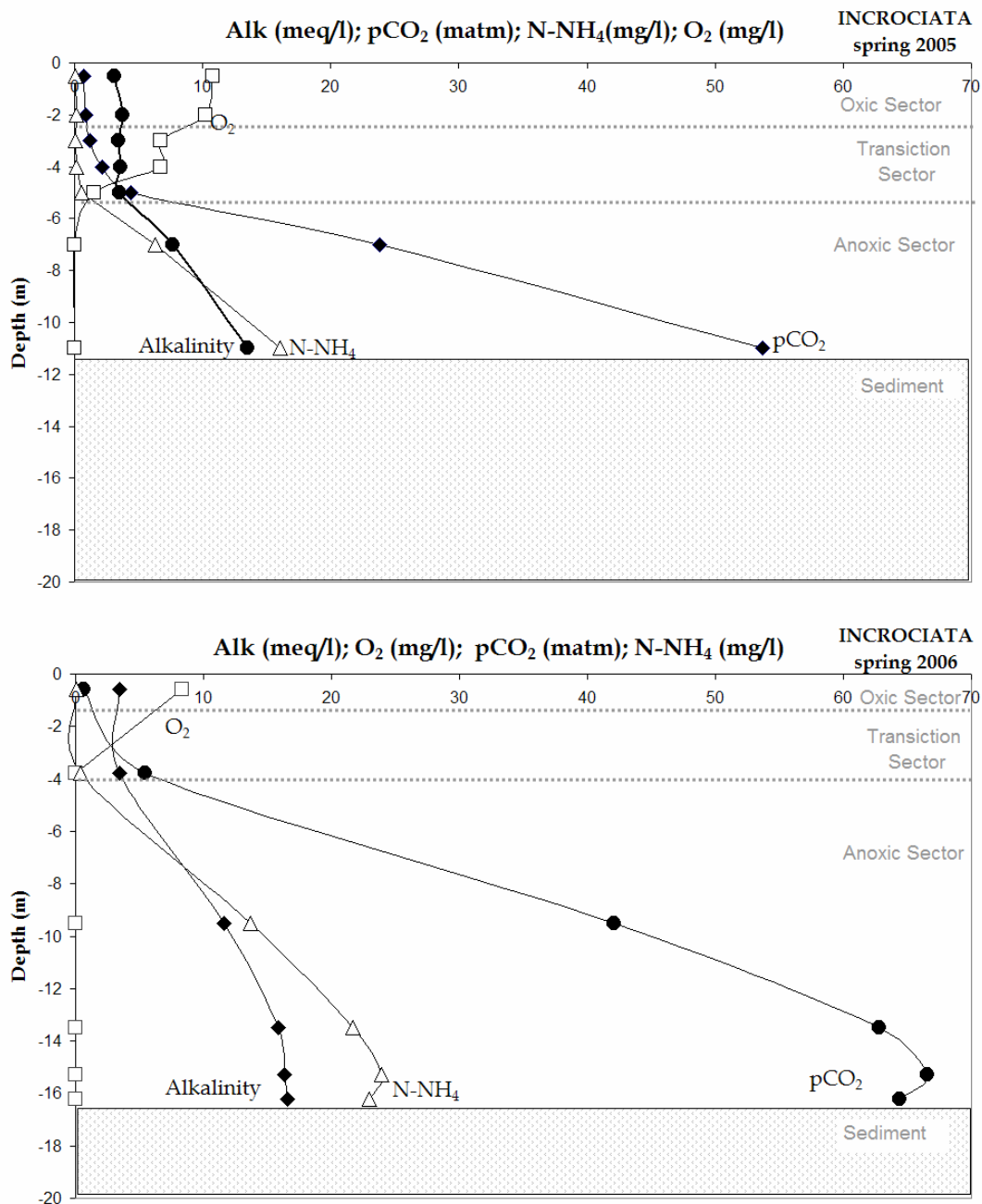


**Figure 5.1.3.2** Alkalinity, dissolved oxygen, pCO<sub>2</sub> and ammonia profiles in Incrociata sandpit

The presence of an oxic-anoxic interface in the water column is expected to influence the stability of iron and manganese aqueous- and solid-phase, as redox-sensitive elements. Trends of iron and manganese with depth in the sandpits are given in Figure 5.1.3.3 and 5.1.3.4. High variability exists in the aqueous phase Mn and Fe data, which may reflect a sediment source for dissolved iron and manganese (Davison *et al.*, 1980). However, the shape of the profiles of these elements in each sandpit is also influenced by reprecipitation and dissolution processes near the oxygen boundary. Hongve (1997) reports these trends for a meromictic lake and by Hong and Kester (1986) in the offshore waters of Peru. In general, soluble Mn and Fe concentrations are often times lower in the oxic overlying water column because of (probable) Fe and Mn oxidation and formation of solid Fe<sub>2</sub>O<sub>3</sub> and MnO<sub>2</sub> phases, respectively; whereas, occasional peaks of aqueous Fe occur at the sediment-water interface of the San Rocchino sandpit in 2002 and Incrociata in 2006, and at the oxic-anoxic boundaries of each sandpit, where a rapid turnover of Fe takes place.

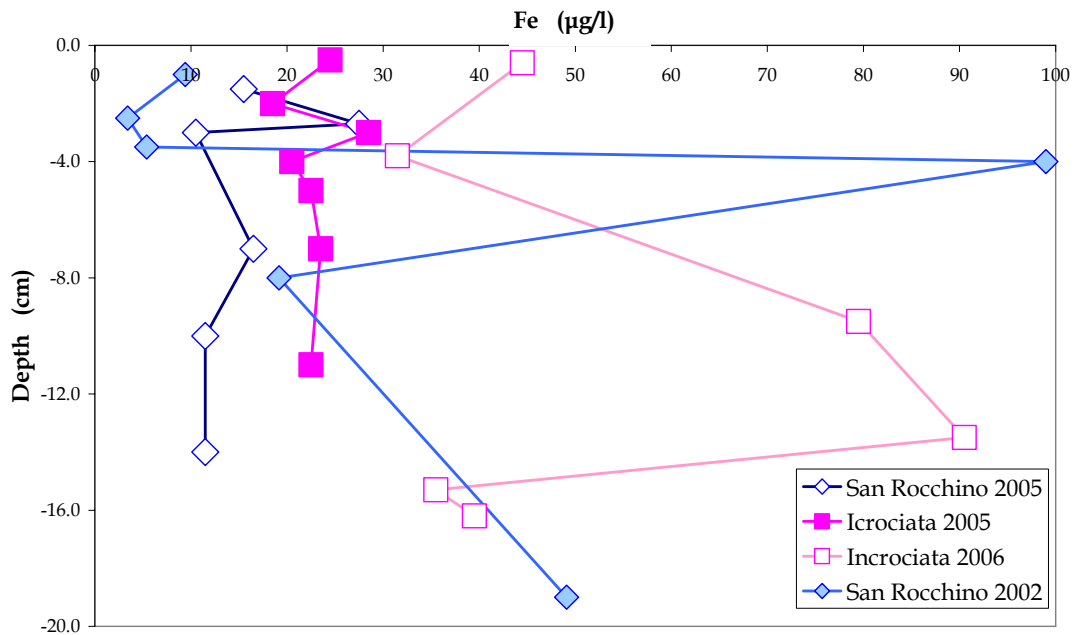


**Figure 5.1.3.3** Dissolved Iron variations along the water column of the quarries

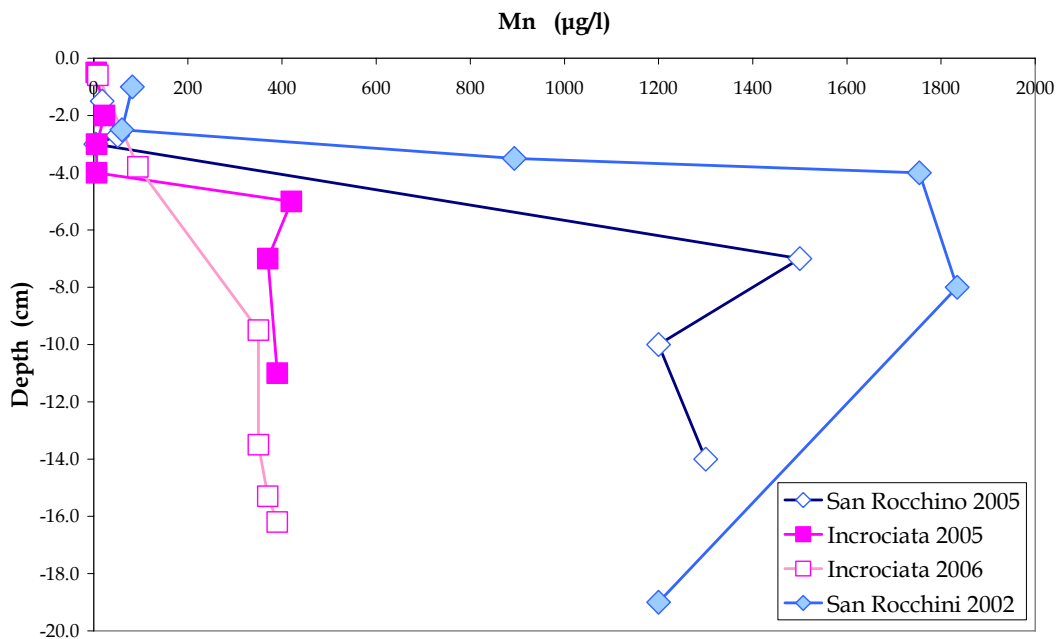


**Figure 5.1.3.4** Dissolved Manganese variations along the water column of the sandpits

In fact, in well-oxygenated epilimnion the stable forms of Fe and Mn are their higher states (Fe(III) and Mn(IV)), which are completely hydrolyzed oxides in the 7-8 pH range (Figure 5.1.3.5). Where oxygen is absent the lower redox states, Fe(II) and Mn(II), are favoured. Because of these properties, where the bottom waters become anoxic, Fe(II) and Mn(II) can accumulate to high concentration, as probably occurred in the San Rocchino 2002 and Incrociata 2006 for Iron.

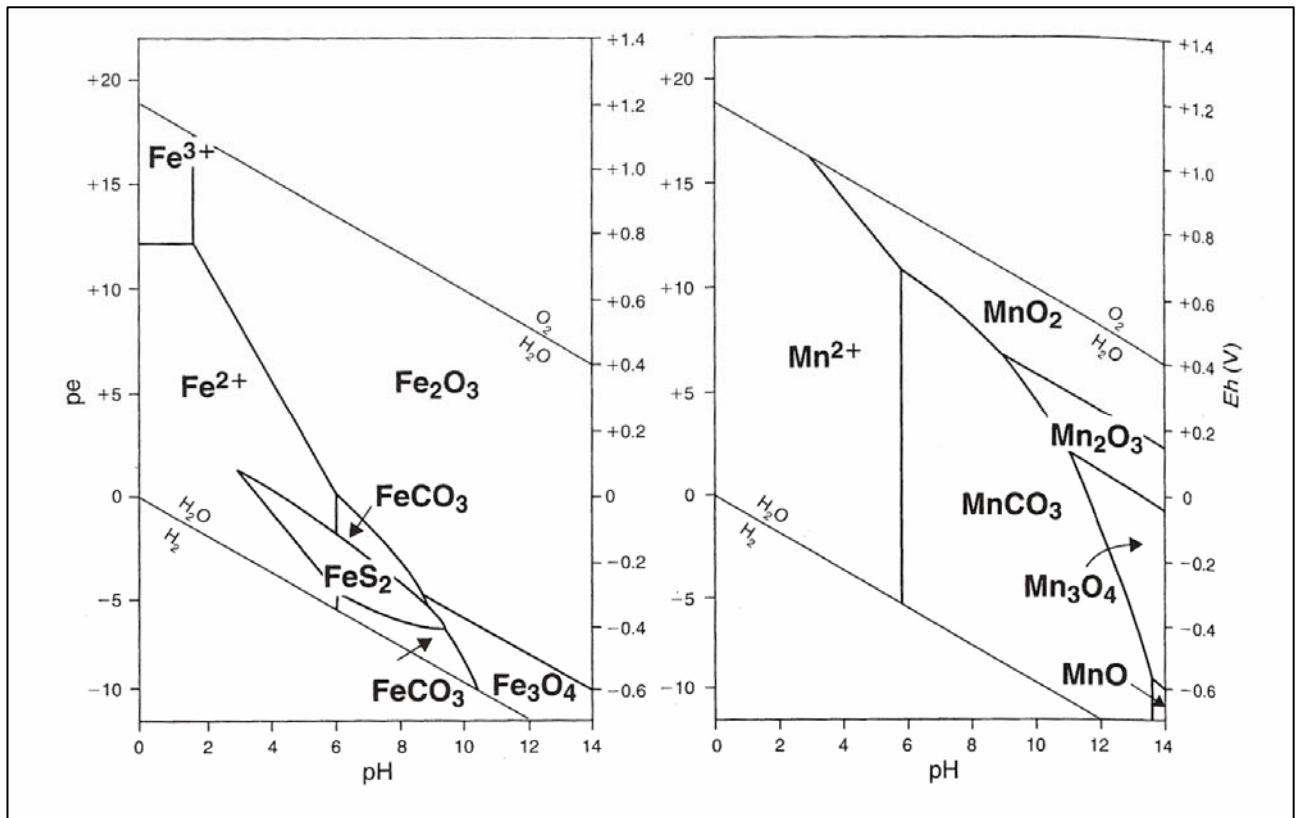


**Figure 5.1.3.5** Stability relations for iron and manganese at 25°C, both assuming that  $\Sigma S=10^{-6}$  and  $TIC=10$  M. Solid Solution boundaries are drawn for  $[Fe^{2+}]=10^{-6}$  (modified from Krauskopf, 1979)

The reduced ions are supplied by reductive dissolution of oxide present in particles sinking through the water column. At the oxic/anoxic boundary in the water column, the upwardly diffusing Fe(II) and Mn(II) may be oxidized to form oxides. However, when anoxic conditions are well advanced, dissolved sulphide can accumulate in the anoxic hypolimnion, leading to the precipitation of FeS (Figure 5.1.3.6) when dissolved sulphide concentrations are higher than  $10^{-6}$  M. Moreover, the samples from the bottom of the sandpits (red triangle in Figure 5.1.3.7) are undersaturated respect to the Siderite ( $FeCO_3$ ). These process can explicate decreasing of Fe concentration in San Rocchino 2005 and Incrociata 2005 sandpits, where sulphide are present at pH values of about 7.

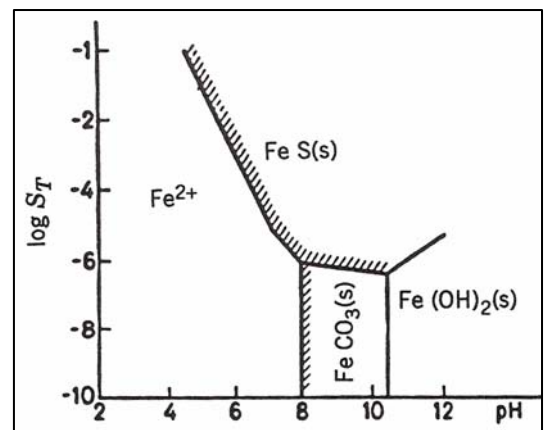


**Figure 5.1.3.6** Concentration conditions for existence of the solid phases  $FeS_{(s)}$ ,  $FeCO_{3(s)}$  and  $Fe(OH)_{2(s)}$ . Conditions  $[Fe^{2+}]=10^{-6}M$ ,  $Alk=5 \times 10^{-3}$  eq liter $^{-1}$  (adapted from Sigg and Stumm, 1994)

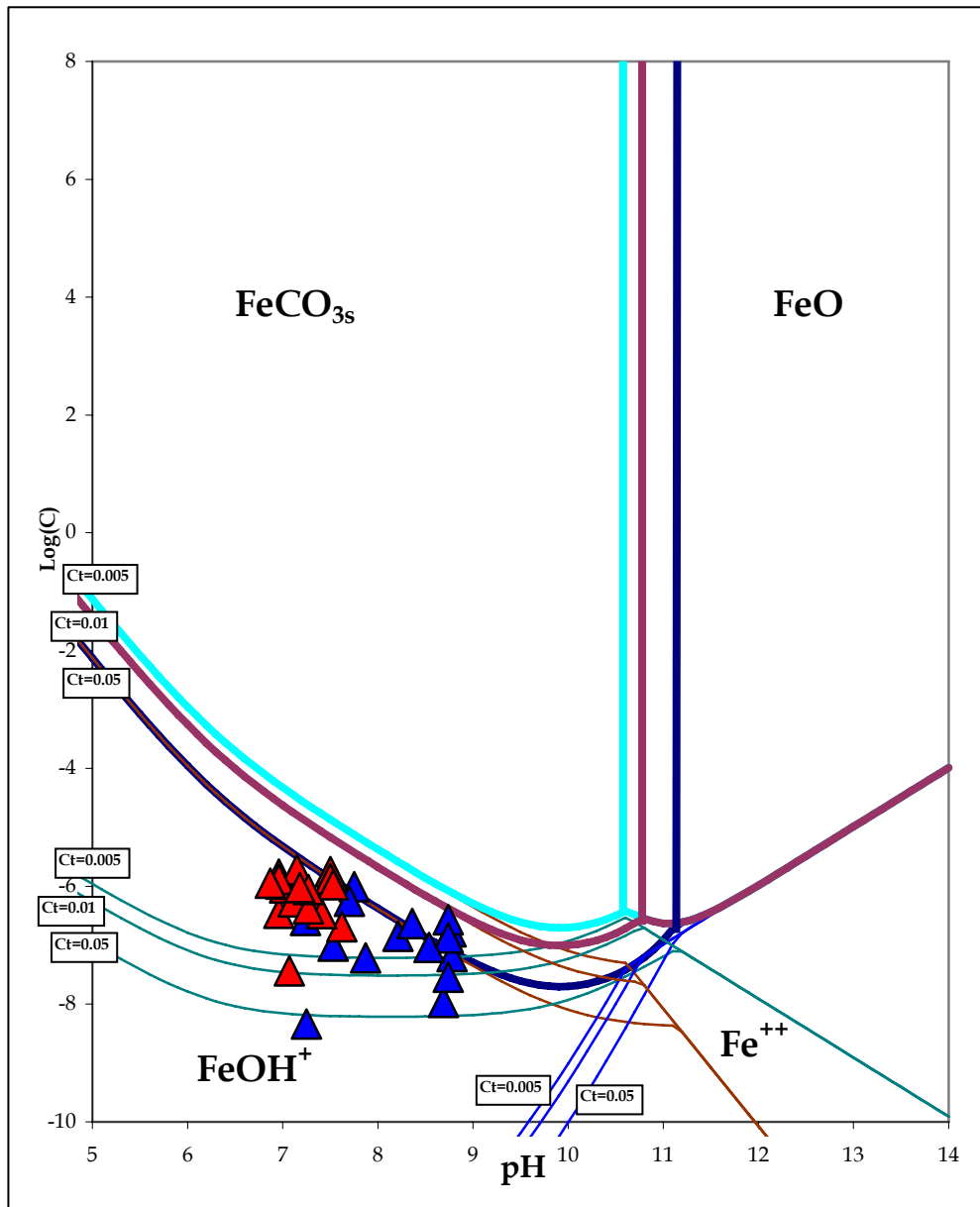
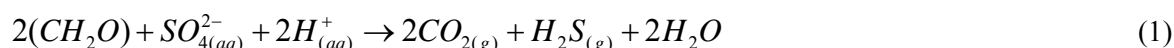


Figure 5.1.3.7 Solubility diagram of Fe(II) in a  $C_T=10^{-3}$  M carbonate system

## 5.2 SULPHATE REDUCTION AND SULPHUR ISOTOPES

As mentioned above, the oxidation of organic matter produces an alkalinity increase. Many models for marine and estuarine systems successfully predict alkalinity production associated to (1) sulphate depletion due to bacterial sulphate reduction, (2) calcium and magnesium increases due to carbonate mineral dissolution, and (3) ammonia production resulting from the decomposition of organic matter (Knull and Richards, 1969; Berner *et al.*, 1970; Einarsson and Stefansson, 1983). The trends in alkalinity described in the previous section, Eh measurements and the presence of H<sub>2</sub>S suggest the occurrence of bacterial SO<sub>4</sub> reduction processes in the waters and substrates of the sandpits. Moreover, in Incrociata sandpit, pCO<sub>2</sub> and alkalinity increases with depth are associated with a depletion of the δ<sup>13</sup>C<sub>DIC</sub> signal. This suggests a biogenic production of CO<sub>2</sub> concurred with sulphate and nitrate reduction.

Fractionation of sulphur isotopes occurs during bacterial reduction of sulphate to sulphide under anoxic conditions. Bacterial (dissimilatory) sulphate reduction (BSR) is a naturally occurring process carried out by a few extant genera, such as *Desulfomonas*, *Desulfovibrio*, *Desulfotomaculum* (Pfennig *et al.*, 1981), *Desulfuromonas* and *Compylobacter* (Pfennig and Biebl, 1981). Under anaerobic conditions, bacteria use sulphate as an electron acceptor for oxidation of organic carbon according to the following generalized reaction (Berner, 1970; 1984; Canfield and Raiswell, 1991):



where decomposing organic matter has been schematically represented as CH<sub>2</sub>O.

The formal oxidation state of the C atom in CH<sub>2</sub>O is 0. However, if this process involves organic compounds with nonzero oxidation states of C, instead of CH<sub>2</sub>O, its stoichiometry diverges from that of reaction (1).

In Figure 5.2.1, sulphate decline with depth is illustrated for Incrociata sandpit during the spring 2005 and 2006. As the sandpit bottom is very irregular and no bathymetry map is available, it is very difficult to sample in the same site at the same depth. For this reason, in spring 2005 samples were collected up to 11 m depth whereas in 2006 sampling was extended up to 16.4 m.

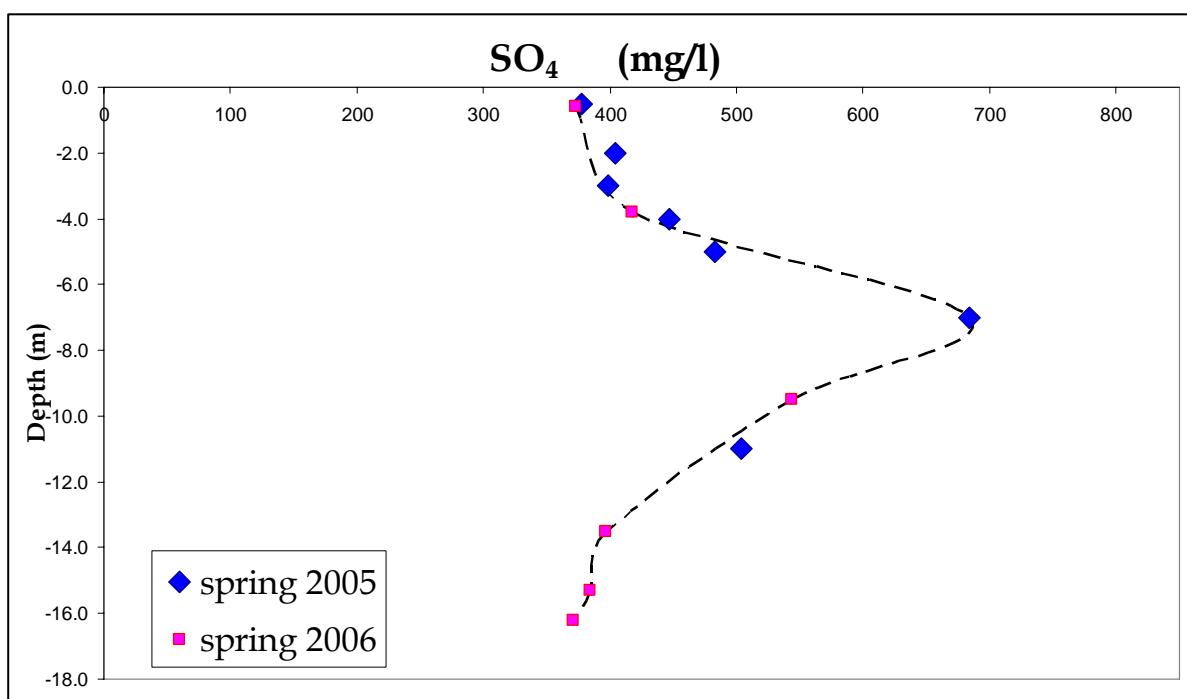


Figure 5.2.1 Sulphate profile in the Incrociata quarry during spring 2005 and spring 2006

The Incrociata sandpit receives seawater, through the San Rocchino sandpit, groundwaters from the east and Massaciuccoli lake waters from the south. We can hypothesize that bottom water results by mixing between seawater and surface water of the sandpit in different proportions. In particular, the percentage of seawater compared with surface less saline waters increase with depth, as indicated by chloride, boron, conductivity and  $\delta^{18}\text{O}$  and  $\delta^2\text{H}$  (chapter 4.3). As in the  $\text{SO}_4$  vs Cl plot (Figure 5.2.2) the samples lie along a hypothetical mixing line between continental waters and seawater, we can calculate the percentage of each end-member by means of the binary mixing equation:

$$[\text{Cl}]_d = \chi_{\text{sea}} \cdot [\text{Cl}]_{\text{sea}} + (1 - \chi_{\text{sea}}) \cdot [\text{Cl}]_{\text{sup}}$$

where  $[\text{Cl}]_d$ ,  $[\text{Cl}]_{\text{sea}}$  and  $[\text{Cl}]_{\text{sup}}$  are the chloride concentration of the Incrociata water at 'd' depth, seawater and surface water, respectively, and  $\chi_{\text{sea}}$  is the percentage of sea water.

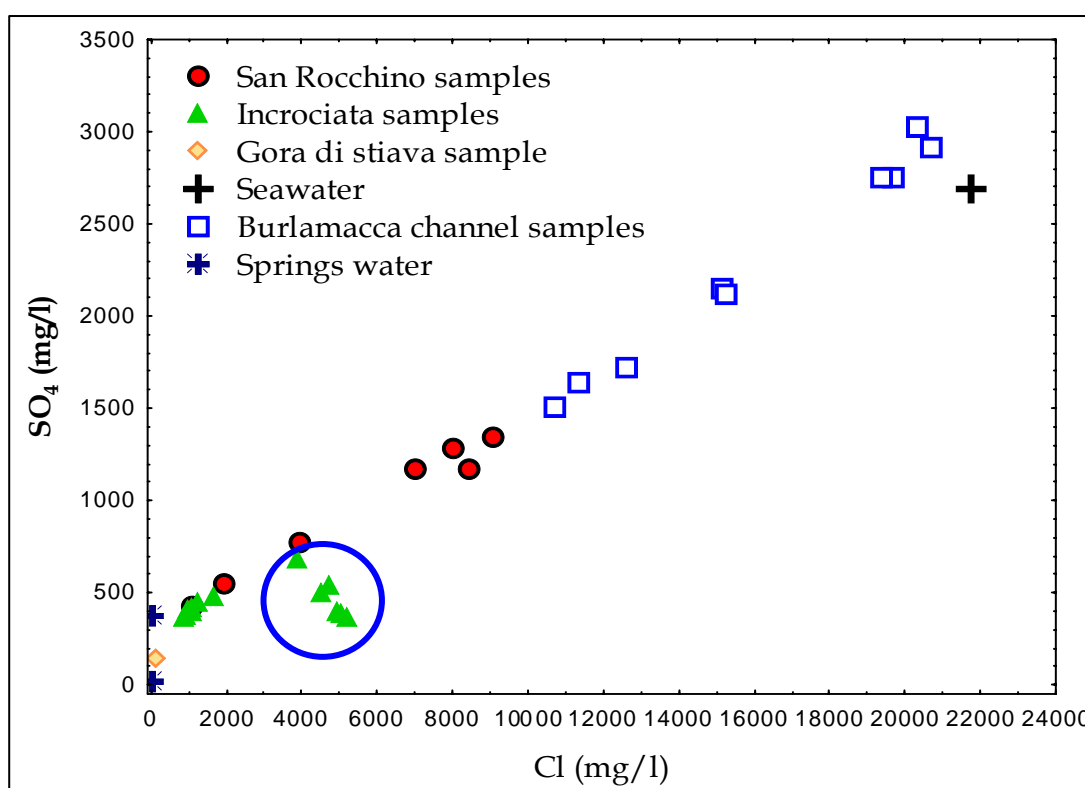


Figure 5.2.2  $\text{SO}_4$  vs Cl diagram

In this way, we first obtain  $\chi_{\text{sea}}$  and then recalculate the  $\text{SO}_4$  content of waters at depth 'd'  $\neq 0$  in the absence of reduction reactions, by mixing the two end members. The sample collected at 3 m depth was considered representative of the surface water because chloride starts to increase below 3 m depth (Figure 5.2.3.). Table 5.2.1 summarizes the results of mixing calculations and the fraction,  $f$ , representing the ratio between measured and calculated sulphate concentrations. This can be considered as the fraction of sulphate unconsumed by the reduction process.



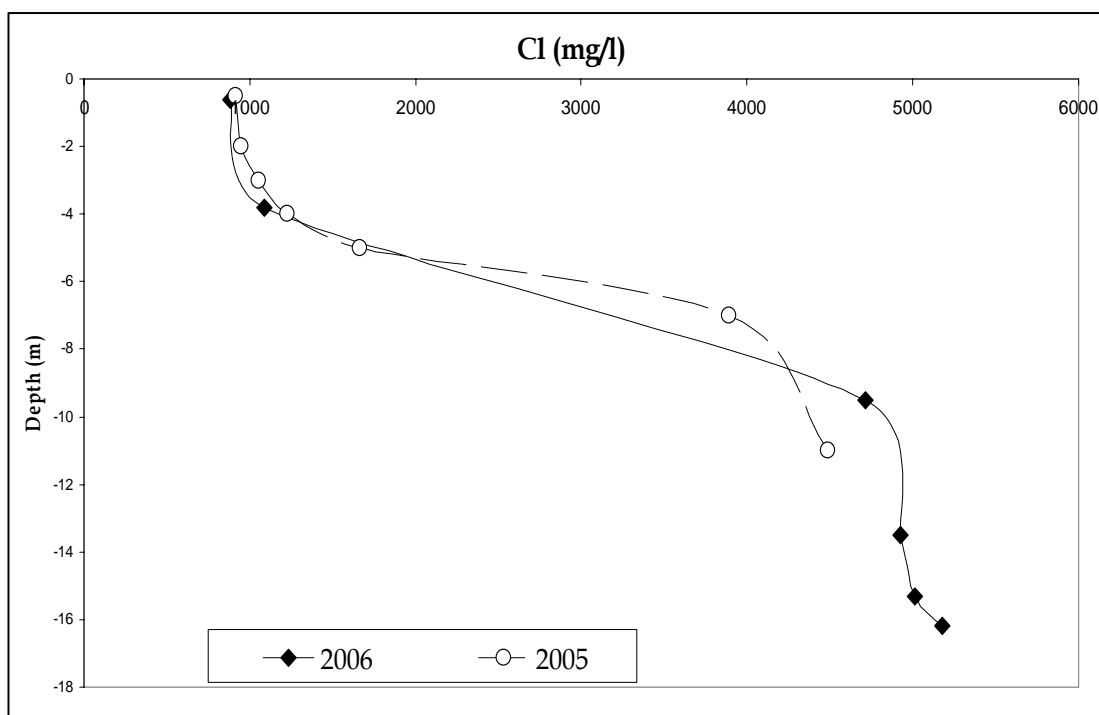


Figure 5.2.3 Chloride profile for the Incrociata quarry during 2006 and 2005 (dotted line)

Table 5.2.1 Reconstruction of sulphate concentration in anoxic waters of Incrociata quarry (Concentrations are in mg/l); f is the fraction of remaining (not consumed by BSR) sulphate

Sample	Cl	SO <sub>4</sub> meas	%seawater	SO <sub>4</sub> calc	f
Inc9.5-sp06	4713	543	17.5	817	66.49487
Inc13.5-sp06	4926	396	18.5	840	47.13845
Inc15.3-sp06	5010	384	19	848	45.28818
Inc16.2-sp06	5180	371	20	867	42.76829
Inc3-sp06	1084	418			
sea	21486	2853			

The relationship between the formal oxidation state of C atoms and reaction stoichiometry is (Marini *et al.*, 2000):

$$\langle C \rangle = \nu_{SO_4} / \nu_{TC}$$

This relationship holds true for any class of organic compounds, and within any given class there is a progressive shift towards the CH<sub>4</sub> point with increasing length of the alkyl chain. The stoichiometry of bacterial SO<sub>4</sub> reduction in samples from the Incrociata sandpit was calculated by means of simple mass balances, based on the sulphate concentration reported in Table 5.2.1. The calculated  $\nu_{SO_4} / \nu_{TC}$  ratios are given in Table 5.2.2; for sample Inc9.5-sp06 we considered the contribution of nitrate reduction, as nitrate is present in superficial samples and is absent below 9.5 m depth. The values are significantly higher than the  $\nu_{SO_4} / \nu_{TC}$  value of -0.5 implied by reaction

(1). It should be noted that if bacterial  $\text{SO}_4$  reduction does not involve total conversion of organic substances to carbonate, as assumed in this discussion,  $\nu_{\text{SO}_4} / \nu_{\text{TC}}$  ratios are higher than calculated. Based on the relationship between the  $\nu_{\text{SO}_4} / \nu_{\text{TC}}$  ratio and the formal oxidation state of C, it can be concluded that the stoichiometry of bacterial  $\text{SO}_4$  reduction in the Incrociata sandpit implies the involvement of substantially oxidized organic substances, with average oxidation state of C of +0.86 to +1.2.

**Table 5.2.2** Calculation of the formal oxidation state of C for the deep samples of the Incrociata quarry

Sample	Alkalinity	N- $\text{NO}_3$	$\Delta\text{Alk}$	$\Delta\text{SO}_4$	$\nu_{\text{SO}_4} / \nu_{\text{TC}}$	formal, average oxidation state of C
	mM/l	mM/l	mM/l	mM/l		
Inc0.6-sp06	3.40	0.23				
Inc3-sp06	3.45	0.28				
Inc9.5-sp06	11.63	<0.1	11.63	-2.84	-0.37	1.22
Inc13.5-sp06	15.83	<0.2	15.83	-4.44	-0.36	1.13
Inc15.3-sp06	16.35	<0.3	16.35	-4.83	-0.37	1
Inc16.2-sp06	16.55	<0.4	16.55	-5.15	-0.39	0.86

Stable isotope techniques constitute a powerful tool to elucidate sulphur transformations in lake systems (Knöller *et al.*, 2004; Faville *et al.*, 2004). BSR is a multistep process that involves kinetic isotope effects for both sulphur and oxygen isotopes. Depending on environmental conditions, sulphur isotope fractionation between sulphate-S and  $\text{H}_2\text{S}$  can be quite variable, with enrichment factors between less than 4‰ and more than 46‰ (Harrison and Thode, 1958; Rees, 1973; Chambers and Trudinger, 1979; Canfield and Thamdrup, 1994; Canfield *et al.*, 1998). However, Canfield (2001) observed that S isotope fractionation ranged only from 8‰ to 21‰ in situations where sulphur-reducing bacteria were provided with no-limiting concentrations of amended substrate such as acetate, ethanol, and lactate. Since bacteria preferentially rupture  $^{32}\text{S}$ - and  $^{16}\text{O}$ -containing bonds during BSR, the residual  $\text{SO}_4$  becomes progressively enriched in  $^{34}\text{S}$  and  $^{18}\text{O}$  as the reaction progresses (Nakai and Jensen, 1964; Mizutani and Rafter, 1973; Holt and Kumar, 1991). Hence, increasing  $\delta^{34}\text{S}$  and  $\delta^{18}\text{O}$  values and simultaneously decreasing concentrations of dissolved sulphate in the water column are expected upon occurrence of BSR. In a closed system, except for sulphide removal, the isotopic enrichment in  $\delta^{34}\text{S}$  and  $\delta^{18}\text{O}$  of the residual sulphate develops as in a Rayleigh distillation model:

$$\delta^{34}\text{S}_{(\text{SO}_4)} = \delta^{34}\text{S}_{(\text{SO}_4)0} + \varepsilon \ln f$$

$$\delta^{18}\text{O}_{(\text{SO}_4)} = \delta^{18}\text{O}_{(\text{SO}_4)0} + \varepsilon \ln f$$

where  $f$  denotes the fraction of unconsumed  $\text{SO}_4$  and  $\delta^{34}\text{S}_{(\text{SO}_4)0}$ ,  $\delta^{18}\text{O}_{(\text{SO}_4)0}$  represent the initial isotope composition of dissolved  $\text{SO}_4$ . Stable isotope fractionation during a reaction, commonly quantified in terms of the fractionation factor,  $\alpha$ , or the isotope enrichment factor,  $\varepsilon$  (in per mil, Hoefs, 2004), represents the slope of the linear regression line in a plot of measured  $\delta^{34}\text{S}$  values against the fraction of remaining, unconsumed  $\text{SO}_4$ .

Therefore, sulphur isotope analyses constitute an elegant tool for monitoring BSR and, in general, redox conditions of waters. For this purpose,  $\delta^{34}\text{S}_{\text{SO}_4}$  and  $\delta^{18}\text{O}_{\text{SO}_4}$  were analyzed in the waters of the Incrociata sandpit. Figures 5.2.4 and 5.2.5 show the isotopic variation in the Incrociata waters.

Differences in the isotopic composition between oxic epilimnic waters and anoxic hypolimnic ones are clearly evident.

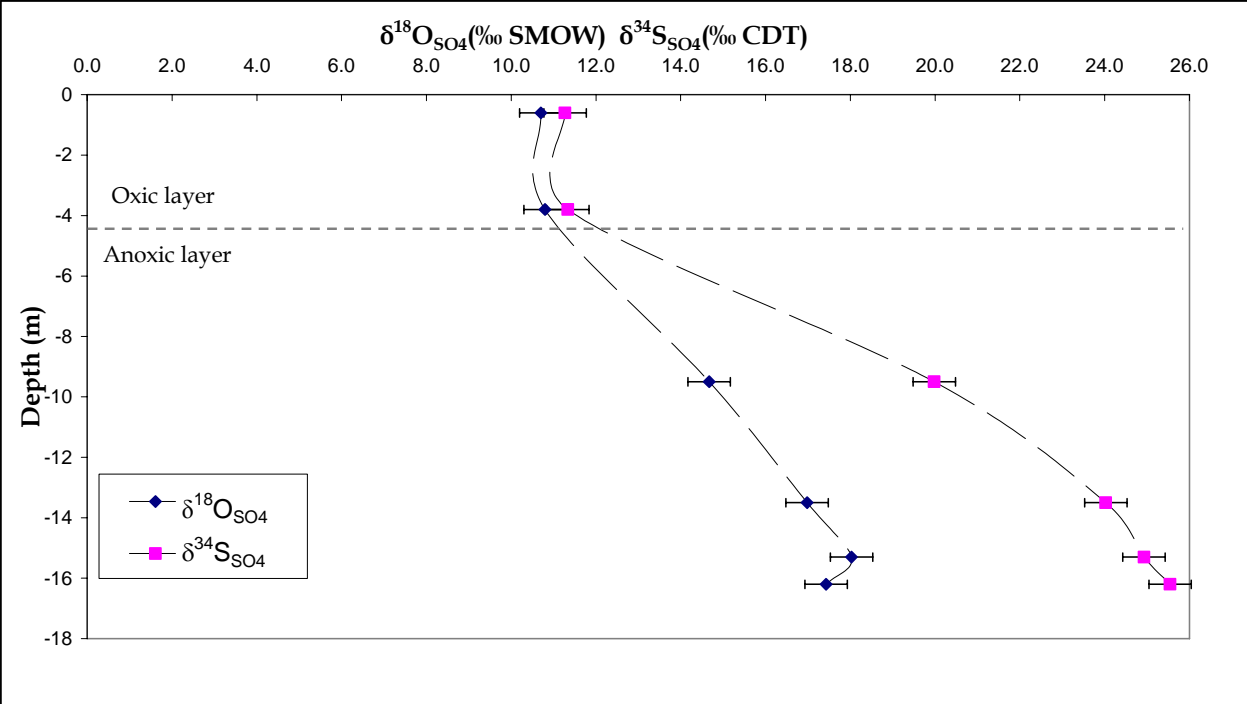


Figure 5.2.4  $\delta^{34}\text{S}_{\text{SO}_4}$  and  $\delta^{18}\text{O}_{\text{SO}_4}$  vertical profiles in the water Incrociata quarry

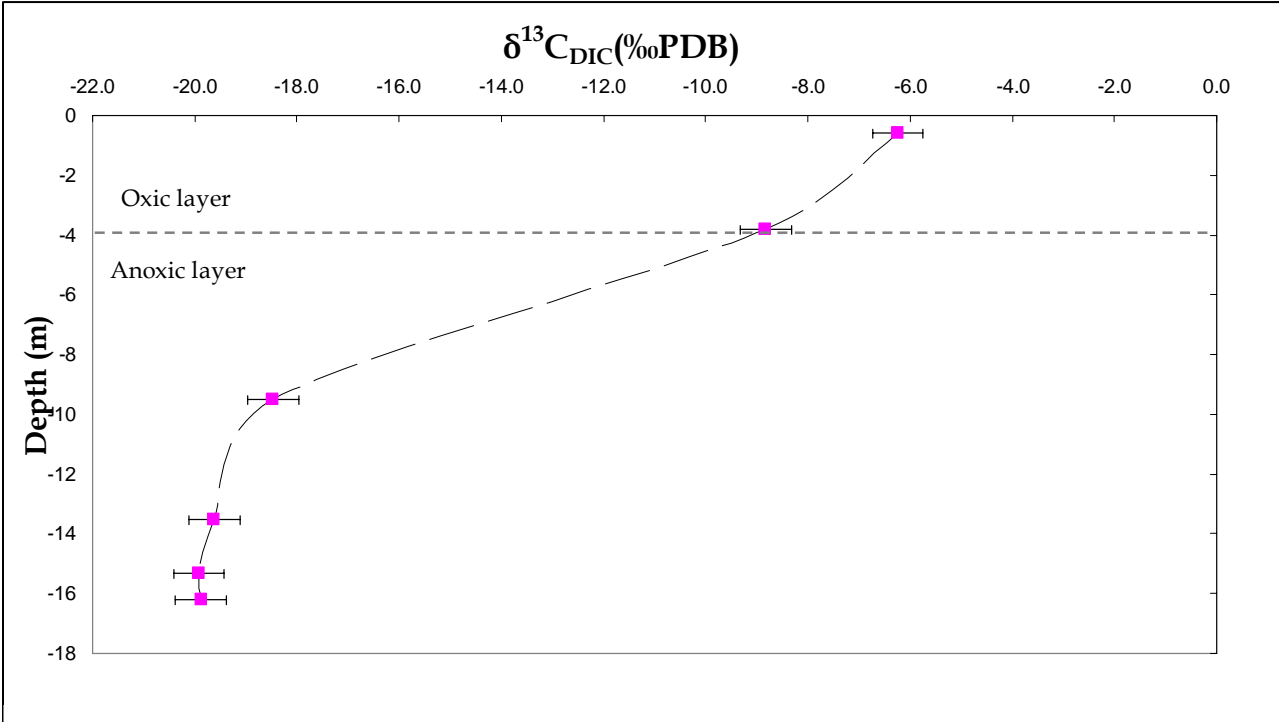
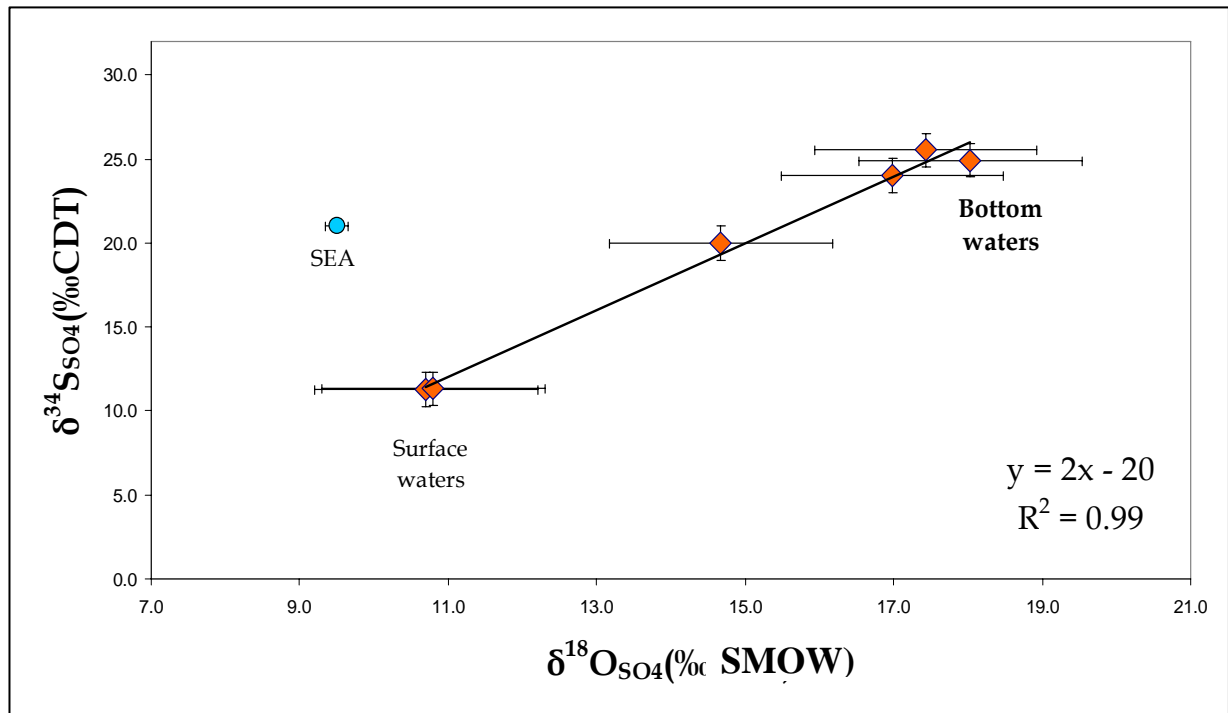


Figure 5.2.5  $\delta^{13}\text{C}_{\text{DIC}}$  vertical profile in the water Incrociata quarry.

The  $\delta^{34}\text{S}_{\text{SO}_4}$  vs  $\delta^{18}\text{O}_{\text{SO}_4}$  diagram (Figure 5.2.6) shows the positive correlation between O and S isotope ratios that fit a straight line of slope close to 2, corresponding to a  $\delta^{34}\text{S}_{\text{SO}_4}/\delta^{18}\text{O}_{\text{SO}_4}$  ratio of 0.5.



**Figure 5.2.7**  $\delta^{34}\text{S}_{\text{SO}_4}/\delta^{18}\text{O}_{\text{SO}_4}$  diagram for the waters of the Incrociata quarry

Mizutani and Rafter (1969) reported that the ratio of  $^{18}\text{O}$  to  $^{34}\text{S}$  for the remaining  $\text{SO}_4$  was approximately 0.25, even if it is very variable. In fact, Aharon and Fu (2000) pointed out that  $\delta^{18}\text{O}$  vs.  $\delta^{34}\text{S}$  relationships of sulphate modified by microbial sulphate reduction have slopes in the range of 0.25 to 0.71.

The values of  $\delta^{18}\text{O}$  and  $\delta^{34}\text{S}$  of the superficial water are +10.7‰ (vs. PDB) and +11.3‰ (vs. CDT), respectively. These values are relatively different from those of seawater reported in the Figure 5.2.5, which has an isotopic composition of  $+9.4 \pm 0.15$  for  $\delta^{18}\text{O}$  and  $20 \pm 0.25$  for  $\delta^{34}\text{S}$  (Leone *et al.*, 1987; Longinelli, 1988; Cortecchi *et al.*, 2001). Sulphates in waters come from both natural and anthropogenic sources. The primary sources of anthropogenic sulphate include mining activity, fertilizers, industrial activities and urban sewage. References values for different sources of  $\text{SO}_4$  are reported in Table. 5.2.3. It is not possible to establish the nature of the sulphate in the considered system by means of one value. Nevertheless, the  $\delta^{34}\text{S}_{\text{SO}_4}$  value is lower than the seawater signal and the Triassic sulphate. A contribution of lighter sulphate has to be supposed, probably derived by pollutants from fertilizers and urban wastes.

**Table 5.2.3** Typical values of  $\delta^{34}\text{S}_{\text{SO}_4}$  and  $\delta^{18}\text{O}_{\text{SO}_4}$  for different sources

Sulphur source	$\delta^{34}\text{S}_{\text{SO}_4\text{-CDT}}$	$\delta^{18}\text{O}_{\text{SO}_4\text{-SMOW}}$	References
Seawater	20‰	9.4‰	Leone <i>et al.</i> , 1987; Longinelli, 1988; Cortecchi <i>et al.</i> , 2001
Precipitation Pisa	1‰		Cortecchi and Longinelli, 1970
Rain from mediterranean coast	5.3-14.3‰		Wakshall and Nielsen, 1982
Tertiary seawater sulphate	16-23‰	11-16‰	Clark and Fritz, 1997
Triassic gypsum and anhydrite (Lucca)	16.4‰	8.9-10.7‰	Boschetti <i>et al.</i> , 2005
Natural oil and gas	0-10‰		Newman <i>et al.</i> , 1991
Anthropogenic $\text{SO}_4$ in European river waters	2-6‰		Hoefs, 2004
Serchio River (near Migliarino)	10.8-12.1‰		Longinelli and Cortecchi, 1969; Arbizzani <i>et al.</i> , 2001
Alum used in paper-mill along the Serchio river	8-9‰		Longinelli and Cortecchi, 1969
Pollutant input in the Serchio catchment	9-14‰		Arbizzani <i>et al.</i> , 2001
$(\text{NH}_4)_2\text{SO}_4$ and $\text{SO}_4$ from phosphatic fertilizers in Northern Europe	0.4-10.3‰		Moncaster <i>et al.</i> , 2000
$\text{Na}_2\text{SO}_4$ from textiles along the Bisenzio river in the Arno river catchment	1.6‰		Cortecchi <i>et al.</i> , 2002
Elemental S applied in agriculture along the Arno river	11.9‰		Cortecchi <i>et al.</i> , 2002

### 5.3 CONCLUSION

Physical profiles carried out in depth in the sandpit ponds pointed out that well defined thermoclines develop in summer. Some ponds are occasionally reached by seawater, where it sinks because of its higher density and, therefore, develop a permanent stratification. Density calculations denoted that during all the year San Rocchino and Incrociata deep waters have a higher density. This situation prevents water mixing but supports the development of anoxic environments.

Vertical profiles of sandpit pond, actually, indicate the occurrence of strong redox gradients. The oxygen concentration decreases within the first 4-5 m from saturation with air to virtually nil, because the water stratification acts a barrier preventing mixing between superficial waters rich in oxygen and deep anoxic waters. In addition, a regular increase of  $\text{CO}_2$  with depth can be observed, together with chloride and sulphate variations. The alkalinity and Eh trend, and the presence of  $\text{H}_2\text{S}$  suggest the occurrence of bacterial  $\text{SO}_4$  reduction at depth. These trends are paralleled by a

$\delta^{13}\text{C}_{\text{DIC}}$  decrease and an increase of  $\delta^{34}\text{S}(\text{SO}_4)$ , suggesting a biogenic production of  $\text{CO}_2$  together with sulphate and nitrate reduction.

Furthermore, the presence of an oxic-anoxic interface in the water column is expected to influence the stability of iron and manganese aqueous- and solid-phase, as redox-sensitive elements. Hence, trends of iron and manganese with depth in the sandpits are analyzed. In well-oxygenated epilimnion the hydrolyzed Fe/Mn oxides dominate, while where oxygen is absent the lower redox states, Fe(II) and Mn(II), are favoured. Because of these properties, where the bottom waters become anoxic, Fe(II) and Mn(II) can accumulate. However, when anoxic conditions are well advanced, dissolved sulphide can accumulate in the anoxic hypolimnion, leading to the precipitation of FeS.

## 6 SEDIMENTS

In this chapter the main chemical characteristics of superficial sediments are presented and discussed.

The sediments collected are described as brown organic silts or grey silts with black layers and vegetal fragments and shells. Samples collected from the Burlamacca channel are rich in sand. Gas bubbles were present in some samples, particularly in the cores near the lake banks or in the agricultural drainage. Samples were sliced in layers of different thickness, based on the visual variations in sediment characteristics. In general, the first level corresponds to the first 5cm (0-5 cm), the second level to 5-10/15 cm in depth and the third level to 25-40cm.

All the sediment layers have high water contents. The mean value is 77%. As a whole, the content of organic and inorganic carbon varies widely, as do Water Content and LOI values. In contrast, the content of nitrogen fluctuates less (Table 6.1).

**Table 6.1** Statistical parameters of sediment samples (significance level of 0.05)

	Water Content	LOI <sub>105</sub>	LOI <sub>375</sub>	LOI <sub>550</sub>	LOI <sub>950</sub>	LOI <sub>res</sub>	TN %	TC %	TOC %	TIC %	C/N
<b>N</b>	49	20	20	20	20	20	36	36	36	36	36
<b>Mean</b>	76.78	6.54	20.58	3.71	10.11	60.18	1.00	19.06	17.89	1.19	20.74
<b>Mediana</b>	78.00	4.78	15.30	3.19	4.99	58.25	0.97	20.05	19.70	0.06	17.72
<b>Min</b>	26.00	0.79	2.11	0.90	1.31	24.49	0.07	3.33	2.33	0.00	12.05
<b>Max</b>	94.00	20.38	53.80	11.61	30.39	92.63	2.18	47.80	47.90	12.90	56.86
<b>Dev.Std.</b>	12.59	4.80	14.77	2.10	10.09	17.34	0.53	10.70	11.59	2.77	9.59

Sequential loss on ignition (LOI) is a simple form of thermogravimetric analysis for estimating the content of organic matter and carbonate minerals in sediments using the linear relations between LOI values and organic. Organic matter is oxidized at temperatures between 70°C and 550°C, and carbonate between 550°C and 1000°C. The organic carbon content has been experimentally calculated as about half the LOI<sub>550</sub> (Dean, 1974). However, high clay content of sediment can influence results (Holliday and Stein, 1989; Smith, 2003; Santisteban *et al.*, 2004), because the heating drives off interstitial water held in clays that can be misinterpreted as organic matter or carbonates. Gypsum, sulphide minerals and metallic oxihydroxides can modify LOI values as well, via oxidation or dehydration (Brauer *et al.*, 2000; Rosen *et al.*, 2002; Ralska-Jasiewiczowa *et al.*, 2003). Additional errors come from loss of inorganic carbon at temperatures between 425 and 520°C in minerals such as siderite, magnesite, rhodochrosite and dolomite (Heiri *et al.*, 2001). The samples collected in the lake contain very little clay, thus, LOI appears to produce an accurate assessment of organic matter content. In particular, the best estimation of organic carbon is LOI<sub>375</sub>. The Figure 6.1 shows the good correlation between TOC and LOI<sub>375</sub> ( $R^2=0.877$ ) and the following relation:  $TOC = 0.6 * LOI_{375}$ .

The superficial sediments of Massaciucoli lake are rich in organic matter and total carbon is exclusively organic carbon, except for the samples collected in the lake (L14 and L15) where inorganic carbon prevails. The sample collected in the Burlamacca channel, L10, has the lowest carbon content. Indeed, the main mineral is quartz and SiO<sub>2</sub> represent the 73% of the chemical bulk composition. For samples L14 and L15 calcite is the main mineral (80%) and quartz represents 10% of the mineralogical composition. In these two samples the SiO<sub>2</sub> is 11% and the CaO content is 43%.

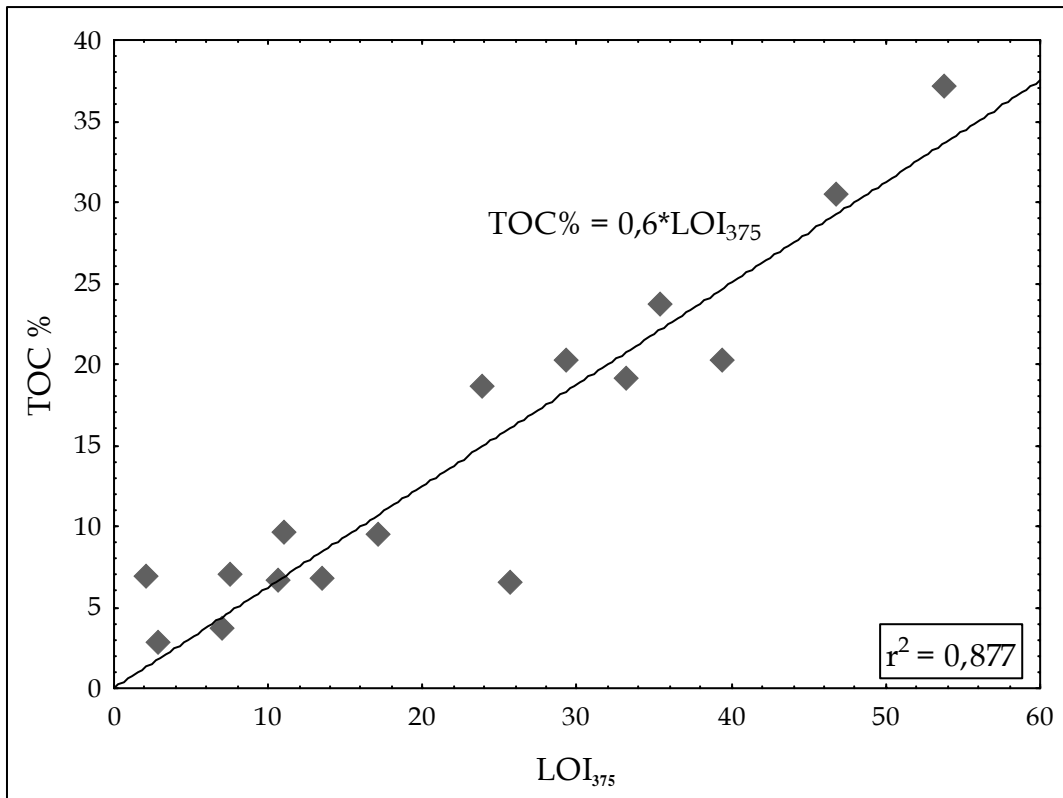


**Figure 6.1** TOCpercentage and  $LOI_{375}$  relation in the sediments of Massaciucoli lake



## 6.1 CARBON DATING

The high organic matter content in the cores allowed us to collect adequate carbon quantities to make analyses of  $^{14}\text{C}$ . Three cores were selected from different lake areas, namely at the Barra mouth (southern part of the lake, L13), at the northern side of the lake (L14) and at the entrance in the lake of the Burlamacca channel, L7. Nuclear weapons' tests in the 1950s–60s produced enough radiocarbon (bomb  $^{14}\text{C}$ ) to double the atmospheric content of  $^{14}\text{C}$ . Long-term measurements of atmospheric  $^{14}\text{C}$  have revealed a distinctive trend (Figure 6.1.1) with a rapid  $^{14}\text{C}$  increase from the late 1950s followed by a peak around 1963 (Levin and Hesshaimer 2000). Subsequently, atmospheric  $^{14}\text{C}$  concentrations declined as the isotope dispersed into other reservoirs involved in the C cycle (Levin and Hesshaimer, 2000). Goodsite *et al.*, (2001) showed the potential of the bomb  $^{14}\text{C}$  pulse for dating surface peat layers. The technique relies on the fact that stratified peat profiles provide a record of the plants that formerly grew on the mire surface. As the  $^{14}\text{C}$  concentration in plant structures reflects the  $^{14}\text{C}$  content of the atmosphere at the time of photosynthesis, stratified peat profiles contain a record of past atmospheric  $^{14}\text{C}$  concentration. Since large changes in atmospheric  $^{14}\text{C}$  occurred as a result of the bomb tests, it should be possible to calibrate the  $^{14}\text{C}$  values of the recently formed peat by matching against the record of atmospheric bomb  $^{14}\text{C}$ .

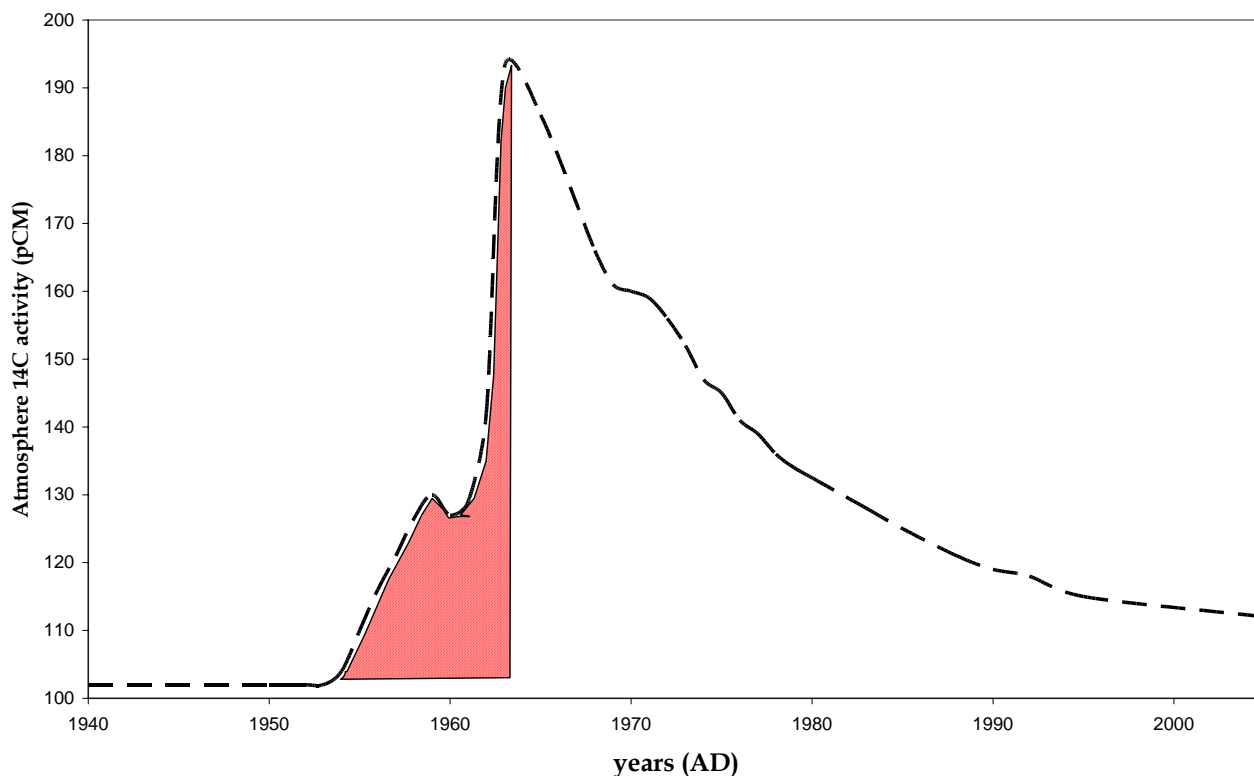


**Figure 6.1.1** Average annual atmospheric  $^{14}\text{CO}_2$  record for the Northern Hemisphere. Annual averaging smoothes the curve and reduces the 1963 peak. Adapted from Levin and Kromer (2004) and Stuiver *et al.* (1998)

Therefore, we analyzed the  $^{14}\text{C}$  profiles in each core to compare these trends with that of atmospheric  $\text{CO}_2$ .

In the southern part of the lake we collected a 90-cm-long core. The  $^{14}\text{C}$  profile is illustrated in Figure 6.1.2.

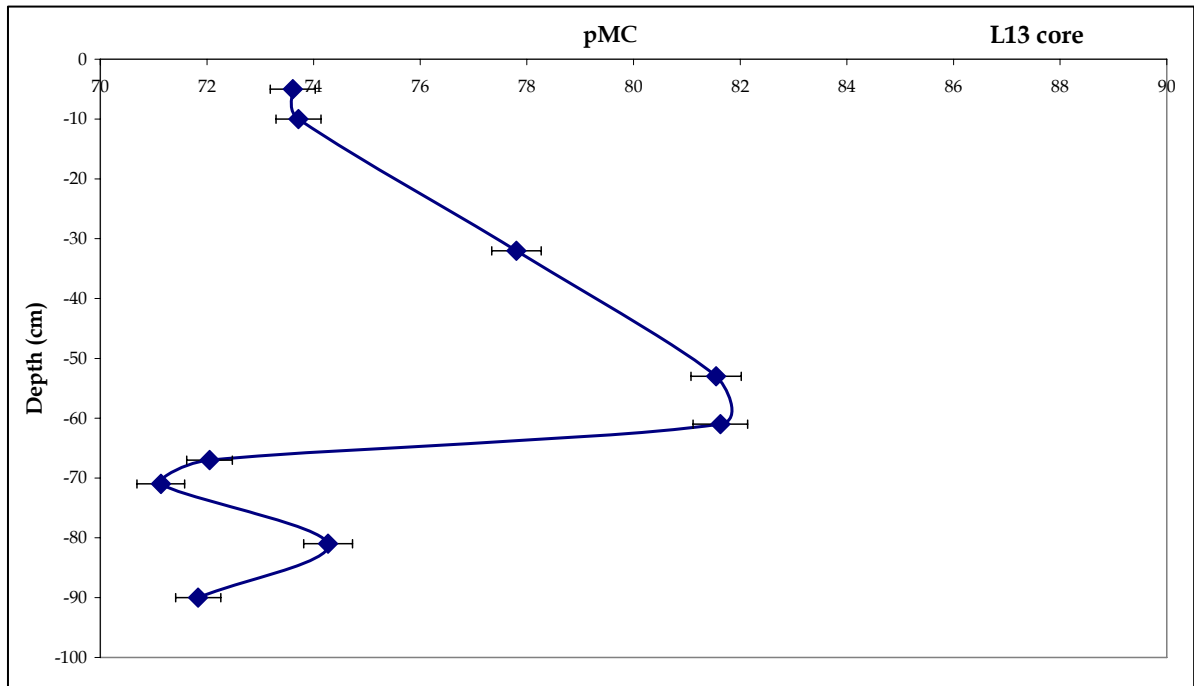


**Figure 6.1.2** <sup>14</sup>C activity profile along the core collected in the southern part of the lake at the site L13

At this site the <sup>14</sup>C activity increases remarkably from the surface up to 55-cm-depth and then it decreases abruptly. We can hypothesize that the peak at -55cm corresponds to the 1963 atmospheric peak. There is another little peak at -80cm and we can suppose that the lower activity at -70cm can be due to the Suess effect. As we collected one long core only, the atmospheric trend was registered only in this sample. Further analyses are necessary other analyses to confirm these data. Figures 6.1.3 and 6.1.4 show the <sup>14</sup>C activity trend in the northern side of the lake.

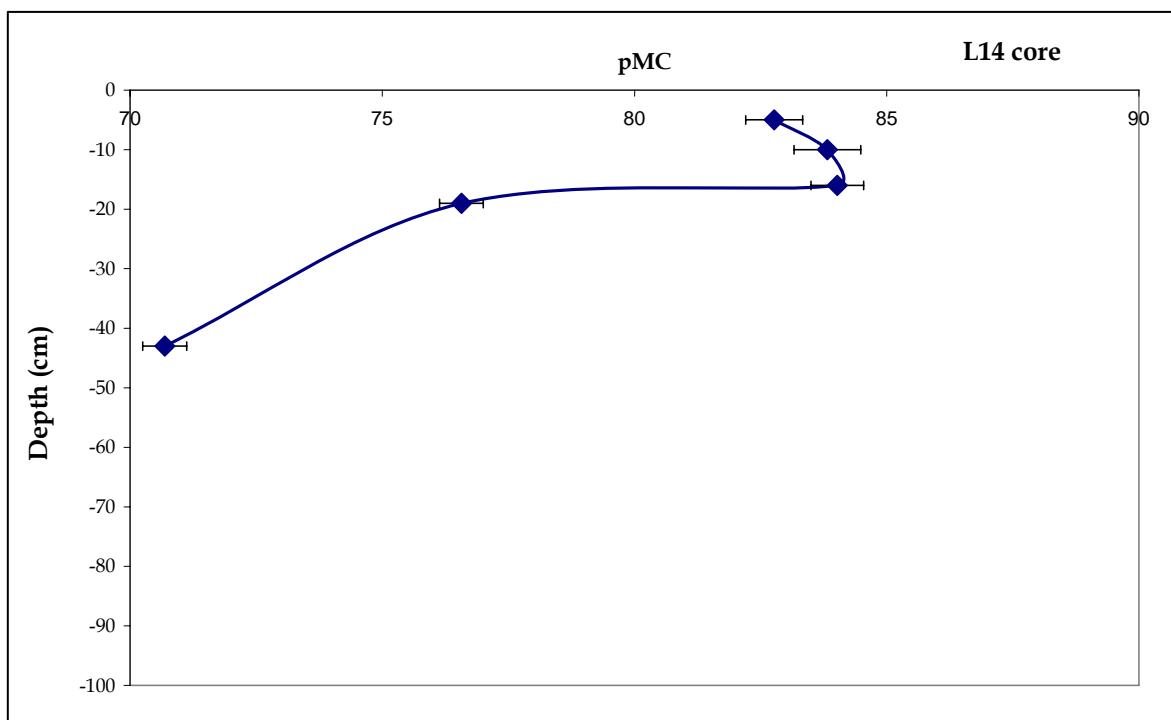


**Figure 6.1.3** <sup>14</sup>C activity profile along the core collected in the northern part of the lake at the site L14

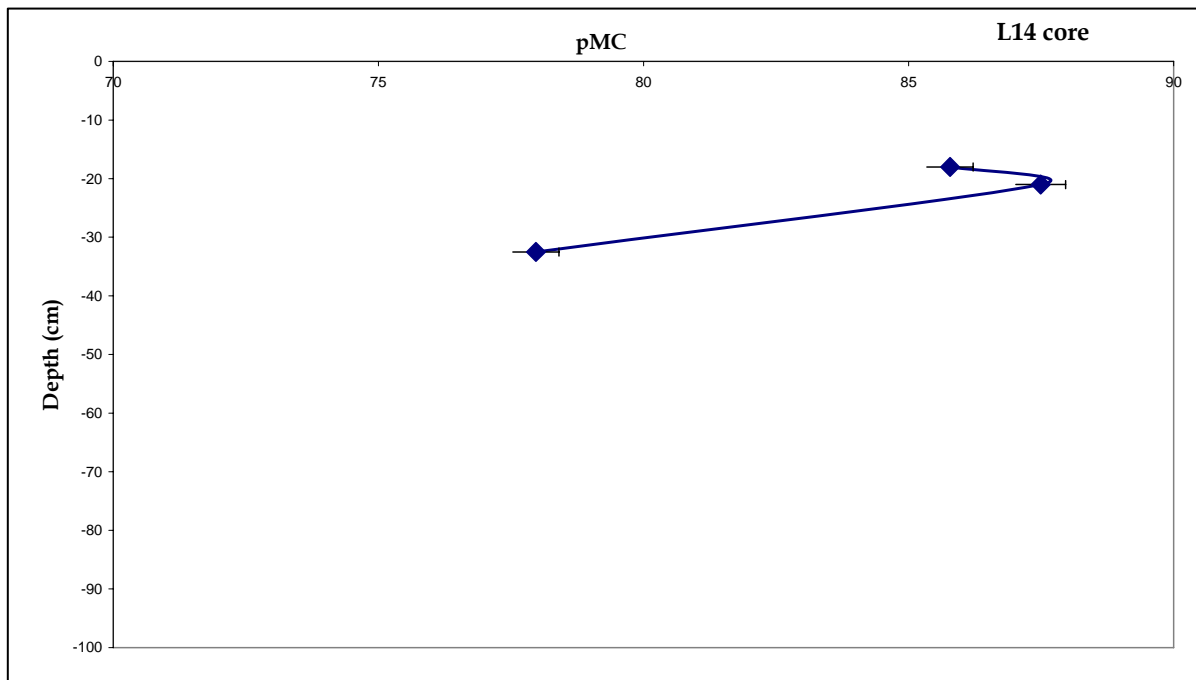


**Figure 6.1.4**  $^{14}\text{C}$  activity profile along the core collected in the northern part of the lake at the site L7

In the cores collected in the northern side of the lake the peak of  $^{14}\text{C}$  activity has a value similar to that recorded in the southern side but it occurs 15-20-cm depth.

Comparing the  $^{14}\text{C}$  activity trend in the three cores it is evident that in the southern part of the lake there is a higher sedimentation rate with respect to its northern section. Remembering that the Barra channel drains the agricultural area, we can hypothesize that it transports a large flux of organic matter into the lake. In fact at this site, the rate of sedimentation can be estimated as 1.3 cm/year, supposing a constant sedimentation through the considered time interval.

Anyhow, there is a large difference in the sedimentation between the southern and the northern side of the lake and this confirms the influence of the agricultural area on the considered system.

## BIBLIOGRAPHY

---

- Aguzzi M., Amorosi A., Sarti G. (2005). "Stratigraphic architecture of Late Quaternary deposits in the Lower Arno Plain (Tuscany, Italy)", *Geologica Romana*, **38**: 1-9.
- Aharon P., Fu B. (2000). "Microbial sulfate reduction rates and sulphur and oxygen fractionations at oil and gas seeps in deepwater Gulf of Mexico", *Geochim. Cosmochim. Acta*, **64**: 233-246.
- AIC Progetti (1982). "Studio idrogeologico del lago di Massaciuccoli", Rapporto per il Consorzio di bonifica del lago e del padule di Massaciuccoli.
- Alessio M., Allegri L., Bella F., Calderoni G., Cortesi C., Dai Pra G., De Rita D., Esu D., Follieri M., Improta S., Magri D., Narcisi B., Petrone V., Sadori L. (1986). "<sup>14</sup>C dating, geochemical features, faunistic and pollen analyses of the uppermost 10 m core from Valle di Castiglione (Rome, Italy)", *Geologica Rom.*, **25**: 287-308.
- Alessio G., Baldaccini G.N., Bianucci P., Duchi A., Esteban Alonso J. (1992). "Fauna ittica e livello trofico del Lago di Massaciuccoli", *Parco Nat. Migliarino - San Rossore - Massaciuccoli. Doc. Tec.* **5**: 167-180.
- Alessio M., Bella ., Cortesi C. (1964). "University of Rome. Carbon-14 dates II", *Radiocarbon* **6**: 77-90.
- Alessio G., Bianucci P., Duchi A. (1995). "I popolamenti del Lago di Massaciuccoli (Toscana) e le prospettive di biomanipolazione", by: "Il bacino del Massaciuccoli IV. Cons. Idraulico II cat.", Pacini Ed.: pp. 79-90.
- Allaway W. G., Osmond C.B., Throughton I. H. (1974). "Environmental Regulation of Growth, Photosynthetic pathway and carbon isotope discrimination ratio in plants capable of Crassulacean acid metabolism", in: R.L. Bialeski, A.R. Ferguson and M.M. Cresswell (Eds). "Mechanisms of Regulation of Plant Growth", *R. Soc. N.Z.*, **12**: 195-202.
- Allegretti G.M., Gentili M., Berrugi D. (2002). "Piano strutturale 2002, Comune di Viareggio (adottato con del C.C. n°9 del 8/2/02, approvato con del. C.C. n°27 del 19/2/2001) ", Public Documentation, Ufficio Piano Regolatore, Comune di Viareggio.
- Allison J.D., Brown D.S., Novo-Gradac K.J. (1990). "MINTEQA2/PRODEFA2--A geochemical assessment model for environmental systems--version 3.0 user's manual", Environmental Research Laboratory, Office of Research and Development, U. S. Environmental Protection Agency, Athens, Georgia, 106 pp.
- American Water Works Association (AWWA) (1998). "Standard Methods for the Examination of Water and wastewater, 20th Edition", American Public Health Association, American Water Works Association and Water Environment Federation.
- Amos C.L., Baneschi, I., Cipollini, P., Friend, P.L., Gulia, L., Helsby R., Scozzari A. (2004). "Study of a highly modified coastal lake by side-scan sonar, modeling and remote sensing", *Geophysical Research Abstracts*, vol. **6**.
- Antonioli F., Girotti O., Improta S., Nisi M.F., Pugliesi C., Verrubbi V. (2000). "Nuovi dati sulla trasgressione marina olocenica nella pianura versiliese", by: Bianchesi P., Angelelli A., Forni S. (eds.), *Atti del Convegno «Le Pianure - Conoscenza e salvaguardia»*, pp. 214-218, Ferrara, 8-11 novembre 1999.
- AQUATER (1980). "Accertamenti ed indagini per la salvaguardia dall'inquinamento del Lago di Massaciuccoli e del suo territorio. Fase II", *Min. Agr. e For.*, Roma, pp. 1-89.
- Arbizzani P., Cortecci G., Dinelli E., Pompilio L., Bencini A., Vaselli O. (2001). "Geochemistry of waters and sediments from the Serchio river catchment (Northern Italy)", *Proceedings International Symposium 10th Water-Rock Interaction, Villasimius (Italy)*, WRI- 10, **2**: 1035 -1038.
- Aucour A.M., Sheppard S. M.F., Guyomar O., Wattelet J. (1999). "Use of <sup>13</sup>C to trace origin and cycling of inorganic carbon in the Rhone river system", *Chem. Geol.*, **159**: 87-105.
- Auterio M., Milano V., Sassoli F., Viti C. (1978). "Fenomeni di subsidenza nel comprensorio del consorzio di bonifica della Versilia", by: "I problemi della subsidenza nella politica del territorio e della difesa del suolo" 9 - 10 Novembre 1978, Pisa.
- Autorità di Bacino del Fiume Serchio (2007). "Bilancio idrico del bacino del lago di Massaciuccoli. Piano di Bacino Stralcio", *Relazione di piano*, 199pp (accessible at: [http://www.serchio-autoritadibacino.it/piani\\_stralcio/bilancio\\_massaciuccoli/relazione\\_di\\_piano](http://www.serchio-autoritadibacino.it/piani_stralcio/bilancio_massaciuccoli/relazione_di_piano)).
- Bade D.L., Carpenter S.R., Cole J.J., Hanson P.C., Hesslein R.H. (2004). "Controls of  $\delta^{13}\text{C}$ -DIC in lakes: Geochemistry, lake metabolism, and morphometry", *Limnol. Oceanogr.*, **49**: 1160-1172.

- Baldacci F., Elter P., Giannini E., Giglia G., Lazzarotto A., Nardi R., Tongiorgi M. (1967). "Nuove osservazioni sul problema della Falda Toscana e sull'interpretazione dei flysch arenacei tipo "Macigno" dell'Appennino Settentrionale", *Mem. Soc. Geol. It.*, **6**: 218-244 .
- Baldacci F., Cecchini S., Lopane G., Raggi G. (1993). "Le risorse idriche del fiume Serchio ed il loro contributo all'alimentazione dei bacini idrografici adiacenti", *Mem. Soc. Geol. It.*, **49**: 365-391, «Scritti in onore di L. Trevisan».
- Baldock D. (1984). "Wetland drainage in Europe. The effect of agricultural policy in four EEC countries", Russel Press, Nottingham.
- Ball J.W., Nordstrom D.K. (1991). "Users manual for WATEQ4F with revised thermodynamic database and test cases for calculating speciation of major, trace, and redox elements in natural waters", USGS Open-File Report 91-183.
- Baneschi I. (2003). "Studio idrochimico ed ambientale delle acque superficiali del sistema lacustre di Massaciuccoli", Tesi di laurea inedita, Facoltà di Scienze M.F.N., Pisa.
- Barth J.A.C., Veizer J. (1999). "Carbon cycle in St. Lawrence aquatic ecosystems at Cornwall (Ontario) Canada: seasonal and spatial variations", *Chem. Geol.*, **159**: 107-128.
- Barth S. (1993). "Boron isotope variations in nature: a synthesis", *Geol. Rundsch.*, **82**: 640-651.
- Barth S. (1998). "Application of boron isotopes for tracing sources of anthropogenic contamination in groundwater", *Water Res.*, **32**: 685-690.
- Barth S.R. (2000a). "Boron Isotopic Compositions of Near-Surface Fluids: A Tracer for Identification of Natural and Anthropogenic Contaminant Sources", *Water Air and Soil Pollut.*, **124**: 49-60.
- Barth S. R. (2000b). "Utilization of boron as a critical parameter in water quality evaluation: implications for thermal and mineral water resources in SW Germany and N Switzerland", *Environ. Geol.*, **40**: 73-89.
- Bassett R. L. (1990). "A critical evaluation of the available measurements for the stable isotopes of boron", *Appl. Geochem.*, **5**: 541-554.
- Basset R.L., Buszka P.M., Davidson G.R., Chong-Diaz D. (1995). "Identification of groundwater solute sources using boron isotopic composition", *Environ. Sci. Technol.*, **29**: 2915-2922.
- Bengtsson L., Enell M. (1986). "Chemical analysis", in Berglund, B. E. (eds.): "Handbook of Holocene Palaeoecology and Palaeohydrology", John Wiley & Sons Ltd., Chichester, 423-451.
- Berner R.A. (1970). "Sedimentary pyrite formation", *Am. J. Sci.*, **268**: 1-23.
- Berner R.A. (1984). "Sedimentary pyrite formation: an update", *Geochim. Cosmochim. Acta*, **48**: 605-615.
- Berner R.A., Scott M.R., Thomlinson C. (1970). "Carbonate alkalinity in pore waters of anoxic marine sediments", *Limnol. Oceanogr.*, **15**: 544-549.
- Bianciardi T. (1999). "Studio palinologico di due sondaggi eseguiti in sedimenti olocenici nell'area del bacino del lago di Massaciuccoli (Lucca)", Tesi di Laurea unpublished, Università di Pisa.
- Blanc A.C., Settepassi F., Tongiorgi E. (1953). "Exursion au Lac de Massaciuccoli (plaine cotière de la basse Versilia)", IV° Congrès International pour l'Etude du Quaternaire, Roma-Pisa, pp. 29.
- Boccaletti M., Coli M., Decandia F.A., Giannini E., Lazzarotto A. (1981). "Evoluzione dell'Appennino settentrionale secondo un nuovo modello strutturale", *Mem. Soc. Geol. It.*, **21**: 359-373.
- Boschetti T., Venturelli G., Toscani L., Barbieri M., Mucchino C. (2005). "The Bagni di Lucca thermal waters (Tuscany, Italy): an example of Ca-SO<sub>4</sub> waters with high Na/Cl and low Ca/SO<sub>4</sub> ratios", *Hydrol. J.*, **307**: 270-293.
- Bossio A., Costantini A., Lazzarotto A., Liotta D., Mazzanti R., Mazzei R., Salvatorini G., Sandrelli S. (1993). "Rassegna delle conoscenze sulla stratigrafia del Neautoctono toscano", *Mem. Soc. Geol. It.*, **49**: 17-98 "Scritti in onore di L. Trevisan".
- Broecker W.S., Kulp J.L., Tucek C.S. (1956). "Lamont natural radiocarbon measurement III", *Science*, **124**: 154-165.
- Canfield D.E. (2001). "Isotope fractionation by natural populations of sulfate-reducing bacteria", *Geochim. Cosmochim. Acta*, **65**: 117-124.
- Canfield D.E., Raiswell R. (1991). "Pyrite formation and fossil preservation", in: Allison P. A., Briggs D. E. G. (Eds.), *Topics Geobiol.* vol. **9**: 337-387. Plenum, New York.

- Canfield D. E., Thamdrup B. (1994). "The production of  $^{34}\text{S}$ -depleted sulfide during bacterial disproportionation of elemental sulfur", *Science* **266**: 1973-1975.
- Canfield D.E., Thamdrup B., Fleischer S. (1998). "Isotope fractionation and sulfur metabolism by pure and enrichment cultures of elemental sulfur disproportionating bacteria" *Limnol. Oceanogr.*, **43**: 253– 264.
- Cantini P., Testa G., Zanchetta G., Cavallini G. (2001). "Tectonostratigraphic evolution of the Pleistocene Montecarlo Basin (Lower Arno Valley, Italy) from new stratigraphic and gravimetric data", *Tectonophysics*, **330**: 25-43.
- Carignan R., Dolors P., Vis C. (2000). "Planktonic production and respiration in oligotrophic Shield lakes", *Limnol. Oceanogr.*, **45**: 189-199.
- Carmignani L., Giglia G., Kligfield R. (1980). "Nuovi dati sulla zona di taglio ensialica delle Alpi Apuane", *Mem. Soc. Geol. It.*, **21**: 93-100.
- Carmignani L., Kligfield R. (1990). "Crustal extension in the Northern Apennines: the transition from compression to extension in the Alpi Apuane core complex", *Tectonics*, **9**: 1275-1303.
- Carmignani L., Decandia F.A., Fantozzi P.L., Lazzarotto A., Liotta D., Meccheri M. (1994). "Tertiary extensional tectonics in Tuscany (northern Apennines Italy)", *Tectonophysics*, **238**: 295-315.
- Carmignani L., Decandia F., Disperati L., Fantozzi P. L., Kligfield R., Liotta D., Meccheri M., Lazzarotto A. (2001). "Inner Northern Apennines", by: Vai G.B. and Martini I.P. (eds.): "Anatomy of an orogen: the Apennines and adjacent mediterranean basins", Kluwer Academic Publishers, pp. 197-213.
- Cartwright I., Weaver T.R., Fifield L.K. (2006). "Cl/Br ratios and environmental isotopes as indicators of recharge variability and groundwater flow: An example from the southeast Murray Basin, Australia", *Chem. Geol.*, **231**: 38-56.
- Casado S., Florin M., Molla S., Montes C. (1992). "Current status of Spanish wetlands", in Finlayson M., Hollis T., Davis T. (Eds.) "Managing Mediterranean Wetlands and their Birds", Proceedings of an IWRB International Symposium, Grado, Italy, February 1991. IWRB Special Publication N° 20, 1992, GB. Istituto Nazionale di Biologia della Selvaggina, Italy. Pages 56-58.
- Cavalli S., Cenni M. (1995). "Carta della natura e ambiti territoriali, scala 1:33.000", Selca, Firenze.
- Cenni M. (1999). "Le azioni dei progetti: Life-natura '97: "Risanamento del Massaciuccoli, sito elettivo del Tarabuso" e Life-natura '99: "Massaciuccoli 2<sup>a</sup> fase: riduzione dei sedimenti e biomanipolazione", in: "Il risanamento del lago di Massaciuccoli", Arpat, pp. 242-253.
- Cerling T.E., Solomon D.K., Quade J., Bowman J.R. (1991). "On the isotopic composition of carbon in soil carbon dioxide", *Geochim. Cosmochim. Acta*, **55**: 3403-3405.
- Chambers L.A., Trudinger P.A. (1979). "Microbial fractionation of stable sulphur isotopes: a review and critique" *Geomicrobiol.*, **1**: 249- 293.
- Chen C.T., Millero F.J. (1986). "Precise thermodynamic properties for natural waters covering only the limnological range", *Limnol. Oceanogr.*, **31**: 657-662.
- Chines C., Nolledi G. (1982). "Studio geologico generale del territorio comunale di Massarosa".
- Ciarapica G., Passeri L. (1980). "Tentativo di ricostruzione paleogeografica a livello del Trias nella Toscana a Nord dell'Arno e sue implicazioni tettoniche", *Mem. Soc. Geol. It.*, **21**: 41-49.
- Ciarapica G., Olivero S., Passeri L. (1985). "Inquadramento geologico delle principali mineralizzazioni apuane ed indizi in favore di una metallogenese triassica", *L'industria mineraria*, **1**: 19-37.
- Clark I.D., Fritz P. (1997). "Environmental Isotopes in Hydrology", Lewis Publishers, Boca Raton, 328 pp.
- Coleman M. L., Shepherd T.J., Durham J.J., Rouse J.E., Moore G.R. (1982). "Reduction of water with zinc for hydrogen isotope analysis", *Anal. Chem.*, **54**, 993-995.
- Convention on Wetlands (Ramsar, Iran, 1971) (1998) website: <http://www.ramsar.org>
- Cooke J.G. (1994). "Nutrient transformations in a natural wetland receiving sewage effluent and the implications for waste treatment", *Water Sci. Technol.*, **4**: 209-217.
- Cortecchi G., Longinelli A. (1970). "Isotopic composition of sulphate in rainwater, Pisa, Italy", *Earth Planet. Sci. Lett.* **8**: 36-40.
- Cortecchi G., Dinelli E., Bolognesi L., Boschetti T., Ferrara G. (2001). "Chemical and isotopic compositions of water and dissolved sulfate from shallow wells at Vulcano Island, Aeolian archipelago, Italy", *Geothermics*, **30**: 69-91.

- Cortecchi G., Dinelli E., Bencini A., Adorni-Braccesi A., La Ruffa G. (2002). "Natural and anthropogenic SO<sub>4</sub> sources in the Arno river catchment, northern Tuscany, Italy: a chemical and isotopic reconnaissance", *Appl. Geochem.*, **17**: 79-92.
- Crites R.W., Dombeck G.D., Watson R.C., Williams C.R. (1997). "Removal of metals and ammonia in constructed wetlands", *Water Environ. Res.*, **69**: 132-135.
- Culberson C., Pytkowicz R.M. (1967). "Effect of pressure on carbonic acid, boric acid and the pH of seawater", *Science*, **157**: 59-61.
- Dallan L., Nardi R. (1979). "Il quadro paleotettonico dell'Appennino settentrionale: un'idea alternativa", *Atti Soc. Tosc. Sc. Mat. Mem.*, **74**: 570-578.
- Dalle Mura G., Giovannini A., Antonelli M. (n.p.). "Corpi idrici superficiali. Individuazione e codifica", Provincia di Lucca Assessorato all'Ambiente, n°4, Nuova Grafica Lucchese, pp. 125.
- Davidson G.R., Bassett R. L. (1993). "Application of boron isotopes for identifying contaminants such as fly ash leachate in groundwater", *Environ. Sci. Technol.*, **27**: 172-176.
- Davison W., Hraney S.I., Etlalling J., Ric E. (1980). "Seasonal transformations and movements of iron in a productive English lake with deep water anoxia", *Schweiz. Z. Hydrol.*, **42**: 196-224.
- Della Rocca B., Mazzanti R., Pranzini E. (1987). "Studio geomorfologico Pianura di Pisa", *Geogr. Fis. Dinam. Quat.*, **10**: 56-84.
- Del Prete, Tomei P.E. (1980). "Indagini sulle zone umide della Toscana. VII. Il contingente orchidologico relitto di Massaciuccoli", in: "Il bacino del Massaciuccoli", I, Pacini, Pisa, pp. 39-50.
- D'Errico M., Simoni F., Volterra L., Gucci P.M.B., Bruno M. (1994). "Crescita *in vitro* di *Prymnesium parvum* (Carter) proveniente dal lago di Massaciuccoli" estratto da "Acqua aria", **9**: 823-828.
- Drever J.I. (1981). "The Geochemistry of natural Waters", Prentice-Hall Inc., Englewood, New Jersey.
- Duchi G., Matraia M., Viti C. (1990). "Contributo alle conoscenze idrogeologiche sul bacino del Massaciuccoli", Massaciuccoli s.r.l., Viareggio.
- Einarsson S., Stefansson U. (1983). "The sources of alkalinity in Lake Miklavatu, North Iceland", *Limnol. Oceanogr.*, **28**: 50-57.
- Eisenhut S., Heumann K.G., Vengosh A. (1996). "Determination of boron isotopic variations in aquatic systems with negative thermal ionization mass spectrometry as a tracer for anthropogenic influences", *Fresenius J. Anal. Chem.*, **354**: 903-909.
- Eisenhut S., Heumann K.G. (1997). "Identification of ground water contaminations by landfills using precise boron isotope ratio measurements with negative thermal ionization mass spectrometry", *Fresenius J. Anal. Chem.*, **359**: 375-377.
- Elter P., Giannini E., Tongiorgi M., Trevisan L. (1960). "Le varie unità tettoniche della Toscana e della Liguria orientale", *Rend. Accad. Naz. Lincei Cl. Sc. Fis. Mat. Nat.*, serie 8, **29**: 497-502.
- Epstein S., Mayeda T. (1953). "Variation of <sup>18</sup>O content of water from natural sources", *Geoch. Cosmoch. Acta* **4**: 213-224.
- Faber E., Vengosh A., Gavrieli I., Marie A., Bullen T.D., Mayers B., Holtzman R., Segal M., Shavit U. (2004). "The origin and mechanisms of salinization of the Lower Jordan River", *Geoch. Cosmoch.*, **68**: 1989-2006.
- Fauville A., Mayer B., Frömmichen R., Friese K., Veizer J. (2004). "Chemical and isotopic evidence for accelerated bacterial sulphate reduction in acid mining lakes after addition of organic carbon: laboratory batch experiments", *Chem. Geol.*, **204**: 325-344.
- Federici P.R. (1983). "Dal Calambrone al Burlamacca: lineamenti geografici e geomorfologici", in: "Guida alla natura del Parco Migliarino - S. Rossore-Massaciuccoli", pp. 3-17.
- Federici P.R. (1987). "Stato attuale delle conoscenze geomorfologiche e geologiche del bacino del Massaciuccoli in Versilia (Toscana)", Consorzio idraulico di II categoria, canali Burlamacca, Malfante, Venti e Quindici: pp. 27-52.
- Federici P.R. (1993). "The Versilian transgression of the Versilia area (Tuscany, Italy) in the light of drillings and radiometric data", *Mem. Soc. Geol. It.*, **49**: 217-225.
- Federici P.R., Mazzanti R. (1988). "L'evoluzione della paleogeografia e della rete idrografica del Valdarno Inferiore", *Boll. Soc. Geogr. It., Ser. XI, vol. V*: 573-615.

- Federici P.R., Mazzanti R. (1995). "Note sulle pianure costiere della Toscana", Mem. Soc. Geol. It., **53**: 165-270.
- Ferrara G., Reinharz M., Tongiorgi E. (1959). "Carbon-14 Dating in Pisa I", Mem. Soc. Geol. It., **49**: 217-225.
- Ferrara G., Fornaca-Rinaldi G., Tongiorgi E. (1961). "Carbon-14 Dating in Pisa II", Radiocarbon, **3**: 99-103.
- Findenegg I. (1935). "Limnologische Untersuchungen in Kärtener Seengebietten", Intern. Rev. Ges. Hydrobiol. Hydrograph., **32**: 369-423.
- Finely O.H., Eberle A.E., Rodden C.J. (1961). "Isotopic boron composition of certain boron minerals", Geochim. Cosmochim. Acta, **26**: 911-914.
- Forzieri R. (2000). "Rapporto 2000-Rapporto sullo stato dell'ambiente in Toscana", Coordinatore del Dipartimento Politiche Territoriali e Ambientali, Regione Toscana.
- Focardi P. (1987). "Problemi ambientali del Lago di Massaciuccoli", VI Convegno Nazionale dell'Ordine dei geologi, Venezia, pp. 101-111.
- Fogg T.R., Duce R.A. (1987). "Boron in the troposphere: distribution and fluxes", J. Geophys. Res., **90**: 3781-3797.
- Foresi L.M., Pascucci V., Sandrelli F. (1997). "Sedimentary and ichnofacies analysis of the Epiligurian Ponsano Sandstone (northern Apennines, Tuscany, Italy)", Giornale di geologia, **59**: 301-314.
- Franceschi R. (1992). "Ricerche preliminari sull'acquifero superficiale e profondo del lago di Massaciuccoli. Aree bonificate: ubicazione e dati di 'pompaggio'", in: "Problemi di Eutrofizzazione e prospettive di risanamento del Lago di Massaciuccoli", Ente Parco Regionale Migliarino-San Rossore-Massaciuccoli, Massarosa.
- Freeze R.A., Cherry J.A. (1979). "Groundwater", Prentice-Hall, pp 96-97.
- Frediani F. (2003). "L'eutrofizzazione e la salinizzazione del lago di Massaciuccoli", Tesi di laurea unpublished, Facoltà di Scienze M.F.N., Pisa.
- Fritz S.J., Whitworth T.M. (1994). "Hyperfiltration-induced fractionation of lithium isotopes: ramifications relating to representativeness of aquifer sampling", Water Resour Res, **30**:225-235.
- Fry B., Sherr E.B. (1984). " $\delta^{13}\text{C}$  measurements as indicators of carbon flow in marine and freshwater ecosystems", Contrib. Mar. Sci., **27**: 13-47.
- Gaillard J. (1995). "Limnologie chimique: principes et processus" In: "Limnologie Generale", R. Pourriot and M. Meybeck (eds.), Masson, Paris, pp. 115-156.
- Gandolfi G., Paganelli L. (1976). "Il litorale pisano-versiliese (Area campione Alto Tirreno). Composizione provenienza e dispersione delle sabbie", Boll. Soc. Geol. It., vol. **94**: 168-199.
- Garbari F. (2003). "Atlante Tematico della Provincia di Pisa", Pacini Editore S.p.a.-Provincia di Pisa, 20-23 pp.
- Gat J.R. (2000). "Atmospheric water balance - the isotopic perspective", Hydrol. Proc., **14**: 1357-1369.
- Gellenbeck D.J., Hunter Y.R. (1994). "Hydrologic data from the study of acidic contamination in the Miami Wash-Pinal Creek area, Arizona, water years 1992-93", U.S. Geological Survey Open-File Report 94-508, 103 pp.
- Gambrell R. P. (1994). "Trace and toxic metals in wetlands - a review", J. Environ. Quality, **23**: 883-891.
- Geoser (1995). "Progetto dell'intervento di bonifica della discarica comunale in località Pioppogatto - Comune di Massarosa", Provincia di Lucca.
- Geotecneco (1975). "Accertamento ed indagini per la salvaguardia dall'inquinamento del lago di Massaciuccoli e del suo territorio", Rapporto per conto del Consorzio di bonifica del lago e del padule di Massaciuccoli.
- Gerritse R.G; George R.J. (1988). "Role of Soil Organic Matter in the Geochemical Cycling of Chloride and Bromide", J. Hydrol., **101**: 83-95.
- Gherlandoni R., Giannini E., Nardi R. (1968). "Ricostruzione paleogeografia dei bacini neogenici e quaternari della bassa valle dell'Arno sulla base dei sondaggi e rilievi sismici", Mem. Soc. Geol. It., **7**: 91-106.
- Ghezzi G. (1994). "La salinizzazione delle acque di falda nelle aree litoranee della Toscana ed evoluzione del cono salino nella pianura del F. Cornia e nella falda superficiale in fregio al F. Serchio", in: "La gestione dell'acqua nell'agricoltura Toscana", Atti convegno ARSIA.



- Giannini E. (1950). "Studio geologico dei monti d'oltre Serchio e di Massarosa", *Boll. Soc. Geol. It.*, vol. **69**: 472-486.
- Giannini E., Nardi R. (1965). "Geologia della zona nord-occidentale del Monte Pisano e dei Monti d'oltre Serchio", *Boll. Soc. Geol. It.*, **84**: 197-270.
- Gilbert R.O. (1987). "Statistical Methods for Environmental Pollution Monitoring", John Wiley & Sons, inc. pp. 320.
- Giovannini A. (1993). "Inquadramento geologico e idrogeologico provincia di Lucca e bacino del fiume Serchio", Provincia di Lucca Assessorato all'Ambiente, n°3, vol. I e II.
- Goldman J.C., Brewer P.G. (1980). "Effect of nitrogen source and growth rate on phytoplankton-mediated changes in alkalinity", *Limnol. Oceanogr.*, **25**: 352-357.
- Gonfiantini R. (1978). "Standard for stable isotope measurement in natural compounds", *Nature* **217**: 534-36.
- Gonfiantini R. (1986). "Environmental Isotopes in Lake Studies. In: Handbook of Environmental Isotope Geochemistry", Fritz and Fontes (ed.), **2**: 113-168.
- Gonfiantini R., Togliatti V., Tongiorgi E. (1962). "Il rapporto  $^{18}\text{O}/^{16}\text{O}$  nell'acqua del lago di Bracciano e delle falde a sud-est del lago", *Not. Com. Naz. Energ. Nucl. (Italy)*, **8**, (6): 39-45.
- Gonfiantini R., Stichler W., Rozanski K., (1995). "Standards and intercomparison materials distributed by the International Atomic Energy Agency for stable isotope measurements", in: "Reference and Intercomparison Materials for Stable Isotopes of Light Elements" IAEA-TECDOC-825, IAEA, Vienna: pp. 13-29.
- Goodsite M.E., Rom W., Heinemeier J., Lange T., Ooi S., Appleby P.G., Shotyk W., van der Knaap W.O., Lohse C., Hansen T.S. (2001). "High Resolution AMS  $^{14}\text{C}$  Dating of Post -Bomb Peat Archives of Atmospheric Pollutants, in Proceedings of the 17<sup>th</sup> International  $^{14}\text{C}$  Conference", I. Carmi and E. Boaretto Ed., *Radiocarbon*, **43**: 453-473.
- Gran G. (1952). "Determination of the equivalence point in potenziometric tritition II", *Analyst*, **77**: 661-671.
- Grassi R., Mariotti-Lippi M., Zanchetta G., Bianciardi T., Bonadonna F.P. (2000). "Studio preliminare di due sondaggi superficiali eseguiti nella piana della bassa Versilia (Toscana Nord-occidentale)", *Atti del Convegno: «Le pianure, conoscenza e salvaguardia - Il contributo delle Scienze della Terra»*, 219 pp.
- Green W.J., Stage B.R., Preston A., Wagers S., Shacat J., Newell S. (2005). "Geochemical processes in the Onyx River, Wright Valley, Antarctica: Major ions, nutrients, trace metals", *Geoch. Cosmoch. Acta*, **69**: 839-850.
- Gu B., Lowe L. E. (1990). "Studies on the adsorption of boron on humic acids", *Can. J. Soil Sci.*, **70**: 305-311.
- Gulia L., Guidi M., Bonadonna F.P., Macera P. (2004). "A preliminary study of two cores from Massaciuccoli eutrophic lake, northern Tuscany, and paleoclimatic implications", *Atti Soc. Tosc. Sci. Nat., Mem., Serie A*, **109**: 97-102.
- Kass A., Gavrielia I., Yechielia Y., Vengosch A., Starinsky A. (2005). "The impact of freshwater and wastewater irrigation on the chemistry of shallow groundwater: a case study from the Israeli Coastal Aquifer", *J. Hydrol.*, **300**: 314-331.
- Kakihana H., Kotaka M., Satoh S., Nomura M., Okamoto M. (1977). "Fundamental studies on the ion exchange separation of boron isotopes", *Bulletin Chemical Society Japan*, **50**: 158-163.
- Kloppmann W. (2003). "Etude isotopique de la pollution azotée de la nappe d'Alsace entre Sierentz et Ottmarsheim" Rapport final BRGM/RP52331-FR.
- Knöller K., Fauville A., Mayer B., Strauch G., Friese K., Veizer J. (2004). "Sulfur cycling in an acid mining lake and its vicinity in Lusatia, Germany", *Chem. Geol.*, **204**: 303-323.
- Knull J.R., Richards F.A. (1969). "A note on the sources of excess alkalinity in anoxic waters", *Deep-Sea Res.*, **16**: 205-212.
- Koch W., Malissa H. (1957). "Dosage précis du carbone au moyen d'un enregistreur de conductivité", *La Metallurgie*, **89**: 719-727.
- Komor S.C. (1997). "Boron contents and isotopic compositions of hog manure, selected fertilizers and water in Minnesota", *J. Environm. Quality*, **26**: 1212-22.
- Köppen W. (1936). "Das Geographische System der Klimate", in: W. Köppen, R.Geiger, "Handbuch der Klimatologie", Bd 1, Teil C., Berlino.

- Krauskopf K.B. (1979). "Introduction to Geochemistry", McGraw-Hill, New York, 617 pp.
- Kroopnick P.M. (1974). "Correlations between  $^{13}\text{C}$  and  $\text{CO}_2$  in surface waters and atmospheric  $\text{CO}_2$ ", *Earth and Planetary Science Letters*, **22**: 397-403.
- Kuchler-Krischun J., Kleiner J. (1990). "Heterogeneously nucleated calcite precipitation in Lake Constance. A short time resolution study", *Aq. Sci.*, **52**: 176-197.
- Hanson P.C., Bade D.L., Carpenter S.R., Kratz T.K. (2003). "Lake metabolism: Relationships with dissolved organic carbon and phosphorus", *Limnol. Oceanogr.*, **48**: 1112-1119.
- Harrison A.G., Thode H.G. (1958). "Mechanisms of the bacterial reduction of sulfate from isotope fractionation studies", *Trans. Faraday Soc.*, **53**: 84-92.
- Harshey J. P., Fernandez M., Milne P. J., Millero F. J. (1986). "The ionization of boric acid in NaCl, Na-Ca-Cl and Na-Mg-Cl solutions at 25°C", *Geochim. Cosmochim. Acta*, **50**: 143-148.
- Heiri O., Lotter A.L., Lemcke G. (2001). "Loss on ignition as a method for estimating organic and carbonate content in sediments: reproducibility and comparabilità of results", *J. Paleolimnol.*, **25**: 101-110.
- Hoefs J. (2004). "Stable Isotope Geochemistry", 5<sup>th</sup> Revised and Updated Edition, Springer, Berlin, 244 pp.
- Hollis G.E. (1992). "Goals and Objectives of Wetland Restoration and Rehabilitation. In Waterfowl and Wetland Conservation in the 1990's - a Global Perspective", *Proc. of IWRB Symposium. St. Petersburg, Florida, 12-19, November, 1992*, pp. 187-94.
- Holt B. D., Kumar R. (1991). "Oxygen isotope fractionation for understanding the sulphur cycle", in H. R. Krouse and V.A. Grinenko (ed.) 'Stable isotopes in the assessment of natural and anthropogenic sulphur in the environment', John Wiley & Sons, New York. pp. 27-41.
- Hong H., Kester D. (1986). "Redox state of iron in the offshore waters of Peru", *Limnol. Oceanogr.*, **31**: 512-524.
- Hongve D. (1997). "Cycling of iron, manganese, and phosphate in a meromictic lake", *Limnol. Oceanogr.*, **42**: 635-647.
- Hudak P.F., Paul F. (2003). "Chloride/bromide ratios in leachate derived from farm-animal waste", *Environm. Poll.*, **121**: 23-25.
- Hutchinson G.E. (1957). "A treatise on Limnology I. Geography, Physics and Chemistry", John Wiley & Sons, Inc., New York.
- IAEA (2004). "Isotope Hydrology Information System. The ISOHIS Database", accessible at: <http://isohis.iaea.org>
- IAEA (2005). "Isotope Composition of precipitation in the Mediterranean basin in relation to air circulation patterns and climate", IAEA-TECDOC-1453, Vienna.
- ISTAT (2002). "5° censimento generale dell'agricoltura. Caratteristiche strutturali aziende agricole - fascicolo provincia di Pisa", *Censimenti*, 50, 262 pp. (accessible at: <http://censagr.istat.it>).
- ISTAT (2005). "8° Censimento generale dell'industria e dei servizi 2001. Distretti industriali e sistemi locali del lavoro 2001", Istituto Nazionale di Statistica, Roma, 150pp. (accessible at: [http://censimenti.istat.it/html/ind\\_home.asp](http://censimenti.istat.it/html/ind_home.asp)).
- ISTAT & ISMEA (1992). "La scomparsa degli ambienti naturali", in Angle T. G.: "Habitat-Guida alla Gestione degli ambienti naturali", WWF, CFS (Eds), 11-17pp.
- Ladouche B., Ghyselinck M., Chery L. (2004). "Détermination de l'origine des nitrates dans quelques sources karstiques du Causse du Quercy (LOT)", *Rapport final BRGM/RP-53114-FR*, 99pp.
- Langelier W.F., Ludwig H. F. (1942). "Graphical methods for indicating the mineral character of natural Water", *J. Amer. Water Works Ass.*, **34**: 335-352.
- Langmuir D. (1997). "Aqueous Environmental Geochemistry", Prentice-Hall, New Jersey, pp.600.
- Leeman W.P., Sisson V.B. (1996). "Geochemistry of boron and its implications for crustal and mantle processes", in: Grew E. S., Anovitz L .M. (Eds.) "Boron: Mineralogy, petrology and Geochemistry", *Reviews in Mineralogy*, vol. **33**, Mineralogical Soc. Of America, Washington, pp. 645-707.
- Lemarchand E., Gaillardet J., Lewin É., Allègre C.J. (2000). "The influence of rivers on marine boron isotopes and implications for reconstructing past ocean pH", *Nature*, **208**: 951-954

- Lemarchand D., Gaillardet J., Lewin É., and Allègre C. J. (2002). "Boron isotope systematics in large rivers: implications for the marine boron budget and paleo-pH reconstruction over the Cenozoic", *Chem. Geol.*, **190**: 123-140.
- Lemarchand E., Schott J., Gaillardet J. (2005). "Boron isotopic fractionation related to boron sorption on humic acid and the structure of surface complexes formed", *Geochim. Cosmochim. Acta*, **69**: 3519-3533.
- Leone G., Ricchiuto T.E., Longinelli A. (1987). "Isotopic composition of dissolved oceanic sulphate", in: "Studies on Isotope Variations in Nature. I.A.E.A.", Vienne, 5-14.
- Lerman J. C. (1972). "Soil-CG- and groundwater: carbon isotope compositions", *Proc. 8<sup>th</sup> Int. Conf. Radiocarbon Dating*, Wellington, **1**: 93- 105.
- Levin I., Hesshaimer V. (2000). "Radiocarbon—a unique tracer of global carbon cycle dynamics", *Radiocarbon*, **42**: 69-80.
- Levin I., Kromer B. (2004). "The tropospheric <sup>14</sup>CO<sub>2</sub> level in mid latitudes of the northern hemisphere (1959-2003) ", *Radiocarbon*, **46**: 1261-1272.
- Longinelli A. (1988). "Oxygen-18 and sulphur-34 in dissolved oceanic sulphate and phosphate", in: "Handbook of Environmental Isotope Geochemistry", vol.3, Fritz P., Fontes J. Ch. (Eds.) Elsevier, Amsterdam.
- Longinelli A., Cortecchi G. (1969). "Isotopic abundance of oxygen and sulphate ions from river water", *Earth Planet. Sci. Letters*, **7**: 376- 380.
- Majoube M. (1971). "Fractionnement en oxygene-18 et en deuterium entre l'eau et la vapeur", *J. Chim. Phys.*, **68**: 423-1235.
- Marini L., Bonaria V., Guidi M., Hunziker J. C., Ottonello G., Vetuschi Zuccolini M. (2000). "Fluid geochemistry of the Acqui Terme-Visone geothermal area (Piemonte, Italy)", *Appl. Geochem.*, **15**: 917-935.
- Marchetti M. (1943). "Una torba glaciale del lago di Massaciuccoli", *Atti Soc. Tosc. Sci. Nat. Proc. Verb.*, **43**: 143-150.
- Marchetti M., Tongiorgi E. (1936). "Ricerche sulla vegetazione dell'Etruria Marittima - VII: una torba glaciale del Lago di Massaciuccoli", *Nuovo Giorn. Bot. It. n.s.*, **43**: 872-884.
- Marchisio M. e D'Onofrio L. (1997). "Indagini geofisiche nel lago di Massaciuccoli e nella fascia costiera tra Migliarino e Torre del Lago", "Lago di Massaciuccoli-13 Ricerche finalizzate al risanamento", Ente Parco Regionale Migliarino-San Rossore-Massaciuccoli: 7-21
- Masini R. (1958). "I bacini costieri delle Alpi Apuane", Pisa.
- Mather J.D., Porteous N.C. (2001). "The geochemistry of boron and its isotopes in groundwaters from marine and non-marine sandstone aquifers", *Appl. Geochem.*, **16**: 821- 834.
- Mazzanti R. (1983). "Il punto sul Quaternario della fascia costiera e dell'arcipelago di Toscana", *Boll. Soc. Geol. It.*, **1**: 55-62.
- Mazzanti R., Trevisan L. (1978). "Evoluzione della rete idrografica nell'Appennino centro-settentrionale", *Geogr. Fis. Dinam. Quat.*, **1**: 55-62.
- Mazzanti R., Pasquinucci M. (1983). "L'evoluzione del litorale lunese-pisano fino alla metà del XIX secolo", *Boll. Soc. Geol. It.*, **12**: 605-628.
- McKnight T.L., Hess D. (2000). "Climate Zones and Types: Mediterranean Climate (Csa, Csb)", in: "Physical Geography: A Landscape Appreciation", pp. 221-3, Upper Saddle River, NJ, Prentice Hall.
- McMullen C. C., Cragg C. B., Thode H. G. (1961). "Absolute ratios of B11/B10 in Searles Lake borax", *Geochim. Cosmochim. Acta*, **23**: 147-149.
- Melis F. (1969). "La bonifica della Versilia del 1559", *Acc. Dei Georgofili*, XV, **144**, Firenze.
- Meriggi A. (1995). "Studio idrogeologico del Bacino del Lago di Massaciuccoli, Tesi di Laurea unpublished, Università di Pisa.
- Ministère de l'environnement (1993). "Proceedings of the Fifth Conference of the Contracting Parties to the Ramsar Convention", Kushiro, Japan, June 1993, National report for France.
- Mitsch W.J., Gosselink J.G. (1993). "Wetlands", 2<sup>nd</sup> Ed. Jon Wiley and Sons, Inc., New York.
- Mizutani Y., Rafter T.A. (1969). "Oxygen isotopic composition of sulphates – Part 4; Bacterial fractionation of oxygen isotopes in the reduction of sulphate and in the oxidation of sulphur", *N. Z. J. Sci.*, **12**: 60-68.

- Mizutani Y., Rafter T.A. (1973). "Isotopic behaviour of sulphate oxygen in the bacterial reduction of sulphate", *Geochem. J.*, **6**: 183-191.
- Moncaster S.J., Bottrell S.H., Tellam J.H., Lloyd J.W., Konhauser K.O. (2000). "Migration and attenuation of agrochemical pollutants: insight from isotopic analysis of groundwater sulphate", *J. Contam. Hydrol.* **43**, 147-163.
- Mook W.G., Tan F.C. (1991). "Stable carbon isotopes in rivers and estuaries", in: Degens E.T., Kempe S., Richey J. E. (Eds.) "Biogeochemistry of Major World Rivers", Wiley, New York, pp. 245-264.
- Mori G., Mattioli M., Madoni P., Ferri G., Baldaccini G.N., Bianucci P., Ricci N. (1996). "Ciliated protozoa from lake Massaciuccoli (western Tuscany)", *Atti Soc. Tosc. Sci. Nat., Mem., Serie B*, **103**: 89-97.
- Mori G., Mattioli M., Madoni P., Ricci N. (1998). "The ciliate communities of different habitats of Lake Massaciuccoli (Tuscany): species composition and distribution", *Italian Journal of Zoology*, **65**: 191-202.
- Munteanu D., N. Toniuc (1992). "The present and future state of the Danube delta", in C. M. Finlayson, G. E. Hollis, T. J. Davis (eds) "Managing Mediterranean Wetlands and their birds", Slimbridge, United Kingdom, IWRB Special Publication No. 20, 43-46 pp.
- Nadeau M.J., Grootes P.M., Schleicher M., Hasselberg P., Rieck A., Bitterling M. (1998). "Sample throughput and data quality at the Leibniz-Labor AMS facility" *Radiocarbon*, **40**: 239-243.
- Nakai N., Jensen M.L. (1964). "The kinetic isotope effect in the bacterial reduction and oxidation of sulphur", *Geochim. Cosmochim. Acta*, **28**: 1893- 1912.
- Natura 2000. [http://biodiversity.eionet.europa.eu/activities/Natura\\_2000/index.html](http://biodiversity.eionet.europa.eu/activities/Natura_2000/index.html)
- Neal C., Fox K.K., Harrow M., Neal M. (1998). "Boron in the major UK rivers entering the North Sea", *Sc.Tot. Environ.*, **210-211**: 41-51.
- Neumann K., Berrylyons W., Priscu J. C., Donahoe R.J. (2001). "CO<sub>2</sub> concentrations in perennially ice-covered lakes of Taylor Valley, Antarctica", *Biogeochem.*, **56**: 27-50.
- Newman L., Krouse H.R., Grinenko V.A. (1991). "Sulphur isotope variations in the atmosphere", in: Krouse, H. R., Grinenko, V.A. (Eds.) "Stable Isotopes-Natural and Anthropogenic Sulphur in the Environment - SCOPE 43", Wiley, Chichester, pp. 133-176.
- Nguyen-Thé D., Widory D. (2006). "Etude isotopique de l'origine des nitrates dans l'aquifère calcaire situé entre l'Aire et la Cousances (Meuse)", *Rapport BRGM/RP-54410-FR*, 38 pp.
- Nolledi G., Bartolini I., Biserna A., Cortopassi P., Nolledi G. (2003). "Indagini geologico-tecnica di supporto al piano strutturale comunale", *Relazione Tecnica*, Comune Massarosa, 90 pp.
- Oana S., Deevet E.S. (1960). "Carbon-13 in lake waters and its possible bearing on paleolimnology", *Am. J. Sci.* **258**: 253-272.
- OECD (Organisation for Economic Cooperation and Development) (1989). "Environmental Data Compendium 1989", OECD, Paris.
- Oi T., Nomura M., Musashi M., Oosaka T., Okamoto M., Kakihana H. (1989). "Boron isotope compositions of some boron minerals", *Geochim. Cosmochim. Acta*, **53**: 3189-3195.
- Oxspring D., McClean S., O'Kane E., Smyth W. (1995). "Study of the chelation of boron with azomethine-H by differential pulse polarography, liquid chromatography and capillary electrophoresis and its analytical applications", *Anal. Chim. Acta*, **317**: 295-301.
- Pagni R., Coco G., Donatini O., Ricci E. (2004). "2° Rapporto sullo Stato dell'ambiente, Provincia di Lucca", Servizio Ambiente.
- Palmer M.R., Spivack A.G., Edmond A.M. (1987). "Temperature and pH controls over isotopic fractionation during adsorption of boron on marine clay", *Geoch. Cosmoch. Acta*, **51**: 2319-2323.
- Palmer M. R., Helvacı C. (1995). "The boron isotope geochemistry of the Kirka borate deposit, western Turkey", *Geochim. Cosmochim. Acta*, **59**: 3599-3605.
- Pantanelli D. (1905). "Di un pozzo artesiano nella pianura tra Viareggio e Pietrasanta", *Atti Soc. Tosc. Sci. Nat.*, **14**: 68-70.
- Psilovikos A. (1992). "Prospects for wetland and waterfowl in Greece", in Finlayson M., Hollis T., Davis T. (Eds.) "Managing Mediterranean Wetlands and their Birds", Proceedings of an IWRB International Symposium, Grado, Italy, February 1991. IWRB Special Publication N° 20, 1992, GB. Istituto Nazionale di Biologia della Selvaggina, Italy. Pages 53-55.

- Park S.C., Yuna S.T., Chaea G.T., Yooa I.S., Shina K. S. Heoa, Leb S.K. (2005). "Regional hydrochemical study on salinization of coastal aquifers, western coastal area of South Korea", *J. Hydrol.*, **313**:182-194.
- Parkhurst D.L., Appelo C.A.J. (1999). "User's guide to PHREEQC (version 2)—a computer program for speciation, batch-reaction, one dimensional transport, and inverse geochemical calculation", U.S. Geological Survey, Water-Resources Investigation, Report 99-4259, 312 pp.
- Pascucci V. (2005). "Neogene evolution of the Viareggio basin, northern Tuscany (Italy) ", *GeoActa*, **4**: 123-138
- Patacca E., Sartori R., Scandone P. (1990). "Tyrrhenian basin and Apenninic areas: kinematic relations since late Tortonian times", *Mem. Soc. Geol. Ital.* **45**: 425-451.
- Pedreschi L. (1956). "Il Lago di Massaciuccoli e il suo territorio", *Mem. Soc. Geogr. It.*, vol. XXII, pp. 225.
- Penman H.L. (1948). "Natural evaporation from open water, bare soil and grass", *Proc. R. Soc. London, Ser. A*, **193**: 120-148.
- Penman, H.L., (1954). "Evaporation over parts of Europe", *IASH*, **36**: 168-176.
- Pfennig N., Widdel F., Trüper H.G. (1981). "The dissimilatory sulfate-reducing bacteria", in: "The Prokaryotes", M. P. Starr, H. Stolp, H. G. Trüper, A. Balows & H. G. Schlegel (Eds.), **1**: 926-940.
- Pfennig N., Biebl H. (1976). "Desulphuromonas acetoxidans gen. nov. sp. nov., a new anaerobic, sulphur-reducing, acetate-oxidizing bacterium" *Arch. Microbiol.*, **110**: 3-12.
- Plummer N.L., Busenberg E. (1982). "The solubilities of calcite, aragonite and vaterite in CO<sub>2</sub>-H<sub>2</sub>O solutions between 0 and 90°C, and an evaluation of the aqueous model for the system CaCO<sub>3</sub>-CO<sub>2</sub>-H<sub>2</sub>O", *Geochim. Cosmochim. Acta*, **46**: 1011-1040.
- Piper A.M. (1944). "A graphic procedure in the geochemical interpretation of water analyses", *Am. Geophys. Union Trans.*, **25**: 914-923.
- Praire Y.T., Bird D.F., Cole J.J. (2002). "The summer metabolic balance in the epilimnion of southeastern Quebec lakes", *Limnol. Oceanogr.*, **47**: 316-321.
- Putschew A., Mania M., Jekel M. (2003). "Occurrence and source of brominated organic compounds in surface waters", *Chemosphere*, **52**: 399-407.
- Rapetti F. (2003). "Atlante Tematico della Provincia di Pisa", Pacini Editore S.p.A & Provincia di Pisa, 16-17 p.
- Rapetti F., Tomei P.E., Vittorini S. (1986). "Aspetti climatici del Lago di Massaciuccoli in rapporto alla presenza di entità vegetali di rilevanza fitogeografica", *Atti Soc. Tosc. Sci. Nat., Mem., Serie A*, **93**: 221-233.
- Reed M.H. (1983). "Seawater-basalt reaction and the origin of greenstones and related ore deposits", *Econ. Geol.*, **78**: 466-485.
- Rees C.E. (1973). "A steady-state model for sulphur isotope fractionation in bacterial reduction processes", *Geochim. Cosmochim. Acta*, **37**: 1141-1162.
- Regione Toscana, Dipartimento Agricoltura e Assetto del Territorio (1973). "Caratteri geologici, geografici, fisici, climatologici e idrogeologici del bacino del Massaciuccoli", Conferenza dei servizi del bacino di Massaciuccoli per il recupero funzionale e culturale delle risorse ambientali, Massarosa.
- Regione Toscana (2005). <http://sira.arpat.toscana.it/sira/MedWet/MEDWET.html>
- Romagnoli L. (1957). "Sondaggi a 200m di profondità nel quaternario recente presso Pisa. Studio delle facies attraversate e considerazioni sulla sedimentazione costiera a carattere ciclico", Pubblicazione n. **45**, Centro studi per la geologia dell'Appennino del CNR.
- Romanek C.S., Grossman E.L., Morse J.W. (1992). "Carbon isotope fractionation in synthetic aragonite and calcite: effects of temperature and precipitation rate", *Geochim. Cosmochim. Acta*, **56**: 419-430.
- Rosler H.J., Lange H. (1972). "Geochemical Tables" Elsevier, Amsterdam, pp. 312-352.
- Salomons W., Mook W.G. (1986). "Isotope geochemistry of carbonates in the weathering zone" In: Fritz, P., Fontes, J. Ch. (Eds.) "Handbook of Environmental Isotope Geochemistry. Vol. **2**, The Terrestrial Environment", B. Elsevier, Amsterdam, pp. 239-269.
- Sartori F., Levi-Minzi R. (1985). "I terreni torbosi del bacino di Massaciuccoli: 1) Fertilità chimica, caratteri geochimici e classificazione. 2) Aspetti mineralogici", *Atti Soc. Tosc. Sci. Nat., Serie A*, **92**: 269-320.

- Shakur M.A. (1982). " $\delta^{34}\text{S}$  and  $\delta^{18}\text{O}$  variations in terrestrial sulphates", PhD thesis, submitted to the Department of Physics, University of Calgary, Calgary, Alberta, Canada.
- Sichel H.S. (1966). "The estimation of means and associated confidence limits for small samples from lognormal populations. Proceedings of the Symposium on Mathematical Statistics and Computer Applications in Ore Valuation", South Africa Institute of Mining and Metallurgy, Johannesburg, pp. 106-123.
- Sigg L., Stumm W., Behra P. (1994). "Chimie des Milieux Aquatiques", Masson ed., Paris.
- Simoni F. (1977). "Sulle cause della moria dei pesci nel lago di Massaciuccoli negli anni 1972-1977", Rivista Italiana d'Igiene, **37**: 363-380, Lischi & figli, Pisa.
- Simoni F., Baldaccini G.N., Bianucci P., Bernacchi G. (1985). "Ultime acquisizioni sulla presenza di *Prymnesium Parvum* Carter (*Chrisomonadinae*) nel lago di Massaciuccoli", Atti Soc. Tosc. Sci. Nat. Mem., Serie B, **91**: 191-199.
- Simoni F., Mattioli M., Di Paolo C. (1999). "Evoluzione del fitoplancton in aree campione e in zone interessate da interventi di risanamento", in "Il risanamento del lago di Massaciuccoli", Arpat, pp. 67-123.
- Simoni F., Di Paolo C., Pesce D., Gianfranchi U., Nuti S., Lepri L. (2002). "Evoluzione trofica di un lago poco profondo con acque salmastre", Biologia Ambientale, XXXII, n.11: 56-68.
- Schmitt-Kopplin P., Hertkorn N., Schulten H.-R., Kettrup A. (1998). "Structural changes in an dissolved humic acid during photochemical degradation", Environ. Sci. Technol., **32**: 2531-2541.
- Spandre R. (1975). "Studio e bilancio idrogeologico del bacino del lago di Massaciuccoli", Tesi di Laurea, Pisa.
- Spivack, A.J., Edmond, J.M., (1986). "Determination of boron isotope ratios by thermal ionization mass spectrometry of the di-caesium metaborate cation", Anal. Chem., **58**: 31-35.
- Striegl R.G., Kortelainen P., Chanton J.P., Wickland K.P., Bugna G.C., Rantakari M. (2001). "Carbon dioxide partial pressure and C-13 content of north temperate and boreal lakes at spring ice melt", Limnol. Oceanogr., **46**: 941-945.
- Stuiver M., Reimer P.J., Bard E., Beck J.W., Burr G.S., Hughen K.A., Kromer B., McCormac G., Van Der Plicht J., Spurk M. (1998). "INTCAL98 radiocarbon age calibration, 24000-0 cal BP", Radiocarbon, **40**: 1041-1083.
- Stumm W., Morgan J.J. (1996). "Aquatic chemistry", 3<sup>th</sup> Edition, John Wiley and Sons, Inc., 1022pp.
- Summa V., Tateo F. (1999). "Geochemistry of two peats suitable for medical uses and their behavior during leaching", Appl. Clay Sc., **15**: 477-489.
- Swihart G. H., Moore P. B., Callis E. L. (1986). "Boron isotopic composition of marine and non-marine evaporite borates", Geochim. Cosmochim. Acta, **50**: 1297-1301.
- Taylor M.J., Grigg J.A., Laban I.H. (1996). "Triol borates and aminoalcohol derivatives of boric acid: their formation and hydrolysis", Polyhedron, **15**: 3261-3270
- Telmer K., Veizer J. (1999). "Carbon fluxes, pCO<sub>2</sub> and substrate weathering in a large northern river basin, Canada: carbon isotope perspectives", Chem. Geol., **159**: 61-86.
- Thornthwaite C.V. (1948). "An approach toward a rational classification of climate", Geogr. Rew., **38**: 55-94.
- Thornthwaite C.V., Mather J.R. (1957). "Instructions and tables for computing potential evapotranspiration and the water balance", Publications in Climatology, **10**: 105-311.
- Throughton J.H. (1972). "Carbon isotope fraction by plants", Proc. 8<sup>th</sup> Int. Cod. Radiocarbon Dating, Wellington, **2**: 421-437.
- Tomei P.E. (1972). "Aspetti naturalistici della macchia lucchese", Atti Soc. Tosc. Sci. Nat., Mem., Serie B, **79**: 8-51.
- Tomei P.E. (1983). "Le zone umide della Toscana: stato attuale delle conoscenze geobotaniche e prospettive di salvaguardia", Atti Soc. Tosc. Sci. Nat., Mem., Serie B, **89**: 345-361, Pisa.
- Tomei P.E., Guazzi E., Barsanti A. (1997). "La carta della vegetazione delle paludi e del lago di Massaciuccoli", da: "Lago di Massaciuccoli: 13 ricerche finalizzate al risanamento", Ente Parco Regionale Migliarino - S. Rossore - Massaciuccoli: pp. 275-288.
- Tomei P.E., Amadei L., Garbari F. (1985) "Données distributives de quelques angiospermes rares de la région méditerranéenne d'Italie", Atti Soc. Tosc. Sci. Nat., Mem., Serie B, **92**: 207-240.

- Tonarini S., Pennisi M., Leeman W.P. (1997). "Precise boron isotopic analysis of complex silicate (rock) samples using alkali carbonate fusion and ion-exchange separation" *Chem. Geol.*, **142**: 129-137.
- Tonarini S., Pennisi M., Adorni-Braccesi A., Dini A., Ferrara G., Gonfiantini R., Wiedenbeck M., Gröning M. (2003). "Intercomparison of boron isotope and concentration measurements. Part I: Selection, preparation and homogeneity tests of the intercomparison materials", *Geostandards Newsletter: The Journal of Geostandards and Geoanalysis*, **27**: 21-39.
- Trevisan L., Dallan L., Nardi R., Raggi G., Squarci P., Taffi L. (1968). "Note illustrative della carta geologica d'Italia" - scala 1 : 100000 Foglio 104-Pisa", *Serv. Geol. It.*, **41**.
- Trujillo P.E., Gladney E., Counce D.A., Mroz E.J., Perrin D.R., Owens J.W., Wangen L.E. (1982). "A comparison study for determining dissolved boron in natural waters and geothermal fluids", *Anal. Lett.*, **15**: 643-655.
- Uppstroem L.R. (1974). "The boron/chlorinity ratio of deep seawater from Pacific Ocean", *Deep Sea Res.*, **21**: 161-162.
- Vai G.B., Martini I.P. (2001). "Anatomy of an Orogen: the Apennines and adjacent Mediterranean basins", *Kluwer Academic Publishers*, pp. 375-400.
- Van Cappellen P., Wang Y. (1996). "Cycling of iron and manganese in surface sediments: A general theory for the coupled transport and reaction of carbon, oxygen, nitrogen, sulfur, iron and manganese", *Amer. J. Sci.* **296**: 197-243.
- Vengosh A. (2003). "Salinization and saline environments", in *Treatise in Geochemistry*, vol. **9**, *Environmental Geochemistry*, edited by B. S. Lollar, pp. 333- 365, Elsevier, New York.
- Vengosh A., Heumann K.G., Juraske S., Kasher R. (1994). "Boron isotope application for tracing sources of contamination in groundwater", *Environ. Sci. Technol.*, **28**: 1968- 74.
- Vengosh A., Pankratov I. (1998). "Chloride/bromide and chloride/fluoride ratios of domestic sewage effluents and associated contaminated groundwater", *Ground Water*, **36**: 815- 24.
- Vengosh A., Barth S., Heumann K. G., Eisenhut S. (1999). "Boron isotopic composition of freshwater lakes from Central Europe and possible contamination sources", *Acta Hydrochim. Hydrobiol.*, **27**: 416-421.
- Vengosh A., Kloppmann W., Marei A., Livshitz Y., Gutierrez A., Banna M., Guerrot C., Pankratov I., Raanan H. (2005). "Sources of salinity and boron in the Gaza strip Natural contaminant flow in the southern Mediterranean coastal aquifer", *Wat. Res. Res.*, **41**: W01013.1-W01013.19.
- Vincini M., Carini F., Silva S. (1994). "Use of alkaline fly ash as an amendment for swine manure", *Bioresour. Technol.*, **49**: 213-222.
- Visentini M. (1936) Association internationale d'hydrologie scientifique. Bulletin No. **22**: 119-137.
- Vittorini S. (1972). "Ricerche sul clima della Toscana in base all'evaporazione potenziale e al bilancio idrico", *Riv. Geogr. It.*, **79**: 1-30.
- Vogt H.J. (1978). "Isotopenttennung bei der Verdünnung von Wasser", Thesis, Institute of Environmental Physics, University of Heidelberg.
- Wachniew P., Różanski K. (1997). "Carbon budget of a mid-latitude, groundwater-controlled lake: Isotopic evidence for the importance of dissolved inorganic carbon recycling", *Geochim. Cosmochim. Acta*, **61**: 2453-2465.
- Wakshall E., Nielsen H. (1982). "Variations of  $\delta^{34}\text{S}(\text{SO}_4)$ ,  $\delta^{18}\text{O}(\text{H}_2\text{O})$  and  $\text{Cl}/\text{SO}_4$  ratio in rainwater over northern Israel, from Mediterranean Coast to Jordan Rift Valley", *Earth Planet Sci. Lett.*, **61**: 272-282.
- Whitmer S., Baker L., Wass R. (2000). "Loss of bromide in a wetland tracer experiment", *J. Environm. Qual.*, **29**: 2043-2045.
- Widory D., Kloppmann W., Chery L., Bonnin J., Rochdi H., Guinamant J. L. (2004). "Nitrate in groundwater: an isotopic multi-tracer approach", *J. Contam. Hydrol.*, **72**: 165- 188.
- Widory D., Petelet-Giraud E., Negrel P., Ladouche B. (2005). "Tracking the Sources of Nitrate in Groundwater Using Coupled Nitrogen and Boron Isotopes: A Synthesis", *Environ. Sci. Technol.*, **39**: 539-548.
- Widory D., Nguyen-Thé D. (2006). "Etude isotopique de l'origine des nitrates dans la nappe alluviale de la Moselle dans le secteur de Yutz (Moselle)", *Rapport BRGM/RP-54409-FR*, 34 pp.

- Xiao Y.K., Sun D., Wang Y., Qi H., Jin L. (1992). "Boron isotopic compositions of brine, sediments, and source water in Da Qaidam Lake, Qinghai, China", *Geochim. Cosmochim. Acta*, **56**: 1561–1568.
- Yan J.P., Hinder M., Einsele G. (2002). "Geochemical evolution of closed-basin lakes: general model and application to Lakes Qinghai and Turkana", *Sed. Geol.*, **148**: 105-122.
- Yermiyahu U., Keren R., Chen Y. (1995). "Boron sorption by soil in the presence of composted organic matter", *Soil Sci. Soc. Am. J.*, **59**: 405–409.
- Zhang J., Quay P.D., Wilbourn D.O. (1995). "Carbon isotope fractionation during gas–water exchange and dissolution of CO<sub>2</sub>", *Geochim. Cosmochim. Acta*, **59**: 107–114.



## CONCLUSION

---

This study highlights some important methodological aspects concerning:

- 1-the role of biotic processes to regulate the contents of several dissolved chemical compounds
- 2-the application of isotopes to trace the chemical-physical processes, taking place at the interface between the different compartments, to establish the origin of the elements and to get dating.

This work gives significant knowledge to understand distinct aspects of the lake system, such as:

- i. the distribution in the system of trace elements depends on the presence and intensity of biotic activity. Photosynthesis and degradation of organic matter are key processes. In fact,
  - a) significant pH,  $p\text{CO}_2$  and  $p\text{O}_2$  variations occur, leading to dissolution/precipitation of the carbonate minerals and such iron and manganese oxides.
  - b) deviations of the molar Cl/Br ratio, related to the DOC content, suggesting the production of brominated organic compounds.
  - c) higher B concentrations in the agricultural network than the mean value of lake water. Indeed, the B/Cl correlation plot underlines three compartments within the studied area: 1) waters draining the agricultural network, 2) lake waters and 3) waters from the Burlamacca channel and the excavation area. Samples with highest B/Cl values are characterized by lowest  $\delta^{11}\text{B}$  values. These anomalies have been ascribed to contamination by animal manure.
  - d) low  $\delta^{13}\text{C}_{\text{DIC}}$  values, approaching the typical isotopic signal of C4 vegetation, are measured within channels with high  $p\text{CO}_2$ . In fact the corn is the main cultivation in the southern basin. In the lake  $\delta^{13}\text{C}$  values correspond to the value expected for equilibrium with the atmosphere. In the excavation area, which represent a meromictic system, a significant increase in alkalinity is detected in the deepest anoxic part, together with a decrease in pH and  $\text{SO}_4$  and  $\text{NH}_3$  and  $\text{H}_2\text{S}$  production. At the same time,  $\delta^{13}\text{C}_{\text{DIC}}$  and  $\delta^{34}\text{S}_{\text{SO}_4}$  signals decrease, suggesting occurrence of oxidation of organic matter and reduction of  $\text{SO}_4$  mediated by sulphate-reducing bacteria.
- ii. The importance of isotope geochemistry to trace the origin of water and active, chemical-physical processes. In particular, the waters of the entire system belong to the NaCl facies, but samples from the Burlamacca channel and the excavation area are characterised by isotopic composition underlining seawater intrusion. In contrast, evapotranspiration processes prevail in the Massaciuccoli lake. The annual evaporation rate is close to 13%.
- iii. Radiocarbon dating of the sedimentary organic matter shows an increase in activity, corresponding to the atomic experiments during the 1960's, at different depths from the sediments of different sites in the lake. In particular, this peak is deeper in sediments near the agricultural channel whereas it is more superficial at the opposite banks of the lake. This suggests a different sedimentation rates.

We can conclude that geochemical research allowed us to underline the influence of agricultural activity on the chemical composition of lake water, the hydrodynamic equilibrium and superficial sediment composition.

The quarries, because of their high water volume, represent a hydraulic barrier for seawater intrusion into the lake. They act also as a sink for nutrients and they have a positive hydraulic function to prevent lake contamination. However, in future, they will become a serious problem if the stratification (chiefly due to chemical stability) disappears or if they are filled up.

# APPENDIX I

**Table I.1** Chemical-physical analyses carried out in-situ

Name	ID	Type	Year	Date	Depth	Water temperature	pH	O <sub>2</sub>	Conductivity 20°C
					m	°C		ppm	µS
<b>Barra-FossaNuova</b>	L1a-04	L	s2004	12/07/2004	-0.25	25.5	9.04	10	3552
	L1m-04	L	s2004	12/07/2004	-0.65	25.1	9.05	10	3493
	L1b-04	L	s2004	12/07/2004	-1.05	24.9	9.05	10	3470
<b>FossaNuova</b>	L2-04	Ch	s2004	12/07/2004	-0.15	26.8	8.89	9	3772
	L2m-04	Ch	s2004	12/07/2004	-0.55	25.2	8.75	9	3566
	L2b-04	Ch	s2004	12/07/2004	-0.95	24.5	8.52	8	3499
<b>Piaggetta</b>	L3aa-04	L	s2004	16/07/2004	-0.15	26.5	8.7	10	3627
	L3a-04	L	s2004	16/07/2004	-0.55	25.9	8.78	10	3544
	L3m-04	L	s2004	16/07/2004	-0.95	25.2	8.95	11	3491
	L3b-04	L	s2004	16/07/2004	-1.35	25	8.92	10	3478
<b>Bufalina Sud</b>	L4aa-04	L	s2004	16/07/2004	-0.25	25	8.97	13	3482
	L4a-04	L	s2004	16/07/2004	-0.65	24.6	8.96	13	3432
	L4m-04	L	s2004	16/07/2004	-1.05	24.4	8.95	12	3423
	L4b-04	L	s2004	16/07/2004	-1.45	24.3	8.88	10	3415
<b>Chiarone</b>	L5m-04	L	s2004	16/07/2004	-0.15	29.3	8.98	11	4023
	L5b-04	L	s2004	16/07/2004	-0.55	29.4	8.98	12	4025
<b>Quiesa</b>	L6m-04	Ch	s2004	19/07/2004	-0.2	20.5	7.52	3	3607
	L6b-04	Ch	s2004	19/07/2004	-0.6	20.5	7.51	4	3606
<b>Burlamacca</b>	L7aa-04	Ch	s2004	19/07/2004	-0.5	26.4	8.33	8	3722
	L7a-04	Ch	s2004	19/07/2004	-0.9	26.3	8.31	3	3716
	L7m-04	Ch	s2004	19/07/2004	-1.3	25.7	7.78	3	3653
	L7b-04	Ch	s2004	19/07/2004	-1.7	25.6	7.69	3	3623
<b>Id.Portovecchio</b>	L8m-04	Ch	s2004	19/07/2004	-0.2	27	8.5	4	4480
	L8b-04	Ch	s2004	19/07/2004	-0.6	27	8.35	4	4466
<b>Torre del Lago</b>	L9aa-04	L	s2004	22/07/2004	-0.4	27.3	8.81	3	3896
	L9a-04	L	s2004	22/07/2004	-0.8	26.5	8.81	3	3798
	L9m-04	L	s2004	22/07/2004	-1.2	26.3	8.71	3	3746
	L9b-04	L	s2004	22/07/2004	-1.6	26.1	8.64	3	3733
<b>Burlamacca FS</b>	L10aa-04	Ch	s2004	22/07/2004	-0.45	29.8	8.54	8	5310
	L10a-04	Ch	s2004	22/07/2004	-0.85	27.7	8.5	9	4773
	L10m-04	Ch	s2004	22/07/2004	-1.25	28.1	8.44	7	6440
	L10b-04	Ch	s2004	22/07/2004	-1.65	28.3	8.37	7	7901
<b>Id. Barra</b>	L11m-04	Ch	s2004	05/08/2004	-0.25	27.6	7.72	8	4920
	L11b-04	Ch	s2004	05/08/2004	-0.65	27.3	7.68	3	4867
<b>Id. Barra 2</b>	L12a-04	Ch	s2004	05/08/2004	-0.15	28	7.84	4	4689
	L12m-04	Ch	s2004	05/08/2004	-0.55	27.9	7.81	3	4655
	L12b-04	Ch	s2004	05/08/2004	-0.95	27.8	7.81	3	4647
<b>Foce Barra</b>	L13a-04	L	s2004	05/08/2004	-0.3	29.7	8.84	8	4414
	L13m-04	L	s2004	05/08/2004	-0.7	29.6	8.84	8	4407
	L13b-04	L	s2004	05/08/2004	-1.1	29.2	8.83	8	4343
<b>Centralino Lago</b>	L14aa-04	L	s2004	20/08/2004	-0.1	27	8.67	8	4078
	L14a-04	L	s2004	20/08/2004	-0.35	27	8.67	8	4078
	L14m-04	L	s2004	20/08/2004	-0.75	27	8.67	7	4078
	L14b-04	L	s2004	20/08/2004	-1.15	26.9	8.67	7	4063

Name	ID	Type	Year	Date	Depth	Water temperature	pH	O <sub>2</sub>	Conductivity 20°C
					m	°C		ppm	µS
<b>Centro Lago</b>	L15aa-04	L	s2004	20/08/2004	-0.5	27.3	8.76	8	4125
	L15a-04	L	s2004	20/08/2004	-0.9	27.3	8.76	8	4123
	L15m-04	L	s2004	20/08/2004	-1.3	27.2	8.75	8	4121
	L15b-04	L	s2004	20/08/2004	-1.7	27.3	8.75	8	4124
<b>FossaNuova</b>	L2-f05	Ch	w2005	09/02/2005	-0.5	4.40	8.08	12	1280
<b>Piaggetta</b>	L3-f05	L	w2005	09/02/2005	-0.5	4.10	8.34	13	1356
<b>Burlamacca</b>	L7-f05	Ch	w2005	09/02/2005	-0.5	5.20	8.04	11	1592
<b>Quiesa</b>	L6-f05	L	w2005	09/02/2005	-0.5	7.00	7.41	0	1871
<b>Massaciuccoli</b>	L5-f05	L	w2005	09/02/2005	-0.5	5.40	8.18	12	1478
<b>Centro Lago</b>	L15-f05	L	w2005	14/02/2005	-0.5	5.90	8.36	12	1495
<b>Barra foce</b>	L13-f05	L	w2005	14/02/2005	-0.5	7.00	7.87	10	1612
<b>Id. Barra 2</b>	L12-f05	L	w2005	14/02/2005	-0.5	7.70	7.74	9	1546
<b>Id. Barra 1</b>	L11-f05	L	w2005	14/02/2005	-0.5	9.10	7.56	8	1852
<b>Bufalina-hangar</b>	L4-f05	L	w2005	14/02/2005	-0.5	6.50	8.00	12	1534
<b>Canale Le 20</b>	L16-f05	Ch	w2005	14/02/2005	-0.5	6.60	8.11	12	1553
<b>Torre del Lago</b>	L9-f05	L	w2005	16/02/2005	-0.5	5.90	7.81	13	1463
<b>Collettore</b>	L17-f05	Ch	w2005	16/02/2005	-0.5	6.00	8.28	14	1490
<b>Malfante</b>	L14c-f05	Ch	w2005	16/02/2005	-0.5	6.30	8.13	13	1533
<b>FossaNuova</b>	L2-m05	Ch	sp2005	19/05/2005	-0.5	23.40	8.56	10	3423
<b>Piaggetta</b>	L3-m05	L	sp2005	05/05/2005	-0.5	21.60	7.92	6	3163
<b>Massaciuccoli</b>	L5-m05	L	sp2005	05/05/2005	-0.5	22.80	8.52	8	3295
<b>Quiesa</b>	L6-m05	Ch	sp2005	05/05/2005	-0.5	17.50	7.30	0	1792
<b>Burlamacca</b>	L7-m05	Ch	sp2005	05/05/2005	-0.5	22.20	8.18	8	3268
<b>Id. Barra</b>	L11-m05	Ch	sp2005	19/05/2005	-0.5	19.80	7.89	6	2697
<b>Id. Barra 2</b>	L12-m05	Ch	sp2005	19/05/2005	-0.5	19.40	6.99	1	2728
<b>Foce Barra</b>	L13-m05	L	sp2005	19/05/2005	-0.5	20.10	8.10	7	2883
<b>Centralino Lago</b>	L14-m05	L	sp2005	19/05/2005	-0.5	20.40	8.67	10	3038
<b>Centro Lago</b>	L15-m05	L	sp2005	19/05/2005	-0.5	20.40	8.67	9	3028
<b>Torre del Lago</b>	L9-m05	L	sp2005	22/06/2005	-0.5	25.90	8.67	9	4035
<b>S.Rocchino 1,5</b>	SR1.5	C	sp2005	14/03/2005	-1.5	9.9	8.21	11	2449
<b>S.Rocchino 2,6-2,9</b>	SR2.7	C	sp2005	14/03/2005	-2.7	9.1	7.24	5	5787
<b>S.Rocchino 3</b>	SR3	C	sp2005	14/03/2005	-3.0	9.7	7.25	0	6749
<b>S.Rocchino 7</b>	SR7	C	sp2005	14/03/2005	-7.0	16.4	7.11	0	17446
<b>S.Rocchino 10</b>	SR10	C	sp2005	14/03/2005	-10.0	17	7.02	0	20210
<b>S.Rocchino 14</b>	SR14	C	sp2005	14/03/2005	-14.0	17	6.98	0	20868
<b>Incrociata -0,5m</b>	Inc05	C	sp2005	26/04/2005	-0.5	16.8	8.27	11	2995
<b>Incrociata -2m</b>	Inc2	C	sp2005	26/04/2005	-2.0	15.9	8.24	10	2938
<b>Incrociata -3m</b>	Inc3	C	sp2005	26/04/2005	-3.0	15.4	8.09	7	3532
<b>Incrociata -4m</b>	Inc4	C	sp2005	26/04/2005	-4.0	14.5	7.84	7	3444
<b>Incrociata -5m</b>	Inc5	C	sp2005	26/04/2005	-5.0	13.1	7.51	2	4051
<b>Incrociata -7m</b>	Inc7	C	sp2005	26/04/2005	-7.0	12.7	7.07	0	8113
<b>Incrociata -11m</b>	Inc11	C	sp2005	26/04/2005	-11.0	14.4	6.96	0	11189
<b>Sisa -0.5m</b>	Sis0.5	C	sp2005	22/06/2005	-0.5	28.2	8.68	10	3962
<b>Sisa -2m</b>	Sis2	C	sp2005	22/06/2005	-2.0	26.7	8.69	11	3567
<b>Sisa -5m</b>	Sis5	C	sp2005	22/06/2005	-5.0	21.7	8.29	5	2852
<b>Sisa -10m</b>	Sis10	C	sp2005	22/06/2005	-10.0	9.5	7.54	0	1753
<b>Sisa -12m</b>	Sis12	C	sp2005	22/06/2005	-12.0	7	7.43	0	1647
<b>Sisa -15m</b>	Sis15	C	sp2005	22/06/2005	-15.0	6.2	7.31	0	1635
<b>Sisa -20m</b>	Sis20	C	sp2005	22/06/2005	-20.0	6.8	6.96	0	2159
<b>Inc0.6-sp06</b>	Inc0.6-sp06	C	sp2006	08/08/2006	-0.6	21.6	8.39	8	3409

Name	ID	Type	Year	Date	Depth	Water temperature	pH	O <sub>2</sub>	Conductivity 20°C
					m	°C		ppm	µS
<b>Inc3.8-sp06</b>	Inc3.8-sp06	C	sp2006	08/08/2006	-3.8	16.8	7.45	0	4166
<b>Inc9.5-sp06</b>	Inc9.5-sp06	C	sp2006	08/08/2006	-9.5	13.9	7	0	12031
<b>Inc13.5-sp06</b>	Inc13.5-sp06	C	sp2006	08/08/2006	-13.5	14.4	6.96	0	11824
<b>Inc15.3-sp06</b>	Inc15.3-sp06	C	sp2006	08/08/2006	-15.3	14.4	6.95	0	11780
<b>Inc16.2-sp06</b>	Inc16.2-sp06	C	sp2006	08/08/2006	-16.2	14.4	6.97	0	11788
<b>B foce sup</b>	Bur7-05	Bur	2005	21/07/2005	-0.5	27.7	8.65	7	10684
<b>B foce fondo</b>	Bur7-05	Bur	2005	21/07/2005	-1.4	28.4	8.72	2	38071
<b>le15FS sup</b>	C15-05	Ch	2005	21/07/2005	-0.5	27.4	8.72	3	8825
<b>le15FS fondo</b>	C15-05	Ch	2005	21/07/2005		28	7.6	0	40291
<b>SR fondo</b>	SR13-s05	C	2005	21/07/2005	-13	16.9	7.15	0	19564
<b>B1 sup</b>	Bur6-05	Bur	2005	08/08/2005	-0.5	25.3	8.42	7	10894
<b>B1 fondo</b>	Bur6-05	Bur	2005	08/08/2005					
<b>B2 sup</b>	Bur5-05	Bur	2005	08/08/2005	-0.5				
<b>B2 fondo</b>	Bur5-05	Bur	2005	08/08/2005	-1.75				
<b>B3 sup</b>	Bur4-05	Bur	2005	08/08/2005	-0.5				
<b>B3 fondo</b>	Bur4-05	Bur	2005	08/08/2005	-1.65				
<b>Burlamacca FS_s</b>	L10-05	Bur	2005	26/08/2005	-0.5	25.3	7.51	9	38931
<b>Burlamacca Ponte Girante_s</b>	Bur2-05	Bur	2005	26/08/2005	-0.5	24.6	7.64	2	55801
<b>Burlamacca molo_s</b>	Bur1-05	Bur	2005	10/08/2005	-0.5	25.6	7.8	3	66831
<b>Burlamacca FS_f</b>	L10-05	Bur	2005	26/08/2005		25.8	7.69	0	67853
<b>Burlamacca Ponte Girante_f</b>	Bur2-05	Bur	2005	26/08/2005		25.2	7.83	2	69883
<b>Burlamacca molo_f</b>	Bur1-05	Bur	2005	10/08/2005	-2.1	25	7.96	4	69520
<b>Farabola0</b>	F0	F	2005	05/08/2005	-0.5	26.6	8.9	3	6158
<b>Farabola1</b>	F1	F	2005	05/08/2005	-0.5	25.7	7.47	2	8489
<b>Farabola2</b>	F2	F	2005	05/08/2005	-0.5	21.8	7.53	2	7345
<b>Farabola3</b>	F3	F	2005	05/08/2005	-0.5	25.3	7.74	7	9158
<b>GoraStiava0</b>	G0	G	2005	10/08/2005	-0.5	23.5	7.66	5	1008
<b>GoraStiava1</b>	G1	G	2005	10/08/2005	-0.5	25.9	8.61	7	12432
<b>GoraStiava2</b>	G2	G	2005	10/08/2005	-0.5	26.2	7.51	5	10498
<b>sea05</b>	sea05	S	2005	10/08/2005	-0.5	26.1	8.02	6	65076
<b>Case Rosse</b>	CaseRosse	well	2005	02/08/2005					
<b>SerchioSIB2</b>	Serchio	Ser	2005	03/05/2005	-1.5	29.4	8.03	9	868

L=lake; Ch=Channel; C=Quarries; S=Sea; Bur=Burlamacca; F=Farabola stream; G=Gora di Stiava stream; Ser= Serchio River; well= deep well

**Table I.2** Chemical analyses of sampled waters

<b>ID</b>	<b>Alk</b>	<b>Cl</b>	<b>SO<sub>4</sub></b>	<b>Na</b>	<b>K</b>	<b>Ca</b>	<b>Mg</b>	<b>Mn</b>	<b>Fe</b>	<b>Si</b>	<b>B</b>	<b>Br</b>
	meq/l	meq/l	meq/l	meq/l	meq/l	meq/l	meq/l	μM/l	μM/l	mM/l	mM/l	mM/l
L1a-04	2.50	21.23	7.92	19.3	0.46	5.49	5.67	7.5	2.700	0.006	0.054	
L1m-04	2.40	20.67	7.59	19.2	0.46	5.36	5.67	1	<0.2			
L1b-04	2.80	20.82	7.92	18.9	0.47	5.49	5.62	1	0.3	0.006	0.045	
L2-04	2.80	20.87	7.68	18.91	0.46	5.49	5.79	2.5	2			
L2m-04	3.10	21.18	7.75	19.01	0.48	5.5	5.73	1.5	<0.2	0.007	0.053	
L2b-04	3.00	21.18	7.69	18.8	0.47	5.49	5.59	1.5	<0.2	0.006	0.046	
L3aa-04	2.45	20.87	7.41	18.07	0.46	5.29	5.45	1	0.2	0.005		
L3a-04	2.40	20.67	7.56	17.76	0.46	5.58	5.56	10	9	0.005	0.054	
L3m-04	2.40	20.67	7.43	18.38	0.45	5.23	5.45	1	<0.2	0.004		
L3b-04	2.46	20.67	7.56	17.87	0.46	5.46	5.56	1	<0.2	0.004	0.048	
L4aa-04	2.50	21.28	7.71	18.71	0.48	5.55	5.58	1		0.005		
L4a-04	2.40	21.18	7.57	18.89	0.47	5.55	5.58	9		0.008	0.053	
L4m-04	2.30	21.18	7.56	18.6	0.48	5.41	5.61	1		0.005		
L4b-04	2.30	21.08	7.89	18.6	0.47	5.28	5.45	1		0.005	0.046	
L5m-04	2.60	20.87	7.68	18.66	0.46	5.28	5.47	1	0.3	0.005	0.051	
L5b-04	2.50	20.46	7.61	18.6	0.46	5.07	5.34	1		0.005	0.045	
L6m-04	3.80	9.28	5.6	8.17	0.19	6.67	2.90	3.5	0.3	0.056		
L6b-04	3.35	8.05	5.65	6.9	0.16	6.67	2.56	3.5	0.3	0.053	0.014	0.006
L7aa-04	3.20	21.18	7.57	18.25	0.46	5.98	5.34	1				
L7a-04	3.20	21.38	7.51	18.19	0.47	6.06	5.41	1.5		0.008	0.046	
L7m-04	2.80	21.38	7.68	17.81	0.46	6.14	5.34	1.5	<0.2	0.01		
L7b-04	3.30	20.87	7.68	18.24	0.46	6.14	5.46	4.5	0	0.012	0.040	
L8m-04	3.40	25.27	8.26	21.42	0.53	6.96	6.33	2	0.2	0.002	0.044	
L8b-04	3.35	25.58	8.2	22.1	0.53	6.82	6.16	2.5	0.4	0.004	0.042	
L9aa-04	2.60	20.98	7.74	18.91	0.46	5.46	5.55	1.5	<0.2	0.002		
L9a-04	2.50	20.77	7.79	18.64	0.47	5.28	5.60	1	0.2	0.004	0.054	
L9m-04	2.30	20.87	7.68	18.77	0.48	5.55	5.66	1	0.3	0.004		
L9b-04	2.30	20.98	7.6	18.37	0.46	5.28	5.66	1	0.2	0.005		0.017
L10aa-04	3.90	27.42	8.69	23.83	0.57	6.89	6.83	2.5		0.002		
L10a-04	3.70	26.29	8.53	23.18	0.54	6.89	6.61	1.5		0.002	0.047	
L10m-04	3.50	36.62	9.56	31.38	0.73	7.56	8.40	1.5	0.2	0.002		
L10b-04	3.80	51.86	10.97	43.79	1.03	8.12	10.99	1.5	0.2	0.004	0.060	
L11m-04	5.40	27.84	7.29	24.44	0.57	6.86	6.93	7.5	1	0.020	0.067	
L11b-04	5.40	27.94	7.21	24.53	0.57	6.9	6.93	8	0.5	0.022	0.065	0.027
L12a-04	4.40	26.14	7.51	23.14	0.54	6.59	6.64	5	<0.2	0.017	0.059	
L12m-04	4.20	26.24	7.83	23.14	0.54	6.53	6.60	4.5	0.2	0.016		
L12b-04	4.30	25.84	7.69	22.58	0.54	6.43	6.58	4.5	0.8	0.017	0.063	
L13a-04	2.80	22.20	8.33	20.28	0.5	5.59	5.88	1		0.008	0.047	
L13m-04	2.50	21.59	8.27	20	0.5	5.48	5.93	1		0.007		
L13b-04	2.30	22.94	8.36	20.18	0.5	5.58	5.88	1		0.008	0.048	
L14aa-04	2.66	23.63	9.01	20.69	0.52	5.82	6.13	6.5	0.3	0.018		
L14a-04	2.60	22.10	8.88	20.78	0.51	5.75	6.08	6.5	0.3	0.018		
L14m-04	2.76	21.90	8.85	20.6	0.5	5.65	6.04	7	0.3	0.02		
L14b-04	2.80	22.10	9.06	20.51	0.51	5.77	6.08	7	0.3	0.02		
L15aa-04	2.20	22.20	8.04	20.64	0.5	5.8	6.18	7.5	0.2	0.021		
L15a-04	2.26	21.69	7.98	20.54	0.51	5.82	6.18	7	0.2	0.019	0.049	
L15m-04	2.46	22.10	8.01	20.54	0.5	5.78	6.18	7.5	0.3	0.02		
L15b-04	2.50	21.08	7.97	20.64	0.51	5.8	6.18	7.5	0.3	0.02	0.053	
L2-f05	3.30	18.95	7.45	17.15	0.44	7.11	5.50	3.5	11			
L3-f05	3.15	19.95	7.92	18.78	0.47	7.01	5.70	3.5	11	0.001	0.046	
L7-f05	3.18	24.96	8.07	21.74	0.53	7.03	6.21	3.5	0.4	0.001	0.047	

ID	Alk	Cl	SO <sub>4</sub>	Na	K	Ca	Mg	Mn	Fe	Si	B	Br
	meq/l	meq/l	meq/l	meq/l	meq/l	meq/l	meq/l	μM/l	μM/l	mM/l	mM/l	mM/l
L6-f05	7.30	25.68	5.52	22.65	0.41	8.7	6.62	26	7		0.041	
L5-f05	3.14	21.90	7.75	19.29	0.49	6.95	5.96	2.5	1		0.045	
L15-f05	3.23	20.35	7.84	18.88	0.47	7.15	5.70	3	0.5		0.048	
L13-f05	4.17	19.41	7.66	18.78	0.47	7.39	6.11	5.5	1		0.052	
L12-f05	6.34	14.83	9.25	13.54	0.39	10.76	6.28	15.5	2		0.059	0.011
L11-f05	7.03	18.95	8.76	17.83	0.45	9.98	7.03	21	3		0.062	
L4-f05	2.97	19.95	7.73	18.44	0.47	6.91	5.75	4	1		0.046	
L16-f05	3.50	20.55	7.97	18.85	0.47	6.89	5.86	5.5	5	0.002	0.048	
L9-f05	3.70	19.75	7.53	18.13	0.46	7.18	5.86	3.5	1	0.001	0.045	
L17-f05	3.48	19.01	8.1	17.54	0.46	7.1	5.86	3	1		0.047	
L14c-f05	3.30	19.01	7.92	17.96	0.47	7.1	5.91	3	0.4	0.001	0.047	
L2-m05	4.13	21.00	7.74	19.12	0.23	7.21	5.99	2		0.087	0.052	
L3-m05	4.02	20.67	7.41	19.22	0.22	6.59	5.96	2.5		0.07	0.05	
L5-m05	5.08	20.26	7.12	19.12	0.22	7.02	6.05	2		0.084	0.053	
L6-m05	4.03	11.47	5.19	10.59	0.1	7.45	3.55	12.5	3	0.160	0.026	0.006
L7-m05	4.05	21.07	7.38	19.42	0.23	6.88	5.86	2.5		0.048	0.044	0.033
L11-m05	6.57	17.48	7.02	16.4	0.23	8.61	5.80	21	3	0.136	0.071	0.027
L12-m05	5.70	17.97	7.7	17.23	0.24	7.26	6.54	28.5	24	0.171	0.091	0.019
L13-m05	4.43	20.45	7.35	19.25	0.23	7.13	6.12	4		0.108	0.054	0.03
L14-m05	4.00	20.75	7.89	19.38	0.24	7.09	6.04	1.5		0.091	0.054	0.03
L15-m05	3.87	21.05	7.55	19.38	0.24	7.02	5.90	1.5		0.099	0.051	0.034
L9-m05	3.43	24.76	7.93	21.45	0.49	6.07	6.54	1		0.120	0.054	0.017
SR1.5	3.24	29.56	8.87	27.39	0.62	7.63	7.28	2.5	0.3	0.075	0.051	
SR2.7	3.30	54.80	11.42	48	1.04	8.42	12.37		1	0.057	0.068	
SR3	3.34	110.88	16.18	96.61	2.07	9.52	22.69	2.5	<0.2	0.083	0.138	
SR7	5.47	196.80	24.51	173.56	3.83	12.02	39.98	73.5	1	0.121	0.272	0.327
SR10	10.10	225.29	26.9	206.52	4.32	12.56	43.48	54	2	0.191	0.215	
SR14	12.44	255.79	28.05	203.3	4.62	12.9	47.71	74	2	0.266	0.223	0.399
Inc05	3.15	25.82	7.86	20.75	0.56	7.24	6.64	2		0.074	0.052	
Inc2	3.77	26.78	8.42	24.2	0.56	6.7	6.81	2		0.068	0.051	
Inc3	3.45	29.81	8.3	26.85	0.61	6.86	7.38	1.5		0.072	0.049	
Inc4	3.57	34.60	9.31	30.37	0.69	7.5	8.70	1.5		0.078	0.054	
Inc5	3.55	46.88	10.05	41.51	0.93	7.68	10.58	7.5		0.081	0.063	
Inc7	7.70	109.71	14.25	95.95	2.03	9.38	22.31	11	<0.2	0.133	0.114	
Inc11	13.47	126.57	10.48	119.47	2.55	10.37	27.41	12.5	3	0.295	0.135	
Sis0.5	3.15	21.66	7.93	19.8	0.48	6.4	6.39	1		0.111	0.05	
Sis2	3.33	21.77	7.98	20.3	0.48	6.06	6.32	1	<0.2	0.116	0.052	
Sis5	3.67	21.97	8.04	20.23	0.48	6.29	6.12	1		0.111	0.049	
Sis10	3.62	20.58	7.92	19.22	0.47	6.9	5.99	3		0.091	0.046	
Sis12	3.83	21.18	8.18	19.56	0.48	6.96	6.06	8.5		0.089	0.046	
Sis15	4.20	22.17	7.66	20.7	0.49	7.1	6.31	19.5	1	0.093	0.048	
Sis20	6.77	32.35	7.21	28.97	0.69	8.29	8.45	27	1	0.122	0.056	
Inc0.6-sp06	3.40	24.79	7.76	25.23	0.54	7.73	5.76	0.2	0.80		0.05	0.038
Inc3.8-sp06	3.45	30.58	8.38	20.88	0.6	7.98	6.83	1.7	0.60		0.05	0.048
Inc9.5-sp06	11.63	132.94	11.31	113.09	2.38	10.98	24.69	6.4	1.40		0.21	0.203
Inc13.5-sp06	15.83	138.94	8.25	117.44	3.07	11.48	26.33	6.4	1.60		0.31	0.216
Inc15.3-sp06	16.35	141.31	8	117.44	2.56	11.48	25.51	6.7	0.60		0.34	0.211
Inc16.2-sp06	16.55	146.11	7.72	117.44	2.56	11.48	25.51	7.1	0.70		0.32	0.218
SR1	3.30	57.16	11.83	51.38	1.1	8.52	13.07	1.5	0.3	0.193		0.082
SR2	3.00	97.53	14.36	82.43	1.53	9.25	20.04	1	<0.2	0.176		0.134
SR3.5	4.00	173.78	22.28	147.7	3.68	11.11	34.41	16.5	0.2	0.172		0.235
SR4	3.80	210.93	25.04	177.49	3.82	11.94	40.29	32	4	0.199		0.26
SR8	5.00	238.52	27.24	200.3	4.27	12.52	43.89	33.5	1	0.592		0.277

ID	Alk	Cl	SO <sub>4</sub>	Na	K	Ca	Mg	Mn	Fe	Si	B	Br
	meq/l	meq/l	meq/l	meq/l	meq/l	meq/l	meq/l	μM/l	μM/l	mM/l	mM/l	mM/l
SR19	11.70	253.06	22.47	220.35	6.16	13.11	48.64	22	2	0.592		0.336
L15-02	3.50	32.13	4.39	25.9	0.65	6.4	7.95	0.5	0	0.214		0.027
Sis1.5	3.30	28.28	7.76	24.94	0.59	6.08	7.37	1	0.3	0.208		0.04
Sis16.5	4.90	31.93	3.74	27.17	0.65	6.62	7.57	18	3	0.239		0.034
C15	3.80	37.07	8.05	32.92	0.78	6.97	9.12	1.5	0.4	0.162		0.052
L10-02	3.75	45.25	9.06	39.92	0.88	7.85	7.98	1.5	0.2	0.186		0.064
Bur1	3.55	302.65	31.54	237.87	5.19	16.1	72.84	3.5	1	0.173		0.422
Sea02	2.70	599.43	62.7	518.59	16.13	22.3	111.36		0	0.014		0.724
L21	3.20	52.55	10.1	47.12	1.12	8.15	12.19	8.5	20	0.213		0.078
L22	3.35	55.55	10.28	48.36	1.08	8.21	12.25	1.5	0.2	0.17		0.079
L23	3.40	75.73	12.74	64.71	1.42	8.69	15.95	1.5	0.4	0.153		0.08
L24	3.60	272.11	36.74	253.25	5.36	13.32	58.42	4.5	1	0.42		0.431
L34(1)	3.90	125.49	15.18	106.08	3.05	9.73	25.80	3.5	1	0.173		0.177
L34(2)	3.70	316.69	38.99	324.3	6.73	15.32	68.90	2.5	<0.2	0.104		0.483
Inc1.5	3.30	39.94	8.86	34.52	0.8	7.05	9.43	1.5	<0.2	0.17		0.058
Inc2.5	3.50	45.14	9.78	39.69	0.88	7.62	11.93	1	1	0.135		0.092
Inc12	11.06	141.20	12.58	116.47	2.51	20.68	27.10	8.5	1	0.42		0.233
SezE1.5	3.20	35.16	8.62	31.23	0.72	6.94	8.51	1.5	<0.2	0.172		0.055
SezE3	3.65	67.47	11.85	58.18	1.3	8.41	14.37	6.5	1	0.135		0.092
SezE7	4.20	55.43	10.48	47.49	1.07	7.89	12.27	26.5	3	0.185		0.069
SezE14	9.50	88.03	8.4	72.04	1.69	8.96	17.89	15.5	2	0.352		0.107
L14c-02	3.45	33.26	8.1	29.11	0.67	6.54	8.12	1	0.2	0.174		0.047
L16-02	3.40	33.36	7.98	29.09	0.67	6.7	8.03	1.5	0.2	0.164		0.049
SezW1.5	3.55	35.25	8.01	31.68	0.73	6.74	8.51	1.5		0.176		0.05
SezW3	3.65	61.45	11.27	52.47	1.18	7.9	13.21	12	2	0.157		0.092
SezW6	5.40	51.16	9.36	44.64	1.02	7.62	11.39	27	2	0.221		0.071
SezW10.5	10.25	83.52	8.4	73.34	1.5	8.83	16.66	19.5	4	0.358		0.099
L21-02	3.60	37.89	9.43	33.16	0.72	9.79	8.80	5	2	0.275		0.041
L20-02	3.40	46.32	9.79	39.75	0.89	7.13	9.47	1.5	0.3	0.174		0.064
SezIV1.5	3.40	35.16	8.48	30.74	1.02	6.64	8.44	1.5	0.2	0.176		0.05
SezIV1.5b	3.60	46.53	9.83	40.4	0.93	7.11	10.47	2	0.5	0.157		0.047
SezIV5	4.50	52.98	10.84	54.35	1.02	7.42	11.81	10	0.4	0.186		0.066
SezIV14	26.59	146.04	0.25	126.96	2.35	14.79	30.73	30	2	1.367		0.193
L18	3.20	27.98	7.85	24.94	0.58	6.38	7.56	1	0.3	0.204		0.038
L14-02	3.10	28.08	7.68	25.17	0.6	6.14	7.20	1.5	0.2	0.217		0.043
L4-02	4.20	19.97	5.28	18.38	0.51	5.58	6.05	2	0.3	0.25		0.027
L13-02	3.20	28.30	7.32	24.72	0.59	6.22	7.33	2.5	3	0.23		0.04
L3-02	3.40	28.10	7.26	24.38	0.58	6.16	7.23	2	1	0.234		0.041
L7-02	3.50	28.20	7.12	24.79	0.58	6.51	7.20	2	0.4	0.258		0.042
L26	3.55	14.91	4.87	11.44	0.29	6.28	3.55	0.5	0.3	0.098		0.015
L27	4.35	17.10	5.62	15.68	0.32	6.87	4.57	1.5	1	0.125		0.021
L8-02	4.60	33.39	7.64	28.99	0.67	6.85	8.10	1.5	0.3	0.165		0.048
L2-02	3.30	28.40	7.22	24.22	0.56	6.26	7.28	1.5	<0.2	0.222		0.038
L5-02	3.50	27.80	7.34	25.58	0.59	6.09	7.19	1.5	1	0.213		0.041
L6-02	6.90	22.10	4.2	18.94	0.36	7.62	5.22	13	5	0.292		0.028
L33	2.90	28.40	7.25	24.83	0.58	6.12	7.19	1	<0.2	0.23		0.045
L11-02	8.80	26.50	6.16	23.76	0.58	8.77	8.14	12	1	0.228		0.035
L12-02	3.10	26.68	7.32	24.54	0.58	6.28	7.09	3.5	1	0.234		0.038
L37	8.60	30.15	5.48	26.91	0.64	7.38	8.15	13.5	3	0.239		0.045
Bur7-05	3.87	65.95	12.3	58.84	1.3	9.16	14.51	1	0.2	0.061	0.092	
Bur7-05		297.52	31.89									
C15-05	4.00	49.62	9.960	42.86	0.98	8.09	11.09	1.5	<0.2	0.039	0.087	
C15-05		318.68	34.18									

<b>ID</b>	<b>Alk</b>	<b>Cl</b>	<b>SO<sub>4</sub></b>	<b>Na</b>	<b>K</b>	<b>Ca</b>	<b>Mg</b>	<b>Mn</b>	<b>Fe</b>	<b>Si</b>	<b>B</b>	<b>Br</b>
	meq/l	meq/l	meq/l	meq/l	meq/l	meq/l	meq/l	μM/l	μM/l	mM/l	mM/l	mM/l
SR13-s05	10.70	237.26	24.43									
Bur6-05	3.90	104.70	15.42	84.51	1.92	9.54	20.90	1.5	<0.2	0.046	0.128	
Bur6-05		355.26	35.9									
Bur5-05	3.90	79.00	12.97	71.23	1.51	9.27	16.79	1	<0.2	0.054	0.098	
Bur5-05		223.19	26.3									
Bur4-05	3.97	82.53	12.36	72.17	1.58	9.07	17.41	1	<0.2	0.059	0.104	0.108
Bur4-05		429.06	44.29									0.580
L10-05	4.75	301.77	31.5	242.04	5.29	13.51	54.56	3	<0.2	0.097	0.245	0.383
Bur2-05	3.57	426.31	44.75	367.88	8.08	17.32	81.87	2	<0.2	0.046	0.336	
Bur1-05	2.93	545.91	57.35	471.58	10.07	20.49	100.53	1	<0.2	0.016	0.416	
L10-05		555.32	57.46									
Bur2-05		572.89	63.03									
Bur1-05		582.66	60.73									
F0	4.97	42.18	7.23	38.31	1.01	6.75	8.60	9	0.2	0.001	0.083	
F1	5.67	59.41	10.98	56.71	1.39	6.96	11.92	5.5	<0.2	0.16	0.092	
F2	5.70	53.69	12.37	51.61	1.32	6.35	10.67	3.5	0.2	0.178	0.092	
F3	5.67	63.44	13.2	61.61	1.49	6.68	12.64	3	0.2	0.13	0.098	
G0	4.03	3.80	2.96	2.73	0.09	5.14	1.72	1	<0.2	0.175	0.039	0.005
G1	5.23	90.29	13.81	82.87	1.94	8.01	17.62	8.5	3	0.018	0.113	
G2	5.23	77.56	14	69.78	1.79	6.96	15.39	3	<0.2	0.109	0.106	
sea05	2.67	612.65	56.11	531.75	10.89	22.81	114.05	<0.2	0.3	<0.001	0.471	0.952
CaseRosse		1.00	0.35	0.94	0.02		0.41					
Serchio	3.25	1.59	3.05	1.68	0.07	4.76	1.24				0.01	
villa spinola	3.07	0.55	7.94	0.37	0.02	7.21	0.89					



**Table I.3** Analyses of nutrients and CO<sub>2</sub> content in waters

ID	N-NH <sub>4</sub>	N-NO <sub>2</sub>	N-NO <sub>3</sub>	Ntot	Ptot	P-PO <sub>4</sub>	TOC	pCO <sub>2</sub>
	mM N/l	mM N/l	mM N/l	mM N/l	μM P/l	μM P/l	mM C/l	atm
L1a-04	1.00E-03		1.00E-03				3.02E+00	8.45E-05
L1m-04	1.00E-03				3.00E+00		3.23E+00	7.86E-05
L1b-04	1.00E-03				3.00E+00		3.15E+00	9.17E-05
L2-04	2.00E-03						3.17E+00	1.49E-04
L2m-04	1.00E-03						2.39E+00	2.39E-04
L2b-04	1.00E-03				3.00E+00		3.12E+00	4.20E-05
L3aa-04	2.00E-03		1.00E-03		2.00E+00		3.09E+00	2.21E-04
L3a-04	1.00E-03						9.28E-01	1.72E-04
L3m-04	2.00E-03		1.00E-03		5.00E+00		8.91E-01	1.06E-04
L3b-04	2.00E-03						2.37E+00	1.18E-04
L4aa-04	1.00E-03		1.00E-03				2.66E+00	1.03E-04
L4a-04	1.00E-03						3.12E+00	1.02E-04
L4m-04	2.00E-03				3.00E+00		2.25E+00	1.00E-04
L4b-04	1.00E-03				3.00E+00		3.01E+00	1.23E-04
L5m-04	1.00E-03						3.97E+00	1.10E-04
L5b-04	2.00E-03						1.22E+00	1.06E-04
L6m-04	4.00E-03		8.60E-02				2.07E+00	5.75E-03
L6b-04	3.00E-03		8.20E-02		5.00E+00		2.39E+00	5.19E-03
L7aa-04	2.00E-03						2.65E+00	7.42E-04
L7a-04	3.00E-03						2.46E+00	7.77E-04
L7m-04	3.00E-03						2.15E+00	2.42E-03
L7b-04	5.00E-03				3.00E+00		3.15E+00	3.51E-03
L8m-04	2.00E-03		3.00E-03				2.36E+00	5.04E-04
L8b-04	6.00E-03		3.00E-03				2.85E+00	7.29E-04
L9aa-04	2.00E-03						3.22E+00	1.74E-04
L9a-04	2.00E-03						3.25E+00	1.67E-04
L9m-04	2.00E-03				3.00E+00		3.35E+00	1.99E-04
L9b-04	3.00E-03						3.41E+00	2.41E-04
L10aa-04	2.00E-03						2.68E+00	5.38E-04
L10a-04	2.00E-03						2.64E+00	5.52E-04
L10m-04	1.00E-03						1.46E+00	5.94E-04
L10b-04	2.00E-03						1.93E+00	7.47E-04
L11m-04	4.00E-03		6.60E-02		1.00E+01		4.19E+00	5.40E-03
L11b-04	2.00E-03		6.60E-02				4.35E+00	5.90E-03
L12a-04	1.60E-02		8.00E-03				4.46E+00	3.35E-03
L12m-04	1.90E-02		5.00E-03		9.00E+00		4.37E+00	3.43E-03
L12b-04	1.80E-02		8.00E-03				3.95E+00	3.51E-03
L13a-04	1.00E-03						4.09E+00	1.76E-04
L13m-04	4.00E-03				3.00E+00		4.08E+00	1.57E-04
L13b-04	4.00E-03						4.08E+00	1.47E-04
L14aa-04	2.00E-03						4.33E+00	2.57E-04
L14a-04	2.00E-03						3.60E+00	2.51E-04
L14m-04	4.00E-03				2.00E+00		3.24E+00	2.67E-04
L14b-04	4.00E-03						4.33E+00	2.70E-04
L15aa-04	3.00E-03						4.25E+00	1.66E-04
L15a-04	3.00E-03						4.49E+00	1.71E-04
L15m-04	2.00E-03						4.28E+00	1.91E-04
L15b-04	5.00E-03						3.83E+00	1.94E-04
L2-f05	1.20E-02	2.00E-03	8.90E-02	1.96E-01	1.00E+00	<0.2	1.56E+00	9.79E-04
L3-f05	1.80E-02	2.00E-03	8.90E-02	2.06E-01		<0.2	2.14E+00	4.98E-04

ID	N-NH <sub>4</sub>	N-NO <sub>2</sub>	N-NO <sub>3</sub>	Ntot	Ptot	P-PO <sub>4</sub>	TOC	pCO <sub>2</sub>
	mM N/l	mM N/l	mM N/l	mM N/l	μM P/l	μM P/l	mM C/l	atm
L7-f05	3.10E-02	3.00E-03	6.50E-02	1.72E-01		<0.2	1.55E+00	1.04E-03
L6-f05	3.84E-01	3.00E-03		4.07E-01	1.00E+01	<0.2	2.47E+00	1.06E-02
L5-f05	2.00E-02	5.00E-03	8.10E-02	1.92E-01	1.00E+00	<0.2	1.61E+00	7.43E-04
L15-f05	1.40E-02	2.00E-03	8.50E-02	1.86E-01	1.00E+00	<0.2	1.99E+00	5.01E-04
L13-f05	6.90E-02	3.00E-03	9.70E-02	2.06E-01	3.00E+00	<0.2	1.75E+00	2.10E-03
L12-f05	8.00E-02	4.00E-03	1.65E-01	3.44E-01	7.00E+00	2.60E+00	2.18E+00	4.35E-03
L11-f05	1.93E-01	5.00E-03	1.01E-01	3.71E-01	1.00E+01	3.20E+00	3.74E+00	7.46E-03
L4-f05	1.90E-02	2.00E-03	7.80E-02	1.66E-01	1.00E+00	<0.2	1.46E+00	1.10E-03
L16-f05	1.70E-02	2.00E-03	8.70E-02	1.82E-01	2.00E+00	<0.2	1.82E+00	1.00E-03
L9-f05	1.70E-02	3.00E-03	1.01E-01	1.69E-01	2.00E+00		1.55E+00	2.12E-03
L17-f05	1.70E-02	2.00E-03	8.60E-02	1.96E-01	2.00E+00		1.96E+00	6.57E-04
L14c-f05	1.70E-02	2.00E-03	8.90E-02	2.06E-01	2.00E+00		1.62E+00	8.96E-04
L2-m05	4.00E-03	2.00E-03	3.00E-03	7.40E-01	2.20E+01	<0.2	0.00E+00	5.01E-04
L3-m05	8.00E-03	2.00E-03	2.20E-02	1.66E+00	3.20E+01		1.20E+00	2.31E-03
L5-m05	5.00E-03	2.00E-03	1.60E-02	9.00E-02	1.60E+01		1.55E+00	6.81E-04
L6-m05	1.15E-01	2.00E-03	3.00E-02	2.55E-01	2.20E+01		7.57E-01	9.47E-03
L7-m05	4.00E-03	1.00E-03	2.40E-02	2.06E+00	2.00E+01		1.47E+00	1.26E-03
L11-m05	3.40E-02	8.00E-03	3.83E-01	5.78E-01	3.50E+01	1.50E+00	3.49E+00	3.92E-03
L12-m05	3.00E-03	1.50E-02	6.48E-01	7.62E-01	3.70E+01		2.76E+00	2.76E-02
L13-m05	7.00E-03	3.00E-03	9.00E-03	3.21E-01	2.70E+01	2.00E-01	2.18E+00	1.61E-03
L14-m05	2.00E-03	2.00E-03	2.00E-03	2.00E+00	2.40E+01	2.00E-01	1.76E+00	3.51E-04
L15-m05	3.00E-03	1.00E-03		2.47E-01	2.60E+01	2.00E-01	1.22E+00	3.40E-04
L9-m05	9.00E-03	9.00E-03		7.33E-01		<0.2	2.59E+00	3.23E-04
SR1.5	1.20E-02	1.00E-03		1.32E-01	2.00E+00	<0.2	1.60E+00	7.51E-04
SR2.7	3.80E-02	3.00E-03		1.77E-01	4.00E+00	<0.2	2.11E+00	6.97E-03
SR3	5.80E-02	1.00E-03		1.43E-01	2.00E+00	<0.2	4.50E-01	6.44E-03
SR7	2.88E-01	5.00E-03		3.90E-01	1.20E+01	4.00E-01	5.56E+00	1.50E-02
SR10	8.59E-01	4.00E-03		8.29E-01	3.60E+01	2.54E+01	2.91E+00	3.37E-02
SR14	1.24E+00	4.00E-03		1.22E+00	6.50E+01	4.84E+01	2.63E+00	4.52E-02
Inc05	7.00E-03	2.00E-03		7.70E-02		<0.2	1.38E+00	7.16E-04
Inc2	9.00E-03	2.00E-03	6.20E-02	1.14E-01	1.00E+00	<0.2	1.09E+00	9.08E-04
Inc3	8.00E-03	2.00E-03	6.10E-02	1.01E-01	1.00E+00	<0.2	8.67E-01	1.17E-03
Inc4	1.20E-02	1.00E-03	5.20E-02	9.00E-02	1.00E+00	<0.2	6.47E-01	2.13E-03
Inc5	3.90E-02	2.00E-03	3.20E-02	2.36E-01	1.00E+00	<0.2	2.35E+00	4.37E-03
Inc7	4.49E-01	1.00E-03	5.00E-03	1.77E-01	9.00E+00	9.80E+00	1.54E+00	2.38E-02
Inc11	1.15E+00	1.00E-03	1.00E-03	3.95E-01	4.80E+01	4.40E+01	1.39E+00	5.37E-02
Sis0.5	6.00E-03	6.00E-03		4.84E-01		<0.2		2.96E-04
Sis2	9.00E-03	7.00E-03		5.41E-01		<0.2		3.01E-04
Sis5	9.00E-03	6.00E-03		6.71E-01		<0.2		8.66E-04
Sis10	4.70E-02	2.70E-02	4.20E-02	5.75E-01		<0.2		4.13E-03
Sis12	5.60E-02	6.60E-02	2.80E-02	3.59E-01		<0.2		5.40E-03
Sis15	1.51E-01	2.00E-03				2.00E-01		7.67E-03
Sis20	8.25E-01	3.00E-03		9.99E-01		1.36E+01		2.72E-02
Inc0.6-sp06								6.12E-01
Inc3.8-sp06								5.44E+00
Inc9.5-sp06								4.21E+01
Inc13.5-sp06								6.28E+01
Inc15.3-sp06								6.66E+01
Inc16.2-sp06								6.44E+01
SR1	5.00E-03				1.00E+00	2.00E-01		2.08E-04
SR2			2.00E-03		1.00E+00	<0.2		1.79E-03

ID	N-NH <sub>4</sub>	N-NO <sub>2</sub>	N-NO <sub>3</sub>	Ntot	Ptot	P-PO <sub>4</sub>	TOC	pCO <sub>2</sub>
	mM N/l	mM N/l	mM N/l	mM N/l	μM P/l	μM P/l	mM C/l	atm
SR3.5	4.80E-02				1.00E+00	<0.2		4.88E-03
SR4	6.70E-02				1.00E+00	3.00E-01		4.50E-03
SR8	2.08E-01				1.00E+00	1.00E+00		6.65E-03
SR19	9.94E-01				3.20E+01	3.21E+01		2.14E-02
L15-02	9.00E-03				2.00E+00	<0.2		2.42E-04
Sis1.5	8.00E-03				1.00E+00	<0.2		2.48E-04
Sis16.5	1.79E-01				1.00E+00	5.00E-01		2.00E-02
C15	2.00E-03				1.00E+00	3.00E-01		2.77E-04
L10-02	2.00E-03				1.00E+00	<0.2		4.51E-04
Bur1	1.11E-01							4.41E-03
Sea02								4.93E-04
L21	3.00E-03				1.00E+00	<0.2		1.62E-04
L22	2.60E-02				1.10E+01	<0.2		5.68E-04
L23			1.10E-02		1.00E+00	<0.2		1.65E-04
L24			3.00E-03		1.10E+01	3.10E+00		4.51E-04
L34(1)	4.30E-02				3.00E+00	2.00E-01		1.61E-04
L34(2)			1.70E-02					1.61E-03
Inc1.5	4.00E-03				1.00E+00	3.00E-01		2.14E-04
Inc2.5					1.00E+00	<0.2		2.48E-04
Inc12	8.19E-01				1.80E+01	1.87E+01		2.09E-02
SezE1.5	8.00E-03				1.00E+00	2.00E-01		2.31E-04
SezE3	1.30E-02					<0.2		3.33E-03
SezE7	5.40E-02		1.00E-03			<0.2		5.30E-03
SezE14	7.35E-01		1.00E-03		1.40E+01	1.37E+01		2.35E-02
L14c-02					1.00E+00	<0.2		2.79E-04
L16-02	1.00E-03				1.00E+00	2.00E-01		3.88E-04
SezW1.5	1.00E-03				1.00E+00	<0.2		3.36E-04
SezW3	1.20E-02				1.00E+00	<0.2		3.02E-03
SezW6	2.33E-01				2.00E+00	2.00E-01		6.82E-03
SezW10.5	7.92E-01				1.10E+01	5.70E+00		2.72E-03
L40	2.20E-02				1.00E+00	2.00E-01		5.90E-03
L41	3.00E-03				1.00E+00	<0.2		2.06E-04
SezIV1.5					1.00E+00	<0.2		4.19E-04
SezIV1.5b	4.00E-03					5.00E-01		7.10E-04
SezIV5	4.90E-02					3.00E-01		4.51E-03
SezIV14	4.12E+00					1.87E+02		1.23E-01
L18	1.00E-03		1.00E-03		1.00E+00	<0.2		2.54E-04
L14-02	5.00E-03							1.66E-04
L4-02	3.00E-03				2.00E+00	<0.2		1.54E-03
L13-02	1.00E-02				2.00E+00	<0.2		3.56E-04
L3-02	1.30E-02		1.00E-03		1.00E+00	2.00E-01		6.14E-04
L7-02	1.00E-03				2.00E+00	2.00E-01		5.55E-04
L26	1.80E-02				1.00E+00	<0.2		1.53E-03
L27	3.40E-02		2.82E-01		1.80E+01	1.22E+01		8.00E-03
L8-02	2.20E-02				1.00E+00	<0.2		4.78E-04
L2-02	6.00E-03				1.00E+00	<0.2		3.45E-04
L5-02	3.00E-03		1.00E-03		1.00E+00	<0.2		2.96E-04
L6-02	4.90E-02		2.28E-01		7.00E+00	9.00E-01		1.37E-02
L33	4.00E-03				1.00E+00	<0.2		1.80E-04
L11-02	8.80E-02		2.31E-01		1.90E+01	5.30E+00		4.50E-03
L12-02	6.00E-03				1.00E+00	3.00E-01		3.41E-04

<b>ID</b>	<b>N-NH<sub>4</sub></b>	<b>N-NO<sub>2</sub></b>	<b>N-NO<sub>3</sub></b>	<b>Ntot</b>	<b>Ptot</b>	<b>P-PO<sub>4</sub></b>	<b>TOC</b>	<b>pCO<sub>2</sub></b>
	mM N/l	mM N/l	mM N/l	mM N/l	μM P/l	μM P/l	mM C/l	atm
L37	1.32E-01		3.30E-02		1.60E+01	9.50E+00		6.12E-03
Bur7-05	2.60E-02	2.00E-03		2.63E-01		6.00E-01	6.70E-01	3.43E-04
C15-05		1.00E-03	1.81E-01	3.91E-01		2.00E-01	7.77E-01	3.06E-04
Bur6-05	7.00E-03	1.76E+00	1.90E-02	4.34E-01		<0.2	3.75E-01	5.89E-04
Bur5-05	7.00E-03	1.76E+00	1.20E-02	2.07E+00		3.00E-01	2.91E-01	
Bur4-05	1.30E-02	1.76E+00	2.60E-02	1.75E+00		3.00E-01	4.13E-01	
L10-05	1.01E-01	1.96E+00	1.20E-02	1.46E+00		5.63E+01	8.40E-02	5.90E-03
Bur2-05	1.46E-01	1.44E+00		8.38E-01		2.38E+01	1.50E+00	3.12E-03
F0	3.00E-03	1.45E+00	1.52E-01			4.00E-01	1.33E+00	2.38E-04
F1	1.54E-01	1.60E+00	5.38E-01	3.08E+00		2.72E+01	8.41E-01	9.82E-03
F2	3.02E-01	1.15E+00	2.08E-01	3.00E+00		8.79E+01	8.02E-01	8.12E-03
F3	3.19E-01	1.37E+00	1.28E-01	2.60E+00		8.24E+01	6.91E-01	5.15E-03
G0	7.00E-03	1.75E+00	1.90E-02	4.67E-01		2.00E-01	2.75E-01	4.74E-03
G1	2.70E-02	1.10E-02	1.28E+00	2.64E+00		3.96E+01	3.24E-01	4.72E-04
G2	3.10E-01	1.10E-02	1.22E+00	3.32E+00		9.60E+01	2.06E-01	7.33E-03
sea05	3.00E-03	1.74E+00		1.22E+00		2.00E-01	2.25E+00	8.50E-04
Serchio	1.10E-02			8.00E-02				1.65E-03

**Table I.4** Isotopic Analyses of waters

ID	$\delta^{18}\text{O}$	$\delta^2\text{H}$	$\delta^{13}\text{C}_{\text{DIC}}$	$\delta^{34}\text{S}_{\text{SO}_4}$	$\delta^{18}\text{O}_{\text{SO}_4}$	$\delta^{11}\text{B}$
	‰SMOW	‰SMOW	‰V-PDB	‰CDT	‰V-PDB	‰NBS
L1a-04						
L1m-04						
L1b-04	-1.49	-13.4				
L2-04	-1.38	-14.1				
L2m-04	-1.37	-13.4				
L2b-04	-1.33	-13.3				
L3aa-04						
L3a-04	-1.54	-13.9				
L3m-04						
L3b-04	-1.48	-13.2				
L4aa-04						
L4a-04						
L4m-04						
L4b-04	-1.44	-13.9				
L5m-04						
L5b-04	-1.5	-13.3				
L6m-04	-4.93	-28.9				
L6b-04	-5.17	-31.9				
L7aa-04						
L7a-04						
L7m-04	-1.84	-16.7				
L7b-04						
L8m-04						
L8b-04	-2.11	-16.7				
L9aa-04						
L9a-04	-1.45	-14				
L9m-04	-1.4	-12.7				
L9b-04	-1.35	-14.1				
L10aa-04						
L10a-04	-1.84	-15.5				
L10m-04						
L10b-04	-2.26	-16.3				
L11m-04						
L11b-04	-1.31	-12.6				
L12a-04						
L12m-04						
L12b-04	-1.2	-12.9				
L13a-04						
L13m-04						
L13b-04	-0.8	-9.4				
L14aa-04						
L14a-04						
L14m-04						
L14b-04	-0.52	-7.3				
L15aa-04						
L15a-04						
L15m-04						
L15b-04	-0.46	-8.9				

ID	$\delta^{18}\text{O}$	$\delta^2\text{H}$	$\delta^{13}\text{C}_{\text{DIC}}$	$\delta^{34}\text{S}_{\text{SO}_4}$	$\delta^{18}\text{O}_{\text{SO}_4}$	$\delta^{11}\text{B}$
	‰SMOW	‰SMOW	‰V-PDB	‰CDT	‰V-PDB	‰NBS
L2-f05	-3.24	-22.3				
L3-f05	-3.16	-22.3				
L7-f05	-2.91	-21.4				
L6-f05	-3.66	-25.2				
L5-f05	-3.11	-23.1				
L15-f05	-3.13	-21.2				
L13-f05	-3.4	-23.2				
L12-f05	-4.41	-28.5				
L11-f05	-4.46	-28.5				
L4-f05	-3.02	-22.5				
L16-f05						
L9-f05	-3.31	-25.8				
L17-f05						
L14c-f05	-3.08	-20.35				
L2-m05						
L3-m05	-2.81	-19.1				
L5-m05	-2.7	-20				
L6-m05	-4.86	-34.3	-10.15			
L7-m05	-2.79	-22.1				23
L11-m05	-3.24	-27.5	-7.73			16.6
L12-m05	-4.74	-31.1	-10.73			23.9
L13-m05	-2.5	-19.9				21.7
L14-m05						
L15-m05	-2.31	-21	-3.03			25.4
L9-m05						
SR1.5	-3.52	-22.8				
SR2.7	-3.38	-21.4				
SR3	-2.7	-19.7				
SR7	-1.48	-8.5				36.6
SR10	-1.37	-9.9				
SR14	-1.34	-8.6				29.9
Inc05	-3.12	-23.5				
Inc2	-3.21	-21.6	-6.39			
Inc3	-3.19	-20.1				
Inc4	-3.25	-23.2	-7.25			
Inc5	-3.05	-20.3	-8.8			
Inc7	-1.7	-12.8	-15.34			
Inc11	-1.49	-8.7	-18.59			
Sis0.5	-1.52	-15.20	-1.02			
Sis2	-1.49	-17.20	-0.96			
Sis5			-3.23			
Sis10	-3.16	-22.50	-7.89			
Sis12	-3.23	-23.50	-8.43			
Sis15	-2.81	-23.20	-8.4			
Sis20	-2.86	-22.70	-7.71			
Inc0.6-sp06	-2.75	-18.8	-6.24	11.27	10.70	
Inc3.8-sp06	-2.89	-19.5	-8.83	11.3	10.80	
Inc9.5-sp06	-1.46	-10.8	-18.47	20	14.67	
Inc13.5-sp06	-1.38	-12.7	-19.62	24	16.98	
Inc15.3-sp06	-1.4	-11.8	-19.92	24.9	18.03	
Inc16.2-sp06	-1.46	-11.5	-19.88	25.5	17.43	

ID	$\delta^{18}\text{O}$	$\delta^2\text{H}$	$\delta^{13}\text{C}_{\text{DIC}}$	$\delta^{34}\text{S}_{\text{SO}_4}$	$\delta^{18}\text{O}_{\text{SO}_4}$	$\delta^{11}\text{B}$
	‰SMOW	‰SMOW	‰V-PDB	‰CDT	‰V-PDB	‰NBS
Bur7-05	-1.68	-15.7	-9.18			27.6
Bur7-05	-1.06	-7.5				
C15-05						
C15-05						
SR13-s05						
Bur6-05						
Bur6-05						
Bur5-05	-1.08	-12.5				
Bur5-05	-0.8	-8				
Bur4-05	-1.68	-12.5	-9.03			30.6
Bur4-05	-0.02	0.5				
L10-05	-2.47	-15	-10.67			37.2
Bur2-05	-0.94	-5.9				
Bur1-05	0.63	5.2				
L10-05	0.63	6				
Bur2-05	0.93	7.9				
Bur1-05	1.02	9.1				
F0						
F1						
F2						
F3						
G0	-4.1	-30.2				
G1						
G2						
sea05	1.22	9.3				
CaseRosse	-6.14	-37.5				
Serchio	-6.81	-44.2				

## APPENDIX II

**Table II.1** Chemical analyses of OC, TC, TIC, N and LOI in the superficial sediments

ID	Core Penetration (cm)*	Subsample Depth in core (cm)**	Water Content %	LOI <sub>105</sub>	LOI <sub>375</sub>	LOI <sub>550</sub>	LOI <sub>950</sub>	LOI <sub>res</sub>	TN %	TC %	TOC %	TIC %	C/N
L1_1	43.5	0-5	76	20.38	23.8	3.8	14.7	37.3	0.73	19.7	18.6	1.1	26.99
L1_2		5-15	86						1.58	21.1	21.2	<0.01	13.35
L1_3		15-41	88						0.87	23.1	23.2	<0.01	26.55
L2_1	44.5	0-3	85	7.22	29.3	5.1	5.5	53.0	1.51	20.3	20.3	0.02	13.44
L2_2		3-33	87						1.51	20.6	20.6	<0.01	13.64
L2_3		33-44.5	87						1.64	23.1	23.1	0.02	14.09
L3_1	40.5	0-5.5	84	2.46	2.1	11.6	26.8	57.0	0.67	11.4	6.96	4.43	17.01
L3_2		5.5-15.5	71	2.23	7.0	3.0	29.2	58.8	0.41	9.08	3.67	5.41	22.15
L3_3		15.5-40.5	72						0.37	8.39	2.33	6.07	22.68
L4_1	36.0	0-5	92	12.77	53.8	4.5	4.5	24.5	1.19	37.2	37.2	0.03	31.26
L4_2		5-17	92						1.49	44.8	44.9	<0.01	30.07
L4_3		17-36	93						1.63	47.8	47.9	<0.01	29.33
L5_1	41.0	0-4.5	91	9.00	35.4	4.2	6.6	48.4	1.68	23.8	23.7	0.07	14.17
L5_2		4.5-15	94						2.18	28.9	28.9	<0.01	13.26
L5_3		15-41	91						1.51	21	21	<0.01	13.91
L6_1	38.0	0-5	74	4.81	13.4	2.8	1.3	78.5	0.56	6.75	6.73	0.02	12.05
L6_2		5-23	76	6.33	17.2	3.1	3.0	70.4	0.73	9.52	9.55	<0.01	13.04
L6_3		23-38	75						0.71	10.4	10.4	0.05	14.65
L7_1	41.5	0-2	86	8.42	33.2	2.0	2.8	56.5	1.22	19.2	19.2	<0.01	15.74
L7_2		2-18	86						1.58	27.5	27.5	<0.01	17.41
L7_3		18-23.5	84						1.47	26.8	26.8	0.08	18.23
L7_4		23.5-41.5	81						1.4	27.7	27.8	<0.01	19.79
L8	30.0	30	81	10.40	39.4	2.8	2.2	49.7	1.3800	20.2	20.2	<0.01	14.64
L9_1	41.0	0-6	89	12.88	46.8	3.4	3.8	33.2	1.450	30.5	30.5	<0.01	21.03
L9_2		6-9	70										
L9_3		9-41	26										
L10_1	18.5	0-6	42	0.79	2.9	0.9	2.8	92.6	0.070	3.33	2.79	0.54	47.57
L10_2		6-18.5	69	4.75	17.3	2.9	3.5	71.5					
L11_1	40.0	0-5	67	4.23	11.0	3.2	1.5	80.6	0.45	10.2	9.6	0.62	22.67
L11_2		5-24	65						0.43	7.75	7.34	0.41	18.02
L11_3		24-37	71						0.59	10	9.87	0.17	16.95
L12_1	41.0	1-10	75	3.55	11.8	3.3	2.1	79.7					
L12_2		10-26	70	4.15	11.0	3.0	8.2	77.7					
L12_3		26-41	65										
L13_1	92	0-5	78	8.22	25.7	5.3	10.0	50.8	0.50	6.77	6.58	0.19	13.54
L13_2		5-10	79						0.46	6.19	6.04	0.15	13.46
L13_3		10-32	78						0.42	6.27	5.98	0.3	14.93
L13_4		32-53	72						1.06	22.5	21.8	0.67	21.23
L13_5		53-61	57						1.09	24.9	24.4	0.46	22.84
L13_6		61-67	80						0.68	14.8	13.7	1.1	21.76
L13_7		67-71	78										
L13_8		71-81	67										
L13_9		81-90	0										
L14_1	43.0	0-5	69	1.94	7.6	2.8	30.4	59.2	0.35	19.9	7	12.9	56.86



ID	Core Penetration (cm)*	Subsample Depth in core (cm)**	Water Content %	LOI <sub>105</sub>	LOI <sub>375</sub>	LOI <sub>550</sub>	LOI <sub>950</sub>	LOI <sub>res</sub>	TN %	TC %	TOC %	TIC %	C/N
<b>L14_2</b>		5-10	69										
<b>L14_3</b>		10-16	77										
<b>L14_4</b>		16-19	75										
<b>L14_5</b>		19-43	89										
<b>L15_1</b>	43.0	0-2.5	74	2.99	10.6	3.7	19.7	66.5	0.52	14.7	6.72	7.94	28.27
<b>L15_2</b>		2.5-29	79	3.24	12.3	3.2	23.6	57.7					
<b>L15_3</b>		29-43	71										
*Recorded in cm as observed in the field													
**Interval of subsample as measured in cm from the top of the core													

**Table II.2**  $^{13}\text{C}$  and  $^{14}\text{C}$  analyses of the organic carbon of the sediments

<b>ID</b>	<b><math>\delta^{13}\text{C}_{\text{DIC}}</math></b>	<b><math>^{14}\text{C}_{\text{OC}}</math></b>	<b>Precision</b>
	<b>‰V-PDB</b>	<b>pMC</b>	
L5_3	-26.3	90.663	0.999
L7_2	-27.8	85.782	0.436
L7_3	-27.6	87.493	0.469
L7_4	-28.3	77.971	0.434
L9_2	-27.2	61.66	0.382
L9_3	-27.2	62.889	0.442
L13_1	-27.6	73.610	0.422
L13_2	-27.5	73.716	0.423
L13_3	-27.4	77.803	0.464
L13_4	-24.4	81.549	0.470
L13_5	-26.8	81.628	0.512
L13_6	-27.7	72.05	0.426
L13_7	-27.2	71.136	0.448
L13_8		74.272	0.456
L13_9	-25.6	71.836	0.424
L14_1	-27.2	82.77	0.564
L14_2	-27.2	83.825	0.662
L14_3	-25.2	84.021	0.523
L14_4	-27.2	76.569	0.432
L14_5	-27.5	70.687	0.436
L15_2		83.083	0.444
L15_3		84.652	0.491